THE
PHYSICAL REVIEW

A journal of experimental and theoretical physics established by E. L. Nichols in 1893

SECOND SERIES, VOL. 71, NO. 7 APRIL 1, 1947

The Mass of the Mesotron as Determined by Cosmic-Ray Measurements

DONALD J. HUGHES*
Argonne National Laboratory, Chicago, Illinois
(Received December 23, 1946)

All quantitative determinations of the masses of individual cosmic-ray mesotrons have been based on cloud-chamber photographs involving measurements of magnetic curvature plus ionization density, range, or energy of knock-on electrons. The errors involved in the different methods are discussed as well as the possibility of reducing these errors by the choice of experimental conditions. The errors and the mass values themselves of 47 published measurements are reviewed in the light of the discussion. The great majority of the results are statistically reconcilable with a single mass; only a very small fraction of the mesotrons seem to have significantly different masses.

I. INTRODUCTION

IN the ten years that have elapsed since the discovery of the mesotron as a component of cosmic rays, many attempts have been made to determine its mass. Although the mass of the mesotron was the property which led to its discovery, and in spite of the many efforts to measure it, the mass is still not known accurately, nor is it known whether it actually has a unique value or a distribution of values. As it is likely that mesotrons will be produced in high voltage accelerators, it seems worth while to review the cosmic-ray measurements of the mesotron mass to serve as a basis for comparison with the accelerator results. Such a review was given by the author at the September, 1946 Physical Society meeting, and the present article includes and extends the material presented at that time. The accuracy which has been, and can be, obtained in mesotron mass determinations will first be discussed, then all of the published measurements will be reviewed in the light of the discussion.

II. THE ACCURACY OF MASS DETERMINATIONS

All measurements of the mass of individual cosmic-ray mesotrons (as distinguished from values of the average mass resulting from measurements of such quantities as the number of electron secondaries, etc.) have been made by determining the momentum of the particle from its magnetic curvature in a cloud chamber, together with some second measurable quantity. This second quantity, which gives essentially the velocity of the particle, has been the ionization density, the range, the rate of loss of momentum or the kinetic energy transferred to an atomic electron. The mass follows directly from the momentum and velocity, but in practice the velocity is not determined explicitly because of its somewhat complicated dependence on the actual measured quantities. It is possible to express directly the dependence of the mass on the measured quantities in simple graphical form and

* On leave from The Institute for Nuclear Studies, University of Chicago, Chicago, Illinois.

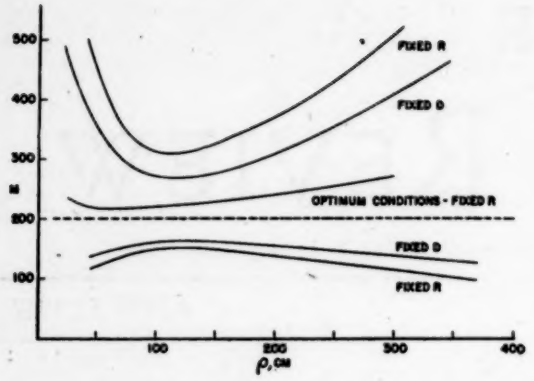

FIG. 1. Variation in mesotron mass (M) as a function of radius of curvature for a true mass of 200 electron masses. Curves labeled "fixed R" and "fixed D" refer to measurements based on range and on ionization density for the chamber described in reference 1. The curve "optimum conditions" is for the same chamber under optimum experimental conditions.

the manner in which mass values depend on the experimental data can thus be clearly shown. A nomograph for this purpose has been given recently as Fig. 1 of an article by Hughes[1] (hereafter referred to as DJH). The nomograph is applicable to cases involving magnetic curvature, change of curvature, density of ionization, and range. Accurate mass measurements based on energy of knock-on electrons are extremely unlikely[2] and the method will not be discussed in this section although several masses based on knock-on electrons will be included in section III.

It was shown in DJH for a particular experimental set-up that the accuracy of mass determination, whether based on curvature and range or curvature and ionization density, is greatest for a particular momentum (curvature) value. For smaller momenta the error caused by spurious curvature due to multiple scattering in the chamber gas lessens the accuracy; for larger momenta the errors in curvature due to gas movements, finite track width, etc., again lessen the accuracy. The calculation of the accuracy as a function of momentum for any chamber can be made by using the formula of Williams[3] for ρ_s (the average radius of curvature caused by multiple scattering), assuming a value for the error in measuring the curvature of a track arising from chamber distortions, and determining the resultant error in mass from the nomograph. The simplified form of Williams' formula applicable to a particular chamber[4] given as Eq. (1) of DJH can be used if the differences in chamber gas and magnetic field are taken into account.

The accuracy of mass determination with the chamber described in DJH was only about 20 percent at best and even this accuracy would be obtained at only a single curvature value ($\rho = 125$ cm) and under the assumption that no error is incurred in the measurement of the ionization density. The operating conditions of the above chamber can be improved with respect to mass determination, and the highest accuracy to be expected is shown in Fig. 1 as the curve marked "optimum" conditions. The other curves in the figure are from Fig. 2 of DJH and refer to the average spread in measured values based on magnetic curvature plus density of ionization ("fixed D") or range ("fixed R"). The true mass of the particle is assumed to be 200 times that of the electron. The "optimum" conditions refer to the same magnetic field of 1165 gauss, and in addition substitution of helium for argon, reduction of chamber distortion to such a point that the magnetic displacement of the center of a track can be fixed to 0.02 cm, and measurement of range in the chamber with negligible error. The minimum error in M under such conditions is 8 percent and is attainable only at a radius of curvature of 65 cm.

It is instructive to consider the effect of supplying a higher magnetic field in order to increase

[1] D. J. Hughes, Phys. Rev. **69**, 371 (1946).
[2] R. Richard-Foy, Cahiers de Physique **2**, 65 (1942); S. Gorodetzky, Ann. de Physique **19**, 5 (1944).
[3] E. J. Williams, Phys. Rev. **58**, 292 (1940).
[4] H. A. Bethe, Phys. Rev. **69**, 689A (1946), has also calculated the effect of scattering on curvature measurements for this same chamber, mainly for very slow particles. *Note added in proof:* Bethe's results have since been published, Phys. Rev. **70**, 821 (1946), and his conclusions are essentially the same as those of the present paper, although he does not consider the errors which become important at high momenta. Bethe calculates that the chance of a mesotron of *assumed* mass 200 giving the *experimental* value of 30 ± 20 reported in DJH, Fig. 5, is 7 percent and hence compatible with the "normal" mesotron mass. The calculations of section III of the present paper, however, give 0.5 percent for the same probability (see left hand point of Fig. 4), a much less compatible value. Bethe's result (see page 825 of his article) is higher than that of the present paper because of (a) his omission of the stopping power of the alcohol, (b) use of the stopping power for 6 Mev alphas whereas the mesotron velocity is actually higher, and (c) the difference (about 20 percent) between Bethe's and Williams' formulas for ρ_s. If Bethe's calculations are corrected for (a) and (b), then the only difference between his results and those given in DJH and in the present article is that caused by (c).

the accuracy further. The particular momentum at which maximum accuracy is obtained is independent of magnetic field strength, but the error in mass is inversely proportional to field strength. Hence, a fourfold increase of H for the above optimum conditions will result in a lowering of the error in mass to two percent, but again only at the same momentum which now means a radius of curvature of only 16 cm. It is obviously very difficult to work at the optimum conditions under such conditions, for particles with such small radii of curvature would tend to be deflected away from the cloud chamber by the magnetic field. On the other hand, the higher magnetic field will give about the same accuracy (8 percent) as the optimum for the lower field, but for particles of four times the momentum. The higher momentum particles will, of course, have the same radius of curvature as the optimum value for the lower field and hence will have the same probability of reaching the chamber. The advantage of the higher field in such a case is that equal accuracy is attained for particles of higher momentum which are much more numerous in the cosmic-ray momentum spectrum. The disadvantage of the higher field is that the higher momentum particles have much greater ranges which are correspondingly harder to measure because they necessitate more absorbers in the chamber.

Thus by increasing the magnetic field it becomes possible to equal the accuracy of the optimum curvature although using correspondingly higher momentum particles of the same curvature in the chamber. However, as particles of much higher momentum are used and the particle velocity becomes relativistic, the accuracy decreases because the error in M relative to a given error in $H\rho$ increases (assuming R measured accurately). In this way the error in M, which is 1.5 times the error in $H\rho$ for low velocities and for a mass of 200 (see nomograph), becomes 2 times at an $H\rho$ of about 5×10^5. The relationships between M, R, and $H\rho$ are shown in Fig. 2 from which the error in M due to a certain error in $H\rho$ can be calculated. Thus the error shown for $M=200$ at an R of 50 g/cm² Pb represents a 10 percent error in $H\rho$ which can be seen to correspond to a 20 percent error in M.

In conclusion it is seen that the highest accuracy is obtained for a gas of low atomic weight, for a chamber of small distortion, for a high magnetic field and at a particular curvature value. As the magnetic field is increased the optimum curvature also increases and it becomes impossible for tracks of such curvature to enter the chamber. It is worth pointing out that the foregoing limitation does not apply if the particles are produced *in* the chamber, which seems to take place for cosmic rays at high altitudes,[5,6] and which can be arranged for particles produced by the high voltage accelerators.[7] The possibility of producing mesotrons inside cloud chambers and hence using high magnetic fields and the optimum curvature seems to be a very promising feature of the mass measurement of artificially produced mesotrons.

III. COSMIC-RAY MEASUREMENTS TO DATE

Up to December 1, 1946 there have been published about 50 measurements made in such a way that the determinations can be considered quantitative measurements of individual mesotron masses. The expected errors of each of these measurements have been recalculated following the principles of section II. The mass value itself has also been recalculated in each case from the original data, using the nomograph of DJH, Fig. 1, to eliminate differences in masses caused by differences in the theoretical formulas used by different experimenters. The main change results

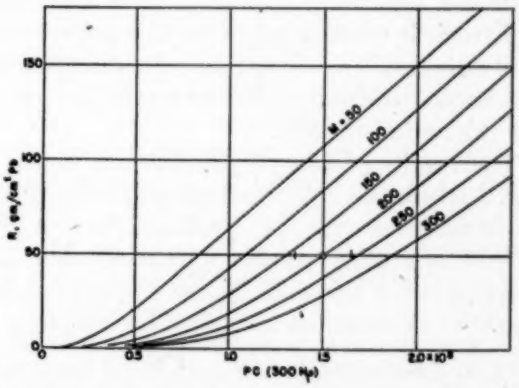

FIG. 2. The relationship between momentum and range for different values of M. The 10 percent error shown in $H\rho$ for a mass of 200 would lead to a 20 percent error in M.

[5] G. Herzog, Phys. Rev. 59, 117 (1941).
[6] D. J. Hughes, Phys. Rev. 60, 414 (1941).
[7] G. C. Baldwin and G. S. Klaiber, Phys. Rev. 70, 259 (1946).

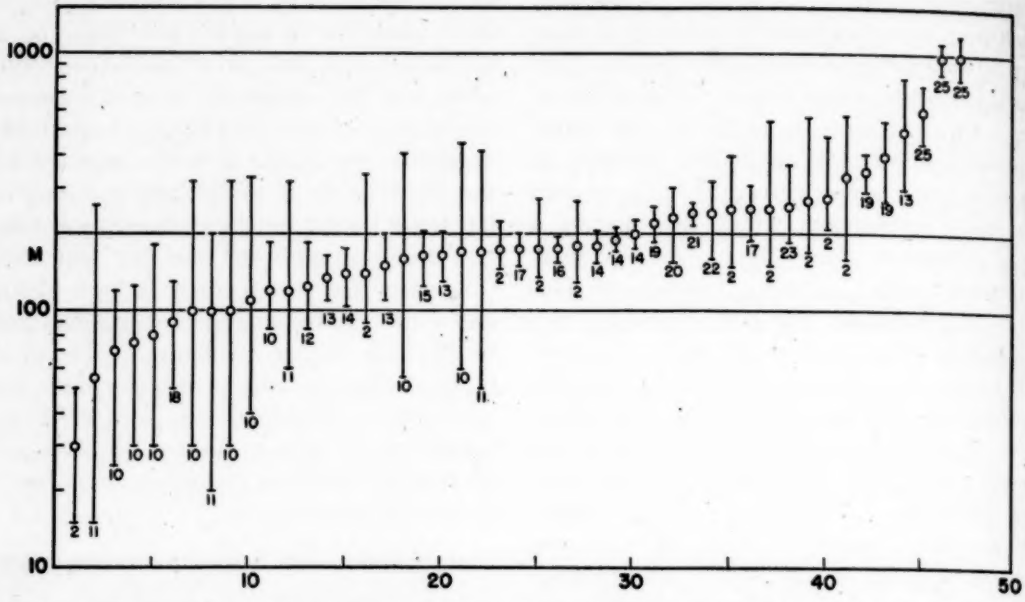

FIG. 3. The experimental determinations of the mass of the mesotron and their expected mean errors. The results are arranged in order of increasing mass and the number identifying each gives the reference for the original publication.

from the use of the theoretical[8] formula for density of ionization, D, as a function of β (approximately $\beta^{-1.8}$ in the usual range) whereas some authors have used experimental values for the exponent of β, such as the value $\beta^{-1.4}$ found by Williams.[9] In many cases the calculated error in M is larger than the error estimated in the original publication because of the omission of some contributory factor by the author. Because pertinent experimental details were sometimes omitted it is undoubtedly true that some of the final estimated errors are themselves in error but it is hoped consistently neither on the pessimistic nor the optimistic side.

The results of the calculations are shown in Fig. 3 where the individual mass determinations are arranged in terms of increasing mass value. The identification number appearing with each mass gives the reference for the original publication.[10–25] Because the formulas[3] for the error in curvature measurement are given in terms of the mean error, and because this error usually predominates, the final errors shown by the vertical lines of Fig. 3 are represented as mean errors also. The mass determinations whose errors are such that only an upper or lower limit for the mass could be obtained have been omitted as have those which give only an average mass value based on some average property of mesotrons (as the average number of knock-on electrons,[26] or the average density in photographic emulsions[27]). Otherwise it is believed that the 47 values of

[8] J. A. Wheeler and R. Ladenburg, Phys. Rev. 60, 754 (1941) (Appendix).
[9] E. J. Williams, Proc. Roy. Soc. A126, 289 (1930); A172, 194 (1939).
[10] J. Ruling and R. Steinmauer, Experientia 2, 108 (1946).
[11] H. Maier-Leibnitz, Zeits. f. Physik 112, 569 (1939).
[12] R. L. Sen Gupta, Nature 154, 706 (1944).
[13] E. J. Williams and E. Pickup, Nature 141, 684 (1938).
[14] C. E. Nielsen and W. M. Powell, Phys. Rev. 63, 384 (1943).
[15] J. C. Street and E. C. Stevenson, Phys. Rev. 52, 1003 (1937).
[16] Y. Nishina, M. Takeuchi, and T. Ichimiya, Phys. Rev. 55, 585 (1939).
[17] J. G. Wilson, Proc. Roy. Soc. A172, 521 (1939).
[18] T. H. Johnson and R. P. Shutt, Phys. Rev. 61, 380 (1942).
[19] S. H. Neddermeyer and C. D. Anderson, Rev. Mod. Phys. 11, 191 (1939) (Figs. 15, 16).
[20] D. R. Corson and R. B. Brode, Phys. Rev. 53, 776 (1938).
[21] L. S. Leprince-Ringuet, S. Gorodetzky, E. Nageotte, and R. Richard-Foy, Phys. Rev. 59, 460 (1941).
[22] P. Ehrenfest, Jr., Comptes rendus Paris 206, 428 (1938).
[23] E. J. Williams and G. E. Roberts, Nature 145, 102 (1940).
[24] S. H. Neddermeyer and C. D. Anderson, Phys. Rev. 50, 263 (1936).
[25] L. Leprince-Ringuet, M. Lheritier, and R. Richard-Foy, Comptes rendus Paris 219, 618 (1944); 221, 465 (1945).

Fig. 3 represent all the quantitative mass determinations of the cosmic-ray mesotron that have been published.[28]

The masses of Fig. 3 cover a wide range, from 30 to 1000 electron masses, but because of the large experimental errors associated with many of them, the number of determinations lying within experimental error of a single mass of 200 is 28, or 60 percent of the total. The number of results agreeing with a single mass would have been much smaller had the errors assigned by the authors themselves been used, because of the increase in many of the calculated errors caused by scattering in the chamber gas. The errors also are much larger than the attainable values discussed in section II because in many cases the experimental conditions were not such as to give the highest accuracy. Nine of the mass values differ from 200 by more than twice the mean error and 3 differ by more than three times (the numbers expected from a Gaussian distribution being 5.2 and 0.8, respectively). Thus, although the majority of the results indicate a single mass, or rather a range in mass smaller than the rather large experimental errors, there is evidence for a few masses of greatly different values.

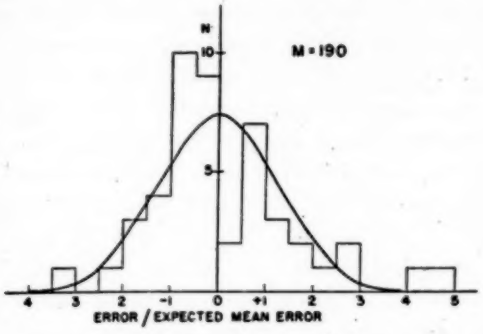

FIG. 4. The errors of the 47 determinations of Fig. 3 relative to the expected mean error of each measurement on the assumption that the true mass is 190. The smooth curve is the Gaussian distribution.

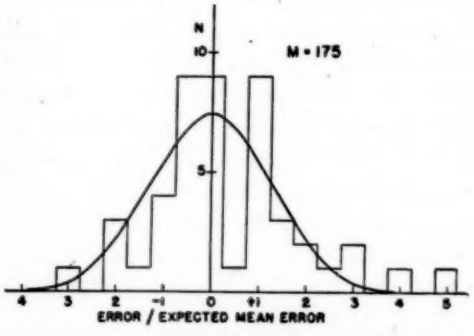

FIG. 5. The same results as in Fig. 4 for a mass of 175.

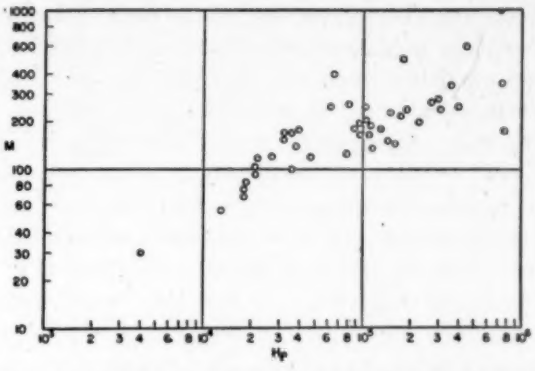

FIG. 6. The experimental mass values plotted against the momentum ($H\rho$) of the mesotron for each measurement.

The errors of Fig. 3 are of course calculated on the basis that the mass involved in each determination is actually the value resulting from the measurement. If it desired to check the possibility that only a single mass is actually involved in all the measurements, then the errors shown in Fig. 3 will be changed somewhat because they are a function of the assumed particle mass. In order to see if the measurements could be reconciled with a single mass, the error in the curvature measurement which would be necessary to give the observed results in each case was calculated under the assumption that the actual mass had a single value. The entire error was assumed to be that of curvature measurement because it is the predominant source of error practically without

[26] H. J. Bhabha, Proc. Roy. Soc. **A164**, 257 (1938).
[27] D. M. Bose and B. Choudhouri, Nature **148**, 259 (1941); **149**, 302 (1942).
[28] The recent measurements of W. B. Fretter and R. B. Brode, which were described at the September, 1946 Physical Society meeting but which have not been published as yet will furnish additional valuable results. *Note added in proof:* This work has since been published, Phys. Rev. **70**, 821 (1946), where 26 mass values are given based on measurement of range and $H\rho$. The errors of individual determinations (expected mean value) are about 18 percent on the average, and the measured masses, if plotted as in Figs. 4, 5 of the present paper, scatter about a single value ($M=202$) in a manner consistent with the expected error. The difference between the mass value of 202 and the 175 of Fig. 4 is not of great significance because of the systematic errors in mass determination (such as the uncertainty in the exact form of the theoretical energy range relation, etc.) which exist in addition to the statistical errors for both values. It should be noted that the mesotrons measured by Fretter all lie in the momentum band 5 to 9×10^5 (see Fig. 5 of present paper and attendant discussion).

exception. The expected mean error for each curvature measurement was also calculated for the particular experimental conditions, again assuming a single particle mass. Although it is true that the expected errors vary with experimental conditions, the results of different measurements can be compared if the errors are taken relative to the expected mean error in each case. The resulting distribution of errors for such a calculation is given in Fig. 4, where the true mass is assumed to be 190, and in Fig. 5 where the mass is taken to be 175. The blocks show the number of measurements which have the indicated errors (in units of the mean expected error, where a positive error signifies a high mass value) under the assumption of a true mass of 190 or 175. The solid curves are the expected Gaussian distributions of errors. The rather close agreement between the observed distribution of "errors" and that expected means that if all the different measurements are considered as repeated trials with varying experimental conditions the distribution of results is about what would be expected. The agreement with mass 175 seems better than with mass 190, but in this connection it must be remembered that the nomograph used to calculate the mass values is based on the theoretical change of ionization with velocity. Experiments[9] seem to show a different change of ionization with velocity and if true would cause the measured masses to increase.

The curves of Figs. 4 and 5 show a few measurements which lie outside the expected distribution but the number is so small that it must be concluded that if there are any mesotrons of mass greatly different from approximately 200 they constitute at most only a few percent of all the mesotrons. This conclusion does not support the suggestion made by Bose and Choudhouri[29] that the average mesotron mass increases with momentum. Actually, if the measured masses are plotted as a function of the particle momentum (Fig. 6), it appears that there is a relationship between mass and momentum. However, the fact that Fig. 6 shows low mass particles only at low momentum can be consistent with either (1), a distribution of masses independent of momentum, because low mass particles would be detectable only at low momentum, or (2) a single mass of about 200, because heavily ionizing tracks ending in the chamber might be neglected unless they show marked curvature which, if owing to scattering, would give erroneously low mass values.

The spread in the observed mass values is much larger than the smallest attainable errors for optimum conditions discussed in section II, hence measurements made under the correct conditions with present apparatus can definitely show whether the spread is real. It is also important, as was pointed out by Blackett at the September, 1946 Physical Society meeting, to measure mesotron masses for as great a range of momentum and altitude as is feasible, because of the possibility that the mesotron mass might vary with these factors.

[29] D. M. Bose and B. Choudhouri, Ind. J. Phys. 18, 285 (1944).

The Determination of the Sign and the Energy Spectrum of Primary Cosmic Radiation*

M. S. VALLARTA, M. L. PERUSQUÍA,** AND J. DE OYARZÁBAL
Instituto de Física, Universidad de México, México, D. F.

(Received November 19, 1946)

An experiment is reported in this paper for the measurement of the complete azimuthal effect. This experiment was performed in Mexico City (geomagnetic latitude 29°, altitude 2242 m above sea level) for constant zenith angles 20°, 40°, and 60°. A characteristic feature is that the length of the atmospheric path is constant, hence the assumption is made that the number of secondaries detected by the cosmic-ray telescope is a measure of the number of primaries. The analysis yields an energy spectrum of the primary radiation of the form $K/E^{1.45}$ (E = energy, K = constant). There is no evidence of negative primary particles. The results are subject to revision because the penumbra bands at this latitude are only imperfectly known, and also because of the resolving power of our present apparatus. The possibility of a bright line spectrum, or of such a spectrum superimposed on a continuous distribution, is not ruled out. The possibility of negative primaries is excluded within the limits of experimental error. The spectrum obtained from our experimental data agrees completely with that determined from the experiment of Gill, carried out at Lahore, Punjab, India. The result is valid in the energy range from about 350 to 600 millistörmers, or 6 to 21 Bev if the primaries are protons.

1. INTRODUCTION

IT has been repeatedly pointed out in the literature that, in principle, the earth is a good magnetic spectrograph suitable for the determination of the energy spectrum of primary cosmic radiation. Several experiments can be suggested with this end in view, of which the measurement of the total latitude effect and of the north-south effect at different latitudes are two examples. The difficulty about the interpretation of these experiments is that of necessity they must be performed not outside, but inside the earth's atmosphere. The passage of primary cosmic rays through air produces many very complicated phenomena which cannot be excluded. Therefore the first requirement is to devise a type of experiment in which some of the atmospheric effects are removed or at least kept constant. It is well known that many of these effects depend essentially on the length of the atmospheric path, hence it appears desirable to plan an experiment in which this parameter is kept constant.

On the occasion of the Symposium on Cosmic Rays held at the University of Chicago in July, 1939 one of us[1] suggested the measurement of the complete azimuthal effect as an experiment satisfying the condition already mentioned. Since the zenith angle is kept fixed, the length of the atmospheric path is also constant. As a matter of fact such an experiment is also suited to obtain very extensive information on the sign of primary cosmic radiation.

It follows from the theory of the allowed cone of cosmic radiation[2] that, at each point of the earth and for each zenith angle, an experiment of the kind already mentioned explores a certain energy range which decreases continuously from the geomagnetic equator to the pole, and, at a given point, from the horizon to the zenith. The theory of the determination of the energy spectrum from the measurement of the azimuthal effect, taking into account the so-called penumbra bands, has been worked out by R. A. Hutner.[3]

2. DESCRIPTION OF THE EXPERIMENT

The experiment was carried out in Mexico City (geomagnetic latitude 29°, altitude 2242 meters). The apparatus was built by A. Baños, Jr. and M. L. Perusquía, and will be described shortly in the literature.[4] It consists essentially of four trains of Geiger-Müller counters connected so as to record triple coincidences. The counters were made in the laboratory of R. D. Evans at the Massachusetts Institute of Technology, and

* Presented by invitation at the New York meeting of the American Physical Society, September 1946.

** Now at Instituto Tecnológico de Monterrey, Monterrey, N. L., México.

[1] M. S. Vallarta, Rev. Mod. Phys. 11, 239 (1939).

[2] See, for example, M. S. Vallarta, *An outline of the theory of the allowed cone of cosmic radiation* (Univ. of Toronto Press, 1938).

[3] R. Albagli Hutner, Phys. Rev. 55, 15, 614 (1939).

[4] Alfredo Baños, Jr. and M. L. Perusquía, to be submitted to Rev. Sci. Inst.

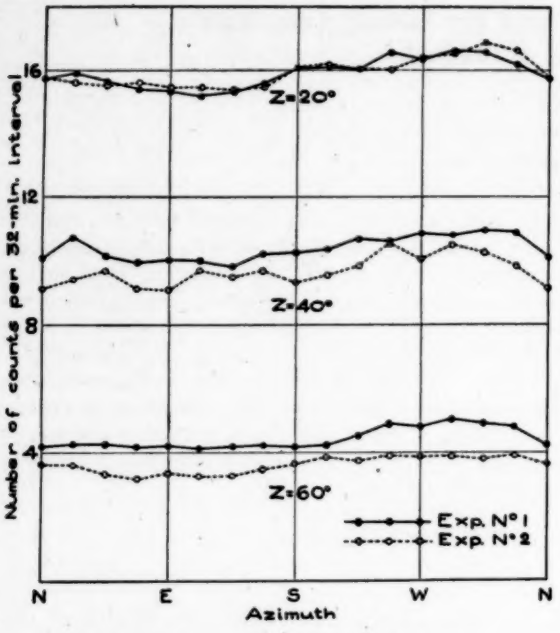

FIG. 1. The experimental azimuthal effect.

were designed specially for high stability over long periods of time. They have proved thoroughly dependable in operation. The trains of counters are placed at zenith angles 0°, 20°, 40°, and 60°, and can be arranged so as to secure best resolution either in zenith angle or in azimuth. The resolving power of each train is 5.5×21.5°. The apparatus rotates about the geomagnetic vertical axis by $\frac{1}{16}$ of a revolution each time, so that each train of counters stays in each azimuth for 32 minutes, and after such an interval the azimuth of each train increases by 22.5°. It is housed in a room built of pressed concrete and fiber boards located on top of a tower. The operation of the apparatus is wholly automatic, and the number of triple coincidences on each of the four trains is recorded photographically at the end of each 32-minute interval. Room temperature is controlled thermostatically at 35°C. Time signals to control the rotation were provided by a master clock at the University Observatory in Tacubaya. In order to secure high precision the apparatus was kept in fairly continuous operation twice for periods of at least 100 days. The first run lasting, with a few interruptions, from July 17, 1943 to September 7, 1944, for a total of 401 days and 32,335 recorded triple coincidences, was made with the counters placed so as to give best resolution in zenith angle; the second, including, with some interruptions, the period from October 21, 1945 to May 19, 1946, for a total of 137 days and 10,546 recorded triple coincidences, was made with the counters placed so as to give best resolution in azimuth.

3. STATISTICAL ANALYSIS

For each azimuth and each zenith angle a statistical analysis was carried out of the frequency distribution of triple coincidences recorded by each train, on the basis of intervals of 32 minutes. The mean value of the number of triple coincidences per interval was calculated from the formula

$$\bar{x}_i = \sum x f_x / n,$$

TABLE I. Azimuthal effect, experiment No. 1.

Zenith distance / Azimuth	20° Mean value	20° Probable error	40° Mean value	40° Probable error	60° Mean value	60° Probable error
N	15.74	0.12	10.07	0.09	4.22	0.07
N N E	15.94	0.12	10.76	0.09	4.27	0.07
N E	15.69	0.11	10.16	0.09	4.28	0.06
E N E	15.40	0.11	9.94	0.09	4.18	0.06
E	15.35	0.11	10.01	0.09	4.22	0.06
E S E	15.19	0.11	10.00	0.09	4.13	0.06
S E	15.30	0.11	9.85	0.10	4.19	0.06
S S E	15.58	0.11	10.21	0.09	4.23	0.06
S	16.03	0.12	10.28	0.09	4.20	0.06
S S W	16.07	0.11	10.37	0.10	4.25	0.07
S W	16.01	0.11	10.73	0.09	4.56	0.07
W S W	16.57	0.11	10.65	0.09	4.91	0.07
W	16.34	0.11	10.88	0.10	4.82	0.07
W N W	16.62	0.11	10.85	0.09	5.05	0.07
N W	16.59	0.12	10.99	0.09	4.92	0.07
N N W	16.18	0.12	10.94	0.09	4.82	0.07

TABLE II. Azimuthal effect, experiment No. 2.

Zenith distance / Azimuth	20° Mean value	20° Probable error	40° Mean value	40° Probable error	60° Mean value	60° Probable error
N	15.76	0.19	9.15	0.26	3.66	0.10
N N E	15.63	0.18	9.45	0.20	3.64	0.09
N E	15.55	0.16	9.72	0.25	3.32	0.07
E N E	15.65	0.18	9.13	0.25	3.17	0.08
E	15.45	0.16	9.11	0.26	3.36	0.09
E S E	15.48	0.18	9.71	0.26	3.25	0.07
S E	15.38	0.18	9.51	0.22	3.28	0.07
S S E	15.44	0.19	9.73	0.24	3.48	0.08
S	16.06	0.20	9.34	0.18	3.64	0.09
S S W	16.18	0.19	9.57	0.24	3.89	0.09
S W	16.01	0.18	9.89	0.26	3.74	0.09
W S W	16.00	0.17	10.59	0.28	3.91	0.09
W	16.38	0.12	10.06	0.28	3.89	0.07
W N W	16.53	0.12	10.54	0.28	3.90	0.09
N W	16.88	0.18	10.30	0.25	3.81	0.10
N N W	16.63	0.18	9.89	0.24	3.94	0.09

TABLE III. East-west, A_w, and north-south, A_s, asymmetries.

Zenith angle→ Asymmetry		20°	40°	60°
A_w	Exp. 1	0.063	0.083	0.134
A_w	Exp. 2	0.058	0.099	0.144
A_s	Exp. 1	0.018	0.021	0
A_s	Exp. 2	0.019	0.021	0

where n is the number of intervals and f_x the frequency of occurrence of the value x. The probable error was calculated from

$$\text{P.E.}(\bar{x}) = 0.67449\sigma/(n)^{\frac{1}{2}}$$

where σ is the standard deviation. For each analysis the x^2-test was made with a discontinuous variable distribution governed by Poisson's law, and the first four coefficients of a Gram-Charlier type B series expansion were obtained. As a final result the adopted mean value of the number of coincidences for each analysis was

$$m = \bar{x} \pm \text{P.E.}(\bar{x})$$

with a limit of perhaps three times the probable error.

The experimental results for the complete azimuthal effect are given in Tables I and II, and in Fig. 1, on the basis of 32-minute intervals.

4. THE NORTH-SOUTH AND EAST-WEST ASYMMETRIES

Particular attention should be paid to the north-south and east-west asymmetries, defined by $A_S = 2(I_S - I_N)/(I_S + I_N)$ and $A_W = 2(I_W - I_E)/(I_W + I_E)$ respectively. They can be readily computed from Tables I and II, and are given in Table III.

These values should be compared with those obtained previously at the same place by Alvarez and Compton,[5] by Johnson[6] and by Schremp and Baños.[7] It will be seen that the agreement is satisfactory. The values of these asymmetries, calculated from the energy spectrum determined in this paper, are given in a later section.

[5] Luis W. Alvarez and A. H. Compton, Phys. Rev. 43, 835 (1933).
[6] T. H. Johnson, Phys. Rev. 47, 91 (1935); ibid. 48, 287 (1935).
[7] E. J. Schremp and A. Baños, Jr., Phys. Rev. 58, 662 (1940).

TABLE IV. Values of the lower limit of integration, $E_{\alpha z}$.

Zenith angle	Azimuth	E (main cone) (mS)	E (penumbra) (mS)
20°	N W	400	380
20°	N E	450	430
40°	N W	385	365
40°	N E	500	480
60°	N W	366	345
60°	N E	580	560

5. THE ENERGY LIMITS

We now turn our attention to the main purpose of this paper: the determination of the energy spectrum of the primary cosmic radiation. The intensity in a given direction, defined by the azimuth α and the zenith angle z, is given by

$$I(\alpha, z) = \int_{E(\alpha, z)}^{\infty} F(E)dE,$$

where $F(E)$ is the energy spectrum and E the energy. The lower limit $E(\alpha, z)$ is given by the theory of the allowed cone, and of course depends on the location and size of the penumbra bands. The penumbra has been fairly completely studied at latitudes near the equator by Tchang Yong-Li[8] and at latitudes up to about 20° by R. Albagli Hutner.[3] No such detailed analysis is yet available for higher latitudes, but from general principles already stated by Schremp[9] and by Albagli Hutner,[3] as well as from the knowledge of the shadow cone obtained by the former,[10] it is possible to determine with fair approximation, which however is subject to revision, the penumbra at 29°, the latitude at which the experiment reported in this paper was performed. It is planned to make a detailed study of the penumbra at this latitude with the help of the new differential analyzer at the Massachusetts Institute of Technology. The results of this work will be reported later. It may be necessary at that time to revise the results obtained here.

The main question now is to determine as accurately as possible, on the basis of these considerations, the lower limit of integration $E(\alpha, z)$ for each zenith angle and each azimuth, that is, the least possible value of the energy of a particle

[8] Tchang Yong-Li, Ann. de la Soc. Sci. de Bruxelles 49, 285 (1939).
[9] E. J. Schremp, Phys. Rev. 54, 153 (1938).
[10] E. J. Schremp, Phys. Rev. 54, 158 (1938).

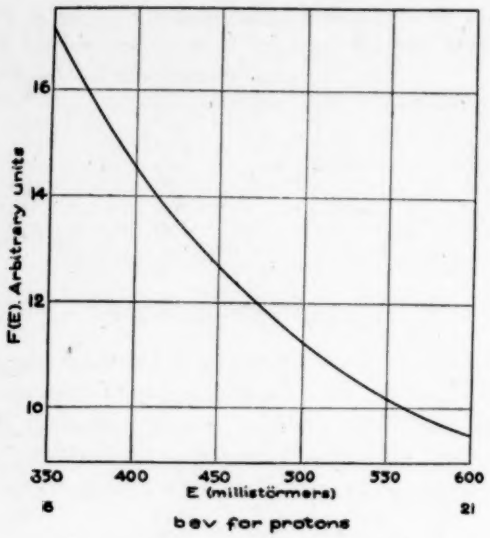

FIG. 2. The energy spectrum.

which can reach the point of observation in the given direction. Typical values thus found are shown in Table IV. These values refer to positive particles and are given in millistörmers (mS). Similar values may be found at other azimuths. Table IV, however, is chosen because it gives the maximum and minimum values of the least energy of arrival. It will be seen from this table that the azimuthal effect at $z=20°$ explores the energy range between 380 and 430 millistörmers, or an interval of 50 mS, that at $z=40°$ it explores between 365 and 480 mS (115 mS), that at $z=60°$ it explores between 345 and 560 mS, or an interval of 215 mS.

6. DETERMINATION OF THE ENERGY SPECTRUM

To determine the spectrum we assume an energy distribution function $F(E)=K/E^c$. We next calculate the intensity $I(z, \alpha)$ using the lower limit of integration $E(z, \alpha)$ obtained as explained in the previous section, and fix the constant K so that the calculated and observed intensities agree at an arbitrarily chosen azimuth, for example the north. To find the exponent c we have, from the discussion above,

$$I(z,\alpha)=\int_{E(z,\alpha)}^{\infty}\frac{K}{E^c}dE=\frac{-K}{c-1}\frac{1}{E(z,\alpha)^{c-1}},$$

therefore

$$-\log\left[\frac{c-1}{-K}I(z,\alpha)\right]=(c-1)\log E(z,\alpha)$$

from which c is determined. A typical calculation is given in Table V. The same value of c is obtained from the other two zenith angles explored, i.e., $z=20°$ and $z=40°$. We therefore conclude that $c=1.45$, and we have the energy distribution function[11] (Fig. 2).

$$F(E)=K/E^{1.45}.$$

A particularly sensitive check of this result is the calculation of the north-south effect. Since the northern and southern boundaries of the allowed cone are only slightly affected by the penumbra, we use the energy limits corresponding to the main cones determined by Lemaitre and Vallarta.[12] The result is shown in Table VI.

7. THE SIGN OF PRIMARY PARTICLES

The question of the sign of the primary particles will now be taken up. From the theory of the allowed cone[13] it is known that the cones for positive and negative particles are symmetrical with respect to the geomagnetic meridian plane. Hence, if there were equal numbers of positive and negative primaries of the same energy, the intensity oscillations due to the penumbra bands should have been symmetrical with respect to the meridian plane; if there were less negatives than positives of the same energy the oscillations should have been asymmetrical as to size, but symmetrical as to position. Finally if the negative primaries had a quite different energy spectrum from the positives, the oscillations on either side

TABLE V. Values of the exponent, c.

	$\lambda=29°$	$z=60°$	Exp. N° 2		
Azimuth	Relative intensity	$E(z,\alpha)$ (mS)	$-\log\frac{I}{K}(c-1)$	$\log E$	$c-1$
N	1	400	1.1685	2.6021	0.45
N E	0.907	570	1.2109	2.7559	0.44
E	0.918	550	1.2055	2.7404	0.44
S E	0.896	490	1.2162	2.6902	0.45
S	0.995	395	1.1703	2.5966	0.45
S W	1.022	360	1.1590	2.5563	0.45
W	1.063	350	1.1421	2.5441	0.45
N W	1.041	350	1.1511	2.5441	0.45

[11] In our preliminary communication (New York meeting of the American Physical Society, September 1946) a variable exponent c was reported. Our preliminary calculations have been shown since to be incorrect, chiefly because the statistical analysis of the experimental results had not yet been completed.

[12] G. Lemaitre and M. S. Vallarta, Phys. Rev. 49, 719 (1936).

[13] Reference 1, or G. Lemaitre and M. S. Vallarta, Phys. Rev. 50, 493 (1936).

of the meridian should have been quite asymmetrical, but there still should have been intensity oscillations on either side of the meridian plane, and these oscillations should have been related for all zenith angles, i.e., they should have gone with the cones of the same energy. In the present experiment oscillations are quite apparent on the side of the meridian plane belonging to positive particles (i.e., on the north to west and west to south quadrants), but none are significant on the side corresponding to negative primaries, within the limits of experimental error, except perhaps that between the north and east at $z=40°$ (Fig. 1). Hence we conclude that within these limits there are no negative particles in primary cosmic radiation, and that the energy spectrum calculated above is that of positive primaries. This conclusion seems to run against the theory of the origin of cosmic rays suggested by Millikan and his collaborators.[14] Although this theory has not yet been fully worked out it would seem to require equal numbers of positive and negative primaries of the same energy, which is ruled out by the present evidence.

The possibility that the energy spectrum may be discontinuous, perhaps consisting of several bright lines, belonging to positive particles, is not ruled out by the present evidence. We take up this question again in a later section.

8. GILL'S EXPERIMENT

The analysis of the energy spectrum outlined above may be extended to higher energies by using the experimental results of Gill,[15] obtained in Lahore at $\lambda=22°$, at a constant zenith angle $z=60°$. Bearing in mind the longitude effect between Lahore and Mexico City,[16] his experiment takes in the energy range from around 380 to nearly 600 mS, with the added advantage that at his latitude the penumbra bands are much better known from the work of Albagli Hutner.[3] An analysis similar to that outlined above yields exactly the same value for c as that obtained here, i.e., $c=1.45$, in agreement with our result. We therefore conclude that the energy spectrum of the primary rays is

$$F(E)=K/E^{1.45},$$

valid in the range from 350 to 600 mS. If now we make the further assumption that the primary particles are protons, as is made very likely by the work of Schein and his collaborators, we may translate the energy range from Störmers to electron-volts. By using the table given by Lemaitre and Vallarta[17] it is seen that this range is from about 6 to 21 Bev.

TABLE VI. North-south effect.

Zenith angle	20°	40°	60°
Energy limits (mS)	420–440	410–430	400–395
A_n calculated	0.0211	0.0212	−0.002
A_n observed	0.018	0.021	0

9. DISCUSSION

The agreement between the energy spectrum determined from Gill's experiment and from that reported in this paper is particularly encouraging, as they were performed at quite different latitudes, longitudes, and altitudes above sea level. This agreement also lends support to the assumption that, so long as the length of the atmospheric path is constant, the number of secondaries detected by a cosmic-ray telescope in a given zenith angle and azimuth is directly related to the number of primaries incident in the same direction, so that the number of secondaries is a measure of the number of primaries.

As already mentioned earlier, the possibility that the energy spectrum may consist of a number of bright lines in the energy range mentioned before is not altogether excluded by the present experiment. For example, if there were three bright lines at 6.6, 7.5, and 13.2 Bev., belonging to the annihilation of nitrogen, oxygen, and silicon, as suggested by Millikan and his collaborators,[14] we should observe sudden changes of intensity as the direction defined by a cosmic-ray telescope measuring the azimuthal effect cuts across the boundary of the allowed cones corresponding to these energies, i.e., from the southeast around to the northwest at $z=60°$. The oscillations observed in the experiment reported here may be accounted for by a continuous energy distribution and the penumbra bands. However, since the latter are not yet known with sufficient

[14] R. A. Millikan, H. V. Neher, and W. H. Pickering, Phys. Rev. **61**, 397 (1942).
[15] P. S. Gill, Phys. Rev. **67**, 347 (1945).
[16] M. S. Vallarta, Phys. Rev. **47**, 647 (1935).
[17] G. Lemaitre and M. S. Vallarta, Phys. Rev. **43**, 87 (1933), Table VI.

precision, and since the resolving power of our instrument does not allow a sufficiently fine exploration of the interesting region of the sky, the possibility suggested by Millikan *et al.* must for the present remain open. What is definitely disproved by the present experiment is their suggestion of a bright line spectrum symmetrical for positive and negative primary particles.

Finally it should be emphasized that the results reported here may still require further revision as soon as the penumbra bands at the latitude of Mexico City have been well determined. It may also be necessary, in order to settle the question of a bright line energy spectrum, to repeat this experiment using an apparatus with much better resolving power than any used so far for work on cosmic rays. A bright line spectrum superimposed on a continuous background may also be a possibility. At any rate, measurements of the complete azimuthal effect at properly chosen latitudes and with properly designed apparatus, as shown here, are quite able to solve the very important problem of the determination of the energy spectrum and sign of primary cosmic radiation.

Our results do not seem to agree with those of Schremp and Baños.[7] Whether this is ascribable to the limitations imposed by the resolving power of our apparatus or to some other reason is still an open question.*

ACKNOWLEDGMENT

We are happy to acknowledge the economic support provided by the Comisión Impulsora y Coordinadora de la Investigación Científica which made the completion of this experiment possible.

* *Note added in proof, February 12, 1947.*
It has been suggested to one of us (M.S.V.) by Professors B. Rossi of Massachusetts Institute of Technology and J. R. Oppenheimer of the University of California that negative primary particles, if they are electrons, may be undetected in this experiment because their secondaries generated by a cascade process would be already absorbed by the atmosphere at 2242 m altitude. In order to test this important point it is planned to repeat the present experiment at an altitude of not less than 5000 m.

PHYSICAL REVIEW VOLUME 71, NUMBER 7 APRIL 1, 1947

Azimuthal Variations of Cosmic Radiation at Lahore

PIARA SINGH GILL*
Forman Christian College, Lahore, India
(Received December 2, 1946)

A study of the azimuthal variations of the cosmic radiation at Lahore (22° N magnetic latitude) shows a large azimuthal effect. The azimuthal effect in the northwest quadrant for a constant zenith angle of 60° is in general agreement with theoretical prediction. These observations lead to the conclusion that (1) primary cosmic-ray particles are positively charged (2) the energy spectrum of the primary cosmic rays within the energy range 7.84×10^9 ev and 14×10^9 ev (for protons) obeys the law $BE^{-\gamma}$ where $\gamma\simeq2.8$.

IN 1940 the author initiated a detailed study of the azimuthal variations of the hard component of cosmic radiation at Lahore (22° N magnetic latitude). Reports on the progress of this work have been published previously.[1] These experiments were planned on the basis of Hutner's[2] calculations of the azimuthal effect of cosmic rays, for a constant zenith angle of 60 degrees, at a geomagnetic latitude of 20 degrees North. Similar studies of the azimuthal variations of cosmic rays have been made by Vallarta, Perusquía, and De Oyarzábal[3] at Mexico City (29° N magnetic latitude). The results obtained

* At present at the University of Chicago, Chicago, Illinois.
[1] P. S. Gill, Phys. Rev. **60**, 153 (1941); **67**, 347 (1945); P. S. Gill, Proc. Ind. Acad. Sci. **12**, 53 (1945); P. S. Gill and S. P. Malhotra, Science and Culture **11**, No. 6, 321 (1945).
[2] R. A. Hutner, Phys. Rev. **55**, 15 (1939); **55**, 614 (1939).
[3] M. S. Vallarta, M. L. Perusquía and J. De Oyarzábal, Phys. Rev. **70**, 785 (1946).

at Mexico City are in general agreement with those reported by the author previously.

In the earlier experiments at Lahore, Geiger-Müller tubes constituting cosmic-ray telescopes of wider cones were used. Measurements were made at all the azimuths in steps of 10° for a fixed zenith angle of 60°. These measurements showed that in the northwest quadrant, the azimuthal irregularities were far more pronounced than in any other quadrant. This is in line with the theoretical predictions of Hutner.

To make a more exact comparison with theory for the northwest quadrant the cone of the telescope was reduced to 5.3° in the vertical and 14.2° in the lateral plane. Two equal telescopes directed oppositely were used. They were frequently interchanged to check the accuracy of their performance. By using the reduced cone of the telescopes the number of triple coincidences decreased to about one to two per hour which made it somewhat more difficult to secure a higher statistical precision. Each point given in the experimental curve of Fig. 1 has a precision of about ten percent.

In Fig. 1 there are drawn the theoretical curve (A) and the experimental curve (B). The ordinate scales represent the counts in arbitrary units for curve (A) and the actual number of coincidences per hour for curve (B), respectively. The theoretical curve was calculated for a zero-degree cone, assuming that the energy spectrum of the primary cosmic-ray particles is represented by the power law $F(E)$ equals $BE^{-2.8}$ where B is a constant and E is the energy. These azimuthal variations result from the fact that the primary cosmic-ray particles are positively charged, i.e., the curve is valid for only positive particles in the northern hemisphere. In the experiment it is assumed that the number of coincidences recorded by the telescope from a given direction is a direct measure of the number of primary particles arriving outside the atmosphere from the same direction. All the telescopes used at Lahore had 10.2 cm of lead inserted between the counters which means that the penetrating high energy secondaries measured by the instrument at lower elevations have practically the same direction as the primaries responsible for their production. The experiments carried out at

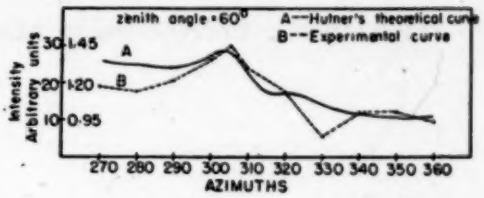

FIG. 1. The azimuthal effect in the northwest quadrant for a fixed zenith angle of 60 degrees.

Mexico City differ in the respect that no lead was placed in the telescopes. Also, the latitude of Lahore is more suitable for a direct comparison with Hutner's calculations than is that at Mexico City.

The curves of Fig. 1 show that the comparison between experiment and theory is as good as can be expected. If a smooth curve is to be drawn through the experimental points the maxima of the two curves would nearly coincide. The difference between the maximum and the minimum of the theoretical curve is nearly fifty percent while that of the experimental curve is close to forty percent. For a still narrower cone this difference might disappear altogether.

These azimuthal measurements in the northwest quadrant at Lahore are in general agreement with the theory. Vallarta[4] has pointed out that measurements of this kind could give (1) the sign, and (2) the energy spectrum of the primary cosmic-ray particles. The azimuthal effect as exhibited by the experimental curve shows that the primary cosmic rays are positively charged particles. This conclusion is in line with that from other sources given by Schein, Jesse, and Wollan.[5] Furthermore, it indicates that the spectrum of the incoming cosmic-ray particles obeys a power law with the exponent approximately 2.8. It can be calculated that the experiment explores the energy band between 0.385 and 0.500 stormer units (7.84×10^9 ev and 14×10^9 ev for protons).

The writer wishes to express his thanks to Professor Marcel Schein for his helpful discussions. The successful execution of the experiment is largely attributed to the grant made by the University of the Punjab.

[4] M. S. Vallarta, Rev. Mod. Phys. 11, 239 (1939).
[5] M. Schein, W. P. Jesse, and E. O. Wollan, Phys. Rev. 59, 615 (1941).

Relativistic Corrections to Magnetic Moments of Nuclear Particles

G. BREIT*
University of Wisconsin, Madison, Wisconsin
(Received December 24, 1946)

ACCORDING to measurements made by W. R. Arnold and A. Roberts[1] the magnetic moment of the deuteron is accounted for by vector addition of proton and neutron moments. They show that the inclusion of the effect of the D state according to Schwinger and Rarita[2] gives agreement with theory within better than the experimental error of ± 0.0012 nuclear Bohr magnetons. In this comparison no correction for relativistic effects to the nuclear moments is made. On the other hand, a recent paper by P. Caldirola[3] indicates as probable a value of -0.006 for the relativistic correction to be added to the sum of the proton and neutron moments in agreement with an older estimate of Margenau.[4] It will be seen that the absolute value of this correction can conceivably be smaller than 0.006 and that a better understanding of interactions between nuclear particles is needed before one can claim that the correction is greater in absolute value than 0.001. The possibility remains open, therefore, that the moments are additive to within about 0.001 of a magneton. The results of Roberts and Arnold[1] when considered in the light of the astounding checks with the measurements of Rabi[5] can thus be reconciled with a simple picture of vector addition of moments of the proton and neutron. The reasoning which leads to this conclusion will now be sketched.

1. The proton moment will be supposed to be partly owing to an intrinsic moment of the type introduced by Pauli[6] and referred to as the "Pauli part." Besides one magneton will be attributed to the Dirac current. This contribution will be called the "Dirac part." The neutron moment will be considered as owing entirely to the Pauli part, as by Caldirola. For the proton, however, other interactions than the four vector type are considered.

2. The relativistic correction factor to the Pauli part is

$$\int [|\psi_3|^2+|\psi_2|^2-|\psi_1|^2]d\tau = 1-2\int |\psi_1|^2 d\tau = 1-\frac{\langle T_z\rangle}{Mc^2}, \quad (1)$$

where the spin is oriented along the z axis and $\langle T_z\rangle$ is the mean value of the part of the kinetic energy due to motion along the z axis. The ψ_μ are the four components of Dirac's wave function with Dirac's original choice of matrices. Since the whole correction in Eq. (1) is owing to ψ_1, it suffices to have a first approximation to ψ_1 in order to ascertain the correction factor to the order v^2/c^2 where v is the velocity of the particle. For spherically symmetric orbital motions (1) becomes

$$1-\langle T\rangle/3Mc^2. \quad (1')$$

The transformation properties of the field which binds the particles do not enter. The magnetic field at the neutron due to the magnetic moment of the proton is neglected in (1) and (1'). This effect is small for the mean distance between proton and neutron and amounts then to a correction of the order $(e^2/r)/Mc^2$ of the momentum. For the mean r this effect is negligible. For very small r it is large. The effect for very small r is neglected here since it involves questions of existence of solutions to the equations. Otherwise one makes the approximation

$$\psi_1 = -\frac{1}{P_0+Mc}\frac{\hbar}{i}\frac{\partial}{\partial z}\psi_1 \cong -\frac{1}{2Mc}\frac{\hbar}{i}\frac{\partial}{\partial z}\psi_1. \quad (2)$$

This approximation is harmless because P_0 differs from its non-relativistic value only in terms of the order v^2/c^2 of itself.

The signs of the correction term are given inconsistently by Caldirola in successive formulas.

* Now at Yale University.
[1] Wayne R. Arnold and Arthur Roberts, Phys. Rev. 70, 766 (1946) (LE).
[2] W. Rarita and J. Schwinger, Phys. Rev. 59, 436 (1941).
[3] P. Caldirola, Phys. Rev. 69, 567 (1946).
[4] H. Margenau, Phys. Rev. 57, 383 (1940); G. Breit, Nature, 122, 649 (1928).
[5] J. M. B. Kellogg, I. I. Rabi, N. F. Ramsey, and J. R. Zacharias, Phys. Rev. 56, 728 (1939).
[6] W. Pauli, *Handbuch der Physik* (Verlagsbuchhandlung, Julius Springer, 1933), Vol. 24/1, p. 221.

His arithmetic shows that he used a plus rather than a minus sign before the correction term in (1′). In the application to the deuteron this makes little difference because the Pauli parts of the moments of proton and neutron are nearly equal and opposite. According to (1′) the correction to the sum due to the Pauli parts is in nuclear Bohr magnetons

$$-\tfrac{1}{3}(1.79-1.93)\langle T/Mc^2\rangle=+0.05\langle T/Mc^2\rangle.$$

Even for the high value $\langle T/Mc^2\rangle\sim 0.012$ used by Caldirola this correction is only 0.0006.

In Eqs. (1), (1′) the kinetic energy that enters is that of the particles separately and not that of their relative motion. The latter is twice the former.

One can verify (1) by (1′) by a consideration involving no quantum theory. A magnetic doublet of unit length directed at angle θ with respect to line of flight suffers a Lorentz contraction changing its projection on the line of flight by $-[1-(1-v^2/c^2)^{\frac{1}{2}}]\cos\theta$ which gives a change $\cong-(v^2/2c^2)\cos^2\theta$ along the doublet's axis. Multiplying numerator and denominator by M one obtains Eq. (1) and averaging over θ one finds Eq. (1′). The quantity T is again seen to be the kinetic energy of an individual particle. Partly for this reason the number 0.012 is too high for $\langle T/Mc^2\rangle$.

3. The relativistic corrections to the Dirac part of the moment depend on transformation properties of the binding energy. The expression for this part of the moment is a sum of contributions containing ψ_1, ψ_2 and their complex conjugates as factors. It is necessary, therefore, to know ψ_1, ψ_2 in the second rather than only in the first approximation. The correction factor

$$1-(2/3)\langle T/Mc^2\rangle \tag{3}$$

has been obtained by Margenau who extended previous calculations[4] to non-inverse square fields of force. This factor corresponds to s states in central fields on the assumption of an interaction of the four vector type. Its difference from unity can be broken down into parts as follows: (a) $-\langle T\rangle/2Mc^2$ due to the effect of ψ_1, ψ_2 on normalization, (b) the same amount as in (a) is contributed by the first correction term to $1/(E-V+Mc^2)$ where V is the potential energy, (c) a term in rdV/dr contributes $\langle T\rangle/3Mc^2$.

For a particle moving in a central scalar[7] field U one can make a similar calculation. The sign of the function U will be chosen so that it will replace V in the non-relativistic approximation. The combination Mc^2+U occurs as a unit everywhere. A breakdown of the difference of the correction factor from unity appears as a consequence as follows: (a) unchanged from previous case, (b) a factor $2Mc^2/(E+U+Mc^2)\cong 1+(T-2W)/2Mc^2$ contributes $\langle T-2W\rangle/2Mc^2$; here W is $E-Mc^2$, (c) in place of rdV/dr there occurs $-rdU/dr$; the sign of this term is reversed in comparison with the four-vector equation. The factor becomes

$$1-\langle W+(T/3)\rangle/Mc^2. \tag{4}$$

Here there is partial cancellation of W and $T/3$. For $W=-2.17$ Mev and $\langle T/Mc^2\rangle=0.012$ one obtains $0.0023-0.0040=-0.0017$ for the correction term in Eq. (4). When combined with the correction to the Pauli part this gives $-0.0017+0.0006=-0.0011$ for the correction to the sum of the moments and is on the limit of experimental error.

4. The value which must be used for W in Eq. (4) is subject to question. A central field was assumed, contrary to reality. It would be better to use the approximately relativistic equations[8] to order v^2/c^2. The choice of available equations is considerable, however. Instead one can use a model in which the proton and neutron move in the same central field and do not interact with each other. For this W is $-2.17/2=-1.08$ Mev and $F(r)=$radial function of relative motion times r can be correlated with the corresponding quantity F_m for the model by requiring agreement of

$$\begin{aligned}&\frac{d^2F}{dr^2}+\frac{M}{\hbar^2}[W-V(r)]F=0,\\ &\frac{d^2F_m}{dr_m^2}+\frac{2M}{\hbar^2}\left[\frac{W}{2}-\frac{1}{2}V_m(r_m)\right]F_m=0\end{aligned} \tag{5}$$

which give the same characteristic values for W provided

$$V_m(r)=V(r),\quad F_m(r)=F(r). \tag{5′}$$

[7] See reference 6 and W. H. Furry, Phys. Rev. 50, 784 (1936).
[8] G. Breit, Phys. Rev. 51, 248 (1937); 53, 153 (1938).

The model attributes to the proton one-half the kinetic and potential energies of the relative motion of the two particles within the deuteron. The scalar field gives, including the Pauli part,

$$\Delta(\mu_p+\mu_n)=\langle -W_p-0.285T_p\rangle/Mc^2 \quad (6)$$

where p stands for "proton" and μ is the magnetic moment. For a "square well" the kinetic energy of relative motion is

$$T_p+T_n=2T_p=\alpha a(D+W)/(1+\alpha a) \quad (7)$$

with

$$\alpha=(-MW/\hbar^2)^{-\frac{1}{2}}, \quad a=\text{radius of well.} \quad (7')$$

For $a=e^2/mc^2$ and $D=21$ Mev one finds, from Eq. (7), $2T_p=14.4mc^2$ corresponding to $T_p=0.0039Mc^2$, and Eq. (6) gives $\Delta(\mu_p+\mu_n)=0.0000$. The four-vector field gives

$$\Delta(\mu_p+\mu_n)=(-0.67+0.05)T_p/Mc^2 = -0.62\times 0.0039=-0.0024.$$

This is also very small.

The model is not believed in as a reality. It has properties in common, however, with Eq. (18.1) of the first paper[8] and gives[7] the inverted fine structure of nuclear levels in agreement with experiment.

5. For a "square well" interaction and range $a=e^2/mc^2$ the proton and neutron spend 45 percent of the time within $r<a$. The additivity of nuclear magnetic moments indicates, therefore, either the retention of individuality by the proton and neutron within the range of force, or a mistaken idea regarding the range of force or a compensation of changes in the moments.

6. It is not intended to say that the relativistic corrections are negligible, but it is believed that the variations in these corrections due to the sensitivity of the Dirac part of the moments to assumptions regarding the interaction between particles have been shown to be so large as to make estimates of the corrections uncertain to within practically their whole magnitude.

Financial support of the Wisconsin Alumni Research Foundation and of the Office of Naval Research is gratefully acknowledged.

PHYSICAL REVIEW VOLUME 71, NUMBER 7 APRIL 1, 1947

Note on the Calculation of Angular Distributions in Resonance Reactions

G. BREIT* AND B. T. DARLING*
University of Wisconsin, Madison, Wisconsin

(Received December 23, 1946)

This note is concerned with pointing out some labor saving devices in the calculation of transformation coefficients arising in the composition of angular momenta which are needed for the calculation of angular distributions of disintegration products arising in nuclear resonance reactions.

THE angular distribution of disintegration products in resonance reactions has been treated theoretically by several authors.[1] The present note is concerned with pointing out a few labor saving devices in the technique of making the necessary calculations of transformation coefficients arising in the representation of the coupling of angular momenta by means of wave functions. It is realized that these coefficients are written out for the general case in Wigner's book on the applications of Group Theory to Quantum Mechanics. The formulas applicable to the general case are rather lengthy, and it is often desirable to have some other way of checking the results or of obtaining them.

Resonance reactions involve transitions from the initial state of the colliding particles *via* one or more states of the compound nucleus to the final state of the disintegration products. The nature of the disintegration products, their yield, and angular distribution depend upon the proper-

*Now at Yale University.

[1] E. Gerjuoy, Phys. Rev. 58, 503 (1940); C. L. Critchfield and E. Teller, Phys. Rev. 60, 10 (1941); E. Eisner, Phys. Rev. 65, 85 (1944).

ties of the intermediate states of the compound nucleus and consequently also on the nature and state of the colliding particles as well as of the disintegration products. The angular distributions depend on the combined effect of products of matrix elements, each product consisting of two factors corresponding respectively to transitions from an initial state to an intermediate one, and to a subsequent transition to a final state. Some of the products have to be added to each other, and the square of the absolute value of the sum enters the formulas for the differential collision cross sections. A knowledge of the relative signs of the transformation coefficients representing the coupling of angular momenta is needed in some cases, and the calculations can be laborious. By applying two general theorems about properties of transformation coefficients of angular momenta, it is possible to shorten the work. The present note is concerned with an explanation of how this can be done.

Usually the beam of incident particles is unpolarized, i.e., their spins $\mathbf{i}_1$ and $\mathbf{i}_2$ are independently and randomly oriented in space. The initial state is described by a modified plane wave in which the spin states are a statistical mixture with equal probabilities and without correlation of the spin states of the individual particles. If ψ_m^l are angular wave functions of the orbital motion for angular momentum $l\hbar$ and projection $m\hbar$ along z, and if the z axis is chosen in the direction of the incident plane wave, then only the components with $m=0$ will occur in the initial state.

The angular wave functions Ψ_M^j of the compound nucleus having angular momentum $j\hbar$, projection $M\hbar$, are linear combinations of $\psi_m^l\psi_{m_1}^{i_1}\psi_{m_2}^{i_2}$, with $\mathbf{l}+\mathbf{i}_1+\mathbf{i}_2=j$, and $m+m_1+m_2=M$. The transition probabilities from initial to intermediate state require the knowledge of the transformation coefficients $(\psi_0^l\psi_{m_1}^{i_1}\psi_{m_2}^{i_2}, \Psi_M^j)$. The evaluation of these quantities is the principal concern of this note.

First of all one can compound the individual spins $\mathbf{i}_1+\mathbf{i}_2=\mathbf{s}$ and use the compound spin states ψ_ν^s instead of $\psi_{m_1}^{i_1}\psi_{m_2}^{i_2}$. The transformation coefficients that are needed are $(\psi_0^l\psi_\nu^s, \Psi_M^j)$ instead of $(\psi_0^l\psi_{m_1}^{i_1}\psi_{m_2}^{i_2}, \Psi_M^j)$. This may be done on account of the following theorem.

(I) A statistical mixture without correlation and with equal probabilities of states having definite projections of two uncoupled spins along an axis is also a statistical mixture in the same sense of states corresponding to compounded spins with definite projections along the same axis.

This theorem is a special case of a theorem proved by J. v. Neumann.[2] It can be proved very simply without direct reference to the more general discussion of v. Neumann. The proof may, for instance, be given as follows:[3] Let u_i, v_j be two complete, orthogonal sets of characteristic functions for a physical system. In the present case the u_i, v_j correspond, respectively, to decoupled and coupled spin states. A statistical mixture of the u_i can be represented by

$$\Sigma_i \epsilon_i u_i,$$

where the ϵ_i are statistical variables subject to the condition,

$$\langle \epsilon_i^* \epsilon_l \rangle = \delta_{il}/N.$$

The sign $\langle\ \rangle$ indicates a statistical average over the statistical mixture, and δ is the Kronecker δ, while N is the total number of states. One can express the u_i in terms of the v_j by means of a unitary transformation

$$u_i = \Sigma_j S_{ij} v_j.$$

The statistical mixture in terms of the v_j is, therefore

$$\Sigma_j \epsilon_j' v_j$$

with

$$\epsilon_j' = \Sigma_i \epsilon_i S_{ij}$$

so that

$$\langle \epsilon_j'^* \epsilon_k' \rangle = \Sigma_{i,l} S_{ij}^* S_{lk} \langle \epsilon_i^* \epsilon_l \rangle = \frac{1}{N} \Sigma S_{ij}^* S_{ik} = \delta_{jk}/N.$$

The statistical mixture of the states u is thus also a statistical mixture of the states v.

Next, to evaluate $(\psi_0^l\psi_\nu^s, \Psi_M^j)$ it is not necessary to calculate the complete set of normalized wave functions Ψ_M^j for the composition of the angular momentum $\mathbf{l}+\mathbf{s}=\mathbf{j}$. To see this, use is made of the following theorem (proof in Appendix).

[2] J. v. Neumann, *Mathematische Grundlagen der Quantenmechanik* (Springer, Berlin, 1932), p. 183.

[3] It will be understood from now on that the words "statistical mixture" stand for "statistical mixture with equal probabilities and without correlation."

(II) Two angular momenta **l**, **s** are compounded to give a resultant **j**. Let $P(j, m_j; m_l)$ be the probability of **l** having a projection m_l along the z axis for a state in which the absolute value of the resultant is j, and its projection on the z axis is m_j. The theorem states that

$$\Sigma_{m_j} P(j, m_j; m_l) = (2j+1)/(2l+1)$$

independently of the value of m_l.

Thus if we can obtain the relative values of $(\psi_0{}^l\psi_\nu{}^s, \Psi_M{}^j)$, we need only determine a common proportionality factor by normalizing the sum of the squares to $(2j+1)/(2l+1)$.

The relative values of $(\psi_0{}^l\psi_\nu{}^s, \Psi_M{}^j)$ can be obtained simply from the symbolic ξ, η method[4] for combining angular momentum wave functions by calculating only those terms containing $\xi_1{}^l\eta_1{}^l(m=0)$. The ξ, η method for the composition of angular momenta $\mathbf{l}+\mathbf{s}=\mathbf{j}$ works as follows: One expands the expression

$$\psi = (-\xi_1\eta_2+\xi_2\eta_1)^{l+s-j} \times(-b\xi_1+a\eta_1)^{l-s+j}(-b\xi_2+a\eta_2)^{s-l+j}$$

in powers of the ξ and η. One then replaces

$$\left[\binom{2l}{l+\mu}\right]^{\frac{1}{2}}\xi_1{}^{l+\mu}\eta_1{}^{l-\mu} \text{ by } \psi_\mu{}^l,$$

and

$$\left[\binom{2s}{s+\nu}\right]^{\frac{1}{2}}\xi_2{}^{s+\nu}\eta_2{}^{s-\nu} \text{ by } \psi_\nu{}^s.$$

Except for a normalizing factor the desired $\Psi_M{}^j$ is then the coefficient of

$$(-)^{j+M}\left[\binom{2j}{j+M}\right]^{\frac{1}{2}}a^{j-M}b^{j+M}$$

in the expansion of ψ.

Example. The procedure will now be illustrated by means of an example. Protons $(i_1=\frac{1}{2})$ are incident on Li^7 $(i_2=\frac{3}{2})$ and give rise to a nuclear disintegration with the emission of two alpha-particles. It is probable that the relative orbital angular momentum before disintegration is $l=1$, and it will be assumed besides that the angular momentum of the compound state is $j=2$ which can be obtained by compounding the spins $i_1=\frac{1}{2}$, $i_2=\frac{3}{2}$ to a resultant $s=\frac{1}{2}+\frac{3}{2}=2$ and compounding $s=2$ with $l=1$ to a resultant $j=2$. One has $l+s-j=1$, $l-s+j=1$, $s-l+j=3$, and the symbolic ψ is

$$\psi = (-\xi_1\eta_2+\xi_2\eta_1)(-b\xi_1+a\eta_1)(-b\xi_2+a\eta_2)^3$$
$$= -\xi_1\eta_1(a\eta_2+b\xi_2)(-b\xi_2+a\eta_2)^3+\cdots.$$

In the symbolic ψ the product $\xi_1\eta_1$ represents within a factor $(\psi_\mu{}^l)_{l=1,\mu=0}$. The product $(a\eta_2+b\xi_2)\times(-b\xi_2+a\eta_2)^3$ gives the coefficients with which the functions $\psi_\nu{}^s$ occur in the $\Psi_M{}^j$ by means of the following replacements:

$\xi_1\eta_1 = u_0 =$ orbital motion function with $l=1$, $\mu=0$

$$d_\nu = (\psi_\nu{}^s)_{s=2}; \quad d_2=\xi_2{}^4, \quad d_1=(4)^{\frac{1}{4}}\xi_2{}^3\eta_2,$$
$$d_0=(6)^{\frac{1}{4}}\xi_2{}^2\eta_2{}^2, \quad d_{-1}=(4)^{\frac{1}{4}}\xi_2\eta_2{}^3, \quad d_{-2}=\eta_2{}^4.$$

To obtain a $(\Psi_M{}^j)_{j=2}$ one needs the coefficients of

$$b^4, \quad -(4)^{\frac{1}{4}}ab^3, \quad (6)^{\frac{1}{4}}a^2b^2, \quad -(4)^{\frac{1}{4}}a^3b, \quad a^4$$

for

$$M=2, \quad 1, \quad 0, \quad -1, \quad -2,$$

and one rearranges the part of ψ containing $\xi_1\eta_1$ into the form

$$\psi = u_0[b^4d_2+\tfrac{1}{2}(-(4)^{\frac{1}{4}}ab^3)d_1 - \tfrac{1}{2}(-(4)^{\frac{1}{4}}a^2b)d_{-1}-a^4d_2]+\cdots.$$

The $(u_0d_M, \Psi_M{}^j)$ are within a proportionality factor the coefficients $1, \frac{1}{2}, -\frac{1}{2}, -1$ occurring in the square brackets. One has thus

$M=$	2	1	0	−1	−2
$(u_0d_M, \Psi_M{}^j)$	$+N$	$+\frac{N}{2}$	0	$-\frac{N}{2}$	$-N$

To determine N^2 one applies Theorem II and finds

$$N^2+\frac{N^2}{4}+\frac{N^2}{4}+N^2=\frac{2j+1}{2l+1}=5/3; \quad N=(\tfrac{2}{3})^{\frac{1}{2}}.$$

The desired transformation coefficients are with-

[4] H. Weyl, *Gruppentheorie und Quantenmechanik* (S. Hirzel, Leipzig, 1928), pp. 154, 159, 193, 261; H. A. Kramers, Proc. Amst. Akad. Sci. **33**, 953 (1930); E. Wigner, *Gruppentheorie und ihre Anwendung auf die Quantenmechanik der Atomspektren* (Friedr. Vierveg & Sohn, Braunschweig, 1931), Chaps. XV, XVII; B. L. van der Waerden, *Die Gruppentheoretische Methode in der Quantenmechanik* (Springer, Berlin, 1932), Section 18.

in a sign which is immaterial here

M	2	1	0	−1	−2
$(\psi_0{}^1\psi_M{}^{(2)}, \Psi_M{}^j)$	$+(\frac{2}{3})^{\frac{1}{2}}$	$+\frac{1}{2}(\frac{2}{3})^{\frac{1}{2}}$	0	$-\frac{1}{2}(\frac{2}{3})^{\frac{1}{2}}$	$-(\frac{2}{3})^{\frac{1}{2}}$

The authors would like to acknowledge their indebtedness to the Office of Naval Research and to the Wisconsin Alumni Research Foundation for financial support.

APPENDIX

Proof of Theorem II

The notation and the general system of Wigner's book[4] are employed here. If

$$\Psi_M{}^j = \Sigma_\mu C_{\mu, M-\mu}{}^j \psi_\mu{}^l \psi_{M-\mu}{}^s$$

is an irreducible state of the angular momentum $\mathbf{j}=\mathbf{l}+\mathbf{s}$, then the matrix

$$X_{\mu'\mu} = \Sigma_{M,\nu}(\psi_{\mu'}{}^l\psi_\nu{}^s, \Psi_M{}^j)(\Psi_M{}^j, \psi_\mu{}^l\psi_\nu{}^s) = X_j{}^l\delta_{\mu'\mu}$$

is diagonal, and

$$X_j{}^l = (2j+1)/(2l+1).$$

Let $D^{(l)}(R)_{\mu'\mu}$ be the irreducible representation induced by the rotation group on $\psi_\mu{}^l$, and similarly for $D^{(s)}(R)_{\nu'\nu}$ on $\psi_\nu{}^s$, and $D^{(j)}(R)_{M'M}$ on $\Psi_M{}^j$. The operator P_R represents the effect of the rotation and is such that

$$P_R\psi_\mu{}^l = \Sigma_{\mu'} D^{(l)}(R)_{\mu'\mu}\psi_{\mu'}{}^l$$

and similarly for $\psi_\nu{}^s$, $\Psi_M{}^j$. Then,

$$X_{\mu'\mu} = P_R X_{\mu'\mu} = \Sigma_{(M,\nu,\mu'',\nu'',M',M'',\mu''',\nu''')} D_{\mu''\mu'}{}^{(l)*} D_{\nu''\nu}{}^{(s)*}(\psi_{\mu''}{}^l\psi_{\nu''}{}^s, \Psi_{M'}{}^j) D_{M'M}{}^{(j)} D_{M''M}{}^{(j)*}$$
$$\cdot(\Psi_{M''}{}^j, \psi_{\mu'''}{}^l\psi_{\nu'''}{}^s) D_{\mu'''\mu}{}^{(l)} D_{\nu'''\nu}{}^{(s)}$$

where R is not explicitly indicated and * means the conjugate complex. Now,

$$\Sigma_\nu D_{\nu''\nu}{}^{(s)*} D_{\nu'''\nu}{}^{(s)} = \delta_{\nu''\nu'''}, \quad \Sigma_M D_{M'M}{}^{(j)} D_{M''M}{}^{(j)*} = \delta_{M'M''},$$

hence

$$X_{\mu'\mu} = P_R X_{\mu'\mu} = \Sigma_{M,\nu,\mu'',\mu'''} D_{\mu''\mu'}{}^{(l)*}(\psi_{\mu''}{}^l\psi_\nu{}^s, \Psi_M{}^j)(\Psi_M{}^j, \psi_{\mu'''}{}^l\psi_\nu{}^s) D_{\mu'''\mu}{}^l$$
$$= \Sigma_{\mu'',\mu'''} D^l(R)_{\mu'\mu''}{}^{-1} X_{\mu''\mu'''} D^l(R)_{\mu'''\mu}$$

for all R. According to Schur's lemma the matrix $(X_{\mu'\mu})$ must be a multiple of the unit matrix,

$$X_{\mu'\mu} = X_j{}^l\delta_{\mu'\mu}.$$

Furthermore,

$$\Sigma_\mu X_{\mu\mu} = 2j+1 = (2l+1)X_j{}^l$$

so that

$$X_j{}^l = (2j+1)/(2l+1).$$

It is only needed to make the further observation that $(\psi_\mu{}^l\psi_{M-\mu}{}^s, \Psi_M{}^j) = C_{\mu, M-\mu}{}^j$, and that

$$\Sigma_M |C_{\mu, M-\mu}{}^j|^2 = X_{\mu\mu} = X_j{}^l = (2j+1)/(2l+1)$$

to see that Theorem II holds.

The *K* X-Ray Absorption Edge of Silicon

VOLA P. BARTON, *Goucher College, Baltimore, Maryland*

AND

GEORGE A. LINDSAY, *University of Michigan, Ann Arbor, Michigan*

(Received December 26, 1946)

The *K* absorption edge of silicon was measured in silicon metal and in the following compounds: quartz, sodium silicate, muscovite, biotite, phlogopite, lepidolite, carborundum, and an organic compound, mono ethyl siloxane. It was found that the quartz, sodium silicate, and the four micas all gave approximately the same wave-length for the absorption edge, namely, about 6700 x.u., while for the siloxane the value was 6706 x.u., and for the silicon metal and for carborundum it rose as high as 6718 x.u. It is to be noted that the surroundings of the silicon atom are the same for all those compounds which gave an edge at 6700 x.u. In the organic compound one oxygen has probably been replaced by the group C_2H_5, while for carborundum and for silicon metal all four oxygens of the tetrahedral group surrounding the silicon atom have been replaced by carbon and by silicon, respectively.

THE *K* absorption edge of silicon in the x-ray spectrum has not been measured very thoroughly up to the present time. In 1920 Fricke[1] photographed and measured the *K* edges of several elements from Na(11) to Cl(17). Although he found the edge for the lighter elements Na(11), Mg(12), and Al(13), the edge of silicon failed to appear. Fricke attributed the difficulty to the presence of an *M* emission line of tungsten which lies in the immediate neighborhood of the silicon edge. The undesirable tungsten line, however, which was caused by the tungsten filament of the x-ray tube, is in the first order, and hence should be absorbed the same as any other radiation of the continuous spectrum. Realizing this fact, Lindh,[2] in 1925, showed that the absorption edge could be observed on the short wave-length side of the broad emission line of tungsten. Lindh used screens of silicon metal and several compounds. His values were:

Substance	λ of edge in x.u.
Si	6731.0
SiO_2	6707.5
Na_2SiO_3	6707.3
K_2SiO_3	6707.7

The only other measurement which has come to the attention of the authors was by Deodhar[3] in 1930. In his work the absorption occurred in the quartz crystal used as a grating, while Lindh used absorbing screens with a gypsum crystal as reflector. Deodhar's value for the Si *K* edge was 6705 x.u. Neither of these workers made any correction for refraction of the x-rays in the reflecting crystal. In fact, at the time when these measurements were made the indices of refraction were not well known and it was not customary to attempt to make such corrections. The correction, however, amounts to several x.u.—in some of the present work to as much as 10 x.u.—and hence it should be made to compare works of different authors as well as to obtain a better absolute value.

In the present work both the methods of absorption in the crystal and in absorbing screens were used. Since in either method the grating space of the reflecting crystal must be more than one half the wave-length to be measured, this requirement immediately rules out the possibility of the first method for those substances which do not have a large enough grating space. The grating spaces of the cleavage faces of the micas are all large enough and to spare, while in quartz the prism face has a value of *d* about 4246 x.u., and hence is qualified to reflect a wave-length of 6700 x.u. The rhombohedral face, although usually better than the prism face, has a *d* of about 3336 x.u. Since this is less than one half the wave-length desired, only the prism face of quartz can be used. Obviously the first method also requires a fairly good crystal. In view of these requirements, quartz and the micas were used as

[1] Hugo Fricke, Phys. Rev. 15, 202 (1920).
[2] Axel E. Lindh, Zeits. f. Physik 31, 210 (1925).
[3] G. B. Deodhar, Nature 125, 777 (1930).

gratings, and so gave the silicon edge without any further absorber, while for sodium silicate, carborundum, the siloxane, and silicon metal a gypsum crystal was used as reflector with absorbing screens of the substance desired. A very fine grade of carborundum was moistened, then allowed to dry on a thin collodion membrane, thus forming the carborundum absorber. Finely powdered sodium silicate and silicon were placed wet on the face of the gypsum crystal in a very thin layer, while the mono-ethyl siloxane was dissolved in isopropyl ether and a few drops of the liquid placed on the surface of water. The thin rubbery layer thus obtained could then be used as an absorbing screen. The radius of the spectrometer was 180.2 mm and the photographic method was used throughout.

As reference line with the micas we used the $K\beta_1$-line of copper in the 5th order which came on during the exposure without moving the film. For the other substances the $K\alpha_1$-line of copper in the 4th order was used, the film being turned through an accurately determined angle between the exposure of the reference line and the exposure of the edge. With the latter procedure the method of calculating the wave-length of the edge was as follows. From the known wave-length of the reference line the actual Bragg angle θ was calculated by using the grating space for the 4th order as determined by Larsson[4] and given by Siegbahn in his *Spektroskopie der Röntgenstrahlen*. Then the angle through which the plate was turned between the exposures for the reference line and the edge was added to 2θ, thus giving the Bragg angle corresponding to the point in the spectrum where the reference line lay while the edge was being photographed. Then the angle corresponding to the position of the edge was calculated by subtracting the angle at the crystal whose arc is the distance on the film from the edge to the reference line. When the Bragg angle for the edge is thus found the grating space for the first order is used to calculate the wave-length of the edge. By thus using the two values of the grating space in the different orders only correction for normal refraction in the crystal is made.

Some trials were made of the effect of anomalous refraction on the position of the edge for

[4] Larsson, Uppsala Univ. Årsskrift 1929.

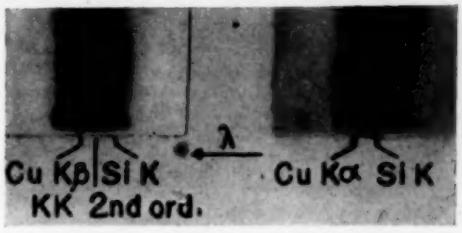

FIG. 1. *K* absorption edge of silicon. Muscovite, left; carborundum, right.

those reflecting crystals which contained silicon. Finely powdered quartz was put on the face of a gypsum crystal and the wave-length of the edge so obtained was compared with that from the quartz as a reflecting crystal. No difference between the two could be definitely established, and since a calculation[5] of the anomalous refraction including the effect of absorption shows that the anomalous refraction is rather small, it was neglected entirely and only the normal refraction was used as indicated above.

The grating space of muscovite has been determined accurately; those of the other micas only approximately. The constants for biotite, phlogopite and lepidolite were accordingly measured with the following results:

Crystal	*d* (x.u.)
Biotite	10006
Phlogopite	10015
Lepidolite	9923

In determining these values the Cu $K\alpha_1$-line was photographed in different orders from the third to the sixth. Since the error in the observed *d*, due to refraction, is only $\frac{1}{9}$ as much in the third order as in the first order, and still less in higher orders, the values obtained were considered to be those for the high orders, and the value for the first order was assumed to be smaller in the same proportion as that found accurately for muscovite by Larsson. This procedure is justified from the consideration that the index of refraction is much the same for all the micas, and because in the reference method used an error in the value of *d* of as much as 10 x.u. would cause a corresponding error in the wave-length of the edge of only 0.3 x.u.

Figure 1 shows two absorption edges, one

[5] See Compton and Allison, *X-Rays in Theory and Experiment*, page 294.

TABLE I. Wave-lengths of the K absorption edge of silicon in various substances.

Substance	λ of edge (x.u.)	Crystal used
Muscovite	6703.0	Muscovite
Phlogopite	6703.2	Phlogopite
Biotite	6703.7	Biotite
Lepidolite	6699.0	Lepidolite
SiO_2	6702.7	Quartz
Na_2SiO_3	6698.4	Gypsum
Si Metal	6715.2	Gypsum
SiC	6717.9	Gypsum
$C_2H_5SiO_{1.5}$	6706.2	Gypsum

taken by a muscovite crystal, the other by a screen of carborundum, using a gypsum crystal. At least three good films were taken for each substance used.

The results of the measurements of the K absorption edge of silicon are set forth in Table I. Each value is the average of at least three good films for that particular substance. The results are corrected for normal refraction in the various crystals used in the manner described above. It will be observed that the wave-length of the edge is nearly the same for all the micas, quartz, and sodium silicate, although for lepidolite it is unexpectedly lower than for the other micas. An extra number of trials was made for lepidolite with independent adjustments of the crystal, but the results had persistently the lower value.

When one considers the crystal structure of the different substances it is easy to see why the first six should be so nearly alike. In all of them the silicon atom is considered to be at the center of a tetrahedron having an oxygen atom at each of the four corners. Any other atoms in the molecule should have little influence on the silicon energy levels, hence one might expect little difference in the wave-length of the edge. In the silicon metal there are also tetrahedrons, but each silicon atom at the center is surrounded by four other silicon atoms instead of oxygens. In carborundum the silicon is surrounded by four carbon atoms. The silicon or carbon atoms would disturb the energy levels of the silicon atoms less than the more negative oxygen atoms would. The result is some 17 x.u. greater wave-length for the silicon metal and the carborundum.

The structure of the silicone is not known, but the formula indicates that one of the oxygen neighbors has been replaced by the ethyl group C_2H_5 so that one might expect the wave-length of the edge to lie between that for the micas and that for the silicon metal or carborundum, but nearer that for the micas. The table shows agreement with this assumption. The difference in the values of the edge for the micas and for silicon or carborundum is about one electron volt, while between the micas and the siloxane it is about $\frac{1}{3}$ volt. This difference in the position of the edge really represents the variation of the difference between the initial and final levels concerned in the absorption process when a change occurs in the neighbors of the silicon atom.

No attempt was made to investigate the fine structure of the edge although such structure could be observed, especially with the carborundum, where it consisted principally of two strong white lines.

Other silicones containing a different proportion of oxygen atoms might well give more information concerning the dependence of the position of the absorption edge on the neighbors of the silicon atom.

Forty-Three Day $_{48}Cd^{115}$

LEO SEREN,* DON ENGELKEMEIR, WILLIAM STURM, H. N. FREIDLANDER, AND S. TURKEL
*Metallurgical Laboratory,** University of Chicago, Chicago, Illinois*

(Received December 24, 1946)

A 43-day isotope of cadmium has been discovered while irradiating cadmium with slow neutrons. The radiation consists of β-rays of energy $\sim$1.5 Mev, and with approximately one 0.5-Mev γ-ray per disintegration. By means of chemical separations, the radio element was identified as cadmium, and the mass assignment to $_{48}Cd^{115}$ was made by a fast neutron $In^{115}(n, p)Cd^{115}$ reaction.

I. PREVIOUS INVESTIGATIONS OF 43-DAY CADMIUM

THE radioactive cadmium isotopes have been studied by several investigators in the past,[1] but only Cork and Lawson[2] have mentioned a long period, beta-emitting Cd isotope. They bombarded cadmium with deuterons and from the chemically separated cadmium fraction found a 40-day activity after the short periods had decayed. They suggested that this negative particle emitter was caused by Cd^{115} or Cd^{117} on the basis of other known isotopes.

At the Argonne Laboratory the radioactivity induced in cadmium by pile neutrons was part of a survey of thermal-neutron-induced activities.[3] In addition to the known periods of 3.75 hr and 2.5 days, a very short period of approximately 2 minutes and a long period of 43 ± 3 days were found. The latter two periods have not previously been found with slow neutron irradiation on cadmium.[4] This paper describes the 43-day period and method of isotopic assignment.

II. CHEMICAL IDENTIFICATION OF LONG PERIOD ACTIVITY AS CADMIUM

The cadmium used in this experiment was commercial strip cadmium so that a small amount of indium impurity[5] would give a 48-day activity which could be mistaken for the observed activity in cadmium (see Fig. 1). Furthermore, the 48-day indium might possibly be produced with slow neutrons on cadmium by a chain of activities. Since 3.75-hr. Cd (from slow neutrons on cadmium) produces 117-min. In, and 2.5-day Cd (also from slow neutrons on cadmium) produces 4.1-hr. In, it seemed reasonable that a third activity from slow neutrons on cadmium could give 48-day In.

To test both of these possibilities chemical separations were made. The cadmium metal

---

* Present addresses of the authors: Leo Seren, General Electric Research Laboratory, Schenectady, New York; Don Engelkemeir, William Sturm, and H. N. Freidlander, University of Chcago, Chicago, Illinois; S. Turkel, Nuclear Engine Powered Aircraft, Fairchild Engine and Airplane Corporation, P.O. Box 415, Oak Ridge, Tennessee.

** This document is based on work done in July, 1943 and performed under Contract No. W-7401-eng-37 for the Manhattan Project at the Argonne National Laboratory. The information covered in this document will appear in Division IV of the Manhattan Project Technical Series as part of the contribution of the Argonne National Laboratory.

[1] See G. T. Seaborg's "Artificial radioactivity," Rev. Mod. Phys. 16, 1 (1944).

[2] J. M. Cork and J. L. Lawson, *Phys. Rev.* 56, 291 (1939).

[3] Cf. L. Seren, H. N. Freidlander, and S. H. Turkel, *Thermal Neutron Activation Cross Sections*, to be published shortly.

[4] Irradiation in the center of the Argonne graphite pile is not strictly a thermal neutron irradiation, but it is practically so for cadmium, atomic No. 48. The spectrum of neutrons in the pile is predominantly thermal and epithermal resonance neutrons, producing (n, γ) reactions. The fission spectrum of neutron energies does have a high energy tail which may extend to 8 Mev, but such high energy neutrons are quite rare. The samples of this experiment were separated from the uranium lumps by a few inches of graphite which reduces even further the number of fast neutrons. Although fast neutrons can cause (n, p) and (n, α) reactions, the potential barrier is quite high for $_{48}Cd$, making these reactions quite improbable. The $(n, 2n)$ reaction requires very high neutron energies, about 8 Mev, so they, too, are quite improbable. The cross sections for the productions of the observed activities in cadmium are:

Half-life	Isotope	Cross section per natural cadmium atom (cf. footnote 3)
2 min.	Cd?	0.05×10^{-24} cm²
3.75 hr.	Cd^{117}	0.1×10^{-24} cm²
2.5 days	Cd^{115}	0.3×10^{-24} cm²
43 days	Cd^{115}	0.04×10^{-24} cm² (may include resonance as well as thermal capture)

These large cross sections leave no doubt that the observed activities were caused by (n, γ) reactions.

[5] The cross section per natural indium atom for the production of 48-day indium with slow neutrons is 2.52×10^{-24} cm², cf. footnote 3. Thus 1.5 percent indium in the thin ($\approx$1 mil) irradiated cadmium strips could account for the activity ascribed to cadmium. A spectrographic report received later showed less than 0.01 percent indium present in the cadmium.

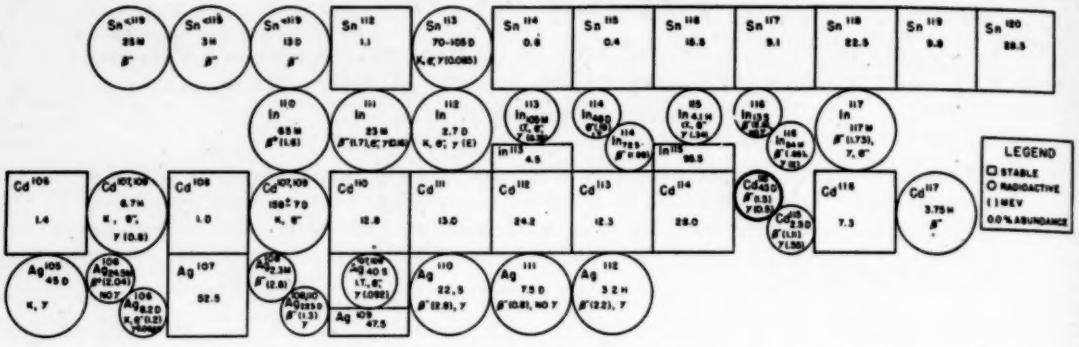

FIG. 1. Partial table of isotopes.

(about two months after irradiation) was dissolved in nitric acid and the indium was then precipitating in an excess of ammonia solution. But the activity remained with the cadmium fraction and did not come down with the indium carrier precipitates. To test the above chemical procedure the following experiments were performed. Cadmium nitrate crystals were irradiated for 10 minutes with pile neutrons and then the indium separated quickly as above. This indium fraction decayed with 2-hr. half-life, hence, it came from the 3.75-hr. cadmium. Next, some more cadmium nitrate crystals were irradiated more strongly and allowed to decay for two days. This indium fraction was then separated and decayed with 4 to 5 hours half-life, hence, it came from 2.5-day cadmium. Thus, the chemical procedure seemed reliable, proving that the 43-day activity was not caused by indium.

There still remained the possibility that the long period activity could be caused by some other impurity in the cadmium metal, such as $_{52}$Te, $_{38}$Sr, $_{51}$Sb, or $_{77}$Ir, which give activities of 32, 55, 60, and 70 days, respectively, when irradiated with slow neutrons. To test this possibility a complete chemical analysis of the cadmium metal was made and the activity remained with the cadmium precipitates and no activity came down with any other precipitates. (This chemical analysis is described at the end of this report.) This proved definitely that the 43-day activity obtained from slow neutrons on cadmium was an isotope of cadmium.

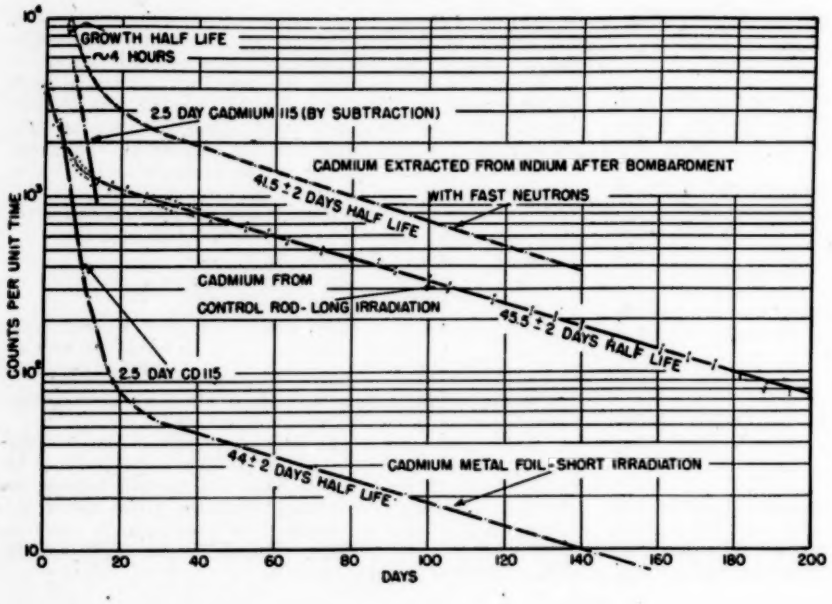

FIG. 2. Cadmium decay curves.

III. HALF-LIFE AND ABSORPTION CURVES

The β-ray activity of three samples[6] of irradiated cadmium metal were followed on a duraluminum Geiger counter for about 150 days, giving half-lives of 44.0±2 days, 41.5±2 days, 45.5±2 days. One of these three samples was followed for 200 days, but tailed off into a longer half-life after 150 days. This is not surprising because no chemical separations were made on these samples of commercial grade cadmium metal. A fourth sample of chemically separated cadmium from indium (bombarded with fast neutrons—see part IV) was followed for 125 days and gave a half-life of 41.5±2 days. These four values give an average value of 43±3 days for the half-life. These decay curves, together with the 2.5 day $_{48}Cd^{115}$ activity, are shown in Fig. 2.

Figure 3 shows one of the β-ray absorption curves taken on a cadmium metal foil (70 mg/cm² thick). The β-rays seem to have a range of ≈640 mg/cm² Al, but to this must be added the self-absorption correction of ≈40 mg/cm² and a counter window plus air correction of 5 mg/cm². The total range of 685 mg/cm² Al corresponds to a maximum β-ray energy of ≈1.5 Mev. This β-ray absorption curve indicates the order of one gamma-ray per beta-particle. Figure 4 shows the absorption of the gamma-rays in Pb which indicates a gamma-ray energy of 0.5 Mev.

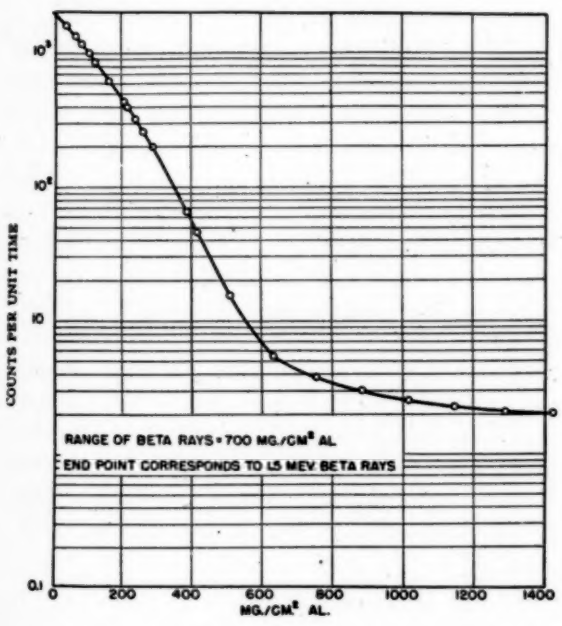

FIG. 3. Absorption of beta-rays from cadmium metal foil showing presence of gamma-rays, 64 days after irradiation with slow neutrons.

[6] One of these samples was prepared from scrapings of the control rod of the pile by Mr. George Miller.

IV. MASS ASSIGNMENT OF $_{48}Cd^{115}$ BY In(n, p)Cd REACTION

Several grams of indium foil were placed on the target assembly of the St. Louis cyclotron of Washington University.[7] Here the indium foil was bombarded with fast neutrons of maximum energy 16 Mev from deuterons on beryllium. After six days of bombardment, totaling 32,730 micro-ampere hours, the foil was shipped to Chicago and a chemical separation of the cadmium made a few days later. The chemically separated Cd precipitate was followed on a beta-counter and showed a 4-hour growth, then a 2.5-day decay and then a 41.5-day decay (see Fig. 2).

Since the chemically separated Cd precipitate represented the end products of an In(n, p)Cd reaction, the 4-hour growth was interpreted as the In^{115} daughter coming back into equilibrium with its 2.5-day Cd^{115} parent. (See Fig. 1.) Also the 43-day Cd activity was thus limited to either Cd^{113} or Cd^{115} because of the two stable isotopes In^{113} and In^{115}.

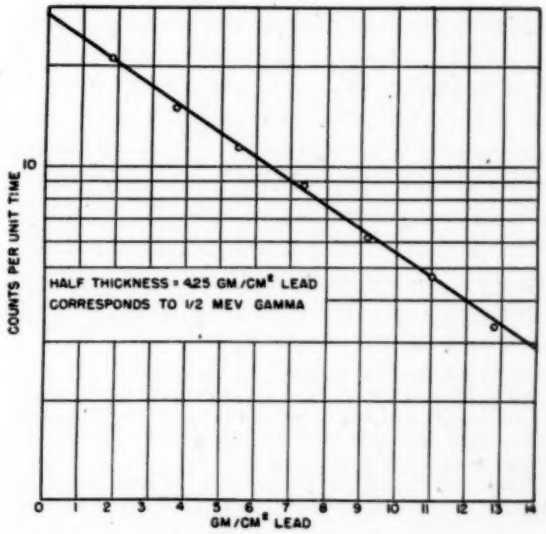

FIG. 4. Absorption of gamma-rays from cadmium metal foil, 64 days after irradiation with slow neutrons.

[7] The assistance of Mr. Harry Fulbright is gratefully acknowledged.

The cyclotron bombardment intensity was logged hourly, so that from this data and the ratio of the initial intensities, it was possible to calculate the ratio of the saturated activities of the 2.5-day and 43-day half-lives. This was found to be 1.1 for the cadmium precipitate from indium.

Since indium has only two stable isotopes, In^{113} and In^{115}, and these are rather similar, the cross section for the fast neutron (n, p) reactions for these two isotopes should be of the same order of magnitude. But the natural abundance is 4.5 percent for In^{113} and 95.5 percent for In^{115}. Thus if the 2.5-day and 43-day activity both came from $In^{115}(n, p)Cd^{115}$ the ratio of the saturated activities should be unity. Actually observed ratio was quite close to this, being 1.1. On the other hand, if the 43-day activity came from $In^{113}(n, p)Cd^{113}$, the ratio of 2.5-day to 43-day saturated activities should be $95.5/4.5 = 21$, which is a different order of magnitude from the observed ratio. The 2.5-day Cd activity has been definitely assigned to $_{48}Cd^{115}$ by Goldhaber, Hill, and Szilard.[8] Thus it seems reasonable to assign both the 2.5-day and the 43-day activities to isomeric states of $_{48}Cd^{115}$.

V. BRANCHING RATIO OF $_{48}Cd^{115}$

For two of the cadmium metal samples irradiated with slow neutrons,[9] the ratio of 2.5-day and 43-day saturated activities could be computed as above. The ratios turned out to be 5.5 and 5.2. (The difference can be ascribed to experimental error.) Thus for slow neutron formation of $_{48}Cd^{115}$ the branching ratio is about $\frac{5}{6}$ for the 2.5-day activity and only about $\frac{1}{6}$ for the 43-day activity. This indicates that the 43-day activity is somewhat forbidden and is consistent with the fact that the ground state of In^{115} has a high spin of 9/2. Also the 2.5-day activity decays to 4.5-hour In^{115*} which seems to have a small spin.[10]

VI. CHEMICAL ANALYSIS OF CADMIUM

The cadmium metal sample was dissolved in HNO_3 and precipitated in 6N-H_2SO_4 with H_2S. The following elements would be precipitated completely—carriers were added: Ag^{+}, As^{+3}, Au^{+3}, Bi^{+3}, Cu^{+2}, Hg^{+2}, Pd^{+4}, Sb^{+3}, Se^{+4}, Sn^{+4}, Te^{+4}, Pt^{+4}, and Pb^{+2} which would precipitate as $PbSO_4$. The following would precipitate incompletely, and no carriers were added for them, except that As and Te carrier was added in the lower valence state. As^{+5}, Ir^{+4}, Mo^{+6}, Os^{+4}, Re^{+7}, Rh^{+3}, Ru^{+4}, Te^{+6}. The cations Cd^{+2}, Se^{+6}, In^{+3} would not precipitate at all.

From the H_2S precipitate the activity on a standard geometry was 0 ± 5 c/m. The supernatant liquid was then made $\frac{1}{2}N$ in H_2SO_4 and again precipitated with H_2S. This brings down the Cd^{+2}, Se^{+6}, and In^{+3}. The activity on the standard geometry was ≈ 1400 c/m. Next, $In(OH)_3$ was precipitated by NH_4OH and this gave ≈ 4 c/m. One-half of the CdS was then dissolved in HNO_3; the solution was then made alkaline with NH_4OH and H_2S passed through. This precipitate gave ≈ 680 c/m, about half of the original activity which was to be expected if all the activity was from the cadmium. Since Ir and Mo would not be precipitated here they are ruled out, leaving Os, Rh, Re, Ru, and Sr. Of these elements, only two have an activity of the same order half-life as 43 days. Re^{184}, 52-days K-capture activity with 1.5-Mev γ's is formed by an $(n, 2n)$ reaction which was highly unlikely in the pile. Sr^{89}, 55 days, with 1.5 Mev β and no γ is formed by slow neutrons. Sr does not precipitate in H_2S at all, but it would be strongly absorbed on $PbSO_4$, hence, would have precipitated in the first step. But since no activity was observed here, the activity could not come from the Sr, leaving only Cd as the carrier of the activity.

[8] M. Goldhaber, R. D. Hill, and Leo Szilard, *Phys. Rev.* **55**, 47 (1939). They showed that the 2.5-day cadmium activity could be produced either by fast (Li+D) neutrons or slow neutrons, and that this 2.5-day Cd activity was actually the parent of 4.5-hour $_{49}In^{115*}$.

[9] Some of this pile neutron activation may have been caused by epi-thermal neutrons, as mentioned in footnote 4.

[10] Cf. page 48 of footnote 8.

The Absorption of Microwaves by Oxygen*

J. H. VAN VLECK
Harvard University, Cambridge, Massachusetts

(Received December 27, 1946)

Even though electrically non-polar, oxygen gas absorbs microwaves because the magnetic moment of the O_2 molecule interacts with electromagnetic fields. The resulting absorption is most pronounced, exceeding 10 db/km, for wave-lengths in the vicinity of $\frac{1}{4}$ cm, for then there is resonance to the spacings in the "rho-type triplet" or spin fine-structure in the $^3\Sigma$ ground state of O_2. There is also a subsidiary resonance near $\frac{1}{7}$ cm, and a non-resonant absorption at long wave-lengths due to diagonal matrix elements. The calculated values of the absorption are given in Table II and depend on the choice of the line-breadth constant $\Delta\nu$ which represents the effect of broadening by collision. Comparison is made of these theoretical results with the absorption in the $\frac{1}{4}$ cm region, observed by various experimentalists with different methods. It is concluded that 0.02 cm^{-1} is probably the best choice for $\Delta\nu/c$. The theoretical dependence of the absorption on pressure is discussed, and is particularly interesting because of the relation to the mechanism of collision-broadening and because the resonances to individual rotational lines are resolved at low pressures.

INTRODUCTION

BOTH the oxygen and nitrogen molecules are electrically non-polar. Hence at first thought, one is likely to conclude that dry, un-ionized air cannot absorb microwaves. The quantum-mechanical basis for this inference is the fact that in non-polar molecules the selection principles allow electric dipole radiation or absorption only when associated with a transition between two different electronic states of a molecule, rather than between two components of a single electronic state. Because the Bohr frequency condition makes frequency proportional to the change in energy of the molecule, switches in electronic state give resonances in the ultraviolet rather than microwave region.

The oxygen molecule, however, is paramagnetic or, in other words, has a permanent magnetic moment. Consequently it can absorb microwaves, since transitions for magnetic dipole radiation are permitted which join closely-spaced components of the ground state, and which hence give resonances in the microwave domain. Usually one thinks of absorption as arising only from electric dipoles, but it can also result from magnetic polarity, since Maxwell's equations are symmetric in E and H. To be sure, the magnetic effect is much weaker than the electric one would be were it present, inasmuch as one Bohr magneton is about 1/100 of a Debye unit of electric polarity. However, because of the great path lengths involved in atmospheric transmission, the magnetic absorption due to oxygen is very pronounced if the wave-length is in the vicinity of $\frac{1}{2}$ cm, where there is a resonance maximum. There is also some absorption, though very much weaker, in the more conventional, longer wave-length microwave region. The purpose of the present paper is to compute the magnitude of the attenuation.

THE FINE STRUCTURE OF THE MOLECULAR SPECTRUM OF OXYGEN

The analysis of the band spectrum of oxygen shows that the oxygen molecule has a $^3\Sigma$ ground state. Since the spin quantum number S consequently is 1, and the gryomagnetic ratio $g(e/2mc)$ has a Landé factor $g=2$, the oxygen molecule carries a magnetic dipole moment of two Bohr magnetons.[1] This magnetic moment interacts with the "end-over-end" rotation of the oxygen molecule to form what the band spectroscopists call a "rho-type triplet." If K be the

* The investigations underlying the present paper were performed largely while the author was serving as consultant for the M.I.T. Radiation Laboratory, NDRC Div. 14, contract OEMsr 262. Most of the results have been presented in its reports 43-2 and 664.

[1] For a resumé of the theory of the magnetic properties of the oxygen molecule, see pp. 262–264 and p. 266 of the writer's *Electric and Magnetic Susceptibilities* (Oxford University Press, New York, 1932). For the theory of rho-type triplets see H. A. Kramers, Zeits. f. Physik 53, 422 (1929); M. H. Hebb, Phys. Rev. 49, 610 (1936); also R. Schlapp, Phys. Rev. 51, 342 (1937).

rotational quantum number exclusive of spin, then K is compounded vectorially with the spin S to yield a resultant inner or rotational quantum number J for the molecule which can take on the values $K-1$, K, and $K+1$. Because the oxygen nucleus is devoid of spin, the Pauli exclusion principle allows K to take on only odd values. The intervals separating states of different K are magnetically inactive, and, anyway, are so large that they would give resonances in the infra-red rather than microwave region. It is only the fine structure of the rho-type triplet, in other words the decomposition of the three states of given K but different J, which is small enough to give microwave resonances. The components $J=K-1$ and $J=K+1$ nearly coincide with each other, and differ from $J=K$ by intervals which depend on K but which, with one exception, are about 2 cm^{-1}, corresponding to a wave-length of $\frac{1}{2}$ cm. Fortunately the selection principle that J cannot change by more than one unit prevents transitions between the components $K-1$ and $K+1$ from being magnetically active, as otherwise the near coincidence of these components would lead to strong absorption in the ordinary microwave region, of the order $\lambda=10$ cm.

In our calculations it is necessary to know the spacings of the components with some accuracy. Fortunately, these have been determined by Dieke and Babcock[2] by measuring the lines of the atmospheric absorption bands of O_2 in stellar spectrograms. The resulting intervals are tabulated in the columns of Table I labelled "spectroscopic." Two sets of values are given. Those listed as "D. & B." are derived from the original article of Dieke and Babcock, while those termed "new B." incorporate the results of new unpublished studies by Professor Babcock which he has kindly made available to us. He is able to improve the accuracy by more careful averaging and appraisal of the experimental data.[2] The difference compared to the earlier values is a relatively slight one, amounting in most cases to only a few thousandths of a wave number.

TABLE I. Energy intervals in the oxygen spin triplets. The intervals separating the components $J=K-1$, $K+1$ from $J=K$ are denoted respectively by $h\nu_{K-}$, $h\nu_{K+}$.

	ν_{K-}/c spectroscopic D. & B.	ν_{K-}/c spectroscopic new B.	ν_{K-}/c theory (Schlapp)	ν_{K+}/c spectroscopic D. & B.	ν_{K+}/c spectroscopic new B.	ν_{K+}/c theory (Schlapp)
$K=1$	——	——	3.962	1.872	1.873	1.878 cm^{-1}
3	2.084	2.085	2.084	1.950	1.951	1.950
5	2.011	2.012	2.012	1.981	1.986	1.988
7	1.976	1.975	1.974	2.021	2.017	2.016
9	1.949	1.949	1.946	2.045	2.041	2.039
11	1.919	1.919	1.922	(2.06)	2.063	2.061
13	1.899	1.900	1.901	(2.08)	2.083	2.081
15	1.877	1.881	1.881	2.10	2.103	2.100
17	1.864	1.862	1.861	2.12	2.124	2.119
19	1.838	1.844	1.843	(2.14)	2.150	2.137
21	1.815	——	1.824	(2.16)	——	2.156
23	1.81	1.813	1.806	2.18	2.180	2.173
25	(1.80)	1.784	1.788	(2.20)	——	2.191
≥ 27	{1.78 $-0.01(K-27)$}		$(-0.0084K$ $+1.985$ $+0.31/K$ $-\cdots)$	{2.22 $+0.01(K-27)$}		$(+0.0084K$ $+1.993$ $-0.31/K$ $+\cdots)$

In other columns of Table I we include for comparison the intervals furnished by a theoretical formula of Schlapp,[3] based on the quantum mechanics of the coupling of spin to molecular rotation in a rho-type triplet. It is quite possible that the individual levels given by Schlapp's expression are more reliable than the spectroscopic values. His formula involves one undetermined constant which is so chosen as to fit the general run of experimental data in the best possible way. The separation between the components $J=0$ and $J=1$ of $K=1$ must be obtained from Schlapp's theory, for this particular interval is not obtainable from the ordi-

[2] G. H. Dieke and H. D. Babcock, Proc. Nat. Acad. Sci. 13, 670 (1927). The intervals can also be obtained from spectroscopic measurements by Badger and Mecke (Zeits. f. Physik 60, 59 (1930)) which use a laboratory rather than solar light source. However, we do not include these values in Table I, since their irregular trend with K indicates that they are probably less accurate than those of Dieke and Babcock, from which they often differ by over 0.01 cm^{-1}. Babcock's new figures are obtained by averaging over a variety of different bands having different vibrational quantum numbers in the upper state, but of course always zero vibration in the lower one, since we are interested only in the characteristics of the normal, vibrationally unexcited ground level. On the other hand, in quoting Dieke and Babcock's data, we give only their measurements on one particular band, the so-called B one ($v=1\rightarrow v=0$).

[3] R. Schlapp, Phys. Rev. 51, 342 (1937). In computing the intervals by means of Schlapp's formula for Table I, slightly different values of the constants B, μ (but not λ) have been used than in his original paper (*vis.* $\mu=-0.00837$, $B=1.43777$ cm^{-1} instead of -0.008, 1.438). Mrs. Herzberg tells us that the fit with the spectroscopic data is improved by the new choice of μ, which is arbitrary. The writer is much indebted to her for supplying him with the results of the calculations with the revised constants. In applying Schlapp's formula (2), care must be exercised to take the proper branch of the radical in the particular case $J=0$, as this may involve a different numerical choice of sign for the root than for other values of J. The appropriate form of Schlapp's expression W_{K-1} for $K=1$ is $-2\lambda-\mu$, as can be verified from the basic theory, or more simply, from the fact that the multiplet intervals must vanish with the spin-orbit constants λ, μ.

nary spectroscopic data. Because of blending, perturbations, or some other reason, the spectroscopic values are not reliable for the level $K=21$. For this value of K, and also for values of K higher than about 25, the intervals are best estimated by interpolation or from theory. Intervals thus obtained, rather than by direct measurement, are inclosed in parentheses when listed in the "spectroscopic" columns of Table I.[4]

Wisely or unwisely, in our calculations of the absorption we have used the spectroscopic rather than theoretical values of the intervals, in order to tie in as closely as possible with direct experiment rather than theory. We used Dieke and Babcock's original values of the intervals, since Babcock's revised figures were not available at the time the calculations were made. As a matter of fact, the differences between the different sets of values, including those based on Schlapp's formula, are far too small to be of consequence except at very low pressures. Thus the curves and tables which we give later in the article for the absorption at atmospheric pressure would have been changed only in a trivial way had we employed Babcock's new figures, or used the Schlapp formula. When the line-breadth constant is as high as 0.05 or 0.1 cm^{-1}, the lines overlap so much at ordinary pressures that sharp resonances are obliterated, and for these values of $\Delta\nu/c$ we have employed "rounded" intervals which are carried only to two decimals. It has nevertheless seemed advisable to give in Table I the best available estimates of the intervals, rather than just those employed in our calculations since in the future improved microwave technique may make it possible to locate individual lines with accuracy.

THE FORMULAS FOR THE ABSORPTION

The general quantum-mechanical expression for the absorption coefficient is

$$\gamma=10^6(\log_{10}e)\left(\frac{8\pi^3\nu N}{3hc}\right)\frac{\Sigma_{i,j}\{|\mu_{ij}|^2 f(\nu_{ij},\nu)\}e^{-E_j/kT}}{\Sigma_j e^{-E_j/kT}}. \tag{1}$$

Here μ_{ij} is the matrix element of the dipole moment connecting two stationary states i, j of energy E_i, E_j, respectively, while ν_{ij} is the frequency of the corresponding spectral line, given by the Bohr frequency condition $h\nu_{ij}=E_i-E_j$. The frequency of the incident radiation is denoted by ν and the number of molecules per cc by N. The factor $10^6\log_{10}e$ is included in order that the absorption be expressed in decibels per kilometer. The factor $f(\nu_{ij},\nu)$ may be termed the "structure-factor" governing the shape of the absorption line, and is given by the expression

$$f(\nu_{ij},\nu)=\frac{\nu}{\pi\nu_{ij}}\left[\frac{\Delta\nu}{(\nu_{ij}-\nu)^2+\Delta\nu^2}+\frac{\Delta\nu}{(\nu_{ij}+\nu)^2+\Delta\nu^2}\right]. \tag{2}$$

Near resonance, (2) is practically identical with

$$f(\nu_{ij},\nu)=\frac{1}{\pi}\left[\frac{\Delta\nu}{(\nu_{ij}-\nu)^2+\Delta\nu^2}\right]. \tag{3}$$

The expression (3) is the form of structure-factor commonly given in the literature, and is a good approximation when $\Delta\nu$ and $|\nu_{ij}-\nu|$ are both small in magnitude compared with ν. These conditions

[4] The spectroscopic determinations of the intervals involved in Table I are based on measurements of the atmospheric bands of O_2, which arise from magnetic dipole radiation in a $^3\Sigma_g^-\!-\!^1\Sigma_g^+$ transition. Because of the selection rules that prohibit combinations of $J=0$ with $J=0$, and of changes of J by more than one unit in dipole radiation, the state $J=0$ of $^3\Sigma_g^-$ cannot combine with any $^1\Sigma_g^+$ level, and so cannot be detected. This statement is no longer true when one allows for the possibility of electric quadrupole radiation, but whether the resulting satellite lines are strong enough to be detectable is uncertain (cf. J. H. Van Vleck, Astrophys. J. 80, 161 (1934)). There are a few electronic states which can combine with $J=0$ of $^3\Sigma_g^-$ even in dipole radiation. Hence in principle the interval ν_{1-} should be detectable if one measured the right bands. However, the known electronic states of O_2 are very limited in number, and to date the experimental difficulties have apparently been prohibitive. For instance, the Schumann-Runge-Fuchtbauer $^3\Sigma_g^-\!-\!^3\Sigma_u^-$ bands are in the ultraviolet, and so the dispersion has not been adequate to resolve the triplet components. The Herzberg $^3\Sigma_g^-\!-\!^3\Sigma_u^+$ bands, though weak, probably offer more chance of success.

are well fulfilled when one deals with the absorption of visible light or infra-red. In studying the absorption of microwaves at frequencies which fall outside sharp resonances, one may encounter cases where $|\nu_{ij}-\nu|$ and even $\Delta\nu$ are of the same order of magnitude as ν. It is then necessary to use the more exact formula (2). The theory involving Eq. (2), which involves inclusion of a term omitted in the standard Lorentz theory of collision broadening, is given in a previous paper by Van Vleck and Weisskopf.[5] In this connection it should be mentioned that their results are obtained essentially by the correspondence principle, and involve the quantum-mechanical transcription of classical formulas. As pointed out to the writer by Professor Dennison, this transcription is not unambiguous, since somewhat different results are obtained according as one applies the correspondence principle directly to absorption, or to emission. With the latter method, the absorption is obtained indirectly by utilizing the Einstein relation between spontaneous radiation and absorption. Thus there is some doubt as to the correct quantal expression for the shape and structure of an absorption line. The uncertainties, however, are of such a character as to be of no consequence if the incident frequency ν and the molecular resonance frequency ν_{ij} are both small compared to kT/h. Fortunately, these conditions are abundantly fulfilled for the oxygen lines studied in the present paper.

The constant $\Delta\nu$ involved in (2) is the so-called line-breadth constant. It represents the effect of damping by collision, which is the most important cause of broadening in the microwave region. Here the wave-length is far too long for the Doppler effect or radiation-damping to have any appreciable effect on the line profile. The constant $\Delta\nu$ cannot be calculated theoretically, as the corresponding collision diameter need not be the same as the gas-kinetic one or the molecular diameter, and usually turns out much larger than the latter. Until recently, uncertainty in the value of $\Delta\nu$ has been a stumbling block in the theoretical calculation of microwave absorption. However, microwave measurements have themselves lately furnished much of the needed information on $\Delta\nu$.

Since $h\nu_{ij}=E_i-E_j=-h\nu_{ji}$ we have $f(\nu_{ij}, \nu)=-f(\nu_{ji}, \nu)$, and the contribution of a typical term i, j in (1) to the absorption is positive or negative according as the energy of the state i is greater or less than that of j. The negative contributions are often called induced emission. If the resonance frequencies are small compared to kT/h, the positive and negative terms nearly cancel. Namely, to any given term i, j in the double sum in (1), there is also a corresponding term j, i whose contribution is of opposite sign, and which would cancel the effect of i, j completely were it not for the difference in the Boltzmann factors for the states i and j. This difficulty of nearly compensating terms may, however, be avoided by using the approximation

$$\nu_{ij}e^{-E_j/kT}+\nu_{ji}e^{-E_i/kT}=\tfrac{1}{2}(h\nu_{ij}^2/kT)(e^{-E_j/kT}+e^{-E_i/kT}) \tag{4}$$

which applies when $|\nu_{ij}|\ll kT/h$. This simplification is well warranted in the application of the present paper, since the width of the rho-type triplet of oxygen is only about 1/100 of kT/h. When (4) is employed, Eq. (1) becomes

$$\gamma=10^6(\log_{10}e)\frac{8\pi^3\nu N}{6ckT}\frac{\Sigma_{i,j}\{|\mu_{ij}|^2\nu_{ij}f(\nu_{ij}, \nu)\}e^{-E_j/kT}}{\Sigma_j e^{-E_j/kT}}. \tag{5}$$

The advantage of using (5) rather than (1) is that all terms in the numerator of (5) are positive.

In our applications to oxygen, the index i (or j) signifies a trio of quantum numbers J, K, M (or J', K', M'), where we have $J=K-1, K, K+1$ as previously explained, and where M is the equatorial or "magnetic" quantum number associated with the space quantization of J. The energy does not depend on M, and only slightly on J. Hence in the Boltzmann factors (but not in the structure-factor given in Eq. (2)) we can make the approximation $E(K, J)=E_K$ where E_K is independent of J.

[5] J. H. Van Vleck and V. F. Weisskopf, Rev. Mod. Phys. 17, 227 (1945); H. Frohlich, Nature 157, 478 (1946).

The matrix elements of the magnetic moment are of the type $K'=K$, $J'=J-1$, J, $J+1$. Consequently (5) takes the specific form

$$\gamma=10^6(\log_{10}e)\frac{4\pi^2\nu N}{3ckT}\frac{\Sigma_K\{2|\nu_{K+}f(\nu_{K+},\nu)|\mu_{K+}{}^2+2|\nu_{K-}f(\nu_{K-},\nu)|^2\mu_{K-}{}^2+F(\nu)\mu_{K0}{}^2\}e^{-E_K/kT}}{\Sigma_K 3(2K+1)e^{-E_K/kT}}, \tag{6}$$

where ν_{K+}, ν_{K-} are defined as in Table I, and where

$$F(\nu)=\lim_{\nu_{ij}\to 0}[\nu_{ij}f(\nu_{ij},\nu)]=\frac{2\nu\Delta\nu}{\pi(\nu^2+\Delta\nu^2)}. \tag{7}$$

The intensity formulas[6] of quantum mechanics appropriate to the type of vector addition involved in a rho-type triplet (Hund's case *b*) show that

$$\mu_{K+}{}^2=\frac{4\beta^2K(2K+3)}{K+1},\quad \mu_{K-}{}^2=\frac{4\beta^2(K+1)(2K-1)}{K},\quad \mu_{K0}{}^2=\frac{8\beta^2(K^2+K+1)(2K+1)}{K(K+1)}, \tag{8}$$

where β is the Bohr magneton $he/4\pi mc$.

The first and second members of (6) represent the resonant absorption of oxygen, which is particularly important in the vicinity of $\nu/c=\frac{1}{2}$ cm. The third member gives the non-resonant or diagonal part of the absorption, which will be discussed and explained more fully below. In the Boltzmann factors, it is an adequate approximation to take $E_K=BK(K+1)$, with $B=1.44$ cm^{-1}, so that at 293°K we have $e^{-E_K/kT}=10^{-0.0030K(K+1)}$. Because of the exclusion principle, only odd values of K are involved in the summation in (6). Without appreciable error, the sum in the denominator may be replaced by the integral

$$3\int_0^\infty K\exp[-BK^2]dK=3kT/2B.$$

On the other hand, the first and second members of the numerator, must be summed in detail, and in this connection it is necessary to know the energy levels or frequency intervals accurately, since $f(\nu_{ij},\nu)$ is sensitive to the value adopted for ν_{ij}. We utilized the D. & B. values in Table I, which has already been discussed. Outside of the resonance region, the absorption becomes less sensitive to the values of the molecular frequencies. It is then adequate to make the centroid approximation of considering all the frequency denominators to be the same. In place of (6) one then has the very simple formula

$$\gamma=0.34\left(\frac{\nu^2}{c^2}\right)\left[\frac{\Delta\nu/c}{[2-(\nu/c)]^2+(\Delta\nu/c)^2}+\frac{\Delta\nu/c}{[2+(\nu/c)]^2+(\Delta\nu/c)^2}+\frac{\Delta\nu/c}{(\nu/c)^2+(\nu\Delta/c)^2}\right], \tag{9}$$

if $T=293°$, $p=76$ cm. Use of (9) is warranted if $\nu/c>4.5$ or <1.5 cm^{-1}. The reason that we say >4.5 rather than >2.5 is that Table I shows that one particular line ν_{1-} has a resonance wave-number of about 4 rather than 2 cm^{-1}, and so gives a peak in the absorption near 4 cm^{-1}, i.e., $\lambda=\frac{1}{4}$ cm, which will be discussed later in connection with Eq. (13).

---

[6] E. U. Condon and G. H. Shortley, *The Theory of Atomic Spectra* (Cambridge University Press, 1935, New York), pp. 64–72. Translated into their notation, our quantities $\mu_{K\pm}{}^2$ are the same as their expression

$$(2\beta/\hbar)^2(2j+1)(\gamma j_1j_2j|J_1|\gamma j_1j_2j')^2\equiv(j,j')$$

provided we take $j_1=1$, $j_2=K$, $j=K$, $j'=K\pm1$. Our quantity $\mu_{K0}{}^2$ is obtained from this espression by taking $j=j'$, and summing over the three components $j=K-1$, K, $K+1$.

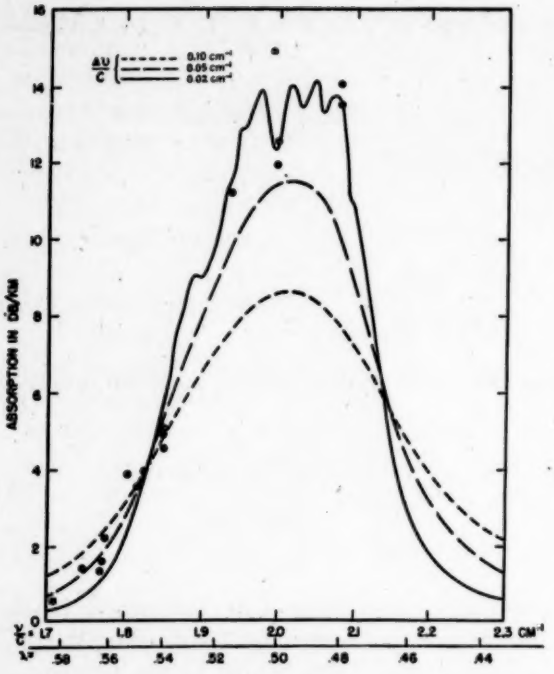

FIG. 1. The absorption, due to oxygen, of dry air at 300°K, 76 cm, for wave-lengths in the vicinity of ½ cm. The curves are calculated theoretically for various values of $\Delta\nu/c$, as indicated. The experimental points are by Beringer. The vertically, horizontally, and diagonally crossed circles refer respectively to measurements made on pure O_2, on O_2-N_2 mixtures with 50 percent O_2, and on 20 percent O_2. The equivalent values for air are obtained from the experimental data by assuming that the cross section is the same for O_2-N_2 and O_2-O_2 collisions, so that the absorption at constant total pressure is directly proportional to the oxygen content.

THE NON-RESONANT OR DIAGONAL PART OF THE ABSORPTION

The third term of (6), i.e., the term with factor $F(\nu)$ represents the non-resonant part of the absorption. It results from the fact that the matrix for the magnetic moment of the oxygen molecule has diagonal matrix elements. Perhaps we have previously given the impression in this paper that the magnetic absorption of oxygen consisted entirely of lines in the vicinity of $\lambda=\frac{1}{2}$ cm, with a satellite at $\frac{1}{4}$ cm. Actually, however, there are also lines whose resonance frequency is zero, and which we hence call non-resonant. They arise from the fact that the matrix for the spin magnetic moment of the oxygen molecule has diagonal elements in addition to the non-diagonal ones which are responsible for the resonance at ½ cm. The diagonal and non-diagonal elements come, respectively, from the projections of the spin vector **S** parallel and perpendicular to the resultant angular moment vector **J** about which **S** precesses. The diagonal members are the quantum analog of a constant term in a classical Fourier expansion. One may wonder how absorption can arise from a constant rather than variable moment. The answer is that the constancy is spoiled by the interruptions due to collisions, and the radiative effect is caused by the pulses attendant to the realignments of collision. The mechanism of absorption due to the diagonal elements is in many ways similar to that in Debye's[7] well-known model of absorption and dispersion of a molecule at radio-frequencies due to redistribution of molecular dipoles by collisions. In fact, when a slight, well-warranted approximation is made, the third member of (6), which is the diagonal effect, has precisely the same form as Debye's expression for the absorption, *viz.*,

$$\gamma=10^6(\log_{10}e)\left(\frac{8\pi^2\nu^2N\mu^2}{3kTc}\right)\frac{\Delta\nu}{\nu^2+\Delta\nu^2}. \qquad (10)$$

The approximation consists in taking $\mu_{K0}^2=8\beta^2\cdot(2K+1)$ instead of using the more accurate value given by (8). Since K is large for the great bulk of the rotational states, this simplification is entirely allowable, and makes the sum cancel from numerator and denominator in the third member of (6). This part then becomes identical with (10) provided the square μ^2 of the dipole moment is given the value

$$\mu^2=g^2S(S+1)\beta^2/3=8\beta^2/3, \qquad (11)$$

where g is the Landé factor and S is the spin quantum number. The factor ⅓ appears in (11) because on the average one-third of the total mean square moment is of the diagonal variety, the other two-thirds being consumed by the non-diagonal type. When (11) is utilized, it is found that the numerical value of the expression (10)

[7] P. Debye, *Polar Molecules* (Chemical Catalog Company, New York, 1929), Chap. V. Debye's derivation of (10) was a classical one. A proof of (10) by means of quantum rather than classical theory, and intended primarily for a magnetic rather than electric moments, has been given by C. J. Gorter and R. de L. Kronig, Physica 3, 1009 (1936) and by Kronig, *ibid.* 5, 65 (1938). See also W. Kauzmann, Rev. Mod. Phys. 14, 12 (1942); Van Vleck and Weisskopf, reference 5.

at 293°, 76 cm becomes

$$\gamma = 0.34\left(\frac{\nu}{c}\right)^2\left[\frac{\Delta\nu/c}{(\nu/c)^2+(\Delta\nu/c)^2}\right] \text{db/km.} \quad (12)$$

Equation (12) gives the principal part of the oxygen absorption if the wave-length is greater than about 1.5 cm.

It should be emphasized that the distinction between resonant and non-resonant absorption is, in a certain sense, a purely artificial one. The diagonal elements can be made of the non-diagonal variety, but of course with zero frequency, by choosing the axis of quantization perpendicular rather than parallel to the incident field. Then the matrix elements of magnetic moment parallel to the field are of the type $\Delta M = \pm 1$ rather than $\Delta M = 0$, where M is the equatorial or magnetic quantum number associated with the axis of quantization. Thus non-resonant absorption is equivalent to resonant absorption when the natural frequency in the latter is made to approach zero as already tacitly implied in (7). This equivalence is secured only when the Lorentz expression for the line profile is modified in the fashion explained by Van Vleck and Weisskopf.[5] Without the revision, the Lorentz result does not reduce to that of Debye and Kronig in the limiting case of zero frequency. Fortunately the diagonal and non-diagonal effects can now be treated by a unified, consistent formalism.

Numerical Values of the Absorption—Comparison with Beringer's Experiments

Before a numerical comparison can be made of the theoretical formulas with experiment, some choice must be made as to the value of the collision parameter $\Delta\nu$. When the theory was first developed by the writer[8] in 1942, no microwave data were available, and the best that could be done was to try to estimate $\Delta\nu$ from measurements on the widths of absorption lines in the infra-red region. Furthermore, the infra-red data were not on oxygen itself, inasmuch as the oxygen molecule is inactive because it is electrically non-polar. The best procedure available was to extrapolate from the infra-red spectra of CO and other molecules somewhat related to O_2. In this fashion the writer concluded[8] that the most reasonable choice for $\Delta\nu/c$ was 0.1 cm^{-1}. Subsequent microwave measurements made on O_2 by Beringer[9] show unequivocally that actually $\Delta\nu/c$ is quite a little lower and is probably between the limits 0.02 and 0.05 cm^{-1}. It is not surprising that the earlier estimates based on infra-red work should prove to be somewhat in error, for infra-red determinations of the width of a spectral line require very high resolving power and involve difficult corrections for slit width, not to mention the fact that the observations are not made on oxygen directly.

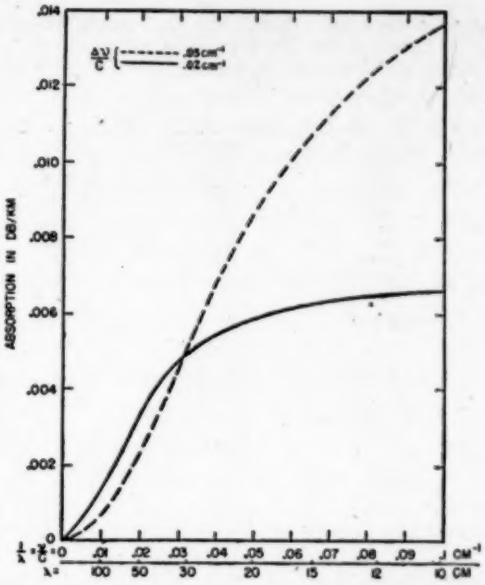

FIG. 2. The absorption, due to oxygen, of dry air at 293°K, 76 cm for wave-lengths greater than 10 cm.

Figure 1 shows the calculated absorption as a function of frequency in the resonance region around $\lambda = \frac{1}{2}$ cm. Beringer's experimental data[9] are also included for comparison, and are indicated by the various points. His measurements on pure or 50 percent O_2 are reduced to "air equivalent" by assuming that at given total pressure the absorption is directly proportional to the concentration of oxygen. This procedure appears legitimate, since Beringer's data show that the collision cross section is substantially the same for O_2-N_2 and O_2-O_2 impacts. For

[8] For details see pp. 10–12 of M.I.T. Radiation Laboratory Report 43-2.

[9] R. Beringer, Phys. Rev. 70, 53 (1946).

TABLE II. Absorption of air, due to oxygen, for various values of the line-breadth constant $\Delta\nu$.

$\Delta\nu/c = \nu/c$	0.01 cm^{-1} γ	0.02 cm^{-1} γ	0.05 γ	0.10 γ
0.1 cm^{-1}	0.0033 db/km	0.0066 db/km	0.014	0.017
.33	.0036	.0072	.018	.033
.67	.0045	.0089	.022	.044
.80	.0052	.010	.026	.051
1.0	.0072	.014	.036	.071
1.3	.017	.033	.083	.17
1.5	.038	.077	.192	.38
1.6	.070	.141	.35	.70
1.7	.166–0.171	.32	.74	1.26
1.77	.66–0.78	1.06	1.83	2.41
1.8		1.99		3.1
1.85	4.8–6.4	5.09–5.5	5.4	4.9
1.90		8.7–9.9		6.9
1.95		12.0–13.5		
2.00	11.4–15.5	12.9–14.1	12.0	8.9
2.05		13.9–14.8		
2.08	11.9–14.9		10.7	8.1
2.10		9.5–13.1		
2.15		5.0	5.7	5.8
2.2		1.70	3.3	4.1
2.3		.51	1.2	2.08
2.5	.096	.19	.48	.95
5.0	.0146	.03	.073	.146

further discussion of this subject and other questions relative to the experimental measurements, the reader is referred to Beringer's paper. Figure 1 shows that his data are scarcely accurate enough to decide between $\Delta\nu/c=0.02$ and 0.05 cm^{-1} but that 0.1 cm^{-1} would be definitely too high. It is interesting to note that at $\nu/c=1.83$ cm^{-1} the various points cross, so that at this particular wave-length the absorption is almost independent of the value chosen for the line breadth. Possibly this feature might be useful in calibrating apparatus in which a constant of proportionality in the absorption is otherwise undetermined.

The wobbles in the curve for $\Delta\nu/c=0.02$ cm^{-1} are caused by the fact that at certain particular wave-lengths there is close resonance to some individual rotational state. This effect does not show up at 0.05 or 0.1 cm^{-1}, as the lines are then so broad that they overlap, whereas at 0.02 cm^{-1}, one has an incipient resolution of the contributions of the different rotational states. By working with low pressures and well-established frequencies, it should ultimately be possible to resolve this fine structure.

Figure 2 gives the absorption at wave-lengths greater than 10 cm. In this region, practically all of the contribution to the absorption comes from the diagonal or non-resonant effect, given by (12) or the third member of (6). The attenuation in this long wave-length region is too small to be of any consequence unless the path is very long. This statement is true regardless of the choice of $\Delta\nu$. At given incident frequency ν, the value of $\Delta\nu$ which maximizes the expression (12) is $\Delta\nu=\nu$, and the resulting upper limit to the attenuation is $0.17/\lambda$ db/km.

Figure 1 does not extend to short enough wave-lengths to show the minor but sharp resonance in the vicinity of $\lambda=\frac{1}{4}$ cm, which comes from the interval ν_{1-} separating the components $J=0$ and $J=1$ of $K=1$ (cf. Table I). The corresponding peak does, however, appear in Fig. 2 of the following paper, where the absorption due to O_2 and H_2O is compared. The formula for the absorption due to the resonance near $\frac{1}{4}$ cm is

$$\gamma=0.048\left[\frac{\Delta\nu/c}{(\nu-\nu_{1-})^2/c^2+(\Delta\nu/c)^2}\right]. \qquad (13)$$

As already mentioned, ν_{1-} cannot be determined spectroscopically, and can only be estimated from Schlapp's theoretical formula. The latter gives $\nu_{1-}/c=3.96$ cm^{-1}, a value which is probably correct to within a few tenths of a cm^{-1}. Oscillators of short enough wave-length to detect this resonance do not exist at present, but with the present rapid development of microwave technique, it should presumably be observable in the not too far distant future.

In Table II we show the calculated absorption numerically rather than graphically. The numerical values in this table are slightly different from those in Fig. 2, since this figure is drawn for a temperature of 300° rather than 293° in order to conform to the approximate temperature of Beringer's experiments. The increase of the temperature from 293 to 300°K reduces the absorption by a factor[10] approximately $(293/300)^2$. It

[10] The proportionality to $1/T^2$ is only approximate, and arises because (6) contains the factor N as well as $1/T$ explicitly, and because for a given the ratio of the sums in the numerator and denominator of (6) is rather insensitive to T as long as the wave-length or line-breadth is such that several lines contribute appreciably to the absorption. Where the absorption is mainly due to one line of excitation energy E_K, there is an additional factor $(1/T)e^{-E_K/kT}$ inasmuch as the sum in the denominator of (6) is nearly proportional to T. For instance, the absorption in the vicinity of $\frac{1}{4}$ cm given by (13), is caused by the state $K=1$ for which $E_K/kT\ll 1$; the proportionality here is hence to $1/T^2$ rather than $1/T^3$. All these statements are on the supposition that $\Delta\nu$ is fixed. Kinetic theory indicates that at constant pressure $\Delta\nu$ should be proportional to $1/T^{1/2}$, but this effect can, of course, be considered only after $\Delta\nu$ has been located. In the many-line case it would make the absorption proportional to $1/T^{3/2}$ at resonance, and to $1/T^{5/2}$ well away from resonance.

will be noticed that for small values of $\Delta\nu/c$ in Table II, the absorption is given only within certain limits. This is because the exact values of the absorption lines are not known experimentally with high precision, and with narrow line-breadths, the exact amount of resonance to a particular doublet belonging to some particular rotational state is, of course, sensitive to the precise values of the resonant wave-length. In their original paper, Dieke and Babcock usually gave their intervals to 0.001 cm^{-1}, but Professor Dieke tells us it is doubtful whether they are more accurate than 0.01 cm^{-1}. The new figures of Babcock are more exact, probably having an accuracy, he tells us, of two thousandths of a cm^{-1},—at least this is suggested by the consistent good agreement with the Schlapp formula. An uncertainty of 0.01 cm^{-1} is sufficient to admit the possibility of a given applied frequency being exactly at resonance with a given rotational line in the $\frac{1}{2}$ cm region, or being midway between two adjacent rotational lines. These two extremes represent, so to speak, the "most resonant" and "least resonant" possible behaviors if the frequencies are not accurately known, and have been used in constructing the upper and lower limits in Table II. If the line-breadth is more than about 0.05 cm^{-1} or so, the lines overlap so much that the resonances to the individual lines are ironed out. They also disappear if one is not in the resonance region, or if the applied frequency is not well stabilized, so that effectively a sort of average frequency over an interval is used. In drawing Fig. 1, we have not attempted to show the curve for $\Delta\nu/c=0.01$ cm^{-1}, because the wobbles are too great. In obtaining the curves for $\Delta\nu/c=0.02$ and 0.05 it has been assumed that Dieke and Babcock's original values

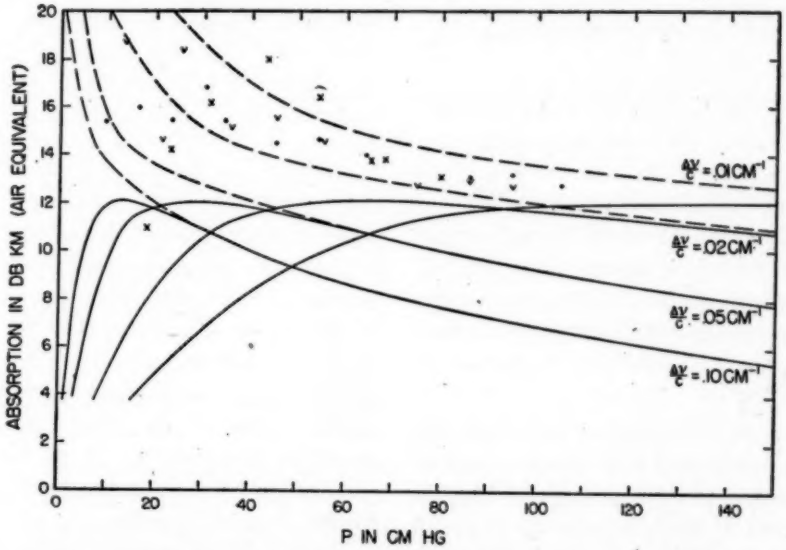

FIG. 3. The dependence of absorption on pressure at $\nu/c=2.08$ cm^{-1}, $\lambda=0.481$ cm. The ordinates are so normalized as to be proportional to the absorption per oxygen molecule, and give the "air-equivalent absorption" which is obtained by multiplying the measured absorption by the ratio of the partial pressure of the oxygen in the actual atmosphere to the partial pressure of the oxygen in the experiment. The solid circles, check marks, and crosses refer, respectively, to measurements made by Beringer on dried tank ("pure") O_2, mixtures of O_2-N_2 with 50 percent O_2, and mixtures with 19 percent O_2. The curves are calculated from theory under the assumption that $\Delta\nu/c$ is proportional to the total pressure; the values of $\Delta\nu/c$ with which the various curves are labelled are those applicable at 76 cm. The divergence between the solid and dashed curves indicates approximately the uncertainty in the calculation due to the fact that the resonance frequency of the line nearest coincidence with the incident frequency is not known with precision. The "on-resonance" case shown by the dashed curves, assumes that $\nu_{2-}/c=2.08$, while the "off-resonance" case, illustrated by the solid curves, supposes that $\nu_{2-}/c=2.09$ cm^{-1}. A line with $K=13$, as well as the one at $K=3$, may cause resonance, but for simplicity it is assumed throughout that $\nu_{13+}/c=2.09$. According to Babcock's latest figures, ν_{2-}/c is 2.085 cm^{-1}.

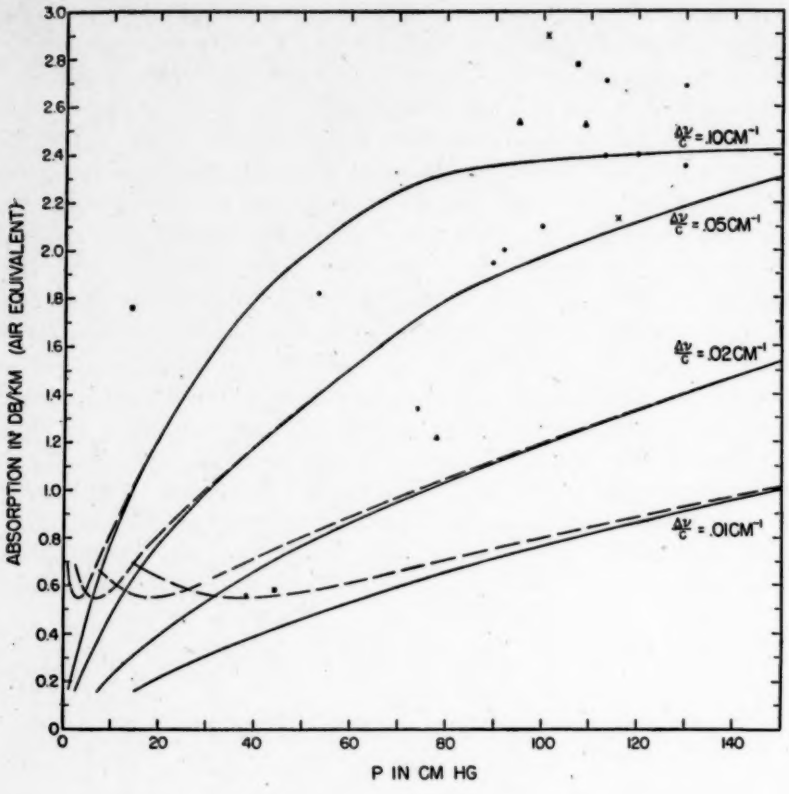

FIG. 4. The dependence of absorption per molecule on pressure at $\nu/c = 1.77$ cm^{-1}, $\lambda = 0.565$ cm. The normalization of the ordinates to the "air-equivalent" absorption and the significance of the $\Delta\nu/c$ labellings are explained in the caption for Fig. 3. The solid circles and squares are Beringer's runs on tank O_2, while the triangles and crosses are for mixtures approximately 50 percent O_2. The solid and dashed curves are for $\nu_{27}/c = 1.78$ and 1.77 cm^{-1}, respectively; both assume $\nu_{23}/c = 1.79$.

are reliable (except that certain irregularities have been smoothed out, as noted in connection with Table I). If the error in the experimental measurements of the frequency intervals amounts to 0.01 cm^{-1}, the positions of the minor peaks and valleys near the maximum in Fig. 1 cannot be trusted.

It is instructive and interesting to graph the absorption per molecule as a function of pressure at a given wave-length. Substantially this is done in Figs. 3 and 4, but in order to have an ordinate which is not an extremely small quantity we use for the vertical scale not the absorption of a single molecule, but rather the "air-equivalent absorption." By this is meant the attenuation in db/km which would result if one had the same number of oxygen molecules per unit volume as actually present in ordinary air, but kept the absorption per molecule the same as that observed experimentally for the pressure in question. In other words, the absorption which is plotted is the actual measured absorption multiplied by $0.21(76/p_{O_2})$, where p_{O_2} is the partial pressure of the oxygen. The curves of the type shown in Figs. 3 and 4 are informative because they exhibit the effect of the variation of $\Delta\nu$ with pressure, and are sensitive to the position of the resonance frequency, as well as to the value of $\Delta\nu$. In drawing the curves it is assumed that $\Delta\nu$ is proportional to the total pressure, and each curve corresponds to a particular value of the line-breadth parameter. A direct proportionality of $\Delta\nu$ to the pressure is required by the ordinary Lorentz theory of collision damping such as we have assumed throughout. We should, however, mention that there is some experimental evidence[11] that in certain polar gases $\Delta\nu$ is proportional to $p^{\frac{1}{2}}$. Also some of the complicated and refined theories[12] of line-broadening developed by various authors indicate that $\Delta\nu$ need not necessarily always be linear in p, but the predicted deviation from linearity is of the opposite type from that required by a proportionality to $p^{\frac{1}{2}}$. On the

[11] For summary of the evidence and references see W. M. Brooks, *Harvard Meteorological Studies*, No. 6, pp. 46–47.

[12] H. Margenau, Phys. Rev. **48**, 755 (1935); E. Lindholm, Arkiv for Matematik, Astronomi och Fysik, **32A**, no. 17 (1945); M. Foley, Phys. Rev. **69**, 616 (1946).

whole, we are inclined to believe that for our purposes it is probably a sufficient approximation to take $\Delta\nu$ proportional to p. With a non-linear dependence of $\Delta\nu$ on p, the curves would be different from those shown in Figs. 3 and 4, and when accurate experimental data become available, they should shed interesting light on this question.[13] The scatter of the Beringer data is too large to test the fine details of the theory, as is clear from the dispersion of the various experimental points in Figs. 3 and 4. Possibly insufficient stabilization of the frequency, with resulting drifting off and on resonance from one run to another accounts for some of the scatter of the absorption measurements, especially those at low pressures which are particularly difficult because the absorption is so small. When the pressure is reduced, the value of $\Delta\nu$ decreases, and the resonance phenomena become more pronounced. This is manifested by the forking of the curves in Figs. 3 and 4. In drawing these curves, instead of trying to use exactly the spectroscopic intervals of Dieke and Babcock, we have assumed that there is uncertainty amounting to 0.01 cm^{-1} or thereabouts, so that we cannot tell whether there is exact resonance to a particular rotational state or whether the incident frequency is midway between two resonances, a situation which we call "off resonance." If the pressure is sufficiently high, the values of the absorption calculated on the basis of maximum and minimum resonance practically coincide, but if the pressure is reduced enough, the two limits diverge, as evidenced by the forking of the curves. Although Beringer's points scatter too much to fix definitely which curve is the correct one, they do confirm the different trends of the absorption with pressure at wave-lengths near to and well removed from resonance. These two cases are exemplified by Figs. 3 and 4, respectively, and represent regions, where, on the whole, the attenuation per molecule tends, respectively, to decrease and increase with increasing pressure. The different behavior at different wave-lengths may be understood qualitatively as follows. If one had a single resonance line, of frequency ν_{ij}, the significant factor in the expression for the absorption would be given by Eq. (3) provided $\Delta\nu$ and $|\nu-\nu_{ij}|$ are small compared to ν. Since $\Delta\nu$ is proportional to p in the Lorentz theory, the attenuation should hence be inversely proportional to pressure in the center of the line, where $|\nu-\nu_{ij}| \ll \Delta\nu$, and directly proportional in the wings, where $|\nu-\nu_{ij}| \gg \Delta\nu$. Actually one has a mixture of various lines, and the situation is consequently more complicated, but the broad outlines of the behavior can be described by the "one-line" formula.

[13] Theoretically, the effect of overlapping collisions studied by Margenau (reference 12) and others enters mainly at high pressures, and so is more likely to manifest itself if the pressure is raised above atmospheric, whereas in the study of individual resonances, the most interesting experiments are at low pressures where the Lorentz assumptions are probably adequate. Some interesting experimental evidence that $\Delta\nu$ is proportional to p over a wide range of pressure may be cited. Namely, the absorption found by Townes and Merritt for water vapor at a pressure of 0.1 mm agrees gratifying well from that calculated under the assumption of such proportionality from the measurements of Becker and Autler at atmospheric pressure. This point is discussed in more detail in the following paper.

COMPARISON WITH OTHER EXPERIMENTAL WORK

So far we have quoted only the experimental measurements by Beringer. In 1944, Mueller[14] made a series of observations on the propagation in air of microwaves having a wave-length $\lambda=0.625$ cm. He found no measurable deviation of the attentuation from that predicted by the inverse square law. This sets an upper limit on the absorption coefficient γ, since with a detectable γ, the transmitted energy should depend on distance in the fashion $(1/r^2)10^{-10\gamma}$. From this type of evidence, and also from unpublished studies of transmission by a wave-guide, he concluded that γ must be less than 0.09 db/km. Since the theoretical value of γ at 0.625 cm is $6.5(\Delta\nu/c)$, Mueller's measurements seem to demand that the line-breadth constant $\Delta\nu$ not exceed 0.014 cm^{-1}, which is lower than the range of values yielded by Beringer's investigations. The cause of this disagreement is not clear. The experiment which Mueller performed requires high sensitivity; the value 0.09 db/km corresponds to a reduction of only 0.8 percent in the transmitted signal over the quarter mile path which he used. He gauged his minimum detectable departure from the inverse square law by the root mean square deviation of his

[14] G. E. Mueller, Bell Lab. Rep. MM-44-160-150.

readings from the mean. This procedure clearly does not allow for systematic errors if present. Mueller informs the writer that perhaps it is allowable to raise his upper limit to 0.13 db/km, corresponding to a line breadth $\Delta\nu/c=0.02$ cm^{-1}. This is just compatible with the lowest value of $\Delta\nu/c$ which seems reasonable in the light of Beringer's experiments, although a sharp delineation of the least admissible $\Delta\nu$ is not possible.

Dicke, Beringer, Kyhl, and Vane[15] have made measurements on the total absorption due to the oxygen in the earth's atmospheric layer, by an ingenious radiometer method described in detail in their paper. The wave-lengths (1, 1¼, 1½ cm) employed in these experiments are so far from resonance that the effect is weak, and hard to determine with precision. Their results do, however, seem to indicate that $\Delta\nu/c$ is of the order 0.02 cm^{-1}. Specifically, the values of $\Delta\nu/c$ required to fit their measurements at 1, 1¼, and 1½ cm are, respectively, 0.025, 0.020, and 0.017 cm^{-1}.

In the combined light of the experiments by Beringer, by Mueller, and by Dicke and collaborators, 0.02 cm^{-1} is probably the most reasonable present choice for $\Delta\nu/c$, and the corresponding column of Table II probably represents the best estimate of the amount of atmospheric absorption due to oxygen.

At Massachusetts Institute of Technology measurements on the oxygen absorption are in progress which, because of improved frequency stabilization, are more refined than any previously attempted. Only a preliminary report of the results has been published,[16] and so we shall not make any attempt to compare the theory with them in any detail. The absolute value of the absorption, according to these new measurements, seems to indicate a line breadth $\Delta\nu/c=0.04$ cm^{-1}. On the other hand, there are fluctuations in the attenuation when the wave-length is changed which are understandable only if $\Delta\nu/c\leqq 0.02$ cm^{-1}. Otherwise the resonances to individual lines responsible for wiggles in our Fig. 1 would not be detectable. The new work does not extend to pressures below 40 cm and so cannot test curves of the type shown in our Figs. 3–4. We should caution that it should not be regarded as highly surprising if the detailed shape of the absorption curve is somewhat different from that calculated by means of our formulas. They are based on the structure factor (2), which in turn presupposes that the collisions are of infinitely short duration. Actually, impacts are not of this idealized character. There is a wealth of literature which tries in one way or another to allow for gradual and overlapping collisions. One of the most recent and comprehensive papers on this subject is that by Lindholm.[13] The more elaborate theories, however, involve undetermined constants associated with the character of the intermolecular forces, and also lead to exceedingly complicated analytical expressions for the line shape. To calculate the final result when there is a plethora of overlapping lines would hence be quite laborious, and so until the experimental data become very accurate and comprehensive, it seems best to use formulas based on the limiting Lorentz concept of infinitely short collisions, leading to the simple structure factor (2). Ultimately, however, microwave measurements, should be the method *par excellence* of testing refined theories of pressure broadening, and obtaining light on related questions concerning the nature of collisions, intermolecular forces, etc. Obviously the theory can be tested far more readily and comprehensively in the microwave region than in the optical domain where the line-breadth is so much smaller compared to frequency.

In closing we would like to emphasize that on the whole the agreement between theory and experiment must be regarded as exceedingly gratifying. Beringer measured absolute values without an undetermined calibration constant, and still the discrepancy between theory and experiment is not more than ten percent or so. The situation is thus quite different from that encountered in many measurements of the absorption coefficients of gases in the infra-red region, which have often disagreed with theory by a factor 10 or so.

[15] R. H. Dicke, R. Beringer, R. L. Kyhl, and A. B. Vane, Phys. Rev. **70**, 340 (1946).

[16] See experiments by Meng, Ingersoll, and Strandberg summarized on p. 19 of Final Report under Contract OEMsr-262, NDRC Div. 14, Research Lab. of Electronics, M.I.T.

PHYSICAL REVIEW VOLUME 71, NUMBER 7 APRIL 1, 1947

The Absorption of Microwaves by Uncondensed Water Vapor*

J. H. VAN VLECK
Harvard University, Cambridge, Massachusetts

(Received December 27, 1946)

The absorption due to uncondensed water vapor in the short microwave region is computed by means of quantum mechanics. The attenuation is attributed to two causes: (a) a single line $\lambda = 1.35$ cm, and (b) the combined residual effect of all the other lines, whose wave-lengths are too short for resonance. There is a sharp peak in the absorption due to (a) at 1.35 cm, amounting to about 0.2 db/km per gram of H_2O per cubic meter. The absorption caused by (b) is inversely proportional to the square of the wave-length. The theory is compared with existing microwave data on damp air, on pure water vapor at low pressures, and on steam. From these data one can determine the precise value of the resonance frequency in (a) and the line-breadth. Until recently these constants could only be roughly estimated from infra-red measurements. On the whole the theory and experiment agree satisfactorily, except that the attenuation due to the residual effect (b) is apparently about four times as large as predicted. Possible causes of this discrepancy are speculated upon—perhaps the Lorentz model of infinitely sharp collisions which we use is too simple. Finally a curve is included of the predicted absorption in the millimeter region, where water vapor is much more opaque than at centimeter wave-lengths, and new resonances come into play.

INTRODUCTION

IN the present paper we consider only the absorption due to uncondensed water vapor. If any condensation is present, as in mists, rains, etc., there is also the absorption due to the drops of water, whose effect has been calculated by Stratton and others.[1] In heavy rains, the absorption due to the Stratton effect can be larger than that computed in the present article, but in any event the absorption due to the uncondensed vapor is always present in addition to any attenuation due to the formation of drops.

The absorption by the uncondensed vapor can only be treated by quantum mechanics, as it is necessary to know the rotational energy states of the water molecule in detail. A sharp contrast is thus presented to the absorption due to the condensed liquid. The latter can be handled entirely by classical theory if one knows the radius of the droplets and the empirical complex dielectric constant of water.

In order to have appreciable absorption by the water molecule, it is essential that there be very closely spaced energy levels which can combine with each other by means of electric dipole radiation. If the levels are not close together, the resonance region will be at frequencies far too high to give any appreciable attenuation of microwaves. It is also obviously necessary that transitions between the nearby states be permitted by the ordinary dipole selection rules of quantum mechanics, since quadrupole effects are of negligible intensity at long wave-lengths. The table of energy levels for the water molecule is honeycombed with pairs of nearly coincident levels, but in practically all cases they cannot combine with each other, owing to the selection rules resulting from symmetry classifications. According to quantum mechanics, the rotational energy levels of the water molecule are of four different symmetry types, which are usually designated as $++$, $--$, $+-$ and $-+$. (The origin of the notation is in the sign behavior of the wave functions under certain kinds of reflections, into whose details we need not enter here.[2]) The selection rules permit the rotational quantum number J to change only by not more than one unit, and allow $++$ to combine only with $--$, and $+-$ only with $-+$. Nonresonant absorption due to diagonal matrix

* The research basic to the present paper was performed mainly while the writer served as consultant for the M.I.T. Radiation Laboratory, NDRC Dv. 14, contract 262. See especially its reports 43-2 and 664.

[1] J. Stratton, Proc. Inst. Rad. Eng. 18, 1064 (1930); for more recent literature see J. W. Ryde, and D. Ryde, Rep. Nos. 7831, 8516, and 8670 of the British General Electric Company; also article by H. Goldstein in Chap. VIII of Book 13 of the forthcoming M.I.T. Radiation Laboratory Series, *Microwave Propagation*.

[2] See D. M. Dennison, Rev. Mod. Phys. 12, 189 (1940).

elements cannot exist in H_2O, for if the initial and final states are identical, they have the same symmetry classification, and hence diagonal matrix elements for the electric dipole moment are wanting. The reason that the non-resonant or diagonal effect is present in O_2, is that the absorption in O_2 is caused by the magnetic dipole moment, for which the rule is that + combines with + and − with −.

Among the levels of the water molecule which are excited at ordinary temperatures, there is only one pair whose members can combine and at the same time are so closely spaced as to give resonance in the microwave region. This pair is formed by the so-called 5_{-1} and 6_{-5} states. According to infra-red measurements as interpreted by Dennison,[2] the energy values of these states, referred to the ground level as origin, are as follows

5_{-1}	446.39 cm^{-1}
6_{-5}	447.17 cm^{-1}

If these figures are accepted, the connecting transition should have a wave-length $1/0.78 = 1.28$ cm. It is, however, obvious that the small energy difference which is involved cannot be determined with precision from infra-red data. In an earlier paper, based on the same experimental work, Randall, Dennison, Ginsburg, and Weber[3] gave the energy levels at 446.52 and 447.20 cm, in which case the wave-length becomes $1/0.68 = 1.47$ cm. The discrepancy 0.19 cm between the two estimates of the wave-length is probably a rough measure of the accuracy of the infra-red data. The wave-length is now known with precision from measurements made with new microwave techniques. Becker and Autler[4] give the wave-length as 1.344 cm, with an estimated error of a little less than one percent. Very recently, by working at low pressures, Townes and Merritt[5] have achieved a still higher degree of accuracy, which they list as two parts in ten thousand, and find the wave-length to be 1.3481 cm.

It is the purpose of the present paper to calculate not only the absorption due to the 1.35 cm line, but also the influence of other lines, of much shorter wave-length, on the attenuation in the microwave region. We shall also see that other resonances come into play if the wave-length is reduced to the millimeter rather than centimeter region.

It is interesting to note now much the whole status of the subject has changed since the writer wrote his first report[6] some five years ago. At that time, no relevant measurements had been made on microwave absorption, and the attenuation could only be predicted. Furthermore the precise amount of absorption could not be calculated with much precision, since there was uncertainty not only in the resonance wave-length but also in the so-called line-breadth constant which tells how much the lines are broadened by collision. Now, however, the constants are quite well known, and correspondingly the emphasis has shifted from prediction of effects not yet observed to comparison of the details of the theory with experiment in the hopes of getting more insight into the mechanism of damping by collision. There are still no measurements for millimeter wave-lengths, but interesting experiments in this domain should be possible when techniques are developed to open it to observation.

FORMULAS FOR THE ABSORPTION

Effect of the 1.35 *cm line.* First we shall give the expression for the absorption due to the line at 1.35 cm. The relevant theory is that given in the preceding article on the absorption by oxygen,[7] but with, of course, the understanding that the dipole moment is now electric rather than magnetic. As we are dealing with but a single line, the expression (5) of our previous paper for the absorption

[3] Randall, Dennison, Ginsburg, and Weber, Phys. Rev. **52**, 160 (1937).
[4] G. E. Becker and S. H. Autler, Phys. Rev. **70**, 300 (1946).
[5] C. H. Townes and F. R. Merritt, Phys. Rev. **70**, 558 (1946).
[6] J. H. Van Vleck, report 43-2 of the M.I.T. Radiation Laboratory.
[7] J. H. Van Vleck, Phys. Rev. **71**, 413 (1947).

γ in db/km for microwaves of wave-length λ becomes

$$\gamma_{1.35}=\frac{\alpha}{\lambda^2}\left[\frac{\Delta\nu/c}{(1.348-1/\lambda)^2+(\Delta\nu/c)^2}+\frac{\Delta\nu/c}{(1.348+1/\lambda)^2+(\Delta\nu/c)^2}\right], \tag{1}$$

with[8]

$$\alpha=10^6(\log_{10}e)(8\pi^2cN/3GkT)\mu_{1.35}^2\exp[-E(5,-1)/kT], \tag{2}$$

$$G=\sum_{J=0}^{\infty}\sum_{\tau=-J}^{J}[2-(-1)^{|\tau|}](2J+1)\exp[-E(J,\tau)/kT]. \tag{3}$$

Here N is the number of water molecules per cc, $\Delta\nu$ is the line-breadth constant representing the effect of broadening by collision, and $E(J,\tau)$ denotes the energy of a state specified by quantum numbers J and τ in Dennison's notation. The factor which immediately follows the summation sign in (3) and which has alternately the values 1 and 3 is caused by nuclear spin. Since $E(5,-1)=447$ cm^{-1}, the Boltzmann factors for the states involved in the 1.35 cm line can be written as $10^{-278/T}$. The factor $\mu_{1.35}^2$ in (3) is the "line-strength" of the electric dipole moment for the transition $5_{-1}\rightarrow 6_{-5}$ inclusive of the augmentation of the statistical weight by a factor 3 due to nuclear spin. The value of $\mu_{1.35}^2$ can be calculated by means of the quantum mechanics of the asymmetrical top applied to the water molecule. We originally[6] computed $\mu_{1.35}^2$ to be $0.17\mu_0^2$, where $\mu_0=1.84\times10^{-18}$ e.s.u. is the permanent dipole moment of the H_2O molecule. The more exact calculations of King, Hainer, and Cross, given in the following article,[9] yield $\mu_{1.35}^2=0.165\mu_0^2$. The partition function G can be evaluated numerically since the energy levels of the water molecule are known from infra-red spectroscopic analysis. At 293°K, the value of G is 170.

When the numerical information given in the preceding paragraph is employed, the constant α defined in (2) acquires at 293°K the value

$$\alpha=0.00350\rho \quad \text{or} \quad \alpha=2.63q, \tag{4}$$

where ρ is the number of grams of water vapor per cubic meter. In the alternative form, q is the fraction of air molecules that are water ones, or, in other words, the ratio of the vapor pressure of water to atmospheric pressure.

Residual Effect of Other Lines. The 1.35 line just discussed is the only one that has a resonance at wave-lengths longer than 1 cm. However, the lines whose resonances are at shorter wave-lengths give a small contribution γ_{RES} to the attenuation in the centimeter region, which we shall term the residual absorption. It may be calculated, to a sufficient approximation, under the assumption that the incident frequency is small compared to the resonance frequency. In other words, the structure factor given in Eq. (2) of the preceding paper[7] may be replaced by $2\nu\cdot\Delta\nu/\pi\nu_{ij}^3$. The general formula (1) of that paper then becomes[10]

$$\gamma_{RES}=\lambda^{-2}\Delta\nu\cdot10^6(\log_{10}e)(16\pi^2Nc/3hG)\Sigma_{J,\tau,J',\tau'}(\mu_{J\tau,J'\tau'}^2/\nu_{J\tau,J'\tau'}^3)\exp[-E(J,\tau)/kT], \tag{5}$$

where $\mu_{J\tau,J'\tau'}^2$ means the line-strength, inclusive of nuclear spin, associated with the transition $J,\tau\rightarrow J',\tau'$. The numerical values of the line-strengths, which are computed by means of the quantum mechanics of the unsymmetrical top, are tabulated in the following paper by King, Hainer, and Cross up to $J=6$, inclusive. From the approximate estimates of Randall, Dennison, Ginsburg, and

[8] Equation (5) of the preceding paper involves all pairs of states symmetrically, so that at first sight it would seem as though our Eq. (2) should contain a Boltzmann factor for the 6, −5 as well as the 5, −1 state. However, this factor is very nearly the same for both states, so we have included a single factor and multiplied by 2.

[9] G. W. King, R. M. Hainer, and P. C. Cross, Phys. Rev. 71, 433 (1947).

[10] For the transitions in which $|\nu_{J\tau,J'\tau'}|$ is small compared with kT/h we may follow a procedure explained in connection with Eq. (4) of the preceding article, and replace the factor $1/\nu_{J\tau,J'\tau'}^{-3}$ in (5) by $1/2kT\nu_{J\tau,J'\tau'}^2$. The need for distinguishing between positive and negative frequencies, and the difficulty of nearly compensating terms, which appears in (5) as it stands, is then avoided. Some of the transitions, however, involve too high frequencies to permit this simplification. It is instructive to examine the magnitude of the centroid frequency $\bar{\nu}$ defined by equating the quadruple sum in (5) to $G\mu_0^2/2kT\bar{\nu}^2$. The numerical value of the sum is such that $\bar{\nu}/c=47$ cm^{-1}.

Weber[3] on the intensities of water lines, or otherwise, it is found that the error involved in omitting the levels higher than $J=6$ is inconsequential, of the order of a percent or so. When the sum in (5) is computed with the aid of the results of King, Hainer, and Cross, Eq. (5) becomes at 293°K

$$\gamma_{RES}=0.0116\rho\Delta\nu/\lambda^2 \quad \text{or} \quad \gamma_{RES}=8.7q\Delta\nu/\lambda^2. \tag{6}$$

In a previous report,[11] we gave the constant as 9.65 instead of 8.7. The discrepancy of about 10 percent is presumably due to the fact that we previously calculated the intensities accurately only up to $J=3$, and thereafter used an approximate method due to Dennison.

VALUE OF THE LINE-BREADTH CONSTANT $\Delta\nu$

Before the absorption can be obtained numerically from (1)–(6), it is necessary to know the value of the constant $\Delta\nu$. In 1942, when the author began his study[6] of the water absorption he considered 0.3 cm^{-1} to be the best choice for $\Delta\nu/c$. This value was derived from experimental measurements by Cornell[12] on the infra-red spectrum of water vapor, which gave 0.20–0.28, and from somewhat higher estimates by Dennison (private communication). In view of the importance of the quantity $\Delta\nu/c$ for microwave physics and problems of radar propagation, improved measurements of the breadth of water-vapor lines in wet air were made by Adel[13] in the infra-red laboratory at the University of Michigan during 1944, and gave at first $\Delta\nu/c=0.17$, later 0.11 cm^{-1}. The error in the final value 0.11 cm^{-1} was estimated not to exceed 0.02 cm^{-1}. It has, however, subsequently proved possible to determine the breadth of the line more accurately with microwave than with infra-red technique, inasmuch as in the microwave region, the breadth is comparable with the frequency of the line itself. The experiments by Becker and Autler[4] at the Columbia Radiation Laboratory reveal the shape of the line in detail, and indicate that, for low densities of water vapor, the best choice of the parameter $\Delta\nu/c$ is 0.087 cm^{-1}, in agreement with the Michigan data to within the limits of accuracy of the latter. An interesting result of the Columbia experiments is that at atmospheric total pressure, the line breadth $\Delta\nu$ depends somewhat on the partial pressure of the water vapor. For instance, at a content of 50 grams/m^3, the value of $\Delta\nu/c$ is 0.107, instead of 0.087 cm^{-1}, the extrapolated value for air with an infinitesimal amount of moisture. As high a density as 50 grams per cubic meter cannot be obtained for water vapor at ordinary temperatures, and was possible in the experiments of Becker and Autler only because the temperature was raised to 45°C. The density of saturated water vapor at ordinary temperatures is about 18 grams/m^3, corresponding by interpolation to a $\Delta\nu/c$ approximately 0.094 cm^{-1}.

TABLE I. γ/ρ gives the absorption in db/km per g of water per cubic meter at 293°K for $\Delta\nu/c=0.1$ cm^{-1}. The contribution of the 1.35 cm line and the residual effect of other lines are denoted, respectively, by $\gamma_{1.35}$ and γ_{RES}.

λ	ν/c	$\gamma_{1.35}/\rho$	γ_{RES}/ρ
10 cm	0.01 cm^{-1}	0.0000133	0.000013
3	0.333	0.000256	0.00013
2	0.50	0.00136	0.00029
1.5	0.667	0.0101	0.00052
1.428	0.700	0.0147	0.00057
1.350	0.740	0.0193	0.00064
1.250	0.800	0.0168	0.00074
1.111	0.900	0.0082	0.00095
1.00	1.000	0.0047	0.00116
0.667	1.500	0.00150	0.00262
0.500	2.000	0.00107	0.0047
0.333	3.000	0.00085	0.013

NUMERICAL VALUES OF THE ABSORPTION

In Table I we use the round value 0.1 cm^{-1} for $\Delta\nu/c$, for the sake of simplicity, since it reflects pretty closely the combined results of the Michigan and Columbia experiments. The third column gives the absorption due to the 1.35 cm line, obtained from Eq. (1), while the

[11] J. H. Van Vleck, report 664 of the M.I.T. Radiation Laboratory. A still earlier report gave the factor as 19.3 rather than 9.65 because the original Lorentz collision theory had not been properly modified to allow for thermal equilibrium at impact.

[12] S. D. Cornell, Phys. Rev. **51**, 739 (1937). We should mention that although the line-breadths reported by Cornell for water vapor in air are apparently too high, his values for steam are compatible with the results of Townes and Merritt and of Becker and Autler on H_2O-H_2O collision cross sections, which we discuss later.

[13] A. Adel, NDRC Div. 14, Rep. No. 320, and especially the supplement thereto. His "half-breadth" is twice our quantity $\Delta\nu/c$.

fourth column gives the residual effect, embodied in Eq. (6), which arises from lines of shorter wave-length. The actual absorption is, of course, the sum of that in the two columns.

COMPARISON WITH EXPERIMENT

The existence of the absorption due to the 1.35 cm line of water has been demonstrated by various investigators in a variety of ways. There is a very noticeable improvement with time in the refinement of method and resulting sensitivity.

Transmission Experiments. The simplest way to show that the absorption is present is merely to verify that if radar signals are propagated over long distances, the attenuation is greater on damp than on dry days. Experiments of this character were made by Bender[14] and collaborators of the M.I.T. Radiation laboratory in aeroplanes in southern climates of high humidity. Even with the best concomitant meteorological data to determine the water content of the atmosphere, the precision cannot be made high. Nevertheless, the experiments do demonstrate unequivocably the reality of the absorption, and show that within the limits of error its magnitude is compatible with the theoretical values calculated on the basis of $\Delta\nu/c=0.10$ cm^{-1}.

Radiometer Method. A very ingenious method for detecting the absorption due to the column of water vapor in the earth's atmosphere has been developed by Dicke and collaborators.[15] It is based on the fact that the "effective temperature" or Johnson noise level of a microwave antenna is determined by the requirement of balance between the absorption and emission of the antenna. The exchange of radiation of radiation with the water vapor makes the temperature different from what it would be were the microwaves propagated through the air without attenuation. For a full account of the interesting theory involved, the reader is referred to the original paper.[15]

Dicke and his colleagues made measurements at wave-lengths of 1, 1¼, and 1½ cm. They found at these wave-lengths absorptions amounting to respectively 0.011, 0.026, and 0.014 when expressed in db/km per gram of H_2O per cubic meter. The corresponding theoretical values given in our Table I, are 0.006, 0.018, and 0.011. The agreement would not be improved if a somewhat lower line breadth, say 0.009 rather than 0.010 cm^{-1}, were used.

Cavity Method. The most accurate existing determinations of the absorption due to water vapor at atmospheric total pressure are probably those of Becker and Autler.[4] By means of thermocouples, they studied how the "Q" of a cavity fed by microwaves was influenced by changing the moisture content of the air in the cavity. In a theoretical paper, Lamb[16] showed that the absorption coefficient can be deduced from their measurements.

The values of the attenuation yielded by the Columbia experiments are somewhat lower than those obtained by the radiometer method, but still are appreciably higher than predicted theoretically. Figure 1, which is reproduced from the paper of Becker and Autler, shows the experimental results, and also the theoretical curve calculated on the assumption $\Delta\nu/c=0.087$. In Fig. 1, the ordinate is not the absorption coefficient, but rather the absorption divided by the square of the wave number. This kind of plot is advantageous, as then the residual effect, due to lines other than 1.35 cm, becomes independent of frequency. In fact, Fig. 1 shows pretty clearly

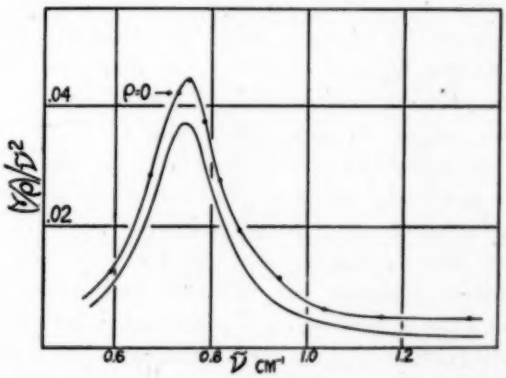

FIG. 1. Dependence of absorption on the wave number ν/c in the vicinity of the resonance at $\lambda=1.35$ cm. The ordinates are the absorption in db/km per gram of H_2O/m^3, divided by the square of the wave number. The upper curve is an experimental one by Becker and Autler for very small water content. The lower curve is calculated from theory on the assumption $\Delta\nu/c=0.087$ cm^{-1}.

[14] R. S. Bender, A. E. Bent and J. W. Miller, Report 729 of the M.I.T. Radiation Laboratory.

[15] R. H. Dicke, R. Beringer, R. L. Kyhl, and A. B. Vane, Phys. Rev. 70, 340 (1946).

[16] W. E. Lamb, Jr., Phys. Rev. 70, 308 (1946).

that the discrepancy between theory and experiment is caused by the residual absorption rather than to the 1.35 cm resonance. If the theoretical ordinate is raised by a uniform amount, then the theoretical curve can be made to coincide with the experimental one within the limits of error of the latter. Such an adjustment, however, involves use of a constant of proportionality in (6) which is between 4 and 5 times larger than the theoretical value 0.0116.

Observations in Water Vapor at Low Pressures. Townes and Merritt[5] have devised a wave-guide method to observe the absorption of pure water vapor at a pressure of only 0.1 mm, where the 1.35 cm line is exceedingly sharp. In their experiments, the resonance wave-length could be determined with high precision, but the attenuation is so weak that the absolute value of the absorption can only be found with an accuracy of 50 percent, or so. The experimentally estimated line-strength agrees with theory within 20 percent, or much less than the limits of error. Owing to the low pressure and resulting very small line-breadth, the residual absorption caused by lines other than 1.35 cm is completely negligible in the cm region. The line-breadth $\Delta\nu$ can be measured to within 20 percent. If it is assumed that $\Delta\nu$ is proportional to pressure, the magnitude of $\Delta\nu/c$ at 76 cm is found to be 0.36 cm^{-1}. This value of the parameter representing the effect of collision-broadening is one appropriate to H_2O-H_2O collisions. Hence we should not expect it to agree with the value 0.1 cm^{-1} which we used in Table I, as there we were interested in relatively low concentrations of water vapor in air, where the collisions are dominantly H_2O-N_2 or H_2O-O_2. By observing how much the line is broadened when the concentration of water is increased to 50 grams per cubic meter, Becker and Autler were able to estimate roughly the collision parameter for H_2O-H_2O collisions as a second-order effect. They concluded that $\Delta\nu$ was about 4.7 times as large for H_2O-H_2O as for H_2O-air collisions. Since they found $\Delta\nu/c$ to be 0.087 cm^{-1} for H_2O-air impacts, their value of $\Delta\nu/c$ for H_2O-H_2O is 0.42. The discrepancy of about 20 percent compared with the extrapolated value 0.36 of Townes and Merritt is well within the limits of error, which amounts perhaps to 50 percent since the H_2O-H_2O effects enter only weakly even in saturated air. Thus we can say that within the experimental error, $\Delta\nu$ is proportional to the pressure p even when the values of p are as diverse as 0.1 mm and 76 cm.

Observations on Steam. Saxton[17] has measured the absorption of steam at 1.6 cm. Here, of course, the relevant collision cross section is for H_2O-H_2O rather than H_2O-air impacts. Consequently, until recently, no information was available on the line-breadth constant. In a previous report,[11] the writer pointed out that the absorption reported by Saxton was larger than could be explained with any reasonable selection of $\Delta\nu/c$. In line with this remark, use of the subsequent value 0.36 of Townes and Merritt gives a theoretical absorption considerably smaller than found by Saxton, provided it is assumed that the residual effect is given correctly by Eq. (6) as it stands. However, if in the light of the Becker and Autler results shown in Fig. 1 it is assumed that the constant of proporrionality should be approximately four times as large as that 0.116 given in (6), then the calculated absorption[18] agrees adequately with Saxton's results. It turns out, if anything, to be a little too high, but the discrepancy is doubtless no more than the experimental error. Thus Saxton's measurements which previously were an enigma to the author, can be now regarded

[17] J. A. Saxton, Paper No. RRBS 17.

[18] Since Saxton's measurements are at 373° rather than 293°K, one cannot apply Eqs. (4) and (6) to them without a temperature correction. At a given pressure the absorption γ/N per molecule varies with temperature according to theory in the following fashion. At resonance $\gamma_{1.35}/N$ is proportional to $T^{-3}10^{-278/T}$, and well away from resonance, to $T^{-3}10^{-278/T}$. On the other hand, γ_{RES}/N is proportional to $T^{-3/2}$. These statements follow from Eqs. (2) and (6) when allowance is made for the fact that $\Delta\nu$ is proportional to T^{-1} at constant p. In (2), the partition function G may, for a rough approximation be considered proportional to $T^{3/2}$. (Explicit numerical calculations give the result that $G_{410}/G_{273}=1.70$ whereas $(410/273)^{3/2}=1.82$.) The temperature dependence of the sum in (5) may be regarded as the same as that of G/T since the centroid frequency defined at the end of footnote 10 varies but slowly with temperature.

The temperature corrections are not completely negligible even in the Columbia experiments, since they were made at 318° rather than 293°K. This explains why the ordinates of the theoretical curve in Fig. 1 are somewhat lower than would be calculated for 293°K as in Table I. The line-breadth $\Delta\nu/c=0.087$ cm^{-1} deduced from the Columbia experiments really applies to 318°. The corresponding value at 293°K is 0.091. This correction is smaller than the experimental error, and so we do not mention it elsewhere in the discussion.

as interesting additional evidence that the residual effect of other lines is greater than that given by (6). Because of the increased line breadth, this effect is relatively greater in steam than in damp air. In fact, at $\lambda = 1.6$ cm the influence of the 1.35 line is overshadowed by the combined residual contributions of other lines if the constant of proportionality in (6) is increased by a factor 4.

SPECULATION ON CAUSES FOR HIGHER RESIDUAL ABSORPTION

The problem for the theoretician is obviously to find a reason why the residual term, i.e., the attenuation due to lines of wave-length other than 1.35 cm, should be so much larger than we have calculated it to be. Any error in the estimation of the line-strengths by the quantum mechanics of the asymmetrical top is undoubtedly far too small to be relevant.[19] A conceivable explanation of the discrepancy, suggested to the writer by W. E. Lamb, is that different lines have different line-breadth constants. This might be the case, for instance, if due to resonance effects in energy exchange, the most effective collisions are those in which the colliding molecules merely exchange rotational states, and hence both have nearly the same Boltzmann factors, inasmuch as the energy transfer is small compared to kT. Then molecules in the populous states have larger line-breadths than those in less occupied ones, since they are more likely to collide with molecules of comparable energy. Thus the effective $\Delta\nu$ to be used in Eq. (6) might be larger than that involved in (1), since the important lines contributing to (5) involve more heavily populated states than the pair involved in the 1.35 cm line. The existing evidence, on the whole, seems to point against this effect being important enough to be the explanation of the trouble. For one thing, there is the fact that line-width measured by Adel[18] agrees fairly well with the value reported by Becker and Autler despite the Michigan and Columbia experiments being made on quite different spectral lines. Also no pronounced variation in line-breadth from line to line has come to light in the now extensive microwave measurements on the ammonia spectrum. Moreover, Townes and Merritt[5] find no great difference in line-breadth between two unrelated lines of H_2O and HDO, respectively.

The only alternative explanation that has occurred to us of why (6) could be wrong is that the collision theory of Lorentz, as slightly revised by Van Vleck and Weisskopf,[20] might be drastically incorrect in the wings of the lines. If the lines tail off much less rapidly away from resonance than predicted by the ordinary formulas, the effect of the lines of short wave-lengths might be stronger in the 1 cm region than (6) would indicate. As has been pointed out by Margenau, Lindholm, Foley, and others,[21] the Lorentz theory involves the idealization of treating the phase change at collision as infinitely sudden. More realistic models give complicated absorption curves which make the attenuation in the wings deviate from the Lorentz expression. It is not clear at present, however, whether the pressure at one atmosphere is high enough to make the modifications of the Lorentz formula really important. The fact that the quotient of line-breadth constant by pressure is the same at 0.1 mm and 76 cm within the limits of experimental error is presumptive but not conclusive evidence in favor of the Lorentz theory.

More study of the question, both experimentally and theoretically, is desirable. Lines should be observed further in the wings, and more measurements should be made on the pressure dependence of $\Delta\nu$. Studies should be made on how $\Delta\nu$ behaves from line to line when it becomes possible to extend the frequency range to embrace more lines. Thus microwave spectroscopy should furnish the clue to interesting theoretical questions connected with the mechanism of collision-damping.

---

[19] The calculations by means of the usual theory of the asymmetrical top do not include the corrections for centrifugal expansion, but this will, in all probability, increase the line-strength by not more than a percent or so,—very likely by only a few parts in a thousand.

[20] J. H. Van Vleck and V. F. Weisskopf, Rev. Mod. Phys. **17**, 227 (1945).

[21] H. Margenau, Phys. Rev. **48**, 755 (1935); E. Lindholm, Arkiv Math., Astron. Fys. **32A**, No. 17 (1945); H. M. Foley, Phys. Rev. **69**, 616 (1946). It should be particularly mentioned that Lindholm's theory gives a less rapid drop of the absorption away from resonance on the low frequency side than does the Lorentz theory, at least if the pressure is sufficiently high to make the divergence between the two theories appreciable. A less rapid drop will make the ordinary infra-red rotational lines of water absorb more strongly in the microwave region than (6) would predict.

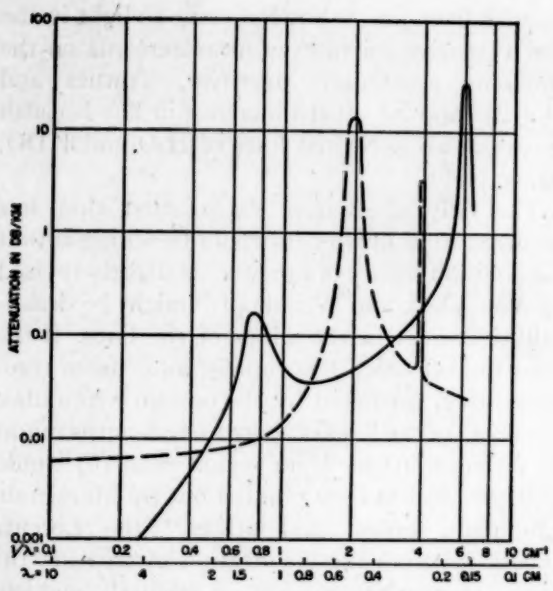

FIG. 2. Theoretical values of the atmospheric attenuation due to uncondensed water vapor and to oxygen at 293°K. The solid curve gives the absorption by water in an atmosphere containing 1.0 percent water molecules ($\rho=7.5$ g/m^3), for $\Delta\nu/c=0.1$ cm^{-1}. The dashed curve is the absorption by oxygen for $\Delta\nu/c=0.02$ cm^{-1}.

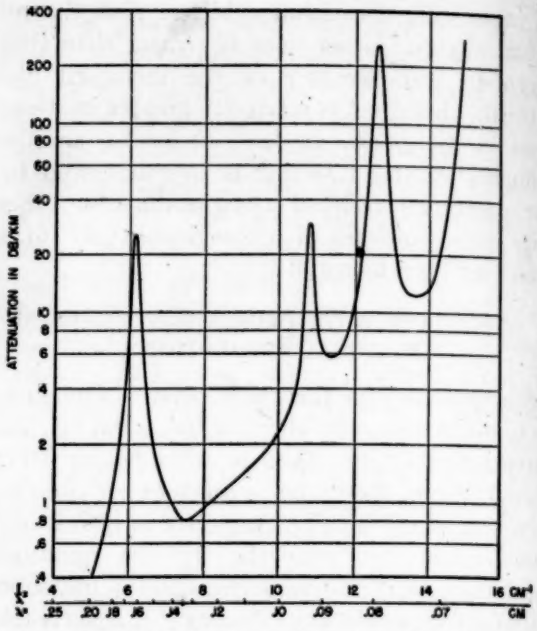

FIG. 3. Theoretical values of the absorption due to uncondensed water vapor in the millimeter region. The curve is for an atmosphere containing 1.0 percent water molecules ($\rho=7.5$ g/m^3), for $\Delta\nu/c=0.11$ cm^{-1}. There is no difficulty in adapting the results to other moisture contents, since short of saturation the absorption is directly proportional to ρ (neglecting the second-order effect of H_2O-H_2O collisions).

COMPARISON OF THE ATTENUATION BY OXYGEN AND BY WATER VAPOR

It is interesting to plot in the same figure the absorption by both the oxygen and the water vapor in the atmosphere as a function of wave number. This is done in Fig. 2. In order to have a basis of comparison, it is assumed that one percent of the molecules in the atmosphere are H_2O. In a temperate climate approximately this amount of water is present in an average day. When there is saturation, the content can be two or three times higher, and in the tropics even greater. There is, of course, then a corresponding increase in the absorption by the uncondensed water vapor.

ABSORPTION BY WATER VAPOR IN THE MILLIMETER REGION

Figure 3 shows the theoretical absorption due to water vapor in the millimeter region. For such short wave-lengths, the attenuation due to oxygen is relatively unimportant, and so has been omitted. As in Fig. 2, it is supposed that the atmosphere has one percent of water molecules. In Fig. 3, it has been assumed that the line-breadth $\Delta\nu/c$ is 0.11 cm^{-1}, the Michigan value, inasmuch as the subsequent Columbia data which somewhat reduce $\Delta\nu$ were not available at the time the calculations for Fig. 3 were made. In view of the uncertainties connected with the constant in (6) it has not seemed worth while to recompute the curve for say 0.10 cm^{-1}. Obviously Fig. 3 loses some of its quantitative significance if $\Delta\nu$ varies from line to line, rather than retaining a constant value as supposed in the calculations, or if the line-structure is more complicated than envisaged by the Lorentz theory. In the latter event, the curve will be affected mainly in the valleys rather than at the peaks. In any case, the graph shows the location of the important resonance maxima. It is to be emphasized that in drawing Fig. 3 (and also in the last line of Table I) it is necessary to use the expression for the absorption given in Eq. (1) of the preceding paper, rather than Eq. (5) or (6) of the present article, in which the structure factor has been simplified by assuming that $|\nu_{J'',J'_r}|\gg c/\lambda$. In the millimeter region one is too close to resonance with many of the lines to warrant this assumption. In fact, here the in-

fluence of the 1.35 cm line is negligible, and the contributions of other lines are dominant rather than residual. Figure 3 shows that there are some very strong resonances in the millimeter region, and that even in the valleys the absorption due to water vapor is so high as to make wave-lengths shorter than a millimeter or so useless for transmission except over exceedingly short distances. Incidentally, any modifications of the standard Lorentz theory such as we discussed previously will tend to make the absorption higher than shown in Fig. 3, especially in the valleys. Of course the opacity does not continue if the wave-length is reduced indefinitely. However, the opening up of the atmosphere to transmission occurs only when the frequency becomes high compared to the rotational frequencies of the water molecule, or in other words falls in the infra-red rather than microwave region.[22]

The writer wishes to express his thanks to Miss Mary Jane Farnsworth and Miss Eleanor Pressly for assistance in the calculations and curve-plotting for this and the preceding paper.

[22] For a calculation of the absorption of water vapor in the infra-red region, see W. M. Elsasser, Astrophys. J. 87, 497 (1938).

PHYSICAL REVIEW VOLUME 71, NUMBER 7 APRIL 1, 1947

Expected Microwave Absorption Coefficients of Water and Related Molecules*

GILBERT W. KING
Arthur D. Little, Inc., and Massachusetts Institute of Technology, Cambridge, Massachusetts

R. M. HAINER
Arthur D. Little, Inc.

AND PAUL C. CROSS
Brown University, Providence, Rhode Island

(Received December 31, 1946)

The microwave absorption of water and related molecules is of interest for practical and theoretical reasons. Since these molecules are asymmetric rotors, the occurrence of lines is a matter of chance and the calculation of their intensities is rather difficult. The line strengths of all transitions of H_2O up to $J=6$ have been calculated exactly and the transformation matrices are given explicitly. Van Vleck has shown that the observed intensity of the $6_{16}-6_{23}$ radar line can be accounted for theoretically, by use of the calculated value of the line strength. The microwave absorption of HDO and D_2O is also predicted with the use of the dipole moment and half-width of H_2O which are presumably the same in the isotopic molecules. In addition, it is pointed out that HDO has components along both the least and intermediate axes of inertia. The selection rules for the former are quite different from the latter (obtaining in H_2O, D_2O), and give rise to transitions between levels which are components of doubly degenerate levels in the limiting case of the symmetric rotor. This splitting varies in magnitude so that lines of HDO should appear throughout the radio and microwave regions. One of these lines has been discovered at 0.7441 cm^{-1}, and is interpreted as the $5_{33}-5_{32}$ transition predicted at 0.79 cm^{-1}. The calculated absorption coefficient is 26×10^{-6} cm^{-1} which is in excellent agreement with the observed value of 30×10^{-6} cm^{-1}. The microwave absorption of H_2S and H_2Se is discussed, and it is pointed out that HDS and HDSe will also have many lines in this region.

INTRODUCTION

THE pure rotation spectra of gaseous molecules extend to the microwave region, where measurements are of value in determinations of molecular structure on account of the relatively great accuracy in which positions and absolute intensities of lines can be determined. The microwave absorption of asymmetric rotors is of particular interest because of the difficulties of analysis of their infra-red vibrational-rotational bands. The spectra of water and similar molecules are of primary interest because the small moments of inertia result in only a few

* Part of this work (on H_2O) was done in 1942 for a thesis presented by R. M. Hainer in partial fulfillment of the requirements for the Degree of Doctor of Philosophy in the Graduate School of Brown University. The calculation of the pure rotational spectra of the other molecules was done on a contract of Arthur D. Little, Inc., with the Office of Naval Research.

lines appearing in the region, so that identification is relatively simple. The microwave spectra of heavier molecules will probably be quite complex, and identification of lines will necessitate elaborate experimentation, such as the determination of Stark effects and temperature coefficients. The three compounds H_2O, H_2S, H_2Se are considered here for various reasons. They form a family of closely related structure, of decreasing dipole moment. Their rotational energy levels are better known than for any other series. Theoretical factors affecting intensity and selection rules can be followed in the spectra of the isotopic molecules HDO, D_2O, etc., which are readily available. The calculation of the microwave absorption of H_2O was carried out by Van Vleck[1] because of its importance in radar. One of the difficult parts of the problem, namely the calculation of line strengths for transitions of the asymmetric rotor, was carried out by us independently, by matrix methods, and has been extended to account for the absorption of some related molecules which have recently been investigated.

In asymmetric-rotor molecules the spacing of energy levels does not follow a simple rule and the existence of permitted transitions in the microwave region accessible to present-day equipment is accidental. To predict or interpret microwave absorption it is necessary to determine all possible transitions between asymmetric-rotor levels about one wave number apart. Since weak lines can be detected, the calculations should be carried to high levels ($J \sim 12$ for water-like molecules) where the Boltzmann population is still appreciable.

The position of the lines depends on the differences between two relatively large numbers, the term values of the zero-vibrational state. These are not known from infra-red spectra with the accuracy to which their differences can be obtained in the microwave region. In fact, one of the purposes of making measurements in this region is to determine the differences in term values accurately. Term values are known for H_2O and D_2O, but for no other molecules of this type. The energy levels of the other molecules considered here have to be estimated from theory based on the rigid-rotor energy levels corrected for various distortions.

An expression for the absorption coefficient of a line in this region has recently been obtained.[2] For absorption at the resonance frequency ν (cm^{-1}) by a gas at partial pressure p (atm.) and absolute temperature T the coefficient is very nearly[3]

$$\alpha = (8\pi^2 N/3kTQ)\mu^2\nu^2 g e^{-E/kT}\Sigma|\Phi|^2 p/\Delta\nu \text{ cm}^{-1}. \quad (1)$$

A detailed discussion of the absorption is given in references 1 and 2.

Here N is Loschmidt's number corrected for temperature (so that Np is the number of molecules per cc in the light path), μ the permanent dipole of the rotor, Q the partition function at $T°K$, E the energy of the initial state. Weight factors due to nuclear spin are indicated by g, which has values for even and odd rotational states of 1 and 3 for H_2X, 6 and 6 for HDX, 6 and 3 for D_2X, X being the central atom. The average of these weights (namely their sum divided by the symmetry number) is used in computing Q. The factor $\Sigma|\Phi|^2$ is the line strength, defined as the squares of the elements of the direction-cosine matrices summed over the Zeeman components and three directions of space. Since the transition probabilities of the asymmetric rotor cannot be approximated by the symmetric-rotor values, especially when "forbidden" lines are considered, it is necessary to calculate the true values. A method of calculating line strengths and a table of values for certain degrees of asymmetry of the rotor have been given.[4] In effect then, the line strengths can be obtained accurately enough, although for the special case of H_2O the line strengths have been calculated for the particular degree of asymmetry in that molecule (Table I).

Thus all the quantities in (1) are known fairly accurately except for the mean free time between collisions, $1/(2\pi\Delta\nu)$. This factor arises from the line shape factor,[2] in which $\Delta\nu$ can be considered as the half-width at half-intensity. Simple kinetic

[1] J. H. Van Vleck, Phys. Rev. 71, 425 (1947).

[2] J. H. Van Vleck and V. F. Weisskopf, Rev. Mod. Phys. 17, 227 (1945).

[3] Actually the peak occurs at the maximum of the function $\nu\nu_{ij}f(\nu_{ij}, \nu)$ of Eq. (13) of reference 2. A correction must be made if $\Delta\nu$ is not very much smaller than ν.

[4] G. W. King, R. M. Hainer, and P. C. Cross, J. Chem. Phys. 11, 27 (1943) and 12, 210 (1944).

theory predicts[5] and experiment indicates that $\Delta\nu$ is proportional to the total pressure P (atm.) so it can be written $P\Delta\nu_0$ where $\Delta\nu_0$ is the half-width for one atmosphere. The value of $\Delta\nu$ for H_2O in air has been determined[6] experimentally from an infra-red line as 0.11 cm^{-1}, and from microwave absorption itself as[7] 0.087 $(1+3.7p)$ cm^{-1}. For pure water vapor $\Delta\nu_0$ can be expected to be much higher, since polar water molecules probably have a much higher collision diameter than the non-polar oxygen and nitrogen molecules in air. This is demonstrated by the above equation obtained by Becker and Autler. From it the value of $\Delta\nu_0$ for pure water can be calculated as 0.41 cm^{-1}. Experiments with pure water vapor discussed below give a value of 0.357 cm^{-1}.

The values of $\Delta\nu_0$ for H_2S and H_2Se can be expected to be smaller than that for H_2O because of the smaller dipole moment of these molecules. Kinetic theory expresses $\Delta\nu_0$ as a product of certain well-known constants and the square of the "optical diameter" ρ,

$$\Delta\nu_0 = N(2kT/\pi)^{\frac{1}{2}}\rho^2((m+M)/mM)^{\frac{1}{2}} \qquad (2)$$

(m and M being masses of the absorbing and colliding molecules, respectively) so that the uncertain part of (1) can be expressed as the ratio $(\mu/\rho)^2$ which will probably be fairly constant for the series H_2O, H_2S, H_2Se. This is a point worth consideration when experimental half-widths have been obtained. However, the values of $\Delta\nu_0$ for the isotopic molecules in each series will be very nearly the same. Thus exact *relative* intensities for lines of H_2O, HDO, D_2O and H_2S, HDS, D_2S, etc., can be calculated independently of uncertainties in $\Delta\nu_0$.

All calculations presented in Table II are based on a uniform value of $\Delta\nu_0 = 0.1$ cm^{-1}. Since this appears as a simple factor, the value of the absorption coefficient for any other estimate of $\Delta\nu_0$ can be found easily.

In this way the order of magnitude of the absorption can be predicted fairly well. The exact value of the absorption coefficient of Eq. (1), can be obtained, however, if any line is actually observed, since $\Delta\nu$ can be directly measured as the half-width. In other words, the product $\alpha\Delta\nu$ can be measured experimentally and compared with a theoretical quantity that can be calculated accurately.

The values of α given in Table II are for the pure gas, so that $p=P$; and as mentioned above, for $\Delta\nu_0 = 0.1$ cm^{-1}. The coefficient for mixtures, such as water vapor in air, or in the equilibrium mixture of H_2O, HDO, and D_2O, can be computed by multiplying the tabulated value by the appropriate ratio of partial to total pressure p/P.

Finally, it should also be pointed out that the tabulated values are computed with the predicted position, ν_{calc}. Since even in the best case, of H_2O, the position is not quite as calculated, the absorption coefficient should be corrected for the observed frequency by multiplying by $(\nu_{obs}/\nu_{calc})^2$.

A temperature of 14.5°C was used in the calculations corresponding to $kT = 200$ cm^{-1}. To find the absorption at any other temperature T a slight correction would have to be applied to allow for the change in various quantities appearing in (1), namely T itself, N, Q, $\Delta\nu$, and the Boltzmann factor. The first four give a factor of $(287.7/T)^3$ which is compensated by the Boltzmann factor to a degree dependent on the lower energy level.

H_2O

The positions of lines of water vapor in the microwave region can be estimated from the term values[8] of the ground state, and those lying above 0.1 cm are listed in Table II*A*. The practical importance of the absorption of water vapor in the radar region of one centimeter led us to compute the transition probabilities very precisely. The probabilities based on the theory of the rigid rotor are of sufficient accuracy.

A method of calculating transition probabilities for the asymmetric rotor has been given.[4] Briefly it depends on the transformation of the known direction-cosine matrices for the symmetric rotor by the orthonormal matrix which diagonalizes the Hamiltonian of the asymmetric rotor. For a

[5] V. Weisskopf, Phys. Zeit. **34**, 1 (1933) and H. Margenau and W. W. Watson, Rev. Mod. Phys. **8**, 22 (1936).
[6] A. Adel, NDRC Report 320 and especially the supplement thereto.
[7] G. E. Becker and S. H. Autler, Phys. Rev. **70**, 300 (1946).
[8] H. M. Randall, D. M. Dennison, N. Ginsburg, and L. R. Weber, Phys. Rev. **52**, 160 (1937), and D. M. Dennison, Rev. Mod. Phys. **12**, 175 (1940).

TABLE I. Line strengths of all possible transitions between levels (through $J=6$) of the water-vapor molecule (dipole moment parallel to the axis of intermediate moment of inertia). The transitions are classified by sub-branches[4] which head the column in which the initial level can be found (identified by $JK_{-1},K_{1};\nu$) and whose final level is in the adjacent column. Thus each value in column 3 corresponds to two transitions, whose lower levels are in columns 1 and 2, respectively.

Transition		Exact value	Exact minus 4 pt. inter.
$\Delta_0 Q_{1,\bar{1}}$	$\Delta_0 Q_{\bar{1},1}$		
$1_{0,1;-1}$	$1_{1,0;1}$	1.5000	.0000
$2_{1,1;0}$	$2_{2,0;2}$	1.2594	−.0010
$3_{2,1;1}$	$3_{3,0;3}$	1.0921	−.0002
$4_{3,1;2}$	$4_{4,0;4}$	1.0883	.0059
$5_{4,1;3}$	$5_{5,0;5}$	1.1011	.0051
$6_{5,1;4}$	$6_{6,0;6}$	1.1117	.0034
$2_{0,2;-2}$	$2_{1,1;0}$	2.0739	.0010
$3_{1,2;-1}$	$3_{2,1;1}$	2.5434	.0073
$4_{2,2;0}$	$4_{3,1;2}$	2.1659	−.0231
$5_{3,2;1}$	$5_{4,1;3}$	2.0658	−.0106
$6_{4,2;2}$	$6_{5,1;4}$	2.0900	.0139
$3_{0,3;-3}$	$3_{1,2;-1}$	2.1809	−.0077
$4_{1,3;-2}$	$4_{2,2;0}$	3.6547	.0221
$5_{2,3;-1}$	$5_{3,2;1}$	3.4462	.0184
$6_{3,3;0}$	$6_{4,2;2}$	3.0719	−.0801
$4_{0,4;-4}$	$4_{1,3;-2}$	2.0369	−.0068
$5_{1,4;-3}$	$5_{2,3;-1}$	4.2239	−.0440
$6_{2,4;-2}$	$6_{3,3;0}$	4.8520	.1564
$5_{0,5;-5}$	$5_{1,4;-3}$	1.8994	.0325
$6_{1,5;-4}$	$6_{2,4;-2}$	4.2180	−.1800
$6_{0,6;-6}$	$6_{1,5;-4}$	1.8411	.0870
$\Delta_0 Q_{1,\bar{1}}$	$\Delta_0 Q_{\bar{1},1}$		
$2_{1,2;-1}$	$2_{2,1;1}$	0.8333	.0000
$3_{2,2;0}$	$3_{3,1;2}$	1.0360	−.0002
$4_{3,2;1}$	$4_{4,1;3}$	1.0831	−.0003
$5_{4,2;2}$	$5_{5,1;4}$	1.1007	.0005
$6_{5,2;3}$	$6_{6,1;5}$	1.1117	.0015
$3_{1,3;-2}$	$3_{2,2;0}$	1.2973	.0002
$4_{2,3;-1}$	$4_{3,2;1}$	1.8497	.0003
$5_{3,3;0}$	$5_{4,2;2}$	2.0248	−.0019
$6_{4,3;1}$	$6_{5,2;3}$	2.0855	−.0041
$4_{1,4;-3}$	$4_{2,3;-1}$	1.5659	−.0002
$5_{2,4;-2}$	$5_{3,3;0}$	2.4942	.0012
$6_{3,4;-1}$	$6_{4,3;1}$	2.8814	.0041
$5_{1,5;-4}$	$5_{2,4;-2}$	1.7088	.0001
$6_{2,5;-3}$	$6_{3,4;-1}$	2.9653	−.0054
$6_{1,6;-5}$	$6_{2,5;-3}$	1.7784	.0039
$\Delta_0 R_{1,1}$	$\Delta_0 P_{\bar{1},\bar{1}}$		
$0_{0,0;0}$	$1_{1,1;0}$	1.0000	.0000
$1_{0,1;-1}$	$2_{1,2;-1}$	1.5000	.0000
$2_{0,2;-2}$	$3_{1,3;-2}$	2.1571	−.0001
$3_{0,3;-3}$	$4_{1,4;-3}$	3.0069	.0021
$4_{0,4;-4}$	$5_{1,5;-4}$	3.9767	−.0016
$5_{0,5;-5}$	$6_{1,6;-5}$	4.9837	−.0152
$1_{1,0;1}$	$2_{2,1;1}$	1.5000	.0000
$2_{1,1;0}$	$3_{2,2;0}$	1.6667	.0000
$3_{1,2;-1}$	$4_{2,3;-1}$	1.9708	−.0005
$4_{1,3;-2}$	$5_{2,4;-2}$	2.4447	−.0032
$5_{1,4;-3}$	$6_{2,5;-3}$	3.1314	.0073
$2_{2,0;2}$	$3_{3,1;2}$	2.3947	.0004
$3_{2,1;1}$	$4_{3,2;1}$	2.3195	−.0010
$4_{2,2;0}$	$5_{3,3;0}$	2.3220	−.0022
$5_{2,3;-1}$	$6_{3,4;-1}$	2.4490	−.0020
$3_{3,0;3}$	$4_{4,1;3}$	3.3931	−.0005
$4_{3,1;2}$	$5_{4,2;2}$	3.2701	.0038
$5_{3,2;1}$	$6_{4,3;1}$	3.1529	.0024
$4_{4,0;4}$	$5_{5,1;4}$	4.3970	−.0014
$5_{4,1;3}$	$6_{5,2;3}$	4.2670	.0007
$5_{5,0;5}$	$6_{6,1;5}$	5.3998	−.0016
$\Delta_0 R_{1,\bar{1}}$	$\Delta_0 P_{\bar{1},1}$		
$1_{1,1;0}$	$2_{2,0;2}$	1.2444	.0006
$2_{2,1;1}$	$3_{3,0;3}$	2.3363	−.0302
$3_{3,1;2}$	$4_{4,0;4}$	3.3904	−.0025
$4_{4,1;3}$	$5_{5,0;5}$	4.3968	−.0025
$5_{5,1;4}$	$6_{6,0;6}$	5.3998	−.0021
$2_{1,2;-1}$	$3_{2,1;1}$	0.9225	−.0041
$3_{2,2;0}$	$4_{3,1;2}$	2.1653	.0078
$4_{3,2;1}$	$5_{4,1;3}$	3.2505	.0030
$5_{4,2;2}$	$6_{5,1;4}$	4.2648	−.0061
$3_{1,3;-2}$	$4_{2,2;0}$	0.6050	−.0019
$4_{2,3;-1}$	$5_{3,2;1}$	1.8396	−.0065
$5_{3,3;0}$	$6_{4,2;2}$	3.0678	.0263
$4_{1,4;-3}$	$5_{2,3;-1}$	0.3804	.0171
$5_{2,4;-2}$	$6_{3,3;0}$	1.4022	−.0427
$5_{1,5;-4}$	$6_{2,4;-2}$	0.2494	.0410
$\Delta_0 R_{3,\bar{1}}$	$\Delta_0 P_{\bar{3},1}$		
$2_{0,2;-2}$	$3_{3,1;2}$	0.0133	−.0003
$3_{1,2;-1}$	$4_{4,1;3}$	0.0045	.0006
$4_{2,2;0}$	$5_{5,1;4}$	0.0020	.0012
$5_{3,2;1}$	$6_{6,1;5}$	0.0013	.0010
$3_{0,3;-3}$	$4_{3,2;1}$	0.0512	.0009
$4_{1,3;-2}$	$5_{4,2;2}$	0.0231	−.0031
$5_{2,3;-1}$	$6_{5,2;3}$	0.0089	.0007
$4_{0,4;-4}$	$5_{3,3;0}$	0.0966	.0033
$5_{1,4;-3}$	$6_{4,3;1}$	0.0708	−.0019
$5_{0,5;-5}$	$6_{3,4;-1}$	0.1240	.0010
$\Delta_0 Q_{3,\bar{3}}$	$\Delta_0 Q_{\bar{3},3}$		
$3_{0,3;-3}$	$3_{3,0;3}$	0.0168	.0004
$4_{1,3;-2}$	$4_{4,0;4}$	0.0059	−.0013
$5_{2,3;-1}$	$5_{5,0;5}$	0.0018	−.0001
$6_{3,3;0}$	$6_{6,0;6}$	0.0008	.0007
$\Delta_0 Q_{3,\bar{3}}$	$\Delta_0 Q_{\bar{3},3}$		
$4_{0,4;-4}$	$4_{3,1;2}$	0.0483	.0031
$5_{1,4;-3}$	$5_{4,1;3}$	0.0317	−.0004
$6_{2,4;-2}$	$6_{5,1;4}$	0.0104	−.0053
$5_{0,5;-5}$	$5_{3,2;1}$	0.0631	−.0011
$6_{1,5;-4}$	$6_{4,2;2}$	0.0858	.0123
$6_{0,6;-6}$	$6_{3,3;0}$	0.0514	−.0084
$\Delta_0 Q_{3,\bar{3}}$	$\Delta_0 Q_{\bar{3},3}$		
$4_{1,4;-3}$	$4_{4,1;3}$	0.0012	.0000
$5_{2,4;-2}$	$5_{5,1;4}$	0.0011	−.0001
$6_{3,4;-1}$	$6_{6,1;5}$	0.0008	−.0001
$5_{1,5;-4}$	$5_{4,2;2}$	0.0036	.0000
$6_{2,5;-3}$	$6_{5,2;3}$	0.0044	.0000
$6_{1,6;-5}$	$6_{4,3;1}$	0.0059	.0001
$\Delta_0 R_{3,\bar{3}}$	$\Delta_0 P_{\bar{3},3}$		
$3_{1,3;-2}$	$4_{4,0;4}$	0.0017	.0000
$4_{2,3;-1}$	$5_{5,0;5}$	0.0016	−.0001
$5_{3,3;0}$	$6_{6,0;6}$	0.0012	−.0001
$4_{1,4;-3}$	$5_{4,1;3}$	0.0048	.0002
$5_{2,4;-2}$	$6_{5,1;4}$	0.0056	−.0003
$5_{1,5;-4}$	$6_{4,2;2}$	0.0076	.0005
$\Delta_0 R_{5,\bar{3}}$	$\Delta_0 P_{\bar{5},3}$		
$4_{0,4;-4}$	$5_{5,1;4}$	0.0001	.0001
$5_{1,4;-3}$	$6_{6,1;5}$	0.0000	.0000
$5_{0,5;-5}$	$6_{5,2;3}$	0.0002	.0000
$\Delta_0 R_{\bar{1},1}$	$\Delta_0 P_{1,\bar{1}}$		
$1_{1,1;0}$	$2_{0,2;-2}$	0.7557	−.0005
$2_{1,2;-1}$	$3_{0,3;-3}$	1.7441	.0040
$3_{1,3;-2}$	$4_{0,4;-4}$	2.8374	.0019
$4_{1,4;-3}$	$5_{0,5;-5}$	3.9184	−.0172
$5_{1,5;-4}$	$6_{0,6;-6}$	4.9646	−.0417
$2_{2,1;1}$	$3_{1,2;-1}$	0.3003	.0002
$3_{2,2;0}$	$4_{1,3;-2}$	0.8347	−.0078
$4_{2,3;-1}$	$5_{1,4;-3}$	1.6407	.0066
$5_{2,4;-2}$	$6_{1,5;-4}$	2.6812	.0425
$3_{3,1;2}$	$4_{2,2;0}$	0.1613	.0023
$4_{3,2;1}$	$5_{2,3;-1}$	0.4349	−.0032
$5_{3,3;0}$	$6_{2,4;-2}$	0.8606	−.0253
$4_{4,1;3}$	$5_{3,2;1}$	0.1193	.0028
$5_{4,2;2}$	$6_{3,3;0}$	0.3030	.0059
$5_{5,1;4}$	$6_{4,2;2}$	0.0990	.0023
$\Delta_0 R_{\bar{1},3}$	$\Delta_0 P_{1,\bar{3}}$		
$2_{2,0;2}$	$3_{1,3;-2}$	0.1015	.0000

TABLE I.—*Continued.*

Transition		Exact value	Exact minus 4 pt. inter.
$\Delta_e R\bar{1},3$	$\Delta_e P1,\bar{3}$		
$3_{2,1;1}$	$4_{1,4;-3}$	0.1224	−.0022
$4_{2,2;0}$	$5_{1,5;-4}$	0.0891	.0014
$5_{2,3;-1}$	$6_{1,6;-5}$	0.0549	.0131
$3_{3,0;3}$	$4_{2,3;-1}$	0.1316	.0003
$4_{3,1;2}$	$5_{2,4;-2}$	0.2622	.0026
$5_{3,2;1}$	$6_{2,5;-3}$	0.3117	−.0064
$4_{4,0;4}$	$5_{3,3;0}$	0.1165	−.0006
$5_{4,1;3}$	$6_{3,4;-1}$	0.2784	.0019
$5_{5,0;5}$	$6_{4,3;1}$	0.0987	−.0006

Transition		Exact value	Exact minus 4 pt. inter.
$\Delta_e R\bar{3},3$	$\Delta_e P3,\bar{3}$		
$3_{3,1;2}$	$4_{0,4;-4}$	0.0042	.0001
$4_{3,2;1}$	$5_{0,5;-5}$	0.0112	.0002
$5_{3,3;0}$	$6_{0,6;-6}$	0.0162	−.0007
$4_{4,1;3}$	$5_{1,4;-3}$	0.0020	−.0001
$5_{4,2;2}$	$6_{1,5;-4}$	0.0099	.0009
$5_{5,1;4}$	$6_{2,4;-2}$	0.0005	−.0002
$\Delta_e R\bar{5},5$	$\Delta_e P3,\bar{3}$		
$4_{4,0;4}$	$5_{1,5;-4}$	0.0002	.0000
$5_{4,1;3}$	$6_{1,6;-5}$	0.0006	.0000
$5_{5,0;5}$	$6_{2,5;-3}$	0.0002	.0000

Transition		Exact value	Exact minus 4 pt. inter.
$\Delta_e Q5,\bar{5}$	$\Delta_e Q\bar{5},5$		
$5_{0,5;-5}$	$5_{5,0;5}$	0.0000	.0000
$6_{0,6;-6}$	$6_{5,1;4}$	0.0002	.0001
$6_{1,5;-4}$	$6_{6,0;6}$	0.0000	−.0001
$\Delta_e Q5,\bar{5}$	$\Delta_e Q\bar{5},5$		
$6_{1,6;-5}$	$6_{6,1;5}$	0.0000	.0000
$\Delta_e R5,\bar{5}$	$\Delta_e P\bar{5},5$		
$5_{1,5;-4}$	$6_{6,0;6}$	0.0000	.0000
$\Delta_e R\bar{5},5$	$\Delta_e P5,\bar{5}$		
$5_{5,1;4}$	$6_{0,6;-6}$	0.0000	.0000

given degree of asymmetry, κ, the elements of this orthonormal matrix can be computed rather simply from the successive convergents of the continued fractions whose roots are the reduced (rigid-rotor) energy levels, $E(\kappa)$, although these are of no value in themselves since the term values of H_2O are known. Because of their importance in defining the orthonormal transformation, used in the computation of transition probabilities, and their use in the more general theory of vibration-rotation interaction, the $E(\kappa)$ for water are tabulated for convenience (Table III) together with the elements of the orthonormal matrices (Table IV) for all levels up to and including $J=6$. The matrices as given were tested by applying them to the Hamiltonian (in the form[4] of Type II^r). The non-diagonal elements were zero, and the diagonal gave the correct values of $E(\kappa)$, with an error in the fifth decimal of 2 or 3 for low J, rising to 50 in the case of the fourth order matrix of $J=6$.

As pointed out in reference 8 the exact values of rigid-rotor moments used in any such calculation have no meaning in the general theory, but form the basis of a framework on which elaborations can be added. The value of κ used was −0.436426, corresponding exactly to the moments used by Randall, Dennison, Ginsburg, and Weber[8] in their rigid-rotor calculations. The elements of the direction-cosine matrices were squared and summed over the Zeeman components and three directions in space to give the line strengths. Table I gives the values of the line strengths of all possible transitions in the pure rotation spectrum of water up to $J=6$ as calculated by the exact method (i.e., for the above value of κ).

Since the calculation of the orthonormal transformation matrix for a given molecule is tedious, the possibility of interpolating the table of line strengths previously given for $\kappa=\pm1$, ±0.5, 0 was investigated by comparing the four-point interpolated values for $\kappa=-0.436$ with the exact values found for water. The "true" minus interpolated values of the line strength are given in column 4 of Table I. Where the error is largest, the line strengths change very rapidly with κ. In these cases interpolation of the logarithms of the line strengths gives an adequate value. For example, the error in the case of the well-known $\Delta_e R\bar{1},3$ line[9] $6_{1,6;-5}-5_{2,3;-1}$ is 0.0131. A four-point interpolation of the logarithms reduces the error to 0.0014. The errors in column 4 were used to indicate the precautions to be taken in interpolating the line strength for the other molecules discussed in this paper.

No difficulty arises in computing the other factors in (1), except for the half-width, which, however, is obtained experimentally. Only one line will appear in the region at present open to experimental investigation. As is well known,

[9] The first two subscripts refer to the absolute values of K for the level in each of the two limiting cases of (prolate and oblate) symmetric rotors. This notation has a descriptive value discussed in the case of HDO. The difference between them is the commonly used τ-value, given as the third subscript.

TABLE II. Predicted absorption lines in the microwave regions. The absorption coefficient, α, is calculated for the predicted position ν and for $\Delta\nu_0 = 0.1$ cm^{-1}.

Sub-branch	Quantum number Upper	Quantum number Lower	Term values Upper	Term values Lower	Position (cm^{-1})	Line strength	α (10^{-6} cm^{-1})
			(*A*) H_2O				
$^{b,c}R\bar{1},3$	$6_{1,6;-5}$	$5_{2,3;-1}$	447.17	446.39	0.78	.0549	37.83
$^{b,c}R\bar{1},3$	$3_{1,3;-2}$	$2_{2,0;2}$	142.30	136.15	6.15	.1015	6838
$^{b,c}R\bar{1},3$	$10_{2,9;-7}$	$9_{3,6;-3}$	1293.80	1283.02	10.78	.0870	174.7
$^{b,c}R\bar{1},3$	$5_{1,5;-4}$	$4_{2,2;0}$	326.50	315.70	10.80	.0891	7544
			(*B*) D_2O				
$^{b,c}R\bar{1},1$	$5_{3,2;1}$	$4_{4,1;3}$	269.34	269.03	0.31	.1136	5.04
$^{b,c}R\bar{1},3$	$3_{1,3;-2}$	$2_{2,0;2}$	74.58	74.03	0.55	.1145	85.1
$^{b,c}P_{1,\bar{1}}$	$8_{7,2;5}$	$9_{6,3;3}$	880.18	879.50	0.68	.1900	1.92
$^{b,c}P_{1,\bar{3}}$	$8_{7,1;6}$	$9_{6,4;2}$	880.18	879.48	0.70	.1902	4.07
$^{b,c}P_{1,\bar{3}}$	$4_{4,0;4}$	$5_{3,3;0}$	269.04	267.41	1.63	.1133	281
$^{b,c}R\bar{1},3$	$4_{2,3;-1}$	$3_{3,0;3}$	158.29	156.46	1.83	.1328	361
$^{b,c}R\bar{1},3$	$6_{1,6;-5}$	$5_{2,3;-1}$	232.60	230.47	2.13	.0919	234
$^{b,c}R\bar{1},3$	$8_{5,4;1}$	$7_{6,1;5}$	671.50	668.83	2.67	.2138	95.5
$^{b,c}R\bar{1},1$	$8_{5,3;2}$	$7_{6,2;4}$	671.60	668.83	2.77	.2132	205
$^{b,c}P_{1,\bar{3}}$	$9_{8,1;7}$	$10_{7,4;3}$	1118.56	1115.45	3.11	.1713	11.1
$^{b,c}P_{1,\bar{1}}$	$9_{8,2;6}$	$10_{7,3;4}$	1118.56	1115.45	3.11	.1713	22.3
$^{b,c}R\bar{1},3$	$11_{2,10;-8}$	$10_{3,7;-4}$	794.33	791.02	3.31	.1020	76.1
$^{b,c}P_{1,\bar{3}}$	$6_{2,4;-2}$	$7_{1,7;-6}$	308.69	305.32	3.37	.0599	525
$^{b,c}P_{1,\bar{3}}$	$10_{9,1;8}$	$11_{8,4;4}$	1383.12	1378.56	4.56	.1557	11.7
$^{b,c}P_{1,\bar{1}}$	$10_{9,2;7}$	$11_{8,3;5}$	1383.12	1378.56	4.56	.1557	5.84
$^{b,c}P_{1,\bar{3}}$	$11_{10,1;9}$	$12_{9,4;5}$	1672.71	1668.15	4.56	.1428	1.26
$^{b,c}P_{1,\bar{1}}$	$11_{10,2;8}$	$12_{9,3;6}$	1672.71	1668.15	4.56	.1428	2.52
			(*C*) HDO				
$^{a,c}Q_{0,\bar{1}}$	$4_{4,0;4}$	$4_{4,1;3}$	405.19	405.19	0.00	7.1950	(498)[a]
$^{a,c}Q_{0,\bar{1}}$	$5_{5,0;5}$	$5_{5,1;4}$	623.35	623.35	0.00	9.1619	(213)
$^{a,c}Q_{0,\bar{1}}$	$6_{5,1;4}$	$6_{5,2;3}$	716.88	716.88	0.00	7.7244	(113)
$^{a,c}Q_{0,\bar{1}}$	$6_{6,0;6}$	$6_{6,1;5}$	888.28	888.28	0.00	11.1382	(68.9)
$^{a,c}Q_{0,\bar{1}}$	$7_{5,2;3}$	$7_{5,3;2}$	826.22	826.22	0.00	6.6753	(56.3)
$^{a,c}Q_{0,\bar{1}}$	$7_{6,1;5}$	$7_{6,2;4}$	997.34	997.34	0.00	9.6292	(34.5)
$^{a,c}Q_{0,\bar{1}}$	$7_{7,0;7}$	$7_{7,1;6}$	1199.96	1199.96	0.00	13.1285	(17.1)
$^{a,c}Q_{0,\bar{1}}$	$8_{6,2;4}$	$8_{6,3;3}$	1122.20	1122.20	0.00	8.4779	(16.3)
$^{a,c}Q_{0,\bar{1}}$	$8_{7,1;6}$	$8_{7,2;5}$	1324.58	1324.58	0.00	11.5106	(8.0)
$^{a,c}Q_{0,\bar{1}}$	$8_{8,0;8}$	$8_{8,1;7}$	1558.39	1558.39	0.00	15.0937	(3.27)
$^{a,c}Q_{0,\bar{1}}$	$9_{6,3;3}$	$9_{6,4;2}$	1262.92	1262.92	0.00	7.5516	(7.17)
$^{a,c}Q_{0,\bar{1}}$	$9_{7,2;5}$	$9_{7,3;4}$	1464.96	1464.96	0.00	10.2371	(3.54)
$^{a,c}Q_{0,\bar{1}}$	$9_{8,1;7}$	$9_{8,2;6}$	1698.56	1698.56	0.00	13.4556	(1.45)
$^{a,c}Q_{0,\bar{1}}$	$9_{9,0;9}$	$9_{9,1;8}$	1963.58	1963.58	0.00	17.0830	(0.49)
$^{a,c}Q_{0,\bar{1}}$	$10_{7,3;4}$	$10_{7,4;3}$	1621.19	1621.19	0.00	9.2432	(1.46)
$^{a,c}Q_{0,\bar{1}}$	$10_{8,2;6}$	$10_{8,3;5}$	1854.49	1854.49	0.00	12.1107	(0.60)
$^{a,c}Q_{0,\bar{1}}$	$10_{9,1;8}$	$10_{9,2;7}$	2119.30	2119.30	0.00	15.4105	(0.20)
$^{a,c}Q_{0,\bar{1}}$	$10_{10,0;10}$	$10_{10,1;9}$	2415.52	2415.52	0.00	19.0743	(0.00)
$^{a,c}Q_{0,\bar{1}}$	$11_{7,4;3}$	$11_{7,5;2}$	1793.30	1793.30	0.00	8.5070	(0.57)
$^{a,c}Q_{0,\bar{1}}$	$11_{8,3;5}$	$11_{8,4;4}$	2026.22	2026.22	0.00	11.0034	(0.23)
$^{a,c}Q_{0,\bar{1}}$	$11_{9,2;7}$	$11_{9,3;6}$	2290.77	2290.77	0.00	14.0118	(0.078)
$^{a,c}Q_{0,\bar{1}}$	$11_{10,1;9}$	$11_{10,2;8}$	2586.81	2586.81	0.00	17.3729	(0.00)
$^{a,c}Q_{0,\bar{1}}$	$11_{11,0;11}$	$11_{11;1;10}$	2914.22	2914.22	0.00	21.0670	(0.00)
$^{a,c}Q_{0,\bar{1}}$	$12_{8,4;4}$	$12_{8,5;3}$	2213.83	2213.83	0.00	10.1401	(0.083)
$^{a,c}Q_{0,\bar{1}}$	$12_{9,3;6}$	$12_{9,4;5}$	2478.02	2478.02	0.00	12.8206	(0.00)
$^{a,c}Q_{0,\bar{1}}$	$12_{10,2;8}$	$12_{10,3;7}$	2773.81	2773.81	0.00	15.9295	(0.00)
$^{a,c}Q_{0,\bar{1}}$	$12_{11,1;10}$	$12_{11,2;9}$	3101.05	3101.05	0.00	19.3408	(0.00)
$^{a,c}Q_{0,\bar{1}}$	$12_{12,0;12}$	$12_{12,1;11}$	3459.66	3459.66	0.00	23.0608	(0.00)
$^{a,c}Q_{0,\bar{1}}$	$5_{4,1;3}$	$5_{4,2;2}$	483.17	483.16	0.01	5.8526	0.027
$^{a,c}Q_{0,\bar{1}}$	$12_{7,5;2}$	$12_{7,6;1}$	1981.42	1981.41	0.01	7.9559	0.00
$^{a,c}Q_{0,\bar{1}}$	$10_{6,4;2}$	$10_{6,5;1}$	1419.61	1419.59	0.02	6.9270	0.001
$^{a,c}Q_{0,\bar{1}}$	$3_{3,0;3}$	$3_{3,1;2}$	233.79	233.76	0.03	5.2440	0.77
$^{a,c}Q_{0,\bar{1}}$	$8_{5,3;2}$	$8_{5,4;1}$	951.50	951.45	0.05	5.8688	0.066
$^{a,c}Q_{0,\bar{1}}$	$11_{6,5;1}$	$11_{6,6;0}$	1592.37	1592.31	0.06	6.3911	0.004
$^{a,c}Q_{0,\bar{1}}$	$6_{4,2;2}$	$6_{4,3;1}$	577.07	576.97	0.10	4.9212	1.44
$^{a,c}Q_{0,\bar{1}}$	$9_{5,4;1}$	$9_{5,5;0}$	1092.82	1092.70	0.12	5.1924	0.17
$^{a,c}Q_{0,\bar{1}}$	$12_{6,6;0}$	$12_{6,7;-1}$	1781.33	1781.19	0.14	5.8191	0.008
$^{a,c}Q_{0,\bar{1}}$	$4_{3,1;2}$	$4_{3,2;1}$	296.34	296.15	0.19	4.0238	17.4
$^{a,c}Q_{0,\bar{1}}$	$7_{4,3;1}$	$7_{4,4;0}$	687.03	686.70	0.33	4.1949	7.7
$^{a,c}Q_{0,\bar{1}}$	$2_{2,0;2}$	$2_{2,1;1}$	109.29	108.95	0.34	3.3168	117
$^{a,c}Q_{0,\bar{1}}$	$10_{5,5;0}$	$10_{5,6;-1}$	1250.41	1250.05	0.36	4.7379	0.62
$^{a,c}Q_{0,\bar{1}}$	$5_{3,2;1}$	$5_{3,3;0}$	375.06	374.27	0.79	3.2083	162

TABLE II.—*Continued.*

Sub-branch	Quantum number Upper	Quantum number Lower	Term values Upper	Term values Lower	Position (cm^{-1})	Line strength	α (10^{-4} cm^{-1})
[a] $^{o}Q_{0,\bar{1}}$	$8_{4,4;0}$	$8_{4,5;-1}$	813.38	812.44	0.94	3.5554	28.4
[a] $^{o}Q_{0,\bar{1}}$	$11_{5,6;-1}$	$11_{5,7;-2}$	1424.54	1423.60	0.94	4.0958	1.54
[a] $^{o}Q_{0,\bar{1}}$	$3_{2,1;1}$	$3_{2,2;0}$	156.98	155.28	1.70	2.2592	1580
[a] $^{o}Q_{0,\bar{1}}$	$12_{5,7;-2}$	$12_{5,8;-3}$	1615.54	1613.37	2.17	3.4302	2.66
[a] $^{o}Q_{0,\bar{1}}$	$6_{3,3;0}$	$6_{3,4;-1}$	470.40	468.14	2.26	2.5695	663
[a] $^{o}Q_{0,\bar{1}}$	$9_{4,5;-1}$	$9_{4,6;-2}$	956.50	954.18	2.32	2.9646	71.0
[a] $^{o}Q_{0,\bar{1}}$	$1_{1,0;1}$	$1_{1,1;0}$	32.44	29.76	2.68	1.5000	4870
[a] $^{o}Q_{0,\bar{1}}$	$4_{2,2;0}$	$4_{2,3;-1}$	221.62	216.77	4.85	1.6472	6880
[a] $^{o}P_{2,\bar{3}}$	$4_{2,2;0}$	$5_{0,5;-5}$	221.62	221.13	0.49	.0250	1.04
[a] $^{o}P_{2,\bar{3}}$	$6_{2,4;-2}$	$7_{0,7;-7}$	403.23	401.92	1.31	.0115	1.39
[a] $^{o}R_{2,3}$	$6_{0,6;-6}$	$5_{2,3;-1}$	305.27	303.70	1.57	.0178	5.05
[a] $^{o}R_{2,3}$	$7_{1,6;-5}$	$6_{3,3;0}$	472.95	470.40	2.55	.0590	19.2
[b] $^{o}R_{1,3}$	$7_{1,7;-6}$	$6_{2,4;-2}$	403.25	403.23	0.02	.1339	0.026
[b] $^{o}R_{1,3}$	$7_{3,5;-2}$	$6_{4,2;2}$	577.63	577.07	0.56	.4666	30.3
[b] $^{o}P_{1,\bar{3}}$	$3_{2,1;1}$	$4_{1,4;-3}$	156.98	155.85	1.13	.2156	468
[b] $^{o}R_{1,3}$	$9_{4,6;-2}$	$8_{5,3;2}$	954.18	951.50	2.68	.6271	143
[b] $^{o}P_{1,\bar{3}}$	$4_{3,1;2}$	$5_{2,4;-2}$	296.34	293.21	3.13	.2988	250
[b] $^{o}R_{1,3}$	$5_{1,5;-4}$	$4_{2,2;0}$	225.12	221.62	3.50	.2226	3330
[b] $^{o}R_{1,3}$	$6_{1,6;-5}$	$5_{2,3;-1}$	307.64	303.70	3.94	.1791	2250
[b] $^{o}R_{1,3}$	$11_{5,7;-2}$	$10_{6,4;2}$	1423.60	1419.61	3.99	.8036	39.2
[b] $^{o}R_{1,1}$	$11_{5,6;-1}$	$10_{6,5;1}$	1424.54	1419.59	4.95	.6841	51.3
[b] $^{o}R_{1,1}$	$9_{4,5;-1}$	$8_{5,4;1}$	956.50	951.45	5.05	.5579	452
			(*D*) H_2S[b]				
[b] $^{o}P_{3,\bar{3}}$	$3_{3,1;2}$	$4_{0,4;-4}$	115.68	114.15	1.53	.0013	0.74
[b] $^{o}R_{3,3}$	$10_{2,8;-6}$	$9_{5,5;0}$	746.69[c]	744.65[c]	2.04	.0047	0.21
[b] $^{o}P_{3,\bar{5}}$	$6_{6,0;6}$	$7_{3,5;-2}$	418.43	416.21	2.22	.0004	0.10
[b] $^{o}R_{3,3}$	$7_{1,6;-5}$	$6_{4,3;1}$	362.59	360.29	2.30	.0034	3.8
[b] $^{o}R_{1,3}$	$10_{3,8;-5}$	$9_{4,5;-1}$	746.69[c]	744.30[c]	2.39	.0047	0.84
[b] $^{o}R_{3,5}$	$9_{4,6;-2}$	$8_{7,1;6}$	687.86	684.32	3.54	.0009	0.16
[b] $^{o}P_{1,\bar{3}}$	$4_{2,2;0}$	$5_{1,5;-4}$	170.76	166.26	4.50	.0014	5.3
[b] $^{o}R_{1,3}$	$7_{2,6;-4}$	$6_{3,3;0}$	362.59	357.37	5.22	.0035	6.9
[b] $^{o}Q_{1,\bar{1}}$	$1_{1,0;1}$	$1_{0,1;-1}$	19.43	13.76	5.67	1.5000	58,330
[b] $^{o}P_{1,\bar{3}}$	$7_{3,4;-1}$	$8_{2,7;-5}$	459.00	452.69	6.31	.0026	14
[b] $^{o}R_{3,5}$	$11_{5,7;-2}$	$10_{8,2;6}$	1032.34[c]	1025.45[c]	6.89	.0011	0.13
[b] $^{o}R_{1,3}$	$4_{1,4;-3}$	$3_{2,1;1}$	114.15	107.65	6.50	.0032	102
[b] $^{o}Q_{1,\bar{1}}$	$2_{2,0;2}$	$2_{1,1;0}$	58.54	51.26	7.28	2.1289	37,710
[b] $^{o}P_{3,\bar{3}}$	$7_{4,4;0}$	$8_{1,7;-6}$	459.74	452.69	7.05	.0026	5.8
[b] $^{o}P_{3,\bar{5}}$	$4_{3,2;1}$	$5_{0,5;-5}$	174.39	166.26	8.13	.0012	45
[b] $^{o}P_{1,\bar{3}}$	$10_{4,6;-2}$	$11_{3,9;-6}$	883.70[c]	875.36[c]	8.34	.0038	1.4
[b] $^{o}P_{3,\bar{3}}$	$10_{5,6;-1}$	$11_{2,9;-7}$	883.75[c]	875.36[c]	8.39	.0038	4.4
[b] $^{o}R_{3,3}$	$6_{1,5;-4}$	$5_{4,2;2}$	281.86	271.85	10.01	.0044	49
[b] $^{o}Q_{1,\bar{1}}$	$3_{3,0;3}$	$3_{2,1;1}$	117.75	107.65	10.10	2.3196	179,000
[b] $^{o}R_{3,5}$	$8_{4,5;-1}$	$7_{7,0;7}$	569.10	559.35	10.75	.0006	5
			(*E*) H_2Se[d]				
[b] $^{o}P_{3,\bar{5}}$	$9_{8,1;7}$	$10_{5,6;-1}$	726.40	725.47	0.93	0.0014	0.012
[b] $^{o}P_{3,\bar{5}}$	$10_{8,2;6}$	$11_{5,7;-2}$	848.92	847.93	0.99	0.0017	0.003
[b] $^{o}P_{1,\bar{3}}$	$4_{2,2;0}$	$5_{1,5;-4}$	138.78	137.21	1.57	0.0035	0.57
[b] $^{o}R_{3,3}$	$7_{1,6;-5}$	$6_{4,3;1}$	299.17	297.58	1.59	0.0100	2.3
[b] $^{o}P_{3,\bar{3}}$	$11_{11,1;10}$	$12_{8,4;4}$	1142.86	1140.99	1.87	0.0004	0.000
[b] $^{o}R_{3,5}$	$11_{6,6;0}$	$10_{9,1;8}$	898.33	895.55	2.78	0.0015	0.017
[b] $^{o}P_{1,\bar{3}}$	$7_{3,4;-1}$	$8_{2,7;-5}$	376.78	373.75	3.03	0.0030	1.7
[b] $^{o}R_{3,3}$	$10_{2,8;-6}$	$9_{5,5;0}$	614.66	611.11	3.55	0.0100	0.78
[b] $^{o}P_{3,\bar{3}}$	$3_{3,1;2}$	$4_{0,4;-4}$	97.80	94.14	3.66	0.0028	3.1
[b] $^{o}R_{3,5}$	$12_{7,6;1}$	$11_{10,1;9}$	1086.64	1082.52	4.12	0.0015	0.044
[b] $^{o}P_{1,\bar{3}}$	$10_{4,6;-2}$	$11_{3,9;-6}$	724.95	720.77	4.18	0.0087	0.55
[b] $^{o}P_{3,\bar{3}}$	$10_{5,6;-1}$	$11_{2,9;-7}$	725.47	720.77	4.70	0.0084	2.0
[b] $^{o}Q_{1,\bar{1}}$	$1_{1,0;1}$	$1_{0,1;-1}$	16.09	11.08	5.01	1.5000	14,000

[a] The lines with predicted values of $\nu=0$ will have $\alpha=0$. The values tabulated in parentheses are α/ν^2. If the lines occur at a finite frequency (as theoretically they will because the splitting is finite although small, and perturbations may increase it substantially), the absorption coefficient can be obtained by multiplying the tabulated value by ν^2.

[b] The line strengths given for H_2S are those for $\kappa=0.5$, since these do not differ appreciably from the interpolated strengths for the actual value of $\kappa=0.523$.

[c] Rigid rotor energy values.

[d] The line strengths given for H_2Se are those for $\kappa=0.3$, since these do not differ appreciably from the interpolated strengths for the actual value of $\kappa=0.315$.

TABLE III. Exact values of the reduced energy, $E(\kappa)$, for H_2O, $\kappa=-0.436426$.

$J_{K_{-1},K_1;\tau}$	$E(\kappa)$	$J_{K_{-1},K_1;\tau}$	$E(\kappa)$
$0_{0,0;0}$	0.00000	$5_{5,0;5}$	21.54000
		$5_{5,1;4}$	21.53968
$1_{1,0;1}$	0.56357	$5_{4,1;3}$	6.37690
$1_{1,1;0}$	0.00000	$5_{4,2;2}$	6.35287
$1_{0,1;-1}$	−1.43643	$5_{3,2;1}$	−4.96391
		$5_{3,3;0}$	−5.49647
$2_{2,0;2}$	2.69953	$5_{2,3;-1}$	−11.75282
$2_{2,1;1}$	2.56357	$5_{2,4;-2}$	−15.08139
$2_{1,1;0}$	−1.74570	$5_{1,4;-3}$	−16.85100
$2_{1,2;-1}$	−3.43643	$5_{1,5;-4}$	−24.77173
$2_{0,2;-2}$	−4.44523	$5_{0,5;-5}$	−24.89899
$3_{3,0;3}$	6.94336	$6_{6,0;6}$	31.84431
$3_{3,1;2}$	6.92214	$6_{6,1;5}$	31.84428
$3_{2,1;1}$	−1.11110	$6_{5,1;4}$	13.27250
$3_{2,2;0}$	−1.74570	$6_{5,2;3}$	13.26907
$3_{1,2;-1}$	−5.30762	$6_{4,2;2}$	−1.71566
$3_{1,3;-2}$	−8.66784	$6_{4,3;1}$	−1.83091
$3_{0,3;-3}$	−9.25316	$6_{3,3;0}$	−12.39928
		$6_{3,4;-1}$	−13.80339
$4_{4,0;4}$	13.23716	$6_{2,4;-2}$	−18.77578
$4_{4,1;3}$	13.23443	$6_{2,5;-3}$	−24.28828
$4_{3,1;2}$	1.53971	$6_{1,5;-4}$	−25.31308
$4_{3,2;1}$	1.39636	$6_{1,6;-5}$	−35.74059
$4_{2,2;0}$	−5.91631	$6_{0,6;-6}$	−35.79273
$4_{2,3;-1}$	−7.59867		
$4_{1,3;-2}$	−10.26823		
$4_{1,4;-3}$	−15.76062		
$4_{0,4;-4}$	−16.04937		

this was discovered as absorption of radar waves. This line, $6_{1,6}-5_{2,3}$, has been observed experimentally.[10, 11, 12]

The observed position of 0.7418 cm^{-1} differs considerably (from the microwave point of view) from the value of 0.78 cm^{-1} predicted from term values, but from inspection of Table II, there can be no doubt that on the basis of position alone this is the correct identification.

The identification is substantiated by the observed intensity. The calculation of the microwave absorption of water vapor and the comparison with experiment are discussed in detail in reference 1. In order to illustrate the use of Table II we can briefly summarize the comparison of calculated and observed absorption coefficients at resonance as follows. The calculated absorption coefficient value (for 14.5°C) at the predicted position of 0.78 cm^{-1} and round value of $\Delta\nu_0=0.1$ cm^{-1} is 37.8×10^{-6} cm^{-1}. When corrected for the observed position[12] and observed half-width[7] of 0.087 cm^{-1}, the absorption coefficient for water vapor in air, at a concentration of 1 g/m^3 and 14.5°C is 0.049×10^{-6} cm^{-1}. At 45°C the coefficient is 0.0522×10^{-6} cm^{-1}, which is in good agreement with the observed[7] absorption coefficient of 0.0573×10^{-6} cm^{-1}.

The theoretical value for pure water vapor is the tabulated value, corrected for position, and for the observed half-width of 0.36 cm^{-1}, namely 9.6×10^{-6} cm^{-1}. This agrees with the observed[12] value of $8\pm4\times10^{-6}$ cm^{-1}.

D_2O

The microwave absorption of D_2O should be as interesting as that of H_2O. On account of the heavier atoms and resulting larger moments of inertia, a few more lines appear in the region. However, the increase in the moments of inertia makes the partition function larger, so that each level has a smaller population. The intensities of the lines are on the average smaller.

The term values of D_2O are known,[13] and the possible transitions in the microwave region (above 0.2 cm) are listed in Table II. The line strengths were obtained by interpolating the basic table[4] in the light of Table I. The dipole moment of D_2O will be very nearly the same as for H_2O. The mean free time will be the same except for a small mass correction, which, according to the simple kinetic theory derivation, makes $\Delta\nu$ for D_2O 0.95 as large as for H_2O. Thus the intensities of the D_2O lines relative to the H_2O lines are quite accurately calculated. Only weak lines are predicted near 1 cm and none have been observed in the region studied[12] (0.73 to 0.89 cm^{-1}).

HDO

Besides having moments of inertia intermediate between H_2O and D_2O, and thus giving rise to a similar selection of lines in the microwave region, HDO is of particular importance because its

[10] R. L. Kyhl, R. H. Dicke, and R. Beringer, Phys. Rev. 69, 694 (1946), estimated the position at 1.34 cm. See also R. H. Dicke, R. Beringer, R. L. Kyhl and A. B. Vane, Phys. Rev. 70, 340 (1946).

[11] S. H. Autler, G. E. Becker, and J. M. B. Kellogg, Phys. Rev. 69, 694 (1946), give 22,320±150 megacycles, or 1.33 cm, or 0.744 cm^{-1}, and the attenuation as 0.044 db/nautical mile for 1 g water vapor per cubic meter. In reference 7 they give the attenuation data in more detail. At 0.751 cm^{-1} it is 0.0249 db/km per g/cu. m.

[12] C. H. Townes and F. R. Merritt, Phys. Rev. 70, 558 (1946), give 22,237±5 megacycles or 0.7418 cm^{-1}, and intensity as $4\pm2\times10^{-6}$ nepers/cm.

[13] N. Fuson, H. M. Randall, and D. M. Dennison, Phys. Rev. 56, 982 (1939).

permanent dipole has components along two axes of inertia. Thus, in addition to the lines of the type where the dipole is parallel only to the axis of the intermediate moment of inertia (b-type) permitted in H_2O and D_2O, there will be lines from transitions permitted when the dipole has a component along the axis of the smallest moment of inertia (a-type). The values of the dipole moments, to be substituted in (1), will be that of H_2O multiplied by $\cos^2\theta$ for the b-type and $\sin^2\theta$ for the a-type, θ being 20° 38′.

The levels of the asymmetric rotor are characterized by the fact that they are split from doubly degenerate symmetric-rotor levels. The amount of splitting depends on the degree of asymmetry, κ. For HDO κ is -0.7, so that the degenerate levels of the prolate symmetric rotor are split, and levels of the same K_{-1} index will be paired, the separation being very small at high K_{-1} values. But it is between exactly these levels that the a-type transitions occur. It is seen then that absorption lines will occur throughout the microwave and radio regions for such a-type transitions.

The expected transitions are listed in Table IIC with position and intensity. It is felt that the intensities are calculable with sufficient accuracy. The position depends on estimates of the rotational energy levels of HDO. There are no term values known for this molecule. The only completely resolved spectrum of HDO is the one at 1.1μ which has been measured and analyzed by L. Herzberg.[14] We have reanalyzed this spectrum on the basis of the asymmetric-rotor intensities and found that the effective moments given by Herzberg are satisfactory. With these one can

TABLE IV. The Hamiltonian is a direct sum of blocks of order $2J+1$ belonging to each value of the quantum number J By the symmetry of the Four Group these blocks can be divided into four submatrices, one for each representation. These are labelled ee, eo, oe, oo, where e, o in the first and second indices refer respectively to the parity of K_{-1} and K_1 which are the absolute values of the internal quantum numbers of the limiting cases of prolate and oblate symmetric rotors. Each state of the asymmetric rotor, $A(J, (K_{-1}, K_1), M, \gamma)$ is identified by the absolute values of the inner quantum numbers (K_{-1}, K_1) it would have in these two limiting cases. This state is a linear combination of Wang functions.

$$A(J, (K_{-1}, K_1), M, \gamma) = \Sigma_K t_{K(K_{-1}, K_1)} S(J, K, M, \gamma). \quad (3)$$

Thus, the columns of the matrices $T = ||t_{ij}||$ in the table refer to asymmetric state, identified by K_{-1}, K_1 (at the head of the columns). The Wang functions $S(J, K, M, \gamma)$ from which the asymmetric states are constructed are identified by the absolute magnitudes of the quantum number K, and γ which describes whether + or − combinations of the symmetric-rotor states were taken. The values of K and γ are indicated in the table on each row of the matrices.

The Hamiltonian diagonalized by these matrices T is of Type II^r, which refers to the fact that the Wang functions used as basis functions are those with symmetry axis parallel to the intermediate axis of inertia. Thus the K's are neither K_{-1} nor K_1 (indeed they may have opposite parity), for the latter refer to inner quantum numbers of Wang functions of symmetry along the least and greatest axes of inertia, respectively. The summation over K in (3) is then over the values listed explicitly on the rows of the submatrices displayed.

	2ee			3eo			3oe			3oo	
	20	02		21	03		30	12		31	13
0+	.78878	.61468	1−	.58817	.80873	1+	.94200	.33560	0+	.74564	.66634
2+	.61468	−.78878	3−	.80873	−.58817	3+	.33560	−.94200	2+	.66634	−.74564

	4eo			4oe			4oo			5ee	
	41	23		32	14		31	13		42	24
1+	.90763	.41976	1−	.55707	.83047	2−	.84957	.52748	2−	.78878	.61468
3+	.41976	−.90763	3−	.83047	−.55707	4−	.52748	−.84957	4−	.61468	−.78878

	4ee				5eo				5oe				5oo		
	40	22	04		41	23	05		50	32	14		51	33	15
0+	.70012	.40889	.58536	1−	.48457	.40145	.77719	1+	.87636	.40298	.26384	0+	.66647	.46684	.58127
2+	.69076	−.18031	−.70024	3−	.81551	.11409	−.56739	3+	.47169	−.80712	−.63947	2+	.70048	−.12321	−.70260
4+	.18077	−.89459	.40868	5−	.31644	−.90875	.27210	5+	.09751	−.58485	.72212	4+	.25523	−.87543	.41046

	6eo			6oe			6oo		
	61	43	25	52	34	16	51	33	15
1+	.84960	.43932	.29185	1− .43478	.47930	.76239	2− .72529	.50319	.46985
3+	.50513	−.51853	−.68991	3− .79528	.19282	−.57476	4− .66290	−.32625	−.67389
5+	.15176	−.73357	.66245	5− .42248	−.85621	.29734	6− .18580	−.80023	.57018

	6ee			
	60	42	24	06
0+	.63933	.44008	.30151	.55379
2+	.70246	−.02605	−.19533	−.68391
4+	.30830	−.77628	−.32937	.44029
6+	.05267	−.45060	.87319	−.17813

[14] L. Herzberg, Zeits. f. Physik **107**, 549 (1937).

compute the rotational energy levels assuming the molecule is a rigid rotor. The corrections to be applied to the rigid-rotor levels will be large, as in H_2O. However, in computing the positions of the microwave lines these corrections cancel to a large extent. For example, levels with same first subscript (K_{-1}) have about the same correction (as in the $5_{3,2}-5_{3,3}$ transition). All the *a*-type lines occur between levels of the same J and K_{-1}, so that the correction cancels in predicting these levels; that is the positions of these lines are given very closely by the splitting of the rigid-rotor levels. Fortunately, the same considerations also apply to the strongest *b*-type line; the correction for H_2O also cancels for the levels involved. On the other hand, the positions of the other *b*-lines are not known within one or more wave numbers, on account of expected deviations from rigid-rotor levels.

All the expected transitions lying at wave-lengths longer than 0.2 cm are listed in Table II*C*. All the "split" levels ${}^{a,o}Q_{0,1}$ are listed first, followed by the other *a*-type lines, and finally by the *b*-type lines. A line of HDO has been observed[12] at 0.7442 cm^{-1}. This is in close agreement with the predicted position of 0.79 cm^{-1} for transition $5_{3,2}-5_{3,3}$. The calculated absorption coefficient of this line is the tabulated value, adjusted for the observed position and half-width ($\Delta\nu_0=0.27$ cm^{-1}), namely 26.2×10^{-6} cm^{-1}. This is in good agreement with the observed intensity of $30\pm14\times10^{-6}$ cm^{-1}. Other lines given in Table II*C* would have approximately the observed intensity, if they appeared at the observed position. However, it seems unlikely that the predicted position would be in error by the amount required.

H_2S

On account of the increased mass of sulphur over oxygen atoms, the microwave spectrum of H_2S should be somewhat richer than H_2O, although the chance that a line will appear in any accessible region remains very small. Again term values are not known, but effective moments of inertia of the ground state have been found with considerable accuracy,[15] and a correction for centrifugal distortion applied. These calculated levels should be accurate to a few hundredths of a wave number, so that the positions given in Table II*D* are equally reliable. The intensities have been calculated as above. The value used for the dipole moment was 1.10×10^{-18} esu-cm.

Several lines between 0.1 and 1.0 cm are very strong, although this is in part due to the ν^2 term. The absorption of H_2S has been measured[16] at two frequencies, 0.31 and 0.81 cm^{-1}. The absorption coefficient (for 1 atm.) was reported as ~0 and $\sim30\times10^{-6}$ cm^{-1}, respectively. Absorption by H_2S at this wave-length would probably be due to the wings of the intense lines at 5.67, 7.28 and 10.10 cm^{-1}, which can be calculated by the shape factor given by Van Vleck and Weisskopf, Eq. (19) of reference 1. If $\Delta\nu_0$ were 0.1 cm^{-1}, the total contribution would only be 1×10^{-6} cm^{-1}. Further investigation of the absorption of H_2S in this region would be of value to estimate the value of $\Delta\nu_0$ for comparison with that of H_2O.

HDS AND D_2S

Infra-red bands of these molecules have not been analyzed so that neither term values nor effective moments of inertia are known. Furthermore, it is not yet possible to estimate the moments of inertia of HDS and D_2S accurately enough by allowing for the increased mass of deuterium, because the effective moments depend on the vibrational quantum number, and hence on the half quantum numbers of the ground state. This introduces a substantial correction which can only be estimated by the isotope effect on the coefficients showing the dependence of the moments of H_2S on vibrational quantum numbers, which is not yet known. Qualitatively, the microwave region spectrum of these molecules will be similar to those of HDO and D_2O, being somewhat richer in lines on account of the increased mass of the central atom.

The spectrum of HDS, like that of HDO, should be composed of both *a*- and *b*-type lines, and should extend throughout the microwave and radio regions.

H_2Se

The H_2Se molecule is similar in shape to that of H_2O and H_2S, and will have the same kind of

[15] B. L. Crawford and P. C. Cross, J. Chem. Phys. **5**, 621 (1937).

[16] J. E. Walter and W. D. Hershberger, J. App. Phys. **17**, 814 (1946).

microwave absorption spectrum. We have made an analysis of the infra-red band[17] of H_2Se at 4.3μ and find the effective moments of inertia are in the neighborhood of $I_A=3.14$, $I_B=3.89$, $I_C=7.18\times10^{-40}$ g cm^2.

These values were substituted in the formulae for the rigid rotor and the positions of the transitions in the microwave region (0.2 cm and longer) calculated as shown in Table II*E*. These positions are only approximate, but indicate that one line might be detectable in the one-centimeter region.

[17] D. M. Cameron, W. C. Sears, and H. H. Nielsen, J. Chem. Phys. **7**, 994 (1939).

The dipole moment of H_2Se is not known. A guess of 0.7×10^{-18} esu-cm was used in estimating the order of magnitude of the absorption coefficient. If the $7_{1,6}-6_{4,3}$ line can be detected, its intensity will serve to determine the dipole moment.

The spectrum of HDSe will be of considerable interest in relation to those of HDO and HDS.

ACKNOWLEDGMENT

The authors are pleased to express their appreciation of the interest and helpful advice of Professor J. H. Van Vleck in the preparation of this material.

PHYSICAL REVIEW VOLUME 71, NUMBER 7 APRIL 1, 1947

Note on the Spherical Harmonic Method As Applied to the Milne Problem for a Sphere*

R. E. MARSHAK
University of Rochester, Rochester, New York

(Received December 20, 1946)

The spherical analog of the Milne problem for the half-plane is treated by an approximate method based on expanding the neutron distribution function in a finite number of spherical harmonics. The results are improved markedly in going from the first to the second approximation and more slowly in higher approximations. The neutron distribution is calculated in the first two approximations. Values of the "extrapolated endpoint"—as predicted by the first three approximations—are tabulated in Table I as a function of the radius of the sphere.

1.

WE consider the following problem: a black sphere of radius a, i.e., a sphere which absorbs completely all neutrons which fall upon it, is surrounded by an infinite non-capturing medium which scatters neutrons isotropically without changing their velocity. No sources are present in the outer medium except that a current density of amount $(F/4\pi r^2)$ (F is a constant) is assumed to exist in the direction $(-r)$. We wish to determine the neutron density in the (outer) medium.[1]

This problem is the complete analog of the Milne problem for the semi-infinite plane since the albedo of the black core is zero just as the albedo of vacuum is zero in the plane case. If the black core is replaced by vacuum, the albedo is no longer zero, and the physical conditions are altered in an essential way. The modified problem is not treated in this note.

* The contents of this note were published in a Montreal Report (MT-49) dated April 15, 1944. The Central Records File Reference giving authority for declassification is 11-5-3, serial No. 47. The spherical harmonic method has been generalized and applied to a great variety of neutron diffusion problems by C. Mark (declassified Montreal report MT-97), B. Carlson (declassified Los Alamos report LADC No. 108), R. Glauber, and W. Rarita. Another approximation method based on the Gauss formula for numerical integration, which is equivalent in certain ways to the spherical harmonic method (cf. footnotes below), was developed independently by G. C. Wick, Zeits. f. Physik **121**, 702 (1943), and applied to problems of the stellar atmosphere by S. Chandrasekhar, Astrophys. J. **100**, 76 (1944) and succeeding papers. Because of the war, Wick's paper did not come to the attention of the author until the present work was completed.

[1] S. Chandrasekhar, Astrophys. J. **101**, 95 (1945) has worked out the converse of this problem, namely the determination of the distribution function due to a point source in a spherical scattering medium surrounded by vacuum, by Wick's method.

An exact solution of the present problem, in contrast to the Milne problem for the plane, seems impossible. Recourse must therefore be had to approximate methods. The simplest approximation is the diffusion approximation which consists in expanding the neutron distribution function up to and including the first spherical harmonic. A natural extension of the diffusion approximation is the inclusion of a larger number of spherical harmonics in the expansion of the neutron distribution function. In the limit, of course, the approximate solutions go over into the exact solution. The great virtue of the spherical harmonic method (as we shall call it) is its rapid convergence in the early approximations.

2.

The transport equation governing the distribution of neutrons in the medium surrounding the black core is:

$$\mu\frac{\partial\psi(r,\mu)}{\partial r}+\frac{(1-\mu^2)}{r}\frac{\partial\psi(r,\mu)}{\partial\mu}+\psi(r,\mu)=\frac{\psi_0(r)}{2}, \quad (1)$$

where the origin of coordinates is taken at the center of the black core, μ is the cosine of the angle between the direction of motion of the neutron and the radius r (pointing away from the origin), and $\psi(r,\mu)d\mu$ is the number of neutrons per unit volume at distance r with direction cosine between μ and $\mu+d\mu$. The quantity $\psi_0(r)$ is the neutron density, defined as $\int_{-1}^{1}\psi(r,\mu)d\mu$. Finally, the mean free path is taken as unit of length, and the neutron velocity is set equal to unity.

It is easy to show, by integrating Eq. (1) over $d\mu$, that the total flux $[4\pi r^2 j(r)]$ $(j(r)=-\int_{-1}^{1}\mu\psi(r,\mu)d\mu)$ is a constant independent of r. We choose the constant as 4π so that $j(r)=1/r^2$. Equation (1) is to be solved, subject to the boundary condition

$$\psi(a,\mu)=0 \quad \text{for} \quad \mu>0, \quad (A)$$

where a is the radius of the black core.

The spherical harmonic method we propose consists in expanding $\psi(r,\mu)$ in a series of Legendre polynomials and breaking off the series after a finite number of terms. Thus we write:

$$\psi(r,\mu)=\sum_{l=0}^{l_0}\tfrac{1}{2}(2l+1)\psi_l(r)P_l(\mu), \quad (2)$$

where $\psi_l(r)=\int_{-1}^{1}P_l(\mu)\psi(r,\mu)d\mu$, and l_0 is an integer which determines the order of the approximation. For example, if l_0 is taken as 1, we say we are dealing with the P_1-approximation, if $l_0=3$, the P_3-approximation, and so on. It is natural to choose l_0 as an odd integer for successive approximations since the even approximations contain singular parts which have no clear physical significance.

The representation of $\psi(r,\mu)$ by a finite number of Legendre polynomials, as defined by Eq. (2), is inconsistant with the boundary condition (A). Instead, this boundary condition must be relaxed and replaced by a series of boundary conditions appropriate to the order of the approximation which is being considered. Thus, if we are working with the P_1-approximation (the diffusion approximation), one boundary condition is sufficient to determine all the arbitrary constants, and it is reasonable to require that the total current entering the (outer) medium from the black core is zero, namely that:

$$\int_0^1\mu\psi(a,\mu)d\mu=0. \quad (3)$$

The next approximation, the P_3-approximation, requires one additional boundary condition besides Eq. (3). There is some arbitrariness involved in the choice of this added boundary condition since we could require that $\int_0^1 P_2(\mu)\psi(a,\mu)d\mu=0$ or $\int_0^1 P_3(\mu)\psi(a,\mu)d\mu=0$, etc. It turns out that the solution for $\psi_0(r)$ is negligibly affected by the particular choice made and always gives a distinct improvement over the P_1-approximation. In an odd approximation, it seems most sensible to choose a boundary condition on an odd moment.[2]

[2] Dr. Mark has pointed out that the apparent ambiguity in the choice of the boundary conditions is removed if one recalls that in the Milne problem for the half-plane the exact even "half-moments" have an infinite derivative at the boundary, whereas the exact odd "half-moments" have a finite derivative, just as they do in any odd P-approximation. Furthermore, it is possible to obtain unique boundary conditions at $r=a$ by regarding the black sphere as *black* not as *vacuum*, i.e., by regarding the black sphere as a second medium which is completely absorbing, solving the equations, and equating (at $r=a$) the ψ_l's to the ψ_l's of the outside medium. The latter procedure turns out to be equivalent to Wick's choice of boundary conditions. The procedure we adopt gives more accurate results for the "extrapolated end point." For example, in the limit $a\to\infty$ (cf. Table I), we obtain 0.667, 0.705, 0.709 for the extrapolated end point in the P_1-, P_3-, P_5-approximations respectively as compared to 0.577, 0.694, 0.704 with the "black" or Wick boundary conditions; the correct value is

We therefore choose as the second boundary condition in the P_3-approximation:

$$\int_0^1 P_3(\mu)\psi(a,\mu)d\mu=0. \tag{4}$$

Since $P_3(\mu)$ is a linear combination of μ and μ^3, Eqs. (3) and (4) are equivalent to (3) and the condition $\int_0^1 \mu^3\psi(a,\mu)d\mu=0$. (This is an added attraction for the "odd moment" boundary conditions.) In this manner it is possible, except for increasing algebraic complications, to arrive at closer and closer approximations to the neutron density $\psi_0(r)$.

3.

We now carry through the P_1 and P_3-approximations in accordance with the procedure outlined above. Let us multiply both sides of Eq. (1) by $P_l(\mu)$. Integrating over $d\mu$ and using well-known relations between Legendre polynomials, we get a series of equations:[3]

$$\frac{1}{(2l+1)}\{l\psi_{l-1}'(r)+(l+1)\psi_{l+1}'(r)\}+\frac{1}{r(2l+1)}\{(l+1)(l+2)\psi_{l+1}(r)-l(l-1)\psi_{l-1}(r)\}+\psi_l(r)=\psi_0(r)\delta_{0l}. \tag{5}$$

In Eq. (5) the primes denote differentiation with respect to r and δ_{0l} is the Kronecker delta-function. If we choose $l_0=1$ (P_1-approximation), then Eq. (5) becomes equivalent to the two equations:

$$\psi_1'(r)+2\psi_1(r)/r=0, \tag{6a}$$

$$\tfrac{1}{3}\psi_0'(r)+\psi_1(r)=0, \tag{6b}$$

of which the solutions are:

$$\psi_1(r)=-1/r^2, \tag{7a}$$

$$\psi_0(r)=-3/r+B \text{ (B is a constant).} \tag{7b}$$

The total flux has been taken as 4π. Equation (7b) is, of course, the usual diffusion result and on the crude assumption, $\psi_0(a)=0$, would lead to the value $B=3/a$. However, one should use the improved boundary condition (3) which becomes in the present case:

$$\tfrac{1}{2}\psi_0(a)+\psi_1(a)=0, \tag{8}$$

from which

$$B=3(1+2/3a)/a. \tag{9}$$

It is convenient to rewrite Eq. (7b) in the form:

$$r\psi_0(r)=B[r-a+r_0] \quad \text{where} \quad r_0=a-3/B.$$

The quantity r_0 is called the extrapolated end point and has the value (in the P_1-approximation):

$$r_0=2/3(1+2/3a). \tag{9a}$$

We consider next the P_3-approximation; setting $l_0=3$ in Eq. (2), we get from Eq. (5) the following set of equations:

$$r\psi_1'(r)+2\psi_1(r)=0; \tag{10a}$$

$$r\psi_0'(r)+2r\psi_2'(r)+6\psi_2(r)+3r\psi_1=0; \tag{10b}$$

$$2r\psi_1'(r)+3r\psi_3'(r)-2\psi_1(r)+12\psi_3(r)+5r\psi_2(r)=0; \tag{10c}$$

$$3r\psi_2'(r)-6\psi_2(r)+7r\psi_3(r)=0. \tag{10d}$$

These equations are to be solved subject to the boundary conditions (3) and (4) which may be rewritten as:

$$4\psi_0(a)+8\psi_1(a)+5\psi_2(a)=0; \tag{11a}$$

$$8\psi_1(a)+25\psi_2(a)+32\psi_3(a)=0. \tag{11b}$$

The solutions are:[4]

$$\psi_0(r)=-3/r+B-2Ge^{-kr}/r; \tag{12a}$$

$$\psi_1(r)=-1/r^2; \tag{12b}$$

$$\psi_2(r)=-6/5r^3+G(1+3/kr+3/k^2r^2)e^{-kr}/r; \tag{12c}$$

$$\psi_3(r)=-18/7r^4+5G(1+6/kr+15/k^2r^2+15/k^3r^3)e^{-kr}/3kr \tag{12d}$$

0.7104. However, the neutron density at the boundary (for the limiting case $a\to\infty$) is given exactly by the Wick method. One would then suppose that for finite a, the present method would give more rapidly converging values of the extrapolated endpoint whereas the Wick method would give more rapidly converging values of the neutron density, at least at the boundary.

[3] The set of Eqs. (5) is a straightforward consequence of the expansion of Eq. (2); compare, however, the roundabout treatment of the spherical problem (see ref. in footnote 1) necessitated by the use of Wick's method. In the end, the final equations are identical. In general, the spherical harmonic method has an advantage over Wick's method in its easy adaptability to problems of several media and different geometries.

[4] The terms having G as coefficient are essentially Hankel functions (of the first kind) of half-integral order having ($i\,kr$) as argument.

where

$$k=(35)^{\frac{1}{2}}/3;$$

$$B=\frac{3}{a}\left[1+\frac{2}{3a}+\frac{1}{2a^2}\right]+\frac{7k\delta}{2a}\left[1-\frac{5}{ka}-\frac{5}{k^2a^2}\right];$$

$$G=14k\delta e^{ka}/3;$$

$$\delta=\frac{[1/8k^2a][1+15/4a+72/7a^2]}{\left\{\left(1+\frac{175}{96k}\right)+\frac{6}{ka}\left(1+\frac{175}{192k}\right)+\frac{15}{k^2a^2}\left(1+\frac{35}{96k}\right)+\frac{15}{k^3a^3}\right\}}.$$

TABLE I. Extrapolated end point r_0.

a	P_1	P_3	P_5
0.5	0.286	0.323	0.334
1.0	0.400	0.480	0.494
2.0	0.500	0.608	0.620
5.0	0.588	0.682	0.690
∞	0.667	0.705	0.709

We rewrite Eq. (12a) to exhibit the extrapolated endpoint and the novel feature of the P_3-approximation:

$$r\psi_0(r)=B[(r-a+r_0)-\gamma e^{-k(r-a)}], \quad (13)$$

where

$$B=3/(a-r_0), \quad \gamma=2G/kB.$$

It is seen from Eq. (13) that the P_3-approximation gives a different (and necessarily improved) value for r_0. Moreover, a correction of exponential order is added to the asymptotic expression $(r-a+r_0)$.

Each higher P-approximation improves the extrapolated end point and adds one more term of exponential order. Thus, we would obtain the following form for $\psi_0(r)$ in the $P_{(2l_0+1)}$-approximation:

$$r\psi_0(r)=B\left\{(r-a+r_0)-\sum_{j=1}^{l_0}\gamma_j e^{-k_j(r-a)}\right\}. \quad (14)$$

Substitution of Eq. (14) into the series of Eq. (6) would lead to an algebraic equation of order l_0 in k^2 which would yield l_0 distinct roots[5] k_j and permit the determination of $\psi_1, \psi_2, \cdots\psi_{(2l_0+1)}$. Knowledge of the ψ_l's together with the application of the (l_0+1) boundary conditions:

$$\int_0^1 \mu^{(2j+1)}\psi(a,\mu)d\mu=0 \quad (j=0, 1, \cdots l_0) \quad (15)$$

would then yield the (l_0+1) constants $r_0, \gamma_1, \gamma_2, \cdots\gamma_{l_0}$.

4.

Since knowledge of the "extrapolated end point," r_0, is of special interest for pile design (e.g., control rods, upper limit on thermal utilization of strongly capturing sphere, etc.) we present some numerical results in Table I. Values of r_0 are given for several values of a in the P_1, P_3, and P_5-approximations. Table I exhibits a fairly general property of the spherical harmonic method: the great improvement of the P_3-approximation over the P_1-approximation and the less rapid improvement registered by still higher approximations.

[5] The roots k_j are identical with the ones obtained by an application of Wick's method; they are independent of the geometry.

Pais' f-Field Theory and the Mirror Nuclei

A. S. WIGHTMAN
Palmer Physical Laboratory, Princeton University, Princeton, New Jersey
(Received January 15, 1947)

It is shown that the f-field theory in its present form cannot simultaneously account for the neutron-proton mass difference and the binding energy differences of mirror nuclei.

A. PAIS has proposed[1] a way of overcoming the self-energy difficulties for electrically charged particles of spin $\frac{1}{2}$, by introducing a scalar short range field in addition to the electromagnetic field. He adjusts its coupling constant, f, so that, at least in first approximation of an expansion in powers of $e^2/\hbar c$, the divergent parts of the electromagnetic and f-field self-energies of a charged particle cancel. This condition requires $f^2=2e^2$, where e is the electronic charge.

The range, a, of the f-field, is not determined by the above condition. However, in this theory, in first approximation, the neutron-proton mass difference is caused by the sum of the electromagnetic and f-field self-energies of the proton. This quantity, as computed in first approximation, has the right sign and order of magnitude when a is greater than, or of the order of magnitude of the classical electron radius, $r_0=e^2/mc^2$.

The static potential between two charged particles now deviates from Coulomb's law

$$V(r)=(e^2/r)(1-2e^{-r/a}).$$

It is the purpose of this note to point out that this modification of the Coulomb potential with $a\sim r_0$ has a drastic effect on the binding energy of nuclei. To see this, one need only examine the mirror nuclei ${}_zX^{2z-1}$ and ${}_{z-1}X^{2z-1}$. On the usual description[2] the difference in nuclear masses, apart from the neutron-proton mass difference, is considered to be the Coulomb energy, ΔE, of the "last proton." (Equality of $n-n$ and $p-p$ specific nuclear forces is assumed.) An estimate of ΔE can be made using a model of the nucleus as a uniformly charged sphere of radius R, where $R=CA^{\frac{1}{3}}$ ($C=0.52r_0$ gives a good fit for the lighter nuclei). If the f-field is introduced one must consider the sum of the Coulomb and f-energies of the last proton. The f-energy has been evaluated in the same way as the electromagnetic energy by considering the f-charge to be distributed uniformly over a sphere, and calculating the total energy of the f-charged sphere.

In Fig. 1 the Coulomb energy difference of mirror nuclei is plotted as a function of Z for several values of a. The lowest curves are for $a=2r_0$ a value which gives a reasonable account of the neutron-proton mass difference. It is apparent that the modification introduced by the f-field is irreconcilable with observation so long as the range of the field is chosen to be as great as $2r_0$.

Apart from the determination of a from the neutron-proton mass difference, one may ask what values of a are compatible with the existing evidence on the mirror nuclei. The middle three curves of Fig. 1 show that it is difficult to fit the data when $a=0.5r_0$. For $a=0.1r_0$ a five

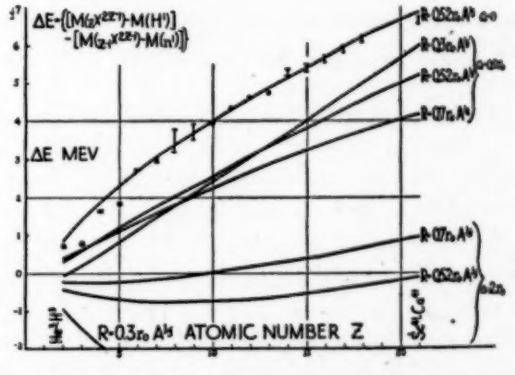

FIG. 1. Coulomb plus f-field energy differences of mirror nuclei, ${}_zX^{2z-1}$ and ${}_{z-1}X^{2z-1}$, plotted against Z. The highest curve is for pure Coulomb energy; the range, a, of the f-field is set equal to zero. The lower curves show how the f-field lowers the energy differences for $a=0.5r_0$ and $a=2r_0$ even when the nuclear radii are varied 40 percent in each direction from the generally accepted values.

[1] A. Pais, Phys. Rev. **68**, 227 (1945); **70**, 796 (1946). An extensive account is given in *On the Theory of Elementary Particles* (Verhandelingen Ac. Amsterdam, 1946).
[2] E. Wigner and E. Feenberg, *Reports on Progress in Physics* **8**, 275 (The Physical Society, London, 1941).

percent variation in C suffices to give agreement, provided C be varied so as to give larger radii for larger Z, and smaller radii for smaller Z. This variation is not in agreement with the nuclear radii deduced from recent fast neutron scattering experiments.[3] However, the nuclear radius is a sufficiently ill-defined quantity that one may perhaps admit such a five percent variation for the light nuclei as lying within the present limits of error of nuclear theory and experiment. In this sense one may say that the experimental evidence requires a range for the assumed f-field of the order of $0.1r_0$ or smaller. But for a range of this size, Pais' theory in the first approximation would predict that the proton should be heavier than the neutron by about four electron masses.

Thus it is concluded that the concept of the f-field in its present form cannot account simultaneously for the neutron-proton mass difference and for the mass differences of the mirror nuclei. It should be pointed out, however, that this conclusion depends on the following assumptions:

(1) The range of the f-field is given to a sufficient accuracy by equating the proton-neutron mass difference as computed in first approximation to the experimental value for this quantity.

(2) The equality of the specific nuclear interaction between like nucleons. It should be noted that, in accordance with the treatment of the nucleon problem given by Pais,[1] the f-interaction is supposed to be *superposed* on that short range proton-proton interaction which, on arguments of charge symmetry, is equal to the neutron-neutron interaction.

(3) A uniform distribution of the charge over the interior of the nucleus. (A supplementary calculation gave similar results when the charged particles were assumed to be concentrated on a shell.) This model is *not* a good approximation if the nucleons have a mean separation greater than the range of the f-field. However in this case the f-energy is small compared to the Coulomb energy. Consequently even a substantial percentage error in the f-energy would at most introduce a correction in Fig. 1 which could not change the order of magnitude, $0.1r_0$, of the maximum range allowable for the f-field.

(4) The possibility of representing the effect of the f-field at all in terms of a purely static potential under nuclear conditions (separations $\sim r_0$, velocities $\sim c/20$). The representation of the interaction of elementary particles by means of a static potential has indeed a limited validity for all theories of short range forces.[4]

There is one further point. According to the hole theory, the field generated by a charged particle polarizes the sea of negative energy electrons which constitute the vacuum. This causes a deviation from Coulomb's Law,[5] which here has been tacitly neglected. The magnitude of the effect will in principle depend on both the electromagnetic and f-fields. The polarization effect of the f-field will be of the same order of magnitude as that of the electromagnetic field. The contribution of the latter to ΔE is negligible, however, in comparison with the direct contribution of the f-field computed above. Thus polarization effects as calculated in first approximation according to the present methods of the hole theory cannot reconcile the f-field theory with the data on the mirror nuclei.

I thank Dr. A. Pais and Professor J. A. Wheeler for much helpful discussion.

[3] R. Scherr, Phys. Rev. 68, 240 (1945).

[4] C. Møller and L. Rosenfeld, Kgl. Danske Vid. Sels. Math.-fys. Medd. 17, 8 (1940).

[5] E. Uehling, Phys. Rev. 48, 55 (1935).

Initial Performance of the 184-Inch Cyclotron of the University of California

W. M. Brobeck, E. O. Lawrence, K. R. MacKenzie,* E. M. McMillan, R. Serber, D. C. Sewell, K. M. Simpson,** and R. L. Thornton
Radiation Laboratory, Physics Department, University of California, Berkeley, California
(Received February 26, 1947)

THE successful application of the *principle of phase stability*[1,2] to a cyclotron has been reported from this Laboratory.[3] The satisfactory results of these experiments, performed on the 37-inch cyclotron, led to the decision to complete the 184-inch cyclotron then under construction as a frequency modulated machine. It is the purpose of this note to describe briefly the equipment and experiments by which deuteron and alpha-particle beams of approximately 200 and 400 Mev, respectively, have been produced.

The angular velocity of such ions in a magnetic field decreases by 11 percent because of the relativistic increase in mass during acceleration. In addition, a radial decrease of magnetic field, essentially linear from the center of a value of 95.4 percent of the central field at a radius of 80 inches, is provided to focus the ion beam properly. This field shape is produced by shims inside the vacuum chamber with contours empirically determined through measurements on a scale model. Thus a total minimum frequency variation of 16 percent is required; in practice it is desirable to provide a substantially greater frequency variation to insure that a satisfactory shape of the frequency *vs.* time curve is obtainable and to make adjustments less critical.

The frequency modulation is produced by a rotating mechanical vacuum capacitor similar in principle to that previously used.[4] Modulation frequencies up to 2000 c.p.s. are obtainable. The single dee and the capacitor are mounted at either end of a shielded line forming a resonant system, whose frequency varies between 12.6 and 9.0 megacycles. The system is excited by means of a grounded grid self-excited oscillator inductively coupled to the resonant circuit.[5] A power input of 18 kilowatts to the plate circuit produces a dee voltage of 15 kilovolts (peak voltage averaged over a frequency-modulation cycle). The magnetic field has a value of 15,000 oersteds at the center; the useful magnetic gap is 19 inches; the height available for the ion beam is 5 inches.

In line with our previous experience, it is necessary to apply a d.c. bias voltage to the dee system to serve as a clearing field; in the absence of such a bias, residual ionization at low dee voltages so loads the oscillator as to prevent the build-up of dee voltage. Similarly it has been found desirable to enclose the dee with grounded shields to reduce the volume available for glow discharges.

A low voltage arc discharge of the type commonly used in cyclotrons serves as ion source. Provision is made for the application of the arc voltage for a time variable between 1 and 110 microseconds at the appropriate point in the frequency-modulation cycle. Our present experience indicates that greater output is obtained from such a pulsed arc than from one operating continuously. For cloud-chamber and similar experiments, a single pulse may be produced at a time controlled by the equipment in question.

All our present experiments are being performed with an internal probe target. It is not planned to attempt to deflect the beam out of the magnetic field in the immediate future.

Under these conditions a deuteron beam is observed at a dee voltage as low as 8 kilovolts and a corresponding optimum capacitor speed of 120 r.p.m. (equivalent to 48 c.p.s.). In accordance with theory, the latter is not critical. At present, normal operating conditions include a dee voltage of 15 kilovolts and a frequency-modulation rate of 120 c.p.s.; with an average energy gain per revolution of one-half the pos-

* Now at the University of British Columbia.
** Now at Santa Barbara College.
[1] E. M. McMillan, Phys. Rev. **68**, 143 (1945).
[2] V. Veksler, J. Phys. U.S.S.R. **9**, 153 (1945).
[3] J. R. Richardson, K. R. MacKenzie, E. J. Lofgren, and B. T. Wright, Phys. Rev. **69**, 669 (1946).
[4] F. H. Schmidt, Rev. Sci. Inst. **17**, 301 (1946).
[5] K. R. MacKenzie and V. Waithman, to be published when patent release can be obtained.

sible maximum, this involves a total number of turns of the order of 10^4, and a time of flight from the ion source to a target at 80 inches radius of approximately 1000 microseconds. The time-average current to a probe at 20 inches radius approximates 0.6 microampere; this current remains constant as the radius is increased to 40 inches corresponding to 52 Mev. At this point the measured current to the target decreases rapidly and is barely measurable ($\sim 2\times 10^{-10}$ amp.) at a radius of 81 inches, and is zero beyond 82 inches. During this decrease the direct neutron radiation from the target increases steadily and falls abruptly to zero in the neighborhood of 82 inches radius. This decrease in current between 40 and 81 inches can be explained by the penetration of the beam through the leading edge of the tapered probe target, and the energy at which it occurs agrees with the calculated range of the deuterons. We do not believe that a substantial fraction of the current is lost between 40 and 81 inches. Measurements of the radiation (which is highly directional) and the induced radioactivity of dee and probe indicate that beyond 82 inches the ion beam is lost to the dee through vertical spreading. In general it may be said that the detailed performance, as far as it has been investigated to date, is in accord with the theory.[6] In view of the fact that this output is more than adequate for our present experimental program, and that the cyclotron is as yet imperfectly shielded, no attempt has been made to increase the current beyond the values obtained initially.

Replacement of the deuterium gas with helium leads (after thorough flushing of the system) to an alpha-particle beam of twice the deuteron energy resulting from the acceleration of doubly charged ions. Radiation yields from such a beam are comparable to those obtained with deuterons, but few experiments using these ions have as yet been carried out.

[6] D. Bohm and L. Foldy, to be published.

No direct measurement of the deuteron or alpha-particle energies has as yet been made. From geometrical considerations, the expected energies at 81 inches radius are 195 Mev for deuterons, and 390 Mev for alpha-particles. Since the conical shape of the magnetic field centers the ion beam quite strongly, we do not believe that the actual energy is substantially lower. It may be noted in this connection that careful measurements of the range of protons accelerated to 15 Mev on the 37-inch f-m cyclotron show excellent agreement with that predicted from the geometry.

Measurement of the directional properties of the neutron radiation emitted from a target, both by means of ionization chambers and the use of radioactive detectors activated by fast neutrons, show that a large fraction of the radiation is emitted in the forward direction in a cone of angle 11 degrees at half-intensity. Disintegrations resulting in the emission of many particles from both deuteron and neutron bombardment are observed from radio-chemical investigations, and from the observation of numerous "stars" in cloud chambers and photographic emulsions. Preliminary estimates of the neutron-energy distribution through proton recoils observed in a cloud chamber using a 10,000 oersted field indicate a distribution extending to the neighborhood of 100 Mev. These and other experiments will be reported in detail by the workers involved when the experiments are completed.

It is a pleasure to acknowledge our indebtedness to the entire staff of the Radiation Laboratory whose cooperation has made the equipment possible. The construction of the cyclotron was made possible by a grant made by the Rockefeller Foundation, supplemented by others from the Research Corporation, the John and Mary Markel Foundation, and the University of California. The later part of the work was partially supported by the Manhattan District under Contract No. W-7405-Eng-48.

Maximum β-Energies and the Mass of the Neutrino

O. KOFOED-HANSEN
Institute for Theoretical Physics, University of Copenhagen, Denmark
(Received March 6, 1947)

OCCASIONALLY it has been mentioned[1] that one might be able to estimate the mass of the neutrino, ν, from the knowledge of maximum β-energies (in the following denoted E^{max} and involving the electron rest mass mc^2) and corresponding mass differences (ΔM) between two neighboring isobars, one of which decays into the other by β-decay. The mass of the neutrino might then be determined from the following relation:

$$\Delta Mc^2 = E^{max} + \nu c^2. \quad (1)$$

It has been hoped that this method would yield a more direct estimate of the mass of the neutrino, than that based on a comparison between experimental β-spectra and the form of these spectra as predicted by the theory of Fermi.[2] Such a comparison gives at present a mass of the neutrino smaller than $\frac{1}{5}$ the electron mass. However, a more detailed analysis of the problem seems to indicate that the maximum β-energy can only be determined from the experimental β-spectra with the same accuracy as can the mass of the neutrino by the original Fermi method, i.e., from the shape of these spectra. If the mass of the neutrino is not zero, but is smaller than the electron mass, this will only affect the shape of the β-spectra near the upper limit. Now, the probability for the emission of a β-particle with an energy near the upper limit is small, and for this reason a determination of the upper limit is usually based on an extrapolation of the curve from points not too near the upper limit. It is true that these points are experimentally more accurately determined, but they are generally not affected by the finite mass of the neutrino, and the extrapolation leads, thus, to a value E^{ex}, which would be equal to that E^{max} which one would find if the mass of the neutrino were zero. In other words, the extrapolated energy value is equal to the true maximum energy augmented by the energy equivalent to the mass of the neutrino. It is thus not possible to estimate νc^2 using the value E^{ex} instead of E^{max} in Eq. (1).

Very often one uses the so-called Fermi plot for this extrapolation. The probability $P(p)dp$ for the emission of a β-particle with momentum p within the limits dp, is as a first approximation in the Fermi theory given by the following formula in which the mass of the neutrino has not been neglected:

$$P(p)dp = \text{const} \cdot p^2(E^{max} + \nu c^2 - E) \times [(E^{max} + \nu c^2 - E)^2 - (\nu c^2)^2]^{\frac{1}{2}} \cdot dp \quad (2)$$

and where E is the β-energy corresponding to the momentum p. In the so-called Fermi plot mentioned above, one plots $[P(p)/p^2]^{\frac{1}{2}}$ against E. If the mass of the neutrino is put equal to zero, we get, in all cases where the experimental curve follows the Fermi curve, a straight line cutting the abscissa at E equal to E^{max}:

$$[P(p)/p^2]^{\frac{1}{2}} = (E^{max} - E). \quad (3)$$

If the mass of the neutrino is not zero, but small, we may remember that the determination of E^{max} is based on an extrapolation, i.e., on points with

$$E^{max} + \nu c^2 - E \gg \nu c^2 \sim 0. \quad (4)$$

We may then neglect the small term $(\nu c^2)^2$ in (2), and the Fermi plot gives

$$[P(p)/p^2]^{\frac{1}{2}} = (E^{max} + \nu c^2 - E). \quad (5)$$

It is thus seen that the extrapolated maximum energy E^{ex} is given by

$$E^{ex} = E^{max} + \nu c^2. \quad (6)$$

As mentioned before, E^{ex} does not permit a determination of νc^2, and only as far as the shape of the curve near E^{max} can be determined, can we find the actual values of E^{max} and, consequently, the value of νc^2.

As an illustration, the theoretical Fermi curves for four different assumptions as regards the mass of the neutrino have been drawn in a

[1] E. M. Lyman, Phys. Rev. **55**, 234 and 1123 (1939); R. O. Haxby, W. E. Shoupp, W. E. Stephens and W. H. Wells, Phys. Rev. **58**, 1035 (1940).
[2] E. Fermi, Zeits. f. Physik **88**, 161 (1934).

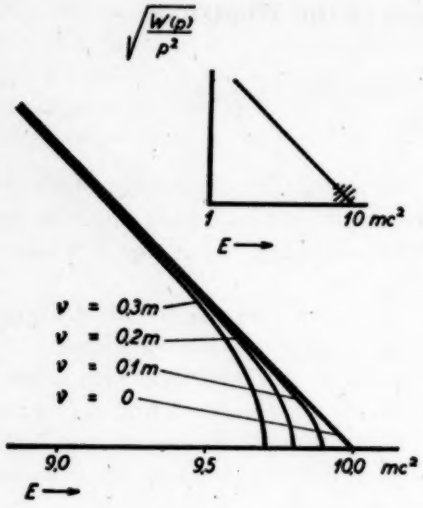

FIG. 1. Theoretical Fermi plots for a β-emitter with $\Delta M = 10 \cdot m$ is shown above to the right. The hatched part of this plot is shown in enlarged scale in the lower part of the figure for four different assumptions about the mass of the neutrino.

Fermi plot in Fig. 1, where the mass difference ΔM has been put equal to $10m$. The deviations from the straight line are small and occur only near the upper limit, practically only in the interval

$$(\Delta M - 2\nu)c^2 < E < \Delta M c^2.$$

The thesis that the maximum β-energy can only be determined with the same accuracy as can the mass of the neutrino, has here been illustrated in the special case of the Fermi theory, which fits experimental data rather closely, but it is not restricted to this theory alone. At any rate, we may say that the probability $P(p)dp$ is a function of the energies and momenta of the neutrino and the electron, which are connected by the law of conservation of energy. The derivation of such an expression is only based on the following assumptions:

(a) The process is one involving three particles, and the mass of the recoil nucleus may be regarded as infinite compared with the two other masses.

(b) The law of conservation of energy and momentum is valid, the conservation of energy being expressed by the following formula:

$$E_\nu + E = E^{\max} + \nu c^2 = \Delta M c^2, \tag{7}$$

so that $P(p)dp$ may be written

$$P(p)dp = f(p, E, p_\nu, E_\nu), \tag{8}$$

where the indices ν refer to the neutrino. Inserting (7) in (8) we get

$$P(p)dp = f\{p, E, (E^{\max} + \nu c^2 - E), \times [(E^{\max} + \nu c^2 - E)^2 - (\nu c^2)^2]\}^{\frac{1}{2}} dp, \tag{9}$$

and it is again seen that E^{ex} may come out in accordance with (6).

Of course, an upper limit for the neutrino mass may be deduced in such cases where $E^{\max}$ may be neglected, e.g., $H^3 \rightarrow He^3$, but the mass difference $H^3 - He^3$ is at present not known with sufficient accuracy. Also, investigations near the upper limit of β-spectra with refined experimental technique might be of interest, and provide a possibility for a better estimate of the mass of the neutrino.

My thanks are due Professor Niels Bohr for his kind interest in the present work and Professor C. Møller for having drawn attention to the problem.

Letters to the Editor

PUBLICATION of brief reports of important discoveries in physics may be secured by addressing them to this department. The closing date for this department is, for the issue of the 1st of the month, the 8th of the preceding month and for the issue of the 15th, the 23rd of the preceding month. No proof will be sent to the authors. The Board of Editors does not hold itself responsible for the opinions expressed by the correspondents. Communications should not exceed 600 words in length.

Showers of Penetrating Particles at Altitude of 26,000 Feet

GLEB WATAGHIN
Department of Physics, University of São Paulo, São Paulo, Brazil
February 17, 1947

THE variation of the frequency of showers of penetrating particles with atmospheric depth was observed during three recent flights in an airplane at altitudes of 22,000 and 26,000 feet. The arrangement and the results are indicated in Fig. 1, where also the results of previous measurements are reported.[1] (Circles indicate measurements made in recent flights, X refers to measurements made in 1944 in the mountains, at 24.2 inches Hg of mean pressure and in 1946 in an airplane at 13.4 inches Hg.) The improved arrangement with 8 counters of 200 cm² of area permitted the observation of a greater number of fourfold coincidences: 157 in 35 min. at the highest altitude (11 inches Hg), 145 in 67 min. at the altitude corresponding to 13 inches Hg. We used a coincidence set with a multivibrator, following the method of Sousa Santos. The resolving time was $\sim 2\times 10^{-6}$ sec. The efficiency was better than . . . 98 percent. The observed variation with altitude is in agreement with the assumption of an exponential absorption law for the shower producing primary radiation. One obtains cross sections per nucleus of O or $N \sim 2.5\times 10^{-25}$ cm² (or $\sim 1.6\times 10^{-26}$ per nucleon). The intensity falls by a factor e in ~ 101 g/cm² of air. This value agrees with the values indicated by Janossy and based on the transition effect in Pb. The author acknowledges the valuable cooperation of the Brazilian Air Force and expresses his special thanks to the Minister of Air, Major-Brigadeiro A. F. Trompowsky, Brigadeiro Eduardo Gomes, and to all persons who helped him in these experiments.

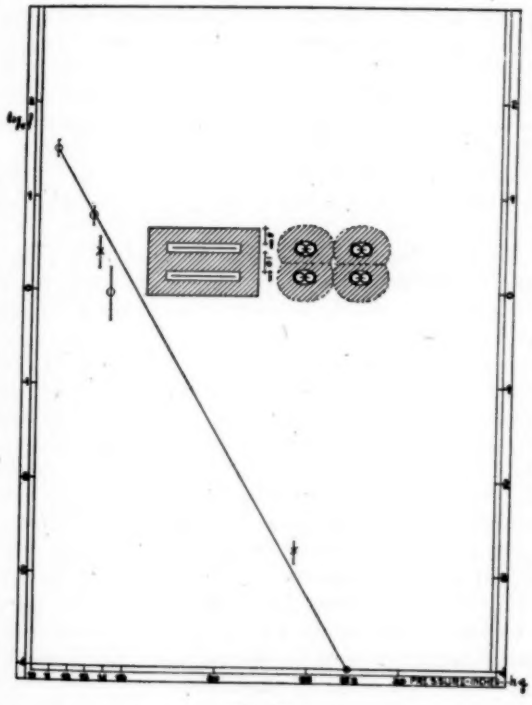

FIG. 1.

[1] O. Sála and G. Wataghin, Phys. Rev. 70, 430 (1946).

The Total Disintegration Energy of Na^{24}*

EDGAR C. BARKER
Clinton Laboratories, Oak Ridge, Tennessee
March 1, 1947

COINCIDENCE measurements[1–5] have shown that the two γ-rays of Na^{24} are probably emitted in cascade. They have energies of 2.76 and 1.38 Mev. Sachs[6] has pointed out that if they are in cascade, the disintegration energy of Na^{24} may be higher than would be expected according to the considerations of Barkas.[7] The following is the result of a different kind of experiment which bears directly on the same question. This was a measurement for Na^{24} analogous to that which was made for RaB and RaC by L. H. Gray.[8] In this type of experiment, the source is placed in a large block of aluminum, and distribution measurement of the γ-energy absorbed in the aluminum are made with small ionization chambers. Integration gives the total energy emitted per second from the source, and a determination of the β-strength gives the average γ-energy emitted per β-particle. In the case of Na^{24} the β-decay is simple, and the result is interpretable as the γ-energy accompanying each disintegration.

Measurements with two separate sources gave the γ-energy per disintegration as 4.15 Mev and 4.19 Mev, respectively, assuming 32.5 ev as the energy required to produce an ion pair. Adding the beta-disintegration energy of 1.39 Mev, one obtains 5.56 Mev for the total disintegration energy of Na^{24}.

* This document is based on work performed under Contract No. W-35-058-eng-71 for the Manhattan Project and the information covered therein will appear in Division IV of the Manhattan Project Technical Series, as part of the contribution of the Clinton Laboratories.

[1] Feather and Dunworth, Proc. Camb. Phil. Soc. 34, 442 (1938).
[2] J. Itoh, Proc. Phys. Math. Soc. Japan 23, 605 (1941).
[3] L. G. Elliot, M. Deutsch, and A. Roberts, Phys. Rev. 63, 386 (1943).
[4] H. Maier-Leibnitz, Zeits. f. Physik 122, 233 (1944).
[5] C. S. Cook, E. Jurney, and L. M. Langer, Phys. Rev. 70, 985 (1946).
[6] R. C. Sachs, Phys. Rev. 70, 572 (1946).
[7] W. H. Barkas, Phys. Rev. 55, 691 (1939).
[8] L. H. Gray, Proc. Roy. Soc. 159A, 263 (1937).

The Reaction $_{38}Sr^{86}(n,\gamma)_{38}Sr^{87*}$ Produced by Thermal Neutrons†

LEO SEREN,†† HERBERT N. FREIDLANDER, AND SOLOMON TURKEL
Metallurgical Laboratory, University of Chicago, Chicago, Illinois
February 28, 1947

THE isotope $_{38}Sr^{87*}$, which is the excited isomer of the stable state $_{38}Sr^{87}$, has been produced by thermal neutron capture of the isotope $_{38}Sr^{86}$. Of the entire species of radio isotopes produced by thermal neutron capture of stable isotopes,[1,2] this is the only known case in which the binding energy released by capture produces an *excited* state of the next *stable* isotope.

In the past, the isotope $_{38}Sr^{87*}$ has easily been produced by *fast* neutrons on Sr with some indication that the reaction $_{38}Sr^{86}(n,\gamma)_{38}Sr^{87*}$ also took place. Stewart *et al.*,[3] produced 2.7 hr. $_{38}Sr^{87*}$ by irradiating Sr inside of a few cm of paraffin with Li+D neutrons. Although thermal neutrons were present, the few cm of paraffin could not remove the fast neutrons, so the experiment was not conclusive. Reddeman[4] showed that the fast neutron activity on Sr was caused by the $_{38}Sr^{87}(n,n)_{38}Sr^{87*}$ reaction. By irradiating in the same geometry with fast and slow neutrons, the 2.7 hr. activity was doubled, thus indicating that the reaction $_{38}Sr^{86}(n,\gamma)_{38}Sr^{87*}$ also took place.

We have observed the 2.7 hr. $_{38}Sr^{87*}$ activity by irradiating $Sr(NO_3)_2$ in the thermal column of the Argonne pile. Since no fast neutrons are found in the thermal column (the cadmium ratio for indium resonance neutrons is greater than 20,000), this seems to indicate conclusively that the thermal neutron reaction $_{38}Sr^{86}(n,\gamma)_{38}Sr^{87*}$ does take place. The identification of our slow neutron produced activity as due to $_{38}Sr^{87*}$ was made from:

(a) the 2.7 hr. half-life;

(b) the shape of the absorption curve which clearly indicates conversion electrons (see Fig. 1 in which the conversion electron absorption curve of $_{38}Sr^{87*}$ is compared to the beta-ray absorption curve of 54 day $_{80}Hg^{203}$);

(c) the absorption end point (visual) of the particles which is at 0.36 Mev.

All of these properties agree with those of $_{38}Sr^{87*}$ listed in Seaborg's Tables.[1]

Using an internal conversion coefficient[5] of 15 percent, the cross section[2] per strontium atom for the thermal neutron reaction $_{38}Sr^{86}(n,\gamma)_{38}Sr^{87*}$ was found to be 0.13 barns.

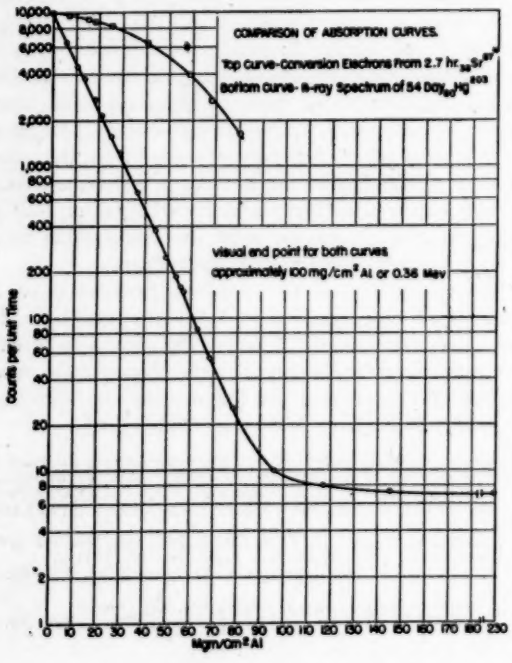
COMPARISON OF ABSORPTION CURVES.
Top curve-Conversion Electrons from 2.7 hr $_{38}Sr^{87*}$
Bottom curve- B-ray Spectrum of 54 Day $_{80}Hg^{203}$
visual end point for both curves
approximately 100 mg/cm² Al or 0.36 Mev
Counts per Unit Time
mgm/cm² Al

FIG. 1.

† Work was completed in June 1944 and submitted for clearance August 1946. This document is based on work performed under Contract No. W-7401-eng-37 for the Manhattan Project and the information covered therein will appear in Division IV of the Manhattan Project Technical Series as part of the contribution of the Argonne National Laboratory.

†† Present addresses of the authors: Leo Seren, General Electric Research Laboratory, Schenectady, New York; Herbert Freidlander, Dept. of Chemistry, University of Chicago; Solomon Turkel, Fairchild Engine and Airplane Corp., Nepa Division, P. O. Box 415, Oak Ridge, Tennessee.

[1] G. T. Seaborg, Rev. Mod. Phys. **16**, 1 (1944).

[2] Refer to "Thermal Neutron Activation Cross Sections," to be published soon by the same authors.

[3] D. W. Stewart, J. L. Lawson, and J. M. Cork, Phys. Rev. **52**, 901 (1937).

[4] H. Reddeman, Naturwiss. **28**, 110 (1940).

[5] L. A. DuBridge and John Marshall, Phys. Rev. **56**, 707 (1939).

On the Existence of Single Magnetic Poles

ELLIOT T. BENEDIKT AND HERTA R. LENG
Rensselaer Polytechnic Institute, Troy, New York
February 17, 1947

THE present paper describes experiments devised to verify the existence of single magnetic poles as claimed by F. Ehrenhaft.[1]

The method used was based on the observation of the motion of ferromagnetic particles under the action of a magnetic field generated by an electric current. If single magnetic poles were present, the magnetic field would cause motion in the direction of the closed lines of magnetic force.

The experimental arrangement consisted of a vertical copper conductor having a section (4.2 cm in length and with a diameter of 1.3 cm) covered by a layer of asbestos and rubber tubing. It was surrounded by a square ebonite container (7.4 cm wide and 2 cm deep) provided with two circular windows. Another section of the conductor was surrounded by a Bakelite jacket. Currents up to 3000 amperes were generated by a "Continous Current Generator, G.E. Company, type M.P." The solution was illuminated by a beam of light from a carbon arc and observed by means of a microscope at a distance of 1.5 cm from the center of the conductor. Heating of the apparatus was avoided as long as possible by the insulation of the conductor, described above, and cooling obtained by means of ice placed into the Bakelite jacket. The observations were discontinued when the thermometer, placed into the liquid, indicated a rise in temperature.

Fifteen observations were performed with a colloidal

solution of Fe_3O_4 (radius as estimated by Elmore[2] equals 17mμ, viscosity: 1.165 dyne sec./cm², density: 1.002 g/cm²). A few experiments were conducted with colloidal solutions of iron and nickel in distilled water prepared with Bredig's method (approximate size of particles: 20mμ). Some of these suspensions were previously placed between the poles of an electromagnet (10,000 gauss) for half an hour in order to produce separation of the two hypothetical kinds of single magnetic poles. The portions of the liquid near the pole-pieces were examined separately. The observations showed that the particles were generally at rest in the liquid or performing a slight Brownian motion. No motion such as would be expected from single magnetic poles was observed.

In order to interpret this result consider a spherical particle having a total magnetic charge m, and acted upon by a magnetic field H. Its motion would be described by the differential equation

$$M'\frac{\partial \mathbf{v}}{\partial t}=m\mathbf{H}-c\mathbf{v}, \qquad (1)$$

where $\mathbf{v}$ is the velocity, c the coefficient of friction, and M' the apparent mass of the particle in the liquid. M' was taken as the sum of the mass of the particle and one-half of the liquid displaced by it. Integrating (1) under the assumption that $\mathbf{H}$ is constant we obtain:

$$\mathbf{v}(t)=(m/c)\mathbf{H}+[\mathbf{v}(0)-(m/c)\mathbf{H}]\exp(-ct/M'). \qquad (2)$$

In the case of the colloidal solution of Fe_3O_4, $M'=1.72\times10^{-16}$ gram. Taking for c the value 3.73×10^{-5} dyne sec./cm calculated from Stokes' law, c/M' becomes 2.16×10^{11} sec.$^{-1}$. The time-dependent term on the right side of (2) can therefore be neglected.

The fact that no motion was detected implies that the magnetic charge of the observed particles does not exceed the quantity

$$m_0=cv_0/H, \qquad (3)$$

where v_0 is the smallest observable velocity. Making the conservative assumption that the smallest displacement with respect to the crosshair of a microscope observable by the eye is 0.05 cm, and having a microscope with the magnification 20, the smallest displacement[3] that could be detected would be 0.005 cm. The observation time in most cases was 3 minutes. Using this time we obtain $v_0=1.4\times10^{-5}$ cm/sec. The magnetic field in the region under observation was 348 gauss. Using this value we find: $m_0=1.5\times10^{-12}$ e.m.u. (A slightly higher value is found from the other colloidal solutions.)

The experiments above described give no evidence of the existence of single magnetic poles. (In case of their existence their pole-strength does not exceed 1.5×10^{-12} e.m.u.)

We wish to express thanks to Dr. G. H. Carragan and Dean M. A. Hunter for their interest in the present work, to Dr. F. W. Schwartz for preparing the solution, to Dr. W. C. Elmore for helpful information and to Mr. O. Rasmussen for building the apparatus.

[1] F. Ehrenhaft, Phys. Rev. 60, 169 (1941); 61, 733 (1942); 63, 216 and 461 (1943); 64, 43 (1943).
[2] W. C. Elmore, Phys. Rev. 54, 309 and 1092 (1938).
[3] The calculated average displacement caused by Brownian motion in the same time is 6.64×10^{-4} cm.

The Origin of Low Frequency Raman Lines in Organic Crystals

A. KASTLER AND A. ROUSSET
University of Paris and University of Bordeaux, France
March 4, 1947

IN the spectrum of the light scattered by crystals of organic molecules of high optical anisotropy, the Russian physicists, Gross and Vuks,[1] discovered in 1936 Raman lines of low frequencies (smaller than 150 cm^{-1}). They attributed them to lattice oscillations: These external or intermolecular lines disappear at melting, while the internal or intramolecular lines persist, with almost the same frequencies, in the liquid state. The frequency-measurements alone, made by Vuks[2] on the paradichloro- and the paradibromo-benzenes and by Gross and Korshunow[3] on the di-iodo-benzenes, did not permit of any conclusion as to the form of these lattice-oscillations. By making a complete study of the polarization and intensity characters of the low frequency lines of a naphthalene-monocrystal in different orientations the authors were able to prove that these lines are produced by rotatory oscillations of the molecules about their three principal axes of inertia, and they showed that the coupling of these motions in the unit cell gives rise to a fine structure of the lines.[4] At the same time Nedungadi[5] in India, working with the same crystals, had come to the same conclusions as a result of polarization measurements.

Later, Rousset and Lochet showed that the hypothesis of rotatory oscillations leads, for the three types of di-iodo-benzene, to a number of low frequency lines in excellent agreement with the experimental results of Gross and Korshunow.[3] An exhaustive study[6] of the polarization of the lines of paradichloro-benzene and of paradibromo-benzene indicated the corresponding axis of rotation for each line.

Polarization measurements on monocrystals of benzene made by Kastler and Fruhling[7] enabled them to study the rotatory oscillations about two axes of the plane of the benzene ring. They found however that the 35 cm^{-1} line behaves as a totally symmetric oscillation. Rousset suggested that this line might be due to a complete rotation of the benzene molecule about its hexagonal axis,[8] and he showed that this hypothesis could explain the curve of specific heat of solid benzene at very low temperatures.[9]

In making a theoretical analysis of the origin of intermolecular forces in a lattice of organic crystals, Rousset[10] was able to prove that the rotatory oscillations of the molecules occur necessarily about the principal axes of inertia if these axes are also principal axes of polarizability. The external motions of translatory type do not appear in the spectra of the light scattered by organic crystals. This is a consequence of the fact that the centers of mass of all molecules form a singular lattice of points even in the case where the unit cell contains more than one molecule.[8] The constancy of the product of the square of the frequency by the corresponding moment of inertia for all dihalogenated benzenes in the para-position is an argument in favor of the hypothesis of rotatory oscillations; this argument has been invoked by Rousset and Lochet,[6] and in recent

publications by Gross and Korshunow,[11] and by Vuks[12] who reach the same conclusions as the French and Indian physicists as to the nature of the low frequency lines. But polarization measurements are necessary to check these conclusions and to determine the orientations of the axes of molecular rotatory oscillation relative to the known crystallographic axes. These rotatory oscillations which appear in the spectra of the light scattered by crystals are included amongst the $3N-6$ fundamental oscillations of the crystal lattice[13] and form optical branches of the spectrum of the elastic vibrations of crystals.

[1] E. Gross and M. Vuks, J. de phys. et rad. 7, 113 (1936).
[2] M. Vuks, Acta Phys. Chim. U.R.S.S. 6, 11, 337 (1937).
[3] E. Gross and A. Korshunow, Comptes rendus Acad. Sci. U.R.S.S. 24, 328 (1939).
[4] A. Kastler and A. Rousset, Comptes rendus 212, 645 (1941); J. de phys. et rad. 2, 49 (1941).
[5] T. M. K. Nedungadi, Proc. Ind. Acad. Sci. A, 13, 161 (1941); 15, 376 (1942).
[6] A. Rousset and R. Lochet, J. de phys. et rad. 3, 146 (1942).
[7] A. Kastler and A. Fruhling, Comptes rendus 218, 998 (1944).
[8] A. Rousset, Comptes rendus 219, 485 (1944).
[9] A. Rousset, Comptes rendus 219, 546 (1944).
[10] A. Rousset, Ann. de physique 20, 53 (1945).
[11] E. Gross and A. Korshunow, Acta Phys. Chim. U.R.S.S. 20, 353 (1945).
[12] M. Vuks, Acta Phys. Chim. U.R.S.S. 20, 851 (1945). Thesis, Acad. Sci. Ukr S.S.R., June 1943.
[13] S. Bhagavantam, Proc. Ind. Acad. Sci. A, 13, 543 (1941).

Electron-Neutrino Angular Correlation in Beta-Decay

DONALD R. HAMILTON
Palmer Physical Laboratory, Princeton University, Princeton, New Jersey
February 21, 1947

BLOCH and Moller have noted[1] an expected correlation between the directions of emission of electron and neutrino in beta-decay; for allowed Fermi transitions they predict a correlation function $W(\theta)\approx(1+\cos\theta)$ for the relative probability of decay with the angle θ between these two directions. Observations on the recoil nucleus[2] have tended to consistency with the above correlation function.

The present note concerns the specific correlation functions for the allowed and first forbidden transitions corresponding to the five invariant forms of beta-interaction. The results of primary interest are the following: (1) even for allowed transitions the correlation functions (in contrast to the energy spectra) are markedly different for the different possible interactions; (2) with increasing order of forbiddenness, emission of the neutrino in the same direction as the electron is increasingly emphasized.

The calculations reported assume plane-wave electrons ($Z\approx 0$, high energies) and are similar to the calculations of electron energy spectra;[3] averaging $W(\theta)$ over θ gives the spectrum correction factors of Konopinski and Uhlenbeck. The correlation functions follow:

Correlation Functions $W(\theta)$

Allowed transitions (W_0):

Scalar:	$W_{0S}=1-(p/E)\cos\theta$;
Polar vector: (Fermi)	$W_{0V}=1+(p/E)\cos\theta$;
Tensor: (Gamow-Teller)	$W_{0T}=1+\frac{1}{3}(p/E)\cos\theta$;
Axial vector:	$W_{0A}=1-\frac{1}{3}(p/E)\cos\theta$;
Pseudoscalar:	$W_{0P}=1-(p/E)\cos\theta$.

First forbidden transitions (W_1):

$$3W_{1S}=\left|\int \mathbf{r}\right|\left[1-(p/E)\cos\theta\right](p^2+q^2+2pq\cos\theta),$$

$$\begin{aligned}4W_{1V}=&\left|\int \mathbf{r}\right|\left[1+(p/E)\cos\theta\right](p^2+q^2+2pq\cos\theta)\\&+\left|\int \boldsymbol{\alpha}\right|^2(3-p\cos\theta/E)\\&+\left\{\left(\int \mathbf{r}\right)^*\cdot\left(\int \boldsymbol{\alpha}\right)-\text{cc}\right\}\\&\times\left[q+p\cos\theta+(p/E)(p+q\cos\theta)\right],\end{aligned}$$

$$\begin{aligned}3W_{1T}=&\frac{1}{20}(\Sigma_{ij}|B_{ij}|^2)\left[\left(5+\frac{p}{E}\cos\theta\right)(p^2+q^2+2pq\cos\theta)\right.\\&\left.-\frac{p^2q}{E}\sin^2\theta\right]+\frac{1}{2}\left|\int \boldsymbol{\sigma}\times\mathbf{r}\right|^2\left[\left(1+\frac{p}{E}\cos\theta\right)\right.\\&\left.\times(p^2+q^2+2pq\cos\theta)+\frac{p^2q}{E}\sin^2\theta\right]\\&+\left|\int \boldsymbol{\alpha}\right|^2\left(3+\frac{p}{E}\cos\theta\right)-\left\{\left(\int \boldsymbol{\sigma}\times\mathbf{r}\right)^*\right.\\&\left.\cdot\left(\int \boldsymbol{\alpha}\right)+\text{cc}\right\}\left[q+p\cos\theta+\frac{p}{E}(p+q\cos\theta)\right]\\&+\frac{1}{3}\left|\int \mathbf{r}\cdot\boldsymbol{\sigma}\right|^2\left[\left(1-\frac{p}{E}\cos\theta\right)\right.\\&\left.\times(p^2+q^2+2pq\cos\theta)-\frac{2p^2q}{E}\sin^2\theta\right],\end{aligned}$$

$$\begin{aligned}3W_{1A}=&\frac{1}{20}(\Sigma_{ij}|B_{ij}|^2)\left[\left(5-\frac{p}{E}\cos\theta\right)(p^2+q^2+2pq\cos\theta)\right.\\&\left.+\frac{p^2q}{E}\sin^2\theta\right]+\frac{1}{2}\left|\int \boldsymbol{\sigma}\times\mathbf{r}\right|^2\left[\left(1-\frac{p}{E}\cos\theta\right)\right.\\&\left.\times(p^2+q^2+2pq\cos\theta)-\frac{p^2q}{E}\sin^2\theta\right]\\&+\frac{1}{3}\left|\int \mathbf{r}\cdot\boldsymbol{\sigma}\right|^2\left[\left(1+\frac{p}{E}\cos\theta\right)(p^2+q^2+2pq\cos\theta)\right.\\&\left.+\frac{2p^2q}{E}\sin^2\theta\right]+3\left|\int \gamma_5\right|^2\left(1+\frac{p}{E}\cos\theta\right)\\&+i\left\{\left(\int \mathbf{r}\cdot\boldsymbol{\sigma}\right)^*\left(\int \gamma_5\right)-\text{cc}\right\}\\&\times\left[(q+p\cos\theta)+\frac{p}{E}(p+q\cos\theta)\right],\end{aligned}$$

$$3W_{1P}=\left|\int \gamma_5\mathbf{r}\right|^2\left(1-\frac{p}{E}\cos\theta\right)(p^2+q^2+2pq\cos\theta).$$

For notation, see reference 3. Electron and neutrino momenta are p and q in units of mc; E is total electron energy in units of mc^2; $E^2=p^2+1$. The abbreviated integrals represent the nuclear matrix elements which determine selection rules and (in part) transition probabilities. Forbidden transitions may in some cases occur *via* the non-vanishing of any of several matrix elements, hence the multiplicity of terms for W_{1V}, W_{1T}, W_{1A}. In specific cases many of these terms vanish; only for $\Delta I=0$ are the complete expressions necessary.

Of the two above introductory generalizations of the results, the second is less clearcut and obvious, and hence will be elaborated. The complication of $W(\theta)$ for first forbidden transitions derives in part from the fact that

these transitions may be allowed either by retardation of electron and neutrino waves across the nucleus (i.e., $(\mathbf{p}+\mathbf{q})\cdot\mathbf{r}\neq 0$) or by the presence in the interaction energy of a small term of order $v/c=$(nucleon velocity)/(velocity of light)$\ll 1$. The basis for the earlier generalization lies in the "constructive interference" effect of the retardation, represented by the introduction into $W(\theta)$ of expressions such as $(p^2+q^2+2pq\cos\theta)\equiv|\mathbf{p}+\mathbf{q}|^2$.

Thus at the midpoint of the spectrum, with $E\approx p\approx q$, the angular dependence of W_1 is most pronounced; the over-all effect of retardation, particularly if $p\gg 1$, is to produce a strong similarity between W_1 and $W_0(1+\cos\theta)$. On the other hand, the factor $|\mathbf{p}+\mathbf{q}|^2$ becomes nearly independent of θ at the upper and lower ends of the spectrum; here W_1 is therefore more isotropic than at the midpoint, and tends to be similar to W_0.

Although first forbidden transitions may occur by grace either of the retardation factor $(\mathbf{p}+\mathbf{q})\cdot\mathbf{r}$ or of the small "v/c" term, more highly forbidden transitions occur only *via* increasingly high powers of $(\mathbf{p}+\mathbf{q})\cdot\mathbf{r}$. Thus the factor $(1+\cos\theta)$ will enter the midpoint correlation function without exception and to higher powers, so that the preference for forward neutrino emission will become more and more marked; a factor $(1-\cos\theta)$, such as will occur for W_{nS} or W_{nP}, may make $W(0)=0$ but the "center of gravity" of the emission will still be in the forward direction.

Thus the predicted correlations for allowed transitions depend markedly upon choice of interaction and the correlation effect furthermore appears to possess a simple asymptotic dependence on order of forbiddenness.

[1] F. Bloch and C. Moller, Nature **136**, 912 (1935).
[2] J. Halpern and H. R. Crane, Phys. Rev. **55**, 1123 (1939). J. S. Allen, Phys. Rev. **61**, 692 (1942). J. C. Jacobsen, Phys. Rev. **70**, 789 (1946).
[3] E. J. Konopinski and G. E. Uhlenbeck, Phys. Rev. **60**, 308 (1941).

On the Magnetic Moment of the Triton*

R. G. Sachs
Argonne National Laboratory, Chicago, Illinois
March 1, 1947

THE recent determination of the magnetic moment of the triton by Anderson and Novick[1] leads to the somewhat surprising result that the moment is slightly greater than the proton moment. This result is surprising because the moment in a ^2P or ^4P or ^4D state, which are the only states that can be admixed with the ^2S state of this nucleus,[2] might be expected to be smaller than the proton moment. Therefore, one might expect that any admixture of these states would lead to a smaller moment than that in the pure S state. It should be pointed out first that, although this statement is correct for the ^2P and ^4P states, in a pure ^4D state the moment need not be less than the proton moment because this state may be formed by combining a wave function which is symmetric for the interchange of ρ and $\mathbf{r}$ and an anti-symmetric function.[3] Here ρ and $\mathbf{r}$ are the distance between the neutrons and the distance from the center of gravity of the neutrons to the proton, respectively. The interference between these symmetric and anti-symmetric functions may lead to a very high moment if the wave function contains states in which the individual particles have sufficiently high orbital angular momenta. However, it seems probable that this latter requirement is not satisfied since the orbital angular momenta of the individual particles probably are small in the ground state. Under this condition the moment in the D state *is* less than that of the proton.

It is still possible to account for the moment of the triton by introducing an admixture of ^2P and ^4P states since there are terms in the expression for the magnetic moment which arise from interference between the ^2P and ^4P states, between the ^2S and ^2P states, and between the ^4P and ^4D states. The signs of these terms depend on the relative phases of the wave functions so that they may be positive. An estimate of their order of magnitude can be made if one makes assumptions consistent with keeping the orbital angular momenta of the individual particles as small as possible and at the same time assumes that the radial parts of the various wave functions are in phase throughout the nucleus. Then it is found that a 6.7 percent increase of the triton moment over the proton moment can be obtained only if the ^2P and ^4P state amplitudes are greater than the D state amplitude. The S state probability is a maximum if the D probability is taken to be zero, the ^4P probability to be 8 percent, and the ^2P probability 20 percent. This rather startling conclusion might be avoided by dropping the above assumption concerning the orbital angular momentum of the individual particles, but it appears that very high configurations indeed would be required to explain the experimental result.

If one assumes that the triton wave function contains about 20 percent ^2P state, 8 percent ^4P state and no ^4D state, then one would draw the same conclusion for He^3 and it would be anticipated that the magnitude of the moment of He^3 would be about 4.0 percent greater than the numerical value of the neutron moment.[3] A measurement of the moment of He^3 would be most valuable for obtaining further information concerning the admixture of states.

The details of these calculations, including a discussion of the other possible ways of compounding a ground state consistent with the observed magnetic moment, will soon be submitted for publication.

* This work has been carried out under the auspices of the Atomic Energy Commission. It was submitted for declassification on January 24, 1947.
[1] H. L. Anderson and A. Novick, Phys. Rev. **71**, 372 (1947).
[2] E. Gerjuoy and J. Schwinger, Phys. Rev. **61**, 138 (1942).
[3] R. G. Sachs and J. Schwinger, Phys. Rev. **70**, 41 (1946).

Erratum: Note on the Scattering of Radiation in an Inhomogeneous Medium

[Phys. Rev. **71**, 268–269 (1947).]
C. L. Pekeris
Columbia University, New York, New York.

THE term $\left[\left(1+\frac{z}{r}\right)\alpha+\frac{x\beta}{r}+\frac{y\gamma}{r}\right]$ in Eqs. (6) and (7) should be changed to $\left[\left(1+\frac{z}{r}\right)\gamma+\frac{\alpha x}{r}+\frac{\beta y}{r}\right]$. In the second integral of Eq. (6) dv'' should be added.

On Molecular Coupling Effects

J. G. VALATIN
Institute of Experimental Physics, University for Technical and Economic Sciences, Budapest, Hungary
March 2, 1947

A CLEARER insight into the mechanism of the rotational coupling effects in a diatomic molecule can be attained by a direct investigation of the wave-mechanical expressions of the corresponding angular momentum operators. In a paper appearing in the *Hungarica Acta Physica* this is described as being performed by using a reference system, the z axis of which is chosen in the direction of the line joining the nuclei, its x, y, and z axes being given with respect to an inertia system by the Eulerian angles ϑ, ψ, φ. Accordingly, the wave functions of molecular states have to obey the additional restriction $-i(\partial\Psi/\partial\varphi)=L_z\Psi$. In such a system we can define operators L_x, L_y, L_z of the components of the resultant electronic angular momentum with the well-known commutation rules, and operators M_x, M_y, M_z of the components of total angular momentum obeying the commutation rules with an opposite sign. The term in the energy operator representing the coupling between rotation and electronic motion can be written in the form

$$-\frac{\hbar^2}{4\pi^2\mu r^2}(M_xL_x+M_yL_y).$$

In a reference system as used by Van Vleck[1] and in Kronig's book[2] where one of the axes is bound to the nuclei and another axis is defined by an arbitrarily chosen plane $x'y'$, one cannot find operators M_x, M_y, M_z with a corresponding physical meaning. On the other hand, in a system as used by Kronig[3] and by Born and Flügge[4] where the xz plane is identified with a plane containing one of the electrons, one cannot define operators L_x, L_y, L_z with a simple commutation rule. To a full description of the interaction between the total and electronic angular momenta the additional variable φ is to be introduced in the diatomic case, in order to characterize a reference system bound to the nuclei.

The observed heterogeneous perturbations in molecular spectra are due to the "accidental" effects of the rotational coupling terms which presents itself besides the regular coupling effects in the case of the closeness of perturbing energy levels. Homogeneous perturbations result by the accidental effect of the other energy terms coupling the wave functions of levels of different electronic states. Owing to the fact that also in the case of the approximate factorization of the molecular wave functions corresponding to an unperturbed electronic state the motion of the nuclei is to be taken into account, and the wave function factor containing the electronic coordinates cannot be identified with an eigenfunction of the two-center problem in general,[5] the non-diagonal matrix elements of the electronic energy terms in the energy operator become important, and these "electronic perturbations" explain the magnitudes of some very strong observed perturbations.

The possibility of a direct experimental verification of this kind of homogeneous perturbation offers itself through constructing the potential curves and radial wave functions belonging to the "unperturbed" electronic states, since the matrix elements of perturbation due to the electronic terms are connected with the product of the radial wave functions of both states, as in the case of the Franck-Condon principle, whereas in neglecting this effect the matrix elements are connected according to Van Vleck with the product of one wave function with the derivative of the other.[6]

[1] J. H. Van Vleck, Phys. Rev. **33**, 467 (1929).
[2] R. de L. Kronig, *Band Spectra and Molecular Structure* (Cambridge University Press, 1930).
[3] R. de L. Kronig, Zeits. f. Physik **50**, 347 (1928).
[4] M. Born and S. Flügge, Ann. d. Physik, No. 5, **16**, 768 (1933).
[5] J. G. Valatin, Proc. Phys. Soc. **58**, 695 (1946).
[6] J. H. Van Vleck, J. Chem. Phys. **4**, 327 (1936).

On the Number of Elements

MIGUEL MASRIERA
Provenza 293, Barcelona, Spain
February 18, 1947

IN 1943 I advanced the hypothesis that the total number of elements should be 96. Considering nuclear charges as elemental particles, the number of possible charges, which is equal to the number of elements, should also be equal to Eddington's number $N_1(96)$ of possible single wave equations. This hypothesis was published in my Spanish translation of Eddington's "New Pathways in Science" and in two notes.[1]

I wish to state that both the theoretical development on which I am still working and the experimental data on new elements published to date, support this point of view.

[1] M. Masriera, Memorias de la Real Academia de Ciencias y Artes de Barcelona (1946), p. 579; Iberica (1946), p. 84.

Magnetic Ions and Magnetic Currents

BROTHER GABRIEL KANE
Department of Physics, Manhattan College, New York, New York
March 6, 1947

THE reported dissociation of water by a magnetic field,[1] with an accompanying loss of pole strength of a permanent magnet,[2] as well as the rotation of colloidal particles in a magnetic field,[3] have been offered as evidence of the existence of a magnetic current. The experimental evidence has been thoroughly investigated by the author and by others.[4] The conclusions reached are that no dissociation of water nor loss of pole strength occurs when proper experimental procedures are observed and that there is a satisfactory electrochemical explanation for the rotation of the colloidal particles.[5]

The polar movement of metallic particles has also been presented as evidence of single magnetic poles. Microscopic metallic particles may move against the force of gravity under the *combined* action of a strong beam of light and a magnetic field; this phenomenon is known as magneto-photophoresis.[6] That this effect does not indicate the presence of a true magnetic charge is shown by the fact that the motion ceases as soon as the light is turned off.[7] Under certain conditions, the particles will move against the gravitational field even without the action of light.[8]

An explanation is here proposed for this latter phenomenon. It cannot be due to the presence of electrostatic fields[9] since the experiment has been performed with the pole pieces shielded by a fine wire cage and the whole apparatus grounded. The explanation may be found by examining the conditions under which the particles jump in the dark. Some fine metal powder such as iron, nickel, cobalt, tungsten, chromium, etc., is placed on the lower pole piece B of a strong electromagnet. When the field is suddenly reversed, a number of these particles jump to the upper pole piece A. The experimental conditions may be improved by agitating the particles slightly with a piece of fine wire before reversing the field. The obvious explanation seems to be that a current is induced in a particle by the rapidly changing magnetic field. If this induced current is more than 90 degrees out of phase with the current in the electromagnet, the particle will be repelled by the lower pole. This phenomenon is similar to Elihu Thomson's "jumping ring" experiment. This interpretation of the phenomenon was checked in two ways. First, when a weak field is used, the particles jump a short distance and fall back to the lower pole face; if they were true single poles, they should continue to rise to the upper pole face. Secondly, the magnetic field was gradually reduced to zero before reversing it and gradually increased after reversal. As a result, no particles were observed to jump.

There appears, then, to be no satisfactory experimental evidence for the existence of either magnetic ions or magnetic currents.[10] However, it has been shown repeatedly that their existence is theoretically possible.[11]

[1] F. Ehrenhaft, Phys. Rev. **63**, 216 (1943).
[2] F. Ehrenhaft, Phys. Rev. **65**, 287 (1944).
[3] F. Ehrenhaft, Phys. Rev. **65**, 62 (1944).
[4] R. J. Hoff, J. J. Naughton, R. Smoluchowski, and H. H. Uhlig, Phys. Rev. **66**, 92 (1944); J. E. Goldman, *ibid.* **66**, 94 (1944); G. Kane and C. B. Reynolds, Science, **100**, 503 (1944).
[5] C. E. Swartz, Phys. Rev. **67**, 201 (1945); C. E. Swartz and W. van der Grinten, *ibid.* **69**, 252 (1946).
[6] F. Ehrenhaft, Ann. de physique **13**, 151.
[7] L. Banet, Phys. Rev. **61**, 733 (1942).
[8] F. Ehrenhaft, Phys. Rev. **61**, 733 (1942); Science **94**, 232 (1941).
[9] V. D. Hopper, Phys. Rev. **66**, 93 (1944).
[10] E. T. Benedikt and H. R. Leng, Bull. Am. Phys. Soc. **22**, 27, paper X 10.
[11] O. Heaviside, *Electromagnetic Theory* (D. Van Nostrand Company, Inc., New York, 1922), Vol. I, pp. 362–385; L. Page and N. I. Adams, *Electrodynamics* (D. Van Nostrand Company, Inc., New York, 1940) p. 160; G. Kane, Phys. Rev. **67**, 201 (1945).

Proceedings of the American Physical Society

1946 Annual Meeting at New York, January 30, 31 and February 1, 1947

THE largest meeting in the history of the American Physical Society was its 277th, the 1946 Annual Meeting held at Columbia University on Thursday, Friday, and Saturday, January thirtieth and thirty-first and February first, 1947. No fewer than 1536 registration cards were filled out, surpassing by over two hundred the previous record set in the same place just one year before. Some of these go to the credit of the American Association of Physics Teachers, which held joint and concurrent meetings with ours; the Division of High-Polymer Physics and the Committee on Fluid Dynamics drew many, the exact number being unknowable. In spite of the huge attendance, the congestion was noticeably less than a year ago, because of the distribution of the sessions among several buildings with adequate auditoriums: we drew upon the Department of Chemistry for the Havemeyer lecture-hall, upon Teachers College for Horace Mann Auditorium and upon Columbia University for daily use of McMillin Theatre. Nevertheless the four-ring circuses which our meetings have become, with their multiple and irreconcilable claims upon the time of the members, form in some ways a dismal contrast with the small congenial meetings of old, and pose insoluble problems. The mere problem of managing so vast a meeting would have been insoluble, but that the junior members of the Department of Physics at Columbia University gave up literally all their time for several days. Special credit is due N. F. Ramsey, Chairman of the Local Committee; to W. W. Havens, G. R. Becker, and to W. S. Gorton of the Bell Telephone Laboratories who provided the acoustical equipment; and to the staff of the American Institute of Physics which tended the registration desk. These brief but needed services can never be repaid except by evanescent words.

The Retiring Presidential Address of E. U. Condon was given under the title "The Franck-Condon Principle and Some Related Topics." This formed a part of the joint session of Friday afternoon with the AAPT, the rest of which comprised the presentation of the Oersted Medal to Duane Roller and the delivery of the Richtmyer Lecture by J. R. Oppenheimer. On Thursday afternoon there was a symposium under the joint sponsorship of the Society and the AAPT, at which General H. S. Aurand and Admiral P. F. Lee spoke, respectively, on "Research and Development in the War Department" and "Research Programmes of the Office of Naval Research in the Physical Sciences." On Friday evening after the dinner D. W. Bronk acquainted his audience with "The Role of the National Research Council in American Science and Education." Nine invited papers on a variety of subjects were interspersed throughout the three days: the speakers and the titles are listed hereinafter. There were ninety-two contributed papers in the general programme of the Society: their abstracts follow.

The Division of High-Polymer Physics held four sessions, and abstracts of all but one of the papers, invited and contributed alike, are printed at the end of these Minutes. The Committee on Fluid Dynamics (R. J. Seeger, Chairman), with the co-sponsorship of the American Mathematical Society, held also four sessions, including a Symposium on Recent Developments in Compressible Flow: abstracts of most of its papers, invited and contributed alike, are printed hereinafter.

The dinner of the Society was divided into two sections, one in the familiar precincts of the Mens' Faculty Club and the other in the no less appreciated John Jay Hall, with a total attendance approaching 550.

At the Business Meeting of the Society, which was held on Friday morning, the Tellers reported the following elections to terms of office commencing at the end of the Annual Meeting: L. A DuBridge, *President;* J. R. Oppenheimer, *Vice President;* K. K. Darrow, *Secretary;* G. B. Pegram, *Treasurer;* J. T. Tate, *Editor* (three-year term); P. M. Morse and J. R. Oppenheimer, *Councillors* (four-year term); H. A. Bethe, L. A. Ridenour, and W. H. Zachariasen, *Members of*

the Board of Editors (three-year term). The Secretary reported that, presuming acceptance of election by all candidates to membership elected at the Council meeting, the membership of the Society stood at 6050.

The Council, meeting on Thursday evening, elected to Fellowship five candidates (Lyle Borst, Ralph Bown, D. O. North, A. H. Snell, and Katherine Way) and to Membership 214 candidates whose names are appended.

Elected to Membership: Edward J. Althaus, Norman Austern, Oscar Beran, Abraham S. Berman, Milton J. Bernstein, William Bernstein, Donald E. Billings, Converse Herrick Blanchard, Sidney A. Bludman, Richard W. Blue, Robert J. Bobber, Sidney Borowitz, Ben Braun, Stuart R. Brinkley, Jr., Herbert Broida, Frederick C. Brown, Robert Reginald Brown, Merle Thomas Burgy, Edwin J. Callan, Jessie Y. Cann, Ann Chamberlain, Herman H. Chanowitz, C. Harmon Chapman, John B. Cladis, John M. Cleveland, Kenneth D. Coleman, Gerald Cohen, Daniel Isaac Cooper, Walter G. Countryman, Clyde L. Cowan, Jr., William Slayter Cowort, Jr., Thomas W. Dakin, Laurence B. Deen, Jr., Charles H. Donelson, Robert G. Dorsch, John J. Dropkin, Stanley L. Ehrlich, C. Eijkman, Roy Arnold Elkind, Willard L. Erickson, Ragnar Ericsson, John L. Everett, John J. Faris, Sherwood L. Fawcett, Lawrence Feldman, Simon Freed, Melvin S. Freedman, Douglas M. French, Gerhart Friedlander, Robert H. Frost, Dudley D. Fuller, James M. Garner, Jr., John E. Garrett, David M. Gates, Lawrence Seymour Germain, Frank E. E. Germann, Thomas Gilmartin, Jacob Burrill Gilstein, Norman Jerome Golden, Stanford Goldman, Morris Goran, Gordon Gould, John R. Green, Melville Saul Green, Joseph Greenspan, John L. Greenstadt, Burgoyne L. Griffing, John J. Guarrera, Glenn Edward Hagen, George B. Harris, Jr., Edward W. Hart, Albert Jerold Hatch, Warren E. Henry, Robert V. Higdon, Bertram L. Hoffman, Ralph E. Hightower, Benjamin Gregory Hogg, Gunnar Hok, Donald F. Hornig, Wendell A. Horning, Paul Von Campen Hough, Erle Howell, Jr., Harry C. Hoyt, Jack A. Hunter, James F. Hurlbut, Carol B. Hyatt, Peter J. Isaacs, Irvin Isenberg, James Madison Jackson, Stanley Anthony Jashemski, Robert Sawyer John, Jr., Gustave Joyet, Edward T. Jurney, Leonard Anthony Kalal, Hugh J. Karr, Jr., Elmer L. Kelly, William Clark Kelly, Donald B. Kerr, J. Kistemaker, Walter Kiszenicky, Murray S. Klamken, George D. Kneip, Jr., Ray L. Kramer, Frank E. Kruesi, Jr., George Czeslaw Kuczynski, Alfred B. Laponsky, Richard A. Laubenstein, Margaret N. Lewis, Leon J. Lidofsky, Hans Wolfgang Liepmann, Arthur Linz, Jr., Robert Lionel Lipton, John Knox Logan, Edward D. Lowry, Joaquin Mazdak Luttinger, Torsten Magnusson, Stephen F. Malakev, Jr., Charles Manneback, Ruth Margolin, Ray W. Mayhew, John R. McCartney, James Prentiss McClellan, Thomas R. McGuire, Lazarus T. Medveson, Edwin P. Meiners, Jr., Harry E. Moses, George M. Muller, Charles J. Munda, Jr., Rodger V. Neidigh, Paul F. Nemenyi, Herman Newhouse, Karl W. Ninnemann, Perley G. Nutting, Jr., George B. Olmsted, Wylie J. Oosterkamp, Alan L. Orvis, George E. Owen, Robert H. Park, Vincent E. Parker, John R. Pasta, Norman Pearlman, Enrico Persico, Ben Petree, Oreste Piccioni, William John Pietenpol, William R. Polye, David Samuel Potter, Ray M. Potter, Robert Clay Prim, III, Sol Raboy, Charles H. Raeth, Russell F. Raitt, Paul I. Richards, Harold N. Ritland, Norman H. Roberts, Y. Rocard, Fritz Rohrlick, Carl L. Rollinson, Harlan Rosenblatt, Morris Rubinoff, Zella Ruthberg, L. A. Sanderman, Tsien San-Tsiang, James Schenek, Huburt W. Schlevning, Warner W. Schultz, Robert N. Schwartz, Harner Selvidge, Philip Anderson Shaffer, Jr., Daniel Shanks, Gerald Shapiro, Jacob Shapiro, Charles Sheer, George William Sherard, Norman Steven Shiren, Jerry Shmoys, W. Sichak, Kai Siegbahn, Siegfried Fred Singer, Lewis Slack, Bernard Smaller, Elmer H. Smith, Harold D. Smith, Newell Hart Smith, James Newton Snyder, William Sollfrey, Irvin L. Sparks, David S. Stacey, John S. Stanton, Ernest J. Sternglass, Richard Griffith Stoner, M. W. P. Strandberg, Max Sucher, Chain Swiatycki, Theodor Teichmann, Jay W. Thornhill, Harold K. Ticho, Bernard E. Tiffany, David Van Meter, Francis Arthur Vick, Walter Geoffrey Wadey, Claude E. Walker, Ernest Wantuch, Paul E. Weiler, Alfred Weissler, Harold Wergeland, William L. Whittemore, Robert W. Willmott, James R. Wilson, Stanislas David Winter, Albert William Wotring, Courtney Wright, Keith H. Wycoff, and Fu-Chun Yu.

The Society has lost through death G. W. Kenrick (Watson Laboratories).

KARL K. DARROW, *Secretary*
American Physical Society
Columbia University
New York 27, New York

Invited Papers on the General Programme

Higher-Order Tyndall Spectra in Mono-Disperse Colloids. V. K. LAMER AND DAVID SINCLAIR, *Columbia University.*

The Production of Ice Crystals in Artificial and in Natural Clouds. IRVING LANGMUIR, V. J. SCHAEFER, AND BERNARD VONNEGUT, *General Electric Company.*

Theories of Helium II. J. G. MAYER, *University of Chicago.*

Behavior of Fission Products and of Very Heavy Elements in Biological Phenomena. J. G. HAMILTON, *University of California.*

The Entropy of Liquids and Solutions. J. H. HILDEBRAND, *University of California.*

Creation and Destruction of Mesons. J. R. OPPENHEIMER, *University of California.*

Operation of a 70-Mev Synchrotron. H. C. POLLOCK, R. V. LANGMUIR, AND F. R. ELDER, *General Electric Company.*

The Use of Electron Multiplier Tubes in Experimental Nuclear Physics. J. S. ALLEN, *University of Chicago.*

Attenuator Materials, Attenuators, and Terminators for Microwaves. G. K. TEAL, M. D. RIGTERINK, AND C. J. FROSCH, *Bell Telephone Laboratories.*

Symposium of the Committee on Fluid Dynamics

Recent Developments in Compressible Flow. Papers by JOHN VON NEUMANN, *Institute for Advanced Study;* G. F. J. TEMPLE, Fluid Motion Committee, *Aeronautical Research Council, London, England;* and THEODORE VON KARMAN, *California Institute of Technology.*

A1. The Variation with Altitude and Latitude of the Vertical Component of the Cosmic Radiation Passing through 15 cm of Lead. W. F. G. SWANN AND PETER A. MORRIS, *Bartol Research Foundation of the Franklin Institute, Swarthmore, Pennsylvania.*—Under the auspices of the National Geographic Society and the Army Air Corps, vertically directed cosmic-ray telescopes, covered with 15 cm of lead, were flown in a B-29 bomber from 58°N magnetic latitude to the magnetic equator in flights at 5000, 15,000, at 25,000, and 33,000 feet with the following results: 1. The ratio of intensity at 58°N to that at the equator was 1.34 at 33,000 ft. and 1.51 at 25,000 ft. At the lower altitudes it was equal to unity within the limit of accuracy of the experiments. 2. However, the actual difference between the intensity at 58°N and at the equator increased in the ratio 1.50 to unity from 25,000 ft. to 33,000 ft. 3. Insofar as the knee of the latitude curve represents a well defined point at all, it occurs at about 48°N magnetic latitude, with no marked variation with altitude from 25,000 ft. to 33,000 ft. Facts (1) and (2) are in harmony with the view that, superposed upon the portion of the hard component originating from a field-sensitive primary, we have a component arising from a non-field-sensitive primary, which is absorbed rapidly (presumably by the creation of mesotrons) between 33,000 ft. and 25,000 ft. and lower. These conclusions are in harmony with the observations of Schein and Wilson.[1]

[1] Schein and Wilson, Phys. Rev. **54**, 304 (1938).

A2. Azimuthal Variations of Cosmic Radiation at Lahore. PIARA SINGH GILL,* *Forman Christian College, Lahore, India.*—A study of the azimuthal variations of the cosmic radiation at Lahore (22°N magnetic latitude) shows a large azimuthal effect. The azimuthal effect in the Northwest Quadrant for a constant zenith angle of 60° is in general agreement with theoretical prediction. These observations lead to the conclusion that (1) primary cosmic-ray particles are positively charged; (2) the energy spectrum of the primary cosmic rays within the energy range 7.84×10^9 ev and 14×10^9 ev (for protons) obeys the law $Be^{-\gamma}$ where $\gamma=2.8$.

* At present at the University of Chicago.

A3. Meson Showers under Lead at Sea-Level. WILLIAM B. FRETTER, *University of California, Berkeley.*—Eleven photographs of meson showers under 30 cm of lead have been obtained using two cloud chambers. One was in a magnetic field, while the other, which contained eight one-half-inch lead plates, was vertically in line below and was simultaneously tripped by counters. Penetrating particles were clearly identified in the lower chamber, and curvature-ionization observations were made in the upper chamber. In two pictures mesons were identified in large electron showers which were associated with heavily ionizing particles in the upper or lower chamber. Few electrons were associated with most of the meson showers in the lower chamber, but heavy tracks often were visible in both chambers. Presence of these heavy tracks indicates that even at sea level meson showers are often accompanied by non-cascade radiation capable of producing nuclear events.

A4. Mechanism of Absorption of Negative Mesons. JOHN A. WHEELER, *Princeton University.*—Under the electrostatic attraction of a nucleus of charge Z, a negative meson can execute a Bohr orbit. The radius is smaller than that of the corresponding electronic orbit by the mass ratio 200, but even in the case of K-orbits is larger than nuclear dimensions for Z less than about 35. The energy release calculated for capture of a thermal meson into the lowest Bohr orbit of iron, for example, is 1.8 Mev; $2s$ or $2p$ orbit, 0.45 Mev. The capture probability is the additive resultant of three effects: emission of the available energy as a photon; transfer of the energy to an atomic electron (Auger

effect); transfer to a negative energy electron to cause pair production (only possible for calcium and heavier nuclei). In solid material the calculated life with respect to such *atomic* capture is far less than the normal life, 2×10^{-6} seconds, with respect to radioactive decay. Subsequent *nuclear* capture of a meson from a K-orbit will be expected to have a probability proportional to Z^4, whether by emission of the mass energy of the meson as a photon or by star formation. Thus, to the extent that direct capture of a thermal meson into the nucleus can be neglected, the probability for decay of a negative meson stopped in a solid element will be expected to depend on atomic number as $[1+(Z/Z_0)^4]^{-1}$, where Z_0 is a constant which must be determined experimentally.

A5. A New Determination of the Mean Life of Mesotrons at an Altitude of 11,500 Feet. HAROLD K. TICHO, *University of Chicago* (Introduced by Marcel Schein).—The mean life of mesotrons stopped in 10 cm of Al was measured at Chicago and Climax (altitude 11,500 ft.). The method consisted essentially of a direct comparison between the time interval due to the decay of each individual mesotron and the period of an accurately calibrated quartz crystal. The crystal frequency of 100 kc per second produced a circular sweep and each time interval appeared as an arc on the oscillograph screen. Exponential disintegration curves were obtained at both altitudes and yielded a mean life of $1.97\pm0.15\times10^{-6}$ sec. at Chicago and $1.78\pm0.10\times10^{-6}$ sec. at Climax. Further experiments are in progress at Chicago. Both values seem lower than those obtained by Nereson and Rossi.[1] Such a difference might be caused by a finite capture probability for negative mesotrons in light materials like Al.

[1] N. Nereson and B. Rossi, Phys. Rev. **64**, 199 (1943).

A6. Production of Cosmic-Ray Stars. EUGENE GROSS, SHUICHI KUSAKA, AND GEORGE SNOW, *Princeton University*.—Data on cosmic-ray stars obtained from cloud-chamber studies and photographic plates by various investigators are analyzed and possible mechanisms for their production studied. The observations are rather meager and not entirely consistent, but the results can be summarized roughly as follows: They occur with a frequency of about 10^{-9} per cc per sec. in air at sea level and increase by a factor of about 50 in going up to an altitude of 14,000 feet. Bagge has attributed the production to γ-rays, but numerical estimates show that the star frequency is about a factor of 100, too large to be accounted for by this process. Lukirsky and Perfilov have considered the production to be caused by absorption of slow negative mesons by air nuclei. This process can account for the number of stars observed at sea level, but not the altitude dependence. Powell has suggested the neutrons as the producers of stars. Calculations made with the assumption that energetic neutrons arise by a cascade process from primary protons show that this hypothesis gives the right order of magnitude both for the number and altitude dependence of stars.

A7. Thermal Neutron Activation Cross Sections.* LEO SEREN,** HERBERT N. FRIEDLANDER, SOLOMON H. TURKEL, *Argonne National Laboratory*.—A survey has been made of cross sections for those nuclei which give rise to radioactive isotopes upon thermal neutron capture. This survey covered 67 elements and cross sections for 133 of the known 160 induced activities. The smallest and largest atomic cross sections measured were 4×10^{-7} barns (10^{-24} cm^2) for the production of 31-second $_8O^{19}$ and 725 barns for the production of 140-minute $_{66}Dy^{165}$. The source of neutrons was the graphite pile and the heavy water pile at the Argonne Laboratory. Incident neutron flux was measured by activated monitors which had previously been calibrated in a standard graphite pile. Captured neutron flux was measured by counting the absolute number of beta-decay particles after irradiation, and reducing this decay rate to a saturated value. The complete table of cross sections will be published soon in *The Physical Review*.

* Work was completed October 1944. This document is based on work performed under Contract No. W-7401-eng-37 for the Manhattan Project at the Argonne National Laboratory.
** Now at General Electric Research Laboratory, Schenectady, New York.

A8. On the Theory of Slowing Down Neutrons in Substances with Periodic Absorption Lines. S. H. BROWNE AND T. DANTZIG, *North American Aviation, Inc.*—The general integral equation for the stationary energy distribution for slowing down of neutrons, as derived by G. Placzek,[1] is applied to the problem of slowing down in an infinite medium in which both $1/v$-capture and capture by resonance absorption lines occur simultaneously. The energy distribution at low energies is obtained from a series solution of the integral equation. To simplify the mathematical problem, instead of the usual expression for cross section for resonance absorption, a trigonometric type of periodic function is used which is applicable to uniformly spaced absorption lines and can be made to agree closely with available experimental data by proper choice of the parameters involved. The energy distribution of neutrons for all energies is discussed. The results are compared with those obtained by the approximation for absorption lines indicated by Placzek, and with his solutions for slowing down without capture and of slowing down with $1/v$-capture. An attempt is made to extend the method to include the case of a medium of finite size.

[1] G. Placzek, Phys. Rev. **69**, 423 (1946).

A9. High Energy Gamma-Rays from U(235) Fission Products. S. BERNSTEIN, W. M. PRESTON, G. WOLFE, R. E. SLATTERY, *Clinton Laboratories*.—The photo-disintegration of the deuteron has been used to study the hard γ-rays emitted by fission products of U^{235}. The neutrons created in the process were used as the indicator of the presence of hard γ-rays. The fission products were placed at the center of a 10" radius sphere of heavy water. Conclusions about the periods and yields of the hard γ-rays were made from the total number of photo-neutrons being captured in a large tank of oil surrounding the sphere of heavy water. Eight half-lives were found: 2.5 sec., 41 sec., 2.4 min., 7.7 min., 27 min., 1.6 hr., 4.4 hr., and 53 hr. The shortest one and longest one of these are least reliable. Eighty-five percent of the photo-neutrons appear in the two shortest half-lives, the 2.5-sec. component being three times as intense as the 30-sec. component. The total saturated activity of

the photo-neutrons for an infinite amount of heavy water was calculated from the 10″ radius sphere measurements to be about 16.5 percent of the saturated delayed neutron activity. It is calculated that there must be of the order of one to two photons of energy above 2.2 Mev emitted per fission by fission products with half-lives greater than one second.

[1] This abstract is based on work performed under Contract No. W-35-058-eng-71 for the Manhattan Project.
[2] This abstract appeared in the Bulletin of the American Physical Society, Vol. 21, No. 6, dated November 29, 1946, but the paper could not be presented at the 275th meeting.

A10. Photographic Neutron Detection.* R. A. PECK, JR., *Yale University.*—For the photographic method of neutron detection and energy measurement,[1] the Eastman fine grain alpha-particle emulsion is the only one readily available in this country. However, this exhibits a large pre-exposure background, which introduces ambiguity in the identification of the beginning of proton tracks. Preliminary "defogging" treatment is thus required. As shown by Perfilov,[2] the defogging oxidizer used (potassium permanganate) must be strong enough to remove background grains, yet not strong enough to desensitize the emulsion for proton detection. Within this concentration range, the $KMnO_4$ even exhibits a sensitizing effect, substantially increasing the visible length of proton tracks. The optimum treatment has been determined for the Eastman emulsion, an 18-minute bath in $KMnO_4$ of concentration 0.66 g/liter. A lead camera is necessary to shield the plates from the high gamma-ray background of the cyclotron. The Li(dn) reaction, investigated by Richards,[3] is used to determine the stopping power of the Eastman emulsion as a function of proton energy.

* This work is conducted as a part of O.N.R. contract N60NR44 Task Order V.
[1] Powell et. al., Proc. Roy. Soc. **183**, 1, 64 (1944).
[2] Perfilov, J. Phys. U.S.S.R. X, No. 1, 1 (1946).
[3] Richards, Phys. Rev. **59**, 796 (1941).

A11. Use of Threshold Detectors for Fast Neutron Studies. BERNARD T. FELD,[1] R. SCALETTAR,[2] AND L. SZILARD.[3] *Metallurgical Laboratory, University of Chicago, Chicago, Illinois.*—Light element (n, p) and (n, α) reactions can be used to compare, qualitatively, the energy distributions of the fast neutrons emitted by various neutron sources. Experiments are described in which a Ra-α-Be and Ra-α-B neutron source are compared by observing their relative activation of a number of light element reactions. Table I summarizes the experimental results. The thresholds for the reactions were calculated by using the best available values of the isotopic masses. The probability for penetration of the Coulomb barrier by the product proton or alpha-particle was calculated from the Gamow formula. The relative values of the activities in the same column have no meaning, since the detectors were not intercalibrated.

TABLE I.

Reaction	Half-life	Calculated threshold (Mev)	Calculated energy for 0.1 penetration (Mev)	Calculated energy for 0.5 penetration (Mev)	Activity Ra-α-Be	Activity $S^{32}(n, p)P^{32}$ Ra-α-B
$S^{32}(n, p)P^{32}$	14.3*d*	.93	2.9	4.0	1.000	1.000
$P^{31}(n, p)Si^{31}$	170*m*	1.02	2.9	3.9	.63	.51
$Al^{27}(n, p)Mg^{27}$	10.2*m*	1.95	3.6	4.6	.29	.058
$Si^{28}(n, p)Al^{28}$	2.4*m*	2.69	4.5	5.5	.95	≤.017
$P^{31}(n, \alpha)Al^{28}$	2.4*m*	.90	6.6	8.3	.24	<.004
$Al^{27}(n, \alpha)Na^{24}$	14.8*h*	2.39	7.5	9.1	.079	<.003

[1] Now at the Massachusetts Institute of Technology, Cambridge, Massachusetts.
[2] Now at Cornell University, Ithaca, New York.
[3] Now at University of Chicago, Chicago, Illinois.

A12. The Scattering of Thermal Neutrons in Polycrystalline Materials. R. M. LANGER AND J. F. DALY, *Bureau of Ships.*—The data of Nix and Clement[1] on thermal neutron scattering in copper can be interpreted quantitatively in terms of the crystal grain size S, the amorphous mass scattering coefficient μ_a/ρ, the rocking angle $\Delta\theta$ through which a crystal grain can be rotated about the Bragg angle without losing its Bragg reflection effectiveness, and finally the crystal thickness S_0 required for a crystal at the Bragg angle to reduce a homogeneous neutron beam by a factor e. The effective mass scattering coefficient μ/ρ including the Bragg scattering is given by the expression

$$\mu/\rho=\mu_a/\rho+\frac{1-\exp[-(2S/S_0)]}{2SN}AJ\Delta\theta\left(\frac{2m^3}{\pi k^3T^3}\right)^{\frac{1}{2}}$$
$$\int_{h/2dm}^{\infty}\exp[-(mv^2/2kT)]v\left(v^2-\left(\frac{h}{2dm}\right)^2\right)^{\frac{1}{2}}dv.$$

Here J is related to the symmetry number of the crystal, ρ is the density, and the other symbols have their customary significance. The second term in the formula is about as large as the atomic mass scattering term μ_a/ρ for grain sizes S less than 10^{-2} cm in the three substances examined so far.

[1] F. C. Nix and G. F. Clement, Phys. Rev. **68**, 159 (1945).

F1. Interferometry of Faster-Than-Sound Phenomena.* RUDOLF LADENBURG, *Princeton University* (30 min.).—Interferometric measurements of supersonic ("faster-than-sound") gas streams enable one to determine the distribution of density, pressure, temperature and gas velocity in the stream throughout the field of view, provided the phenomenon under investigation is two-dimensional or has axial symmetry. Also the apparently discontinuous rise of density, pressure, velocity, etc., through a shock wave can be measured by interferometry. So far studied are: (1) Air flow around bullets in flight (Cranz, Schardin, and others); (2) homogeneous air-streams escaping through a Laval nozzle into the atmosphere ("open wind tunnel") and the air flow around various objects supported in the stream[1]); (3) inhomogeneous air jets escaping from pressure tanks through various circular nozzles at pressure ratios up to 100; and (4) air flow and boundary layers in two-dimensional channel flow. New results with inhomogeneous air jets at widely varying pressure ratios have been obtained by letting the air discharge from a pressure tank into a vacuum tank. Of special interest is the change in the shock formation from a cone with oblique shocks to a kind of truncated cone where a strong plane shock intersects with two conical

shocks. The measured angles and shock strengths are compared with the present theory of von Neumann. Further, the information obtained about distribution of density, temperature and velocity in a two-dimensional channel and especially in the boundary layer, when flow is supersonic, will be discussed.

* This work was done in Palmer Physical Laboratory under the sponsorship of the Navy Department, Bureau of Ordnance.
[1] R. Ladenburg, C. C. VanVoorhis, and J. Winckler, Phys. Rev. 69 251(A), 1946.

F2. Refraction of Shocks in Ideal Gases.* A. H. TAUB, *University of Washington* (20 min.).—It is assumed that when a plane shock is incident on an interface between two gases of different densities ρ and ρ_1 and different ratios of specific heats γ and γ_1, respectively, a three-shock configuration results, involving an incident shock, a reflected shock, and a transmitted shock. It is further assumed that in the various angular domains the pressure is constant. The Rankine-Hugoniot equations may be used to formulate the following boundary conditions: (1) the pressure across the interface is continuous and (2) the deflection of the flow caused by the incident and reflected wave is equal to that caused by the transmitted wave. Rational polynomial equations of twelfth degree are obtained, the roots of which determine the position and strength of the reflected and transmitted wave as functions of the strength and angle of incidence of the incident wave. Ranges of these parameters where certain types of solutions are possible are determined by analytical methods. The equations were solved numerically, for various values of ρ_1/ρ and γ_1/γ, on the Eniac which was made available through the cooperation of the Army Ordnance department. Mrs. Adele Goldstine superintended the computations.

* This work was begun while the author was employed at Princeton University on work sponsored by the Office of Naval Research.

F3. On the Interaction between Boundary Layer and Shock Waves. H. W. LIEPMANN, *California Institute of Technology* (20 min.).—Hydrodynamics of real fluids has been, to a large extent, governed by the concept of the boundary layer initiated by Prandtl in 1904. The existence of a boundary layer and the possibility of dividing the solution of a fluid flow problem into two parts, an "outer" inviscid solution giving the pressures and an "inner" solution including viscosity or turbulence giving the shear forces, has become almost self-evident. The extension of fluid mechanics to problems involving supersonic flow requires, however, a critical analysis of the applicability of the classical boundary layer concept. The assumptions underlying the classical theory are certainly not correct near the base of a shock wave and recent experiments have shown that boundary layer effects in transonic flow have a considerable influence upon the external flow field and the form of the shock wave. Hence, there exists a shock wave-boundary layer interaction which makes, at least in some cases, a simultaneous solution of the outer and inner fields of flow necessary. Further experiments have been carried out to clarify the interaction problem and to pave the way for a rational theoretical analysis of this typical non-linear problem.

F4. The Formation and Stability of Normal Shock Waves in Channel Flows. ARTHUR KANTROWITZ, *Cornell University* (20 min.).—There is experimental evidence that channel flows involving shock-free deceleration through the speed of sound are unstable. This paper presents an analysis of non-viscous unsteady channel flow which was made to gain some insight into this apparent instability and to study the closely related (small shock intensity) stable flows. In Part I, Riemann's theory of the propagation of finite amplitude disturbances in a homogeneous medium is extended to the case where upstream moving pulses are superposed on a decelerating transonic channel flow. Shock waves are formed as the pulse is propagated, as in Riemann's problem. If it is assumed that the intensity of the shocks is very small, then the pulse approaches a "trapped" state in which a portion of the decelerating channel flow is converted to an accelerating flow which is an alternate steady-state solution for the channel. In Part II, the assumption of weak shocks is dropped to study the later development of the trapped pulses. It is concluded that smooth transonic deceleration is unstable to compression pulses coming from the rear of the channel and that the shock position is stable in diverging channels and unstable in converging channels.

F5. Notes on the Thermodynamic Propulsion of Wind Tunnels. FRANCIS CLAUSER, *Johns Hopkins University* (20 min.).—In view of the current trend toward wind tunnels of very great cost and power for supersonic research, this paper undertakes to investigate the feasibility of using thermodynamic propulsion for such tunnels. This is based on the experience with aircraft and missiles that thermodynamic propulsion systems (ram jets, turbo jets, pulse jets, etc.) have been able to supply large amounts of power with relatively simple installations. The present paper deals largely with purely thermodynamic means of propulsion (i.e., without compressors or turbines). It is shown that a ram jet cannot be used to furnish the sustaining motive power for a tunnel. However, the analysis shows what combinations of thermodynamic systems can be used for sustained wind tunnel propulsion. Several installations are analyzed with a view toward practical utilization, and it is concluded that there is hope for success. However, the aerodynamic design of such installations must be carefully considered because they are so constituted that the losses can easily outweigh the gains.

F6. Variation of Aerodynamic Lift in the Transonic Speed Range. W. F. HILTON, *Johns Hopkins University* (20 min.).—Certain difficulties are experienced when attempting free flight in the transonic speed range (0.8 to 1.2 of the speed of sound). These difficulties fall into two main classes: namely, (1) overcoming the somewhat high air resistance by means of improvements in engine design; and (2) balancing the aircraft for stable horizontal flight. The latter problem is considered in the paper. Changes of trim are caused by sudden loss of wing lift in the transonic range, decreasing the downwash over the tail, and possibly resulting in an uncontrollable nose-heavy dive. A qualitative explanation is given of the observed changes of lift,

and an approximate calculation of the magnitude of the effect has been made. A method of minimizing these effects is indicated and is found to be verified by wind tunnel experiments.

B1. The Width of the Nuclear Magnetic Resonance Absorption Line in Gases, Liquids, and Solids. N. BLOEMBERGEN, R. V. POUND, AND E. M. PURCELL, *Harvard University.*—Magnetic resonance absorption and dispersion were observed, at 30 Mc/sec., in various substances containing hydrogen or fluorine. The strong field H_0 (approximately 7000 gauss) was modulated with adjustable amplitude at 30 c.p.s., allowing observation of the entire absorption or dispersion curve on an oscilloscope or point-by-point measurement of the slope of either curve with a lock-in amplifier. In water, many other liquids, and hydrogen gas, the line width is less than 0.15 gauss. This upper limit is set by inhomogeneities in H_0. The narrowness of the line can be understood by noting that the local fields from neighboring nuclear or molecular moments (in magnitude several gauss) must nearly average out as the changes in these fields due to molecular motion are rapid compared to the radio frequency. Moreover an estimate of the intensity of the "local field spectrum" at 30 Mc/sec. permits a prediction of the relaxation time in these substances which is in reasonable agreement with our observations. In a single crystal of CaF_2, by contrast, the observed width of the fluorine resonance agrees with that computed under the assumption of fixed neighbors, displaying the predicted dependence on the angle between H_0 and a crystal axis.

B2. Measurements of Nuclear Quadrupole Interactions. W. A. NIERENBERG, N. F. RAMSEY, S. B. BRODY, *Columbia University.*—The resonance minima of the Na^{23} nucleus in NaCl, NaBr, and NaI have been studied using the molecular beam magnetic resonance method. The resultant resonance patterns of beam intensity *versus* frequency for fixed fields ~9.000 gauss are similar to predicted[1] for the interaction of a nuclear electrical quadrupole moment in the molecular field and for an assumed spin of $\frac{3}{2}$. Comparison with theory[1] yields the values for the interaction $e^2qQ/2h$ of 1.35, 1.17, and 0.97 megacycles/sec. for NaCl, NaBr, and NaI respectively, where Q is the quadrupole moment of the nucleus and q is simply related to the gradient at the nucleus of the electric field intensity of the electrons and the other nucleus of the molecule. A new type of resonance minimum was employed to further the investigation. Minima were observed for a very low (less than 4 gauss) magnetic field. The frequency at which the resonance occurs is due to the electric quadrupole interaction. These minima gave values for the interaction agreeing within 5 percent with those listed above. This technique based on the quadrupole interaction should, in addition, provide a method of determining nuclear spins. However, the theory of the resonance patterns observed in some other compounds is not understood as yet.

[1] B. T. Feld and W. E. Lamb, Jr., Phys. Rev. 67, 15 (1945).

B3. Determination of Stable Species $_{39}Y^{89}$, $_{40}Zr^{90}$, and $_{56}Ba^{134}$ Produced by Nuclear Transmutations. M. H. KURBATOV AND J. D. KURBATOV, *Ohio State University, Columbus.*—An experimental procedure has been developed for determination of stable atoms formed by the nuclear transmutations $_{38}Sr^{88}(d, n)_{39}Y^{89}$; $_{39}Y^{89}(d, n)_{40}Zr^{90}$; and $_{55}Cs^{133}(d, n)_{56}Ba^{134}$, when the products are in quantities below 10^{-8} gram. The aim of the work was to evaluate the yield of the competitive reactions d, n producing stable species and d, p or $d, 2n$ producing radioactive species for a given target. The procedure consists in obtaining by means of radioactive tracers reference coagulation isotherms for $_{39}Y^{89}$ and $_{40}Zr^{90}$ and an adsorption isotherm for $_{56}Ba^{134}$ under such conditions that the fraction coagulated or adsorbed respectively changes with the quantity of stable species present. The unknown quantity of stable species is determined from the isotherm after the fraction coagulated or adsorbed is found by means of radioactive tracer.

B4. Thresholds for the Photo-Disintegration of Li^7, Mg^{24}, Al^{27}, Si^{28}, S^{32}, and Ca^{40}. ROBERT A. BECKER, A. O. HANSON AND B. C. DIVEN, *University of Illinois.*—The photo-thresholds for the production of short-lived activities from several substances have been observed using x-rays from the 20-Mev betatron. The technique was similar to that employed by Baldwin and Koch.[1] With the exception of Li^7 the observed activities were produced by (γ, n) reactions. The thresholds in most cases are not well defined, and the estimates of the thresholds are limited by the observed intensity of the activity as compared to that caused by various backgrounds. The approximate periods and estimated thresholds for the observed reactions are presented in the Table I. The calculated thresholds are based on the masses given in Segrè's isotope chart of May 1945. No attempt was made to determine the periods accurately.

TABLE I.

Reaction	Period (sec.)	Threshold (Mev) Observed	Calculated
$Li^7(\gamma, p)He^6$	1	9.5±.3	10.1
$Mg^{24}(\gamma, n)Mg^{23}$	11	16.4±.3	15.5
$Al^{27}(\gamma, n)Al^{26}$	7	14.4±.3	11.1
$Si^{28}(\gamma, n)Si^{27}$	5	16.9±.3	16.0
$S^{32}(\gamma, n)S^{31}$	3	15.0±.3	16.7
$Ca^{40}(\gamma, n)Ca^{39}$	1	16.0±.3	13.7

[1] Baldwin and Koch, Phys. Rev. 67, 1 (1945).

B5. Energy Levels in the Nucleus Mn^{56}. A. B. MARTIN, *Yale University.*—The energies of the protons emitted in the reaction $Mn^{55}(d, p)Mn^{56}$ have been measured by an absorption method. It is found that six distinct groups occur in the energy range from zero to 4.3 Mev above the ground state of Mn^{56}. The nuclear energy change values corresponding to these groups are 0.38, 1.15, 2.28, 2.99, 3.69, and 4.76 Mev. From these results it is seen that the spacings of the most prominent energy levels in the Mn^{56} nucleus which are exhibited in a d, p process are, in order of increasing excitation, 1.07, 0.70, 0.71, 1.13, and 0.77 Mev. The Mn^{56} nucleus contains a sufficient number of particles to render the statistical approach to the problem

at least reasonably valid. The lack of agreement between the results quoted and the 5-kev level spacing predicted by theory[1] suggests that strong selection rules are operating to restrict the number of energy levels participating in reactions of this type to a very small fraction of the total number that are theoretically possible. Other work has shown that in practically all cases the level spacings observed for excitations up to 5 Mev are of the order of 1 Mev or greater, while the spacings predicted by theory range from 5 kev to 100 kev.

[1] H. A. Bethe, Rev. Mod. Phys. 9, 86 (1937).

B6. Yields of Protons in Transmutations.* ERNEST POLLARD, *Yale University.*—A survey of proton yields from elements of low and medium atomic weight due to aphalparticle and deuteron bombardment has been carried out in this laboratory. One general trend seems to be definite. The greater the excitation energy the greater the proton yield. To a first-order approximation the yield is given by $Y=Ae^{U/B}$ where A, B are constants for any one element and U is the excitation energy. No consistent evidence for a maximum in the yield as predicted by Volkoff[1] for the O-P process seems to exist. Nor is there apparent any reduction in yield as a result of the emergent Coulomb barrier.

* Work done under Navy Contract N6ori-44.
[1] G. M. Volkoff, Phys. Rev. 57, 866 (1940).

B7. *L*-Converted Isomeric Transition. M. GOLDHABER, C. O. MUEHLHAUSE, AND S. H. TURKEL, *Argonne National Laboratory.*—It is shown that the radioactive isotope with a half-lifetime of 1.5 min.,[1] formed by capture of slow neutrons in Ir, does not decay by β-emission as was previously believed, but by an isomeric transition which is largely converted in the L-shell. L-radiation of Ir has been detected, and the energy of the transition has been determined by absorption of the internal conversion electrons to be approximately 60 kev. A γ-ray component of similar energy has been found. This energy is smaller than the energy needed for conversion in the K-shell of Ir (76 kev).

[1] E. McMillan, M. Kamen, and S. Ruben, Phys. Rev. 52, 375* (1937).

B8. Disintegration Scheme of the 21-Minute Isomer of Mn^{52}. R. K. OSBORNE AND M. DEUTSCH, *Massachusetts Institute of Technology.*—The beta- and gamma-spectra of the 21-minute isomer of Mn^{52} have been studied by the same techniques as reported previously for the 6.5-day isomer.* The positron spectrum is simple with an end point at 2.66±0.05 Mev. For such large disintegration energies, orbital electron capture would not be expected to be important. One gamma-ray (besides annihilation radiation) of energy 1.46±0.04 Mev was observed. Beta-gamma coincidence measurements show that all the positrons are followed by this, and only this, gamma-ray. The same gamma-ray energy occurs in the decay of Mn^{52} (6.5 day) and of V^{52}. Thus all three decays have the 1.46-Mev excited state of Cr^{52} in common. With the established disintegration scheme of the 6.5-day isomer, these data show that the 21-minute level in Mn^{52} lies 0.40±0.05 Mev above the 6.5-day level. Conversion electrons corresponding to a 0.392±0.008-Mev transition were observed in the spectrometer with an intensity of 5×10^{-4} conversion electron per positron. The accompanying gamma-rays were not observed because of their low intensity. Some new details of the decay of Mn^{52} (6.5 day) and V^{52} will be reported.

* Peacock and Deutsch, Phys. Rev. 69, 306 (1946).

B9. Internally Converted Gamma-Radiation from Tantalum (182). JAMES M. CORK AND FRANKLIN B. SHULL, *University of Michigan.*—The beta-radiation from a sample of tantalum, radiated in the pile, is being studied in a large semi-circular focusing magnetic spectrometer. On using a photographic method about 16 sharp lines are observed caused by electrons with energies less than 200 kev. These can be arranged in several K-L-M and L-M groups characteristic of the level differences in tungsten, indicating that in the decay (half-life 97 days) a beta emission is followed by the gamma-radiation. An attempt is made to arrange a level scheme capable of accounting for the many lines.

B10. Neutron-Proton and Proton-Proton Scattering at 200 Mev. J. ASHKIN AND R. E. MARSHAK, *University of Rochester.*—To get some orientation with regard to high energy scattering experiments, the cross section for n-p and p-p scattering at 200 Mev is calculated using the Born approximation. Calculations are performed for the S(symmetrical), C(charged), and N(neutral) theories on the basis of a square well. The constants (range, depth, amount of tensor force, etc.) are taken from Rarita and Schwinger's paper.[1] The total cross section for n-p scattering is 1.0×10^{-25} cm² and does not vary more than 10 percent, depending on the theory used. However, the angular distribution is very sensitive to the particular theory. In the S theory, backward scattering (in the c.g. system) is 4 times as great as forward scattering. The C theory gives a backward scattering 400 times as great as the forward scattering. The N theory predicts an angular distribution just the reverse of that predicted by the C theory. The S, C, and N theories do not predict such strikingly different angular distributions for p-p scattering. But the total cross sections for p-p scattering do vary considerably (by a factor of 7). The sensitivity of the results to the shape of the potential will also be discussed.

[1] W. Rarita and J. Schwinger, Phys. Rev. 59, 436 (1941).

B11. Results of H^3 Bombardments on Ag and Rh. D. N. KUNDU AND M. L. POOL, *Ohio State University.*—H^3 has been used as the bombarding particle to effect nuclear reactions. The 13-hour Pd^{109} activity has been produced by bombarding silver with H^3 according to the reaction $Ag^{109}(H^3, He^3)Pd^{109}$. The assignment[1] of this activity to Pd^{109} and not to Pd^{107} has been further checked by observing that this activity is not produced on prolonged alpha bombardment of Ru. The possibility of a (d, α) reaction leading to any confusion as to results has been obviated. The effect of the reaction $Ag^{109}(n, p)Pd^{109}$ has been estimated and corrected for. There is reason to believe that the reaction (H^3, p) also takes place. The 7.5-day Ag^{111} activity appears to be produced because of $Ag^{109}(H^3, p)Ag^{111}$ and also with a much longer bombardment, the reaction

$Rh^{103}(H^3, p)Rh^{105}$ seems to be evident, resulting in the 35-hour Rh^{105} activity. The energy of the H^3 particles used is approximately 10 Mev.

[1] W. Rall, Phys. Rev. 70, 112 (1946).

B12. The Nuclear Energy Surface. EUGENE FEENBERG, *Washington University.*—The semi-empirical theory of the nuclear energy surface as sum of volume, surface, symmetry, Coulomb, and expansion terms has been subjected to critical revision. A quantitative correlation appears to exist between the windings of the mass valley in the $N-Z$, A-plane and irregularities (plateaus) in the packing fraction curve. The theoretical pf curve and the various energy parameters are fixed within narrow limits by the mass differences of odd isobars ($N-Z=\pm 1$) independent, within wide limits, of the value assigned to the compressibility coefficient. Two procedures (the analysis of nuclear fission, the fitting of the theoretical pf curve) yield independent values for the ratio surface energy/Coulomb energy. These values differ, presumably because the first involves the size of the real nucleus, whereas the second, through the assumption $R=r_0A^{\frac{1}{3}}$, refers to a uniform state of nuclear matter as it would be in the absence of internal pressures tending to produce expansion. A reasonable value of the compressibility coefficient, consistent with estimates based on the virial theorem, suffices to account for the computed 10 percent difference. A general proof is found for Wigner's rule that isotopic numbers $N-Z=2n-1$ and $N-Z=2n$ first occur at nearly the same values of A.

C1. Stability of Polyelectrons. EGIL A. HYLLERAAS, *University of Oslo,* AND AADNE ORE, *Yale University.*—Previous calculations gave little evidence for the stability of the four-electron $(++--)$.[1] In the present paper some mathematical simplifications have been obtained, which involve a reduction in the number of independent variables and facilitate the calculation of matrix elements with suitably chosen wave functions. The function

$$\psi\sim\exp-\left[\frac{1+\beta}{2}(r_{1a}+r_{2b})+\frac{1-\beta}{2}(r_{1b}+r_{2a})\right]+\exp-\left[\frac{1-\beta}{2}(r_{1a}+r_{2b})+\frac{1+\beta}{2}(r_{1b}+r_{2a})\right]$$

yields a lower limit for the binding energy of roughly 0.11 ev for $\beta^2=0.50$. (1, 2 and a, b refer to electrons and positrons, respectively.) The dynamical stability of the neutral four-electron has thus been proved and an affirmative answer is thereby given to the rather fundamental question regarding the stability of larger aggregates of positrons and electrons, such as those suggested by Wheeler.

[1] J. A. Wheeler, Ann. New York Acad. Sci. 48, Art. 3, 219 (1946); A. Ore, Phys. Rev. 70, 90 (1946).

C2. On the Heitler Theory of Radiation Damping. JOHN M. BLATT, *Massachusetts Institute of Technology.*—Heitler[1] has developed a method of including radiation damping in scattering problems. It involves an integral equation for the scattered field amplitude far from the scatterer. We derived this integral equation classically for a special group of problems. The essential neglect in our deviation also appears in the usual quantum-mechanical derivation.[2] Our derivation allows a comparison between the Heitler method and the Wentzel-Dirac λ-process. Two simple problems are discussed, involving the interaction of an oscillator with scalar and vector meson fields, respectively. Both problems have exact solutions, which we compare with approximate solutions by the Heitler method. The Heitler method preserves the shape of the resonance, but neglects the shift in resonance frequency caused by the additional mass of the oscillator coming from the coupling to the meson field. The strong radiation damping encountered in vector meson theory appears in the second example, although we assumed no spin interaction. The damping can be traced to the Lorentz condition $\sum_{i=1}^{4}\partial U_i/\partial x_i=0$ on the 4-vector field quantity U_i.

[1] W. Heitler, Proc. Camb. Phil. Soc. 37, 291 (1941).
[2] S. T. Ma and C. F. Hsüeh, Proc. Camb. Phil. Soc. 40, 167 (1944)

C3. A Remark on the Correspondence Treatment of Radiation. W. H. FURRY, *Harvard University.*—If expressions for E and H in the wave zone are calculated from the wave-mechanical formulas for charge and current of an atomic system, an approximately correct account of the emission of radiation can be obtained only if this E and H are still regarded as subject to matrix rules of multiplication. This is most clearly indicated in Pauli's exposition of the treatment by the correspondence principle.[1] One can then raise the question as to what this approach gives for the commutation rules of E and H. When it is assumed that the region in question is surrounded by a distribution of oscillators sufficiently numerous to serve as a complete absorber, it turns out that the commutation rules obtained are just those of quantum electrodynamics. This may be regarded as adding to the evidence that quantum electrodynamics must be accepted as a logical development of the correspondence treatment of radiation.

[1] Pauli, *Handbuch der Physik,* Vol. XXIV, no. 1.

C4. Formula for the Coupling of Nuclear Quadrupole Moments in Symmetrical Polyatomic Molecules. J. H. VAN VLECK, *Harvard University.*—If the nucleus has a quadrupole moment and a spin greater than $\frac{1}{2}$, its various possible orientations cause a hyperfine structure, even if the magnetic effects of the nuclear spin are negligible. The dependence of this structure on the quantum numbers J and K of a "symmetrical top molecule" is calculated by quantum mechanics. The effect of the quantum number K is to introduce an extra factor $1-3K^2/(J^2+J)$ not present in the formulas derived by Kramers or Casimir for molecules with $K=0$. It is assumed that the nucleus with the quadrupole moment is located on the axis of symmetry and that the spin effects of other nuclei are unimportant. The calculations thus apply to NH_3 if the hyperfine structure comes mainly from the N nucleus. The predicted dependence on J and K is confirmed with amazing precision in the measurements of Dailey, Kyhl, Strandberg, and Wilson on the microwave inversion spectrum of ammonia.[1] From

the absolute magnitude of the observed structure one concludes that the product of the gradient of the electric field at the N nucleus and the latter's quadrupole moment is eighteen times as large as the corresponding product for the D nucleus in HD.

[1] Dalley, Kyhl, Strandberg, Van Vleck, and Wilson, Phys. Rev. 70, 984(L) (1946).

C5. Thermal Analog of the High Frequency Electron Distribution.[1] LAWTON M. HARTMAN, *Yale University.*—It has been shown[2] that when only elastic collisions occur between electrons and gas molecules the isotropic part of the distribution function under a high frequency field may under suitable conditions be approximated by a Maxwellian function at an effective temperature T', which is determined by the field strength and frequency and differs from the gas temperature T. This conclusion is extended to include inelastic collisions: if the period of the field is much smaller than the mean free time of the electron, the isotropic part of the distribution function always will be identical with the distribution function in a field free gas whose temperature is T'. Utilizing this fact, the distribution function is obtained for the case of a single type of inelastic encounter, assuming a linear cross section. The result may be expressed in terms of the confluent hypergeometric function for the energy range above the excitation potential and may be computed numerically for smaller values by two quadratures.

[1] Sponsored by Office of Naval Research.
[2] H. Margenau, Phys. Rev. 69, 508–513 (1946).

C6. Irreversible Processes in Stellar Dynamics. HERBERT JEHLE, *Franklin Institute.*—The discussion of Boltzmann's H-theorem (cf. Ehrenfest, Encyclopaedie der mathematischen Wissenschaften) centered around the inquiry after the cause of irreversibility, i.e., of the trends in the development of a distribution function $f(x_1, x_2, x_3, v_1, v_2, v_3, t)$ in phase space, notwithstanding the reversibility of classical mechanics. It was recognized that a statistical treatment of the interaction between molecules provided for the deduction of the second law of thermodynamics as a statistical law. If the particles move in a smooth field of force, besides interaction (encounter) forces, the force fluctuation method gives account of the irreversible diffusion superimposed on the smooth streaming of representative points in phase space (Brownian motion in a field of force[1]). In stellar dynamics we are not only concerned about time-dependent solutions of Boltzmann-Gibbs' hydrodynamical equation of transport in a given field of force, but in particular about hydrodynamical self-consistent fields, steady and transient solutions, trying to account for trends of development like the flattening of a galactic system. Such a coupling of the hydrodynamical equations with Poisson's equation is non-linear, but so far still reversible. The superimposing of a statistical "tapping effect" originating from force fluctuations (encounter forces), however, brings about the irreversibility we are looking for.

[1] H. A. Kramers, Physica (1940).

C7. Note on the Recurrence Time Problem for the Two-Dimensional Markoffian Random Function. ARNOLD J. F. SIEGERT, *Syracuse University.*—We have shown (for the two-dimensional Markoffian random function[1]) the equivalence of two seemingly different approaches to the problem of finding the conditional probability that a random function $y(t)$, which has a root at t_0, returns to zero for the first time in $(t, t+dt)$. Wiener[2] and Rice[3] have given a formal solution in form of a series, while, generalizing an argument of Schroedinger,[4] one obtains the integral equation

$$\bar{P}_0(t_0\dot{y}_0/t\dot{y}) = p(t_0\dot{y}_0/t\dot{y}) - \int_{t_0}^{t} d\vartheta \int_{-\infty}^{\infty} d\dot{\eta}\, \bar{P}_0(t_0 y_0/\vartheta\dot{\eta})\, p(\vartheta\dot{\eta}/t\dot{y}),$$

where $\bar{P}_k(t_0\dot{y}_0/t\dot{y})d\dot{y}dt$ denotes the conditional probability that $y(t)$—after starting from zero at t_0 with derivative $\dot{y}_0$—returns to zero in the interval $(t, t+dt)$ for the $(k+1)$th time; $p(t_0\dot{y}_0/t\dot{y}) = \sum_{k=0}^{\infty} \bar{P}_k(t_0\dot{y}_0/t\dot{y})$ being easily obtained from $P_2(y_0\dot{y}_0 t_0/y\dot{y}t)$. The Wiener-Rice series for this process is obtained from the integral-equation by iteration.

[1] Such as the coordinate of a harmonic oscillator in Brownian motion, M. C. Wang and G. E. Uhlenbeck, Rev. Mod. Phys. 17, 323 (1945).
[2] N. Wiener, verbal communication.
[3] S. O. Rice, Bur. Stand. J. Research 24, 46 (1945); Eqs. (3.4–11).
[4] E. Schroedinger, Physik. Zeits. 16, 289 (1915).

C8. Scattering from Statistically Distributed Scatterers. PETER G. BERGMANN, *Sonar Analysis Group.*—The notion of the self-correlation coefficient, the importance of which was first recognized by N. Wiener, has been applied to scattering problems, when the statistical distribution of the scatterers is such that a spatial self-correlation coefficient can be defined. It is possible to express the intensity of the scattered radiation as a function of the scattering angle in terms of the Fourier transform of the self-correlation coefficient of the scatterers. A few cases which are of interest in x-ray diffraction work have been worked out and will be presented. The principal application of the method lies probably in the interpretation of x-ray patterns of imperfect crystals, polycrystalline materials, and partially ordered matter.

C9. Motion of Charged Particles in Inhomogeneous Anisotropic Media. N. CHAKO, *Kansas State College.*—The equivalence between the path of light rays of geometrical optics in inhomogeneous anisotropic media and the trajectories of charged particles in electromagnetic fields is established by a single function, the characteristic function of Hamilton V, commonly called the *point eiconal.* This function responds to the action function S which appears in the Hamilton-Jacobi theory of classical mechanics. Starting with the action function, $S(x_i, x_i')$, which is a function of both the positional and directional coordinated (generalized coordinates and momenta qi, pi), the equations of motion of charged particles in inhomogeneous anisotropic media and a general expression for the refractive index of the particles are obtained. As a special case, the expression of the refractive index[1] of an electron in an electromagnetic field is obtained, as well as the more general case, where the electron moves according to special relativity theory. Further, the fifth-order theory of image errors is developed and it is applied to axial symmetric electron optical system. Besides the nine (actually ten) errors in geometrical optics obtained by Schwarzschild,[2] one finds 6 additional errors,[3]

which are due to the anisotropy of the medium due to the magnetic field. These errors have been studied in an extensive manner with the hope of future application in connection with high energy apparatus.

[1] P. Frank, Phys. Rev. 62, 241 (1942).
[2] K. Schwarzschild, Untersuchungen zur geometrischen Optik, König. Gess. Wiss. zu Göttingen 4, 1 (1905–1906).
[3] In general, one obtains for additional errors, but for this particular case they do not appear in the development of the Seidel's eiconal function.

C10. An Investigation of Thick Target X-Ray Production in the Range from 1250 to 2350 kv. W. W. BUECHNER, R. J. VAN DE GRAAFF, E. A. BURRILL, AND A. SPERDUTO, *Massachusetts Institute of Technology.*—An experimental investigation has been made of the thick target production of x-rays using electrons from an electrostatic accelerator. Measurements of x-ray intensity at various angles with respect to the incident electron beam were made with an ionization chamber for targets of beryllium, aluminum, copper, silver, tungsten, and gold. The radiation was filtered to reduce the softer components. Various voltages from 1250 to 2350 kv were used and the angular range covered was from 0 to 140 degrees. The radiation intensity and its angular distribution are in agreement with the results of Petrauskas, Van Atta, and Myers[1] for gold. The total radiation intensity, integrated over all angles, is found to be accurately linear with atomic number in this energy range. From these measurements, the efficiency of x-ray production may be calculated. The values of efficiency obtained are in general agreement with the measurements and theoretical calculations of Arcimovic and Chramov[2] for the case of copper and of Ivanov, Walter, Sinelnikov, Taranov, and Abramovich[3] for the case of lead.

[1] Petrauskas, Van Atta, and Myers, Phys. Rev. 63, 389 (1943).
[2] L. A. Arcimovic and V. A. Chramov, Comptes Rendus Acad. Sci. U.S.S.R. 7, 415 (1938).
[3] Ivanov, Walter, Sinelnikov, Taranov, and Abramovich, J. Phys. U.S.S.R. 4, 319 (1941).

C11. Probability of *K*-Ionization of Nickel by Electrons. L. T. POCKMAN, D. L. WEBSTER, P. KIRKPATRICK, AND K. HARWORTH, *Stanford University.*—Absolute *K*-ionization cross sections Φ_k, calculated from our relative measurements[1] of nickel K_α line intensity and an absolute measurement[2] are well expressed empirically by

$$\Phi_k = 7.27(e/V_k^2)(V/V_k)^{-0.837}\log_{10}(V/V_k).$$

V and V_k are bombarding and *K*-ionizing potentials. Burhop's[3] theory fits these absolute cross sections as well as could be expected of a Born-approximation, non-relativistic theory. Since non-relativistic theories make $\Phi_k V_k^2$ nearly the same for nickel and silver at any V/V_k, we ascribe our observed differences[4] to relativity and deduce cross sections for hypothetical non-relativistic nickel. These confirm Burhop still better. Comparison with helium ionization data[5] suggests that each helium electron considerably reduces the cross sections for the other at low voltages.

[1] D. L. Webster, L. T. Pockman, K. Harworth, and P. Kirkpatrick, Phys. Rev. 55, 682 (1939).
[2] A. E. Smick and P. Kirkpatrick, Phys. Rev. 67, 153 (1945).
[3] E. H. S. Burhop, Proc. Camb. Phil. Soc. 36, 43 (1940).
[4] D. L. Webster, W. W. Hansen, and F. B. Duveneck, Phys. Rev. 43, 839 (1933).
[5] P. T. Smith, Phys. Rev. 36, 1293 (1930).

C12. Absolute Energy of $K\alpha$ Radiation from Thick Silver Targets. PAUL KIRKPATRICK AND A. V. BAEZ, *Stanford University.*—$K\alpha$ radiation from a thick silver target bombarded at 40 kv was isolated by Ross filters of 42 Mo and 45 Rh and the total energy measured with a large air-filled ion chamber and found to be 8.6×10^{-12} erg per electron. This standardizes the curve of intensity *vs.* bombardment voltage measured in arbitrary units up to 180 kv by Webster, Hansen, and Duveneck. A quantitative explanation of the curve may be developed upon the basis of the absolute cross section of the silver atom for *K*-ionization by electron impact, known over a considerable range of bombardment voltages from measurements by Webster, Hansen, and Duveneck and by J. C. Clark. From this cross section and the rate of energy loss of the bombardment electron it is possible to determine the number of *K*-ionizations produced by the electron. The radiation energy follows readily after due account has been taken of the silver fluorescence yield, the relative intensities of the several *K* lines, the *K*-ionizations produced by fluorescence, and the bombardment electrons lost by rediffusion. Corresponding ordinates of the calculated and observed curves of absolute $K\alpha$ intensity *vs.* bombardment voltage differ by five to ten percent, which is no more than their probable errors.

G1. Scale Factors in Water Entry. HAROLD WAYLAND, *Underwater Ordnance Division, Naval Ordnance Test Station* (20 min.).—In 1943 facilities were constructed by the California Institute of Technology under OSRD contract for the Bureau of Ordnance, Navy Department, for studying water entry of large weapons such as aircraft torpedoes. The existence of these facilities made possible the first critical study of the modeling of water entry phenomena wherein accurate quantitative data were available from large scale objects. Fundamental difficulties in modeling the oblique entry of fine-nosed projectiles were encountered, which were associated with the properties of the atmosphere above the fluid medium. The effect of the atmosphere on cavity behavior had been recognized, but these experiments showed that the force pattern on the projectile nose was seriously modified before the nose was symmetrically wetted. This proved to be due to viscous effects of the gas. In light of these and other anomalies, the general problem of modeling water entry is briefly reviewed.

G2. Fluid Flow Patterns. GARRETT BIRKHOFF AND THOMAS E. CAYWOOD, *Harvard University* (20 min.).—Quantitative discussion is given of the velocity fields caused by the entry of solids into water. Our main experimental technique used is high speed multiflash photography of 1-mm diameter air bubbles located in a fixed vertical plane; this was first developed by L. B. Slichter. We conjectured from "virtual mass" theory, and verified experimentally, that the air bubbles may move twice as far as the surrounding water, and in a different direction. We developed mathematical "corrections" applicable to various cases, for inferring the water velocity from the air bubble displacement. A modification of Slichter's technique is described, based on silhouette photography of dyed oil drops, which is often much easier to correct. Various specific flow patterns are

exhibited, and conclusions reached regarding the physical applicability of certain branches of classical mathematical hydrodynamics—especially so-called Dirichlet flow, wake theory, and jet theory.

G3. The Interaction of Shock-Waves, the Spectra of Cavity Charge Explosions, and the Production of Artificial Meteors. R. W. WOOD, *Johns Hopkins University* (20 min.).—An account is given of the examination of interfering shock-waves in air by "Schlieren" photography, and by the patterns which they trace on plates of smoked glass, in an attempt to verify von Neumann's theory that the armor piercing jet of a cavity charge (Bazooka projectile) was a "Mach wave" of high intensity. Experiments made at the Aberdeen Proving Ground in 1944 on the photography of the spectrum of the exceedingly narrow and very brilliant flash or "jet" of light that shoots up to a height of a hundred or more feet, when the charge is fired on the ground at night, proved that it was a "fireball" or slug of metal, heated to incandescence by air friction—in other words an artificial meteor. Its velocity, found to be around 30,000 feet per second, and its spectrum, obtained by mounting a high intensity replica diffraction grating in front of the lens of a camera, was that of the metal forming the V-shaped liner of the hollow charge. This is the so-called "man made meteor" that is to be fired from the nose of a V2 rocket at White Sands, New Mexico.

(Title not received.) H. W. EMMONS, *Harvard University* (20 min.).

Some Recent Investigations in Hydrodynamic Stability. C. C. LIN, *Brown University* (20 min.).—Much theoretical investigation of the stability of parallel flows has been carried out recently. The results obtained in the case of the boundary layer in an incompressible fluid agree with the excellent experimental work of Schubauer and Skramstad and of Liepmann. L. Lees and the present writer extended the work to include the effect of compressibility, and heat transfer. Periodic disturbances of the usual type are considered, and many results are established analogous to those obtained in the incompressible case. Some further conclusions are reached by L. Lees, three of which are quoted below. (1) The withdrawal of heat from the solid boundary makes the boundary layer more stable, while the addition of heat through the solid boundary makes it less stable. (2) For an insulated boundary, the boundary layer becomes less stable as the Mach number of the free-stream is increased. (3) For supersonic free stream, the flow may be completely stabilized by the removal of heat through the boundary beyond a certain critical rate.

Linearization of Solutions in Supersonic Flow. J. W. TUKEY, *Princeton University* (10 min.).

L1. Hall Effect and Magneto-Resistance in Germanium. W. CRAWFORD DUNLAP, JR. *General Electric Company.*—Resistivity, Hall effect, and magneto-resistance measurements were made upon twelve samples of germanium including both polycrystalline and single crystal specimens. Room temperature resistivity ranged from 2 to 30 ohm cm. Magnetic fields up to 15,000 gauss and temperatures from −195°C to 450°C were used. The Hall coefficient decreased linearly with increasing field in most cases, and by as much as 50 percent at 12,500 gauss. The resistivity increased from 10 to 20 percent at 12,500 gauss and 25°C, and the increase ranged from 40 to 100 percent at −195°C, and the same field. No tendency toward saturation was observed at 15,000 gauss. $\Delta\rho/\rho_0$ decreased with temperature increase roughly proportional to the mobility (R/ρ). The room temperature mobility ranged from 1200 to 3000 cm²/volt sec. The magneto-resistance effect in germanium appears to be at least an order of magnitude larger than is expected from the free electron theory for semi-conductors, which predicts saturation at 12 percent. A discussion is given of possible sources of the discrepancy.

L2. Temperature Dependence of the Diamagnetic Susceptibility of Gamma-Brasses.* JULES A. MARCUS, *Yale University.*—The temperature dependence (14-290°K) of the magnetic susceptibility of gamma-brass has been measured for several polycrystalline specimens synthesized from copper and zinc of highest purity. The susceptibility was determined relative to that of a pure bismuth standard by measuring the force in an inhomogeneous magnetic field. The forces of order two dynes were measured by means of a Sucksmith ring balance. At room temperature the susceptibility varied linearly with composition in agreement with the results of other investigators. At the copper-rich end of the phase, the susceptibility decreased almost linearly with decrease in temperature, the total decrease being 10 percent; at the zinc-rich end, the susceptibility increased with decrease in temperature, the total increase being only 3 percent. The band theory of metals indicates that the gamma-phase should be very similar magnetically to bismuth and accounts for the large diamagnetic susceptibility at room temperature. However, the above results show that the temperature coefficient of susceptibility for gamma-brass at low temperatures is considerably less than for bismuth. Also, the susceptibility of gamma-brass was found to be independent of field strength at 14°K.

* The research described in this abstract was supported by the Office of Research and Inventions of the U. S. Navy under contract N6Ori-44.

L3. Magnetic Transition Curves in Superconducting Tantalum.* ROBERT T. WEBBER, *Yale University.*—The behavior of thin wires of pure (99.9+ percent Fansteel) tantalum in uniform, longitudinal magnetic fields has been measured at the temperatures of liquid helium. The resistances of the wires were measured by the potentiometer method, the potential drop being recorded by a Brown potentiometer. In unannealed wires containing a small, but unknown, quantity of absorbed gas, the results were in some respects more similar to alloy behavior than to that of a pure metal. The zero field transition temperature was 4.16°K. The slope of the critical field was $dH_c/dT = 1300$ Gauss per degree, in fair agreement with the results of Mendelssohn and Moore,[1] but much larger than the results of induction measurements of Daunt and Mendelssohn.[2]

We found no hysteresis, but considerable evidence of intermediate state, particularly at the lowest temperatures studied. The effect of annealing and outgassing the wires at high temperature and high vacuum was also determined. Preliminary results will also be given on an attempt to determine the relaxation time occuring in the transitions of the wires under pulsed magnetic fields.

* Work done under Navy Contract N6Ori-44.
[1] K. Mendelssohn and J. R. Moore, Phil. Mag. [7] 21, 532 (1936).
[2] J. G. Daunt and K. Mendelssohn, Proc. Roy. Soc. 160, 127 (1937).

L4. A Method to Measure Complex Permeabilities of Metals at UHF. M. H. JOHNSON, G. T. RADO, AND M. MALOOF, *Naval Research Laboratory.*—Complex permeabilities in the surface layer of ferromagnetics with known d.c. resistivity can be computed from the attenuation and phase velocity in a coaxial line whose center conductor is ferromagnetic. These quantities can be found experimentally by measuring simultaneously the change in Q and in the resonant frequency ($\sim$.01 percent) when a metal is substituted for the ferromagnetic portion of the center conductor in a coaxial resonator. A mechanical substitution invariably produces a greater change in resonant frequency by alteration of geometrical conditions than by removal of the ferromagnetism. The difficulty can be circumvented with the use of a polarizing field which is parallel to the small r-f field and is strong enough to completely saturate the ferromagnetic material. It is thus possible to compare resonant frequencies (and Q's) for the actual permeability and for unit permeability without altering the geometrical conditions. High power dissipation and the transient skin effect of the current producing the polarizing field in the center conductor require, respectively, pulse technique and millisecond periods. Application of the method at 200 Mc to magnetic iron and Mo-permalloy show that their permeabilities ($\sim$100) are much smaller than the d.c. values and have a large out-of-phase component.

L5. Complex Permeability of Magnetic Iron at 200 Mc as a Function of Polarizing Field. G. T. RADO, M. H. JOHNSON, AND M. MALOOF, *Naval Research Laboratory.*—The method of the previous abstract can readily be extended to determine the complex permeability[1] in the surface layer of a ferromagnetic metal as a function of the polarizing magnetic field. It is only necessary to compare the Q and the resonant frequency of the cavity for any polarizing field with the corresponding quantities for a saturating field ($\sim$1000 oersteds). In this way the real and imaginary components of the permeability of magnetic iron have been determined from zero to saturating fields. The r-f permeability shows no appreciable change until the d.c. magnetization is well beyond the knee of the magnetization curve. Hence the domain changes (wall displacements) supposedly responsible for the d.c. susceptibility below the knee have already become inoperative at 200 Mc. In high polarizing fields the imaginary component becomes small compared to the real component. The correlation between r-f and incremental d.c. permeabilities and the interpretation of the experimental results will be discussed.

[1] The complex permeability, $\mu_1 - i\mu_2$, is defined as the ratio of B to H in the metal. $\mu_2 \neq 0$ means that the magnetization and the magnetizing field are not in phase.

L6. A New Material of High Permeability. O. L. BOOTHBY AND R. M. BOZORTH, *Bell Telephone Laboratories.*—Magnetic permeabilities of over one million, and initial permeabilities of over 150,000, have been obtained in an alloy containing iron, nickel, and molybdenum (79 Ni, 5 Mo, 15 iron, <1 Mn). Representative properties of specimens 0.014 in. thick are: maximum permeability, 800,000; initial permeability, 100,000; coercive force, 0.003 oersted; hysteresis loss, 4 ergs/cm^3/cycle at $B_m = 5000$; saturation induction, 8000; resistivity, 65 microhm-cm. The alloy is prepared by vacuum melting of commercial materials of high purity, fabrication in the usual way, heat treatment in pure dry hydrogen at about 1300°C, and cooling at a critical rate. The purity and the cooling rate are both essential for good magnetic quality. The cooling rate appears to control the amount of atomic ordering present, and the hypothesis is made that, when a critical amount of ordering is present, the magnetostriction and the magnetic crystal anisotropy both tend toward zero in the alloy of this composition. The material has been named supermalloy (su-perm'-al-loy).

L7. Pulsed Ultrasonic Measurements on Some Single Crystals.* H. B. HUNTINGTON, *Rensselaer Polytechnic Institute.*—Measurements of acoustic velocity and attenuation have been made at 10 Mc/sec. by a pulsed technique on Rochelle salt and several alkali halides. Values of elastic moduli for LiF, NaCl, KBr, and KI will be reported. The attenuation of the ultrasonic beam in these media is small. Corresponding measurements on the elastic moduli of Rochelle salt have been carried out. Under the assumption of plane wave transmission many of these observed moduli automatically correspond to those measured on foiled crystals by other methods. Attenuation is considerable in Rochelle salt and appears to be excessively high for transmission involving the temperature-dependent C_{44} (foiled case). As a result, it has not yet been possible to carry out a direct measurement of this quantity for a temperature range within 2°C of the upper Curie point. Where this modulus is involved, marked effects have been observed from electric bias and mechanical pressure. A complete set of elastic moduli have been obtained and used to calculate the corresponding values for the moduli of compliance.

* Based on work done for the Office of Scientific Research and Development under OSRD Contract OEMsr-262 with Massachusetts Institute of Technology.

L8. The Transmission of Energy from Radiation on Silicon Crystals. F. C. BROWN, *Massachusetts Institute of Technology.*—Pulsed radiation, of duration 3 to 60 μ sec. on silicon crystals produces an effect that is propagated along the crystal with velocity of 400 meters/sec. The effect is detected and measured through change of resistance. Since the velocity is of the same order of magnitude as a thermal pulse, further experiments were conducted. A thermocouple showed a transmitted temperature rise accounting largely for the resistance change. There was inappreciable transmission if metal flats, extending between electrodes and point of impingement of radiation, pressed against opposite crystal faces. Neither black paint nor

opaque wax on crystal materially altered the so-called photo-effect—i.e., the effect depends on energy received. Finally, the pulsed energy was transmitted to the crystal electrode contact over a tungsten wire and repeated by transmission over a nickel wire. The resistance changes were almost identical to the transmission over the silicon crystal. The velocity in tungsten is 730 meters/sec., and in nickel 250 meters/sec. It would seem that the photo-conductivity in silicon crystals can be more readily explained as a thermal effect.

L9. Infra-Red Vibrations in NaCl. JORDAN J. MARKHAM, *Brown University.**—A theoretical study has been made of the propagation properties of the lattice vibrations in NaCl. The phase velocity, the group velocity, displacement angle (angle between the particle displacement and the direction of propagation), and the displacement ratio were calculated as a function of wave-length for three directions of propagation. In these calculations, Born's theory was used. The transmission characteristic of the crystal resembles a filter with a low pass band (acoustical) and an upper band (optical). At the lowest frequency, the waves are simply elastic ones. As the frequency increases, the structure exhibits strong dispersion. In the limit of shortest wave-length, the group velocity approaches zero. The optical branch is highly dispersive at all frequencies. The group velocity is negative (on the single zone scheme), and is zero at both the short and long wave-length limits. Generally, for both branches at the short wave-length limit the particle displacement lines up along the direction of nearest neighbors. Exceptions to this occur for propagation along some highly symmetrical direction.

* Now at Clinton Laboratories, Oak Ridge, Tennessee.

L10. Total-Energy Distributions of Photoelectrons from Polycrystalline Tungsten. L. APKER, E. TAFT, AND J. DICKEY, *General Electric Company.*—The total-energy distributions of photoelectrons from an aged polycrystalline tungsten ribbon were determined at λ2138 and λ2537.[1] Shields for the ribbon supports eliminated extraneous contact potentials in the usual type of spherical-condenser photo-cell, which was magnetically shielded in this case. Data were obtained within 30 seconds after flashing at 2900°K. Current-voltage curves could be divided into three regions: (1) the high-energy portion investigated by DuBridge and Roehr[2]; (2) a portion showing a parabolic approach to a pseudo-saturation point independent of wave-length; (3) a pseudo-saturation portion characterized by the well-known slow increase of current with voltage. Region 2 is of interest in evaluating the effects of non-uniform work function[3] and of electron reflection at the graphite anode. Extraneous contact potentials of only a few tenths of a volt distorted the curves seriously.

[1] We are indebted to the University of Rochester Physics Department for the loan of a monochromator.
[2] L. A. DuBridge, Phys. Rev. 43, 727 (1933); W. W. Roehr, *ibid.* 44, 866 (1933).
[3] R. P. Johnson and W. Shockley, Phys. Rev. 49, 436 (1936); C. E. Mendenhall and C. F. DeVoe, *ibid.* 51, 346 (1937); M. H. Nichols, *ibid.* 57, 297 (1940).

L11. A Study of the Barium Silicate Interface of Oxide Coated Cathodes. A. EISENSTEIN,* *Massachusetts Institute of Technology.*—Previous studies[1] have shown (1) the presence of a crystalline material at the interface of oxide cathodes prepared on a Si-Ni base metal and (2) the existence of an anomalous voltage at the interface region under certain conditions of pulsed measurements. The interface compound which is formed in the case of a BaO or (BaSr)O coating on a Si-Ni base is believed to be Ba_2SiO_4 rather than $BaSiO_3$ as previously reported.[1] The relationship between (1) and (2) above has been investigated by comparing the electrical conductivities of (BaSr)O and Ba_2SiO_4 in the temperature range 1100°K to 1300°K. Conductivities were determined for materials activated by (a) high d-c current drain, (b) CH_4 gas, and (c) H_2 gas and deactivated in CO_2 gas. In general, the specific conductivity of the silicate is lower than that of the oxide by a factor of 10 to 1000. The thickness of the interface, found in actual cathodes, has been determined by an x-ray method[2] to lie in the range 5×10^{-4} to 10^{-3} cm. The relationship of the interface to the thermionic emission characteristics will be discussed.

* Frank B. Jewett Fellow.
[1] A. Fineman and A. Eisenstein, J. App. Phys. 17, 663 (1946).
[2] A. Eisenstein, J. App. Phys. 17, 874 (1946).

H1. On the Hydraulic Analogy between Surface Waves on a Liquid and Pressure Waves in a Compressible Fluid. H. A. EINSTEIN, *California Institute of Technology.*—The intersection of strong shock waves in compressible fluids is being studied by means of this analogy. As the linear approximation cannot be used for strong waves, the validity of the analogy must first be proved. It is found that only the combinations of p and v can be duplicated by surface waves for which the condition $[1-(\pi/p)][1-(b/v)]=1$ is fulfilled. The introduction of this additional condition made it desirable to solve mathematically the intersection problem of two identical surface shock waves. The case of the regular intersection with constant state between shock waves has been solved in general and the numerical solutions for a number of wave heights and for some angles of intersection are tabulated. Also, the extreme angle which allows a regular intersection is found. All these values duplicate very closely the corresponding results for pressure waves. The experimental check of these solutions was accomplished by the study of transient shock waves in a shallow tank with still water. The "extreme" solution (maximum angle at which a regular intersection is possible) very closely checks the beginning of a Mach-type intersection. Also, the water depth (pressure) immediately behind the intersection duplicates very closely the calculated value. The angle of the reflected waves, however, never could be checked because the reflected waves had a curved front with a corresponding pressure drop along the front.

H2. On Nearly Glancing Reflection of Shocks.* V. BARGMANN, *Princeton University.*—The oblique reflection of plane shocks from a plane rigid wall follows a simple pattern—that of "regular reflection"—as long as the angle of incidence α is smaller than a critical angle depending on

the strength of the incident shock. For larger values of α the more complex pattern of the "Mach reflection" is observed. A detailed hydrodynamical treatment of Mach reflection seems extremely difficult, and therefore the discussion has been generally confined to the immediate neighborhood of the intersection of the three shocks. In the limiting case of nearly glancing incidence, however, it has been possible to obtain an approximate solution of the hydrodynamical equations, and to derive explicit expressions for the pressure distribution behind the shocks.

* Work carried out under an OSRD contract at the Institute for Advanced Study, Princeton, New Jersey.

H3. Compressible Flows with Degenerate Hodographs. JOHN H. GIESE, *Ballistic Research Laboratories (Introduced by R. H. Kent)*.—Non-linearized, three-dimensional, steady, isentropic, compressible, potential flows for which the maps of the physical space on to the hodograph space have fewer than three dimensions have been systematically studied by applying a Legendre transformation to the equation of the velocity potential. This leads naturally to a synthesis of a number of familiar types of flows, such as (1) Prandtl-Meyer expansion around a corner; (2) Ringleb's or Binnie's and Hooker's spiral flows; (3) general plane flow; (4) Busemann's cylindrical and general conical flows, including Taylor-Maccoll flow. The most general flow with a one-dimensional map is a straightforward generalization of (1). Flows with two-dimensional maps must be either of types (4) or of modified conical type. The differential geometry of these flows has been thoroughly investigated to find analogues for many of the well-known properties of plane flow. As an example, all axisymmetric flows with degenerate hodographs have been determined.

H4. On an Operator Method in the Theory of Two-Dimensional Flows of a Compressible Fluid.* STEFAN BERGMAN, *Harvard University*.—Using the hodograph method, the author represents the stream lines of an adiabatic two-dimensional flow of a compressible fluid in an implicit form $x=x(f,g)$, $y=y(f,g)$, $\psi(f,g)=\text{const}$, $f(\xi)$ and $g(\eta)$ are functions of one variable $\xi=(\theta+i\lambda(M))$ and $\eta=(\theta-i\lambda(M))$, respectively. In the subsonic case, f and $g=\bar{f}$ are conjugate complex functions of a complex variable; in the supersonic case λ becomes purely imaginary, f and g are two independent functions of a real variable. ψ satisfies the equation $\psi_{\lambda\lambda}+\psi_{\theta\theta}+N(\lambda)\psi_\lambda=0$ where $N(\lambda)$ is a known function.[1] The representation obtained is used for the study of the behavior of the solutions in the neighborhood of $\lambda=0$, which corresponds to Mach number $M=1$. This investigation is particularly simplified if N is approximated by $C\lambda^{-1}$, where C is a properly chosen constant. The author indicates how the functions f, g have to be chosen in order to obtain a flow around a contour which approximates the boundary curve given in the physical plane. The considerations show that for certain contours no solutions of a certain kind exist without shock-waves.

* Work done under contract with Bureau of Ordnance, Navy Department.
[1] See also N.A.C.A.; Tec. Notes 972, 973, 1018, 1096.

H5. Some Remarks on the Limitations of Linearized Theory of Supersonic Flow Around Cones. ZDENĚK KOPAL, *Massachusetts Institute of Technology*.—The purpose of these notes is to compare the consequences of Karman-Moore's linearized equations of axial flow, and of their extension, by Tsien, to non-axial flow, with the corresponding rigorous solutions of non-linear equations in the case of a supersonic flow around cones. The outcome of such a comparison may be summarized as follows: 1. The linearized equations do not predict the existence of a shock-wave in front of a solid cone in supersonic flight. 2. In the neighborhood of the sonic velocity, they lead to a solution for every Mach number larger than one—and therefore fail to predict the non-existence of a conical regime for Mach numbers in the neighborhood of unity. 3. They fail to lead to a solution for velocities high enough for the Mach cone to become smaller than the solid—whereas, in reality, the solution does exist up to infinite velocities. 4. For axial flow, they lead to head-drags which are systematically too small, and their errors increase with increasing velocity as well as increasing angle of the cone. 5. For non-axial flow, they make the coefficients of normal force to decrease with increasing Mach number, and to vanish when the Mach cone becomes identical with the solid, whereas the coefficients derived from the non-linear theory are found to behave in exactly the opposite way and would not vanish even should the Mach number become infinite. 6. The fact that the linearized equations predict correctly the order of magnitude of both drags can be quoted as the only point on their credit side.

H6. Supersonic Problems in Astronomy. FRED L. WHIPPLE (*Introduced by R. J. Seeger*).—Until recently the meteor problem has represented the most obvious case of supersonic ballistic problem in Astronomy. The V-2 experiments and laboratory experiments on shaped charges are in the process of bridging the gap between the theories of the meteoric and the ballistic processes. The types of observations and the theoretical approach needed or anticipated in this field are outlined briefly. Other supersonic processes of importance in Astronomy are, however, recognized. The atmosphere of the Sun shows a complex of supersonic motions. Novae, supernovae, and certain other variable stars represent atmospheric motions with tremendous velocities. There is also good reason to suspect that the interiors of the stars are in a state of great turbulence, and possibly a considerable amount of energy and momentum are transmitted from the interiors by shock-waves. On a much greater scale of dimensions the interstellar medium of gas and dust also shows evidence of shock-wave phenomena, which probably play important roles in galactic, stellar, and planetary evolution problems as well as in the production of observed radiation. The nature of each of these astronomical problems is discussed and related to the more familiar physical point of view.

H7. Comments on the Motion of a Solid Body at High Velocity through a Compressible Medium. R. N. THOMAS, *Harvard Observatory*.—The motion of a solid body through a resisting medium provides one phase of a general astro-

nomical interest in the motion of a body of one density through a medium of another, and arises directly in the motion of a meteor through the atmosphere. There exists a wide gap between the laboratory experimental ballistic case, and the meteor case. To the limit of the ballistic velocities yet reached, and in atmospheric conditions, the theoretical formulation of the ballistic problem may be said to describe satisfactorily the situation. Ballistics provides essentially no information, however, on the high velocity important process of heating of the body to evaporation. The work of Whipple at Harvard provides the only analysis of the meteor case from adequate experimental data. Recent V-2 soundings indicate surprisingly exact agreement with the "meteoric" atmosphere. A detailed discussion is made of the explicity inferences which may be drawn from the Whipple analysis concerning the details of the interaction between medium and meteor.

H8. Laminar Boundary-Layer Oscillations and Stability of Laminar Flow. H. K. SKRAMSTAD AND G. B. SCHUBAUER *National Bureau of Standards.*—An experimental investigation carried out in 1940 and 1941 in a wind tunnel of very low turbulence led to the discovery of sinusoidal velocity fluctuations in the laminar boundary layer of a flat plate. The characteristics of these fluctuations were found to agree with those predicted earlier by the stability theory of Tollmein and Schlichting, throwing new light on the causes of transition from laminar to turbulent flow. The fluctuations are termed "laminar boundary layer oscillations" to distinguish them from the irregular velocity fluctuations previously observed by other investigators. In earlier investigations these oscillations were not found, probably because of the high turbulence in the wind tunnels in which the investigations were conducted. Methods were found to produce these oscillations artificially in the boundary layer, and studies were made of the frequency, wave-length, amplitude, and amplification or damping of the natural and the artificially produced oscillations. Transition occurred where conditions in the boundary layer were such that these oscillations had been amplified to a sufficiently large value to cause a breaking into irregular high frequency fluctuations characteristic of turbulent flow. This work was done with the cooperation and financial assistance of the National Advisory Committee for Aeronautics.

H9. Drag Coefficient of Steel Spheres Entering Water. ALBERT MAY AND JEAN C. WOODHULL, *Naval Ordnance Laboratory.*—The drag coefficient has been measured for steel spheres in the cavity stage after entering water normally. Data were obtained from high speed motion pictures of 77 shots of $\frac{1}{4}''$ to $1\frac{1}{2}''$ spheres with entrance velocities of 16 to 126 ft./sec. giving a range of Reynold's number from 0.3×10^5 to 15×10^5. Before using $1/v$ *versus* t plots, it was found necessary, on most shots, to correct for gravity, for hydrostatic pressure due to depth, and for the pressure in the cavity behind the sphere. The last of these corrections requires a knowledge of the time at which the cavity closes near the water surface. Analysis shows this time to be considerably later than the time at which the spray dome appears to close. The drag coefficient was found to increase with the Reynold's number at water entry from about 0.28 to 0.33 over the range investigated. The curve of drag coefficient *versus* log$R$ appears to be concave upwards and the standard deviation from this curve was 0.012.

H10. Drag and Cavity of Fast Spheres Shot into Water.* J. HOWARD MCMILLEN** AND E. NEWTON HARVEY, *Princeton University.*—Drag forces and cavity formation for fast spheres entering water vertically were studied by means of high speed motion pictures. The impact velocity was varied from 800 to 3300 ft./sec. and sphere diameter from $\frac{1}{16}''$ to $\frac{1}{4}''$. The drag coefficient in the cavity stage was 0.297 ± 0.01 for steel spheres, 0.318 ± 0.011 for aluminum spheres. The unimportance of viscous forces in this velocity range was verified by measuring drag in a syrup which was 2100 times more viscous than water; the measured drag coefficient showed only a 60 percent increase over water. The small effect of structural forces in this velocity range was revealed in the measurement of the drag coefficient in 20 percent gelatin gel at 24°C; it was found to be 0.35. The cavity in water was observed to expand laterally to about sixteen sphere diameters for the highest velocities. The maximum cross-sectional area of this cavity at any level was found to be proportional to the space rate at which the sphere lost energy at that level, the constant being 8.92×10^{-7} cm³/erg. A large portion of the cavity became detached to from a bubble resembling the bubble of underwater explosions. This "explosive" bubble was observed to oscillate with a period proportional to the cube root of the impact energy, the constant being 0.8×10^{-4} sec. erg$^{-\frac{1}{3}}$.

* Work done under contract with the Office of Scientific Research and Development, the Committee on Medical Research.
** Now at Naval Ordnance Laboratory, Washington, D. C.

H11. Impact Pressure Produced by Flat Plate Striking Water Surface. P. N. METZELAAR AND D. E. ALLMAND, *Naval Ordnance Laboratory, Washington, D. C.* (*Introduced by J. Howard McMillen*).—Measurements were made of the peak pressure which a flat-nosed cylinder experiences when the cylinder is shot end foremost into water with a near-sonic velocity. The velocities V ranged from 1000 to 2000 ft./sec. and the pressures were measured by means of diaphragm gauges. These gauges consisted of 0.015" sheet of steel stretched over holes having diameters ranging from 0.016" to 0.031". The gauges were calibrated statically up to 130,000 p.s.i. and their response time calculated to be less than ten microseconds, the time depending on the magnitude of the deformation. The peak pressure at 2000 ft./sec. was found to be 125,000 p.s.i. According to the simple theory the peak pressure should be equal to RV or $d^{\frac{1}{2}}Ve^{\frac{1}{2}}$ where e and R are the elastic constant and acoustic impedance, and d is the density of the liquid, respectively. It was found that the measured peak pressure followed the simple theory curve with a standard deviation of 7300 p.s.i. The effect of shear-rate on performance of the gauge will be discussed. Shots into ether and glycerine, having acoustic impedances equal to 0.5 and 1.7 that of water, show the expected dependence of impact pressure on acoustic impedance.

H12. On the Characterization of Fields of Diabatic Flow. BRUCE L. HICKS, *Ballistic Research Laboratories.*—In continuing the previously reported investigations of steady diabatic flow,[1] the transformation $\bar{N}=\bar{V}/[g(N)RT]^{\frac{1}{2}}$, $N=|\bar{N}|$ has been introduced. The Crocco vector $\bar{N}_W\bar{W}=(\bar{V}/V_t)$,

$$\left(g_W=\frac{2\gamma}{\gamma-1}(1-W^2)^{-1}\right)$$

is in the general case the best $\bar{N}$ to use in describing a steady, *rotational*, diabatic field of flow. There is an infinite number of distinguishable types of *irrotational* diabatic flows determined by $g(N)$ and $F(\varphi_N)$, an arbitrary function appearing in the p.d.e. for the $\bar{N}$ potential, φ_N. Specification of $g(N)$ determines the change of (mathematical) type of the flow which may, for example, be always elliptic, of mixed type, partially hyperbolic, etc., irrespective of the ratio of the Mach number to unity. By contrast, in adiabatic compressible flow, the flow always changes type at $M=1$ from elliptic to hyperbolic. Specification of both $g(N)$ and $F(\varphi_N)$ restricts the nature of the distribution of heat sources q_N within the fluid by requiring that a relation be satisfied among $F(\varphi_N)$, q_N and $\nabla\cdot\bar{s}$, the fractional rate of variation of stream-tube area along a stream line. A number of types of irrotational diabatic flow have been studied as illustrations of these characteristics.

[1] B. L. Hicks, Phys. Rev. **69**, 135(A), 250(A) (1946).

H13. On the Initial Motion of a Strong Spherical Shock. Y. H. KUO, *Cornell University.*—A special problem of the production and of the propagation of a spherical shock wave is studied by considering the motion produced by a spherical shell expanding with a prescribed motion given by $x_2=\text{const.}\ t^\beta$ during a short time interval. G. I. Taylor[1] considered the case $\beta=0$ and in the present case $\beta=-\frac{1}{2}$. A shock wave, according to a previous paper,[2] is assumed to be formed instantly and to propagate into still air with a velocity $x_1=\text{const.}\ t^{-\frac{1}{2}}$. The solution is so chosen that it satisfies exactly the boundary conditions at the spherical shell and approximately at the shock wave. In the case of a very strong shock, the error introduced through the latter condition is believed to be negligible. The shock strength decays according to the law $p=\text{const.}\ x^{-2}$, x being the instantaneous radius of the shock.

[1] G. I. Taylor, Proc. Roy. Soc. **186A**, 243 (1946).
[2] Y. H. Kuo, Quart. App. Math. (January 1947).

W1. Some New Results on the Recrystallization of Quartz. D. D'EUSTACHIO, *Collman Manufacturing Corporation.*—The recrystallization of thin single crystals of quartz on moderate heating has been previously reported.[1] An improved x-ray technique for observing the phenomenon will be described. The new method makes possible the observation of much smaller changes and permits quantitative measurement of the extent to which recrystallization has taken place. As a result, marked changes have been observed in plates up to .07 mm thick. The magnitude of the effect in crystals 0.2 mm thick (if it exists at all) is less than one-tenth of that observed with crystals .07 mm thick. The major portion of the change occurs within a few microns of the surface when the wafers are more than 20 microns thick, but throughout the entire volume when they are thinner than 10–15 microns. The argument put forth by D'Eustachio[2] for the formation of "polycrystalline" surface layers on valence crystals can easily be extended to explain thermal recrystallization, but it alone cannot account for the dependence of the effect on thickness.

[1] D. D'Eustachio and S. Greenwald, Phys. Rev. **69**, 532 (1946).
[2] D. D'Eustachio, Phys. Rev. **70**, 522 (1946).

W2. The Band Theory of Graphite. P. R. WALLACE, *Chalk River Laboratory.**—Electronic energy bands are calculated by the "tight binding" approximation[1] for the $2p$ electrons in graphite having their nodes in the graphite planes. For a single hexagonal plane, the electronic energy level splits into two bands separated by a zero energy gap. To the lower band corresponds a hexagonal Brillouin zone containing one electron per atom. When interactions between layers are taken into account, the zone becomes a hexagonal "pill-box," the zero energy gap remains, and inside and outside energy correspond at twelve points on the vertical edges of the pill-box. Thus graphite may be considered a semi-conductor with zero activation energy. The surfaces of constant energy near the zone boundary are very anisotropic, which gives rise to very anisotropic conductivity; at room temperatures, about 100 times as great in the layers as across them. The anisotropy increases for decreasing temperature. Also, a strong diamagnetic susceptibility is predicted, which is anisotropic but somewhat less so than the conductivity. In addition, the zero energy gap ensures a volume optical absorption stretching from the longest wave-lengths down into the ultraviolet.

* Now at McGill University, Montreal.
[1] Mott and Jones, *Properties of Metals and Alloys*, p. 65.

W3. The Effect of X-Rays on the Elastic Constants of Quartz.* VIRGIL E. BOTTOM, *Colorado A & M College.*—The resonance frequencies of certain quartz oscillator plates are decreased by irradiation with x-rays. The magnitude of the frequency change depends upon the orientation of the plate with respect to the crystallographic axes. The effect, which is attributable to changes in the elastic constants, is accompanied by a change in the color of the quartz. Both effects differ widely in different samples of quartz. The magnitude of the changes in certain of the elastic constants have been determined. It is found that irradiation to saturation causes a change of -0.013×10^{10} dynes/cm^2 or -0.07 percent in c_{14}; -0.020 dynes/cm^2 or -0.03 percent in c_{44} and -0.008 dyne/cm^2 or -0.02 percent in c_{66}.

* This paper is based on work done at the Signal Corps Laboratories at Fort Monmouth, New Jersey.

W4. The Structure of Evaporated Antimony Films. H. LEVINSTEIN AND H. R. CRANE, *University of Michigan.*—The structure of evaporated antimony films as a function of rate of evaporation and substrate has been investigated by transmission electron diffraction and by electron microscopy. When antimony is evaporated rapidly on collodion the film consists of very small particles, all crystalline and

oriented preferentially with respect to the substrate. When antimony is evaporated slowly large amorphous patches are formed. While most of these amorphous patches are stable, some crystallize after several days or weeks. These crystallites generally have no preferred orientation. Crystallization of individual patches is often produced by the electron beam in the electron microscope and may be followed visually on the viewing screen. Variation of substrate does not affect crystal structure, but changes the size and appearance of the patches composing the film. These effects may be explained on a basis of varying degrees of mobility of antimony molecules on different substrates.

W5. Temperature Dependence of "Second Sound" Velocity.* HENRY FAIRBANK, WILLIAM FAIRBANK, AND C. T. LANE, *Yale University.*—According to theoretical predictions of Tisza and Landau, two types of wave motion are possible in liquid helium II, i.e., pressure waves (sound) and temperature waves ("second sound"). We have measured this second sound velocity as a function of temperature using the following resonance method. A cylindrical Lucite cavity, containing a resistance heater at the bottom as a source and a magnetic microphone at the top as a detector was partially filled with liquid helium. The second sound induced in the liquid is converted into normal sound in the vapor and hence second sound resonances in the liquid are detectable. Knowing the length of the liquid column at each resonance and the frequency of the source, we are able to determine the velocity of the "second sound" to within ±0.5 percent. The velocity is 0 at the λ-point, a maximum of 20.5 m/sec. at 1.70°K and decreases to a value of 19.8 m/sec. at 1.43°K, the lowest temperature reached. These results are in excellent agreement with those obtained by Peshkov, using a different method, and the agreement with theory is very good. In the low temperature region where Landau and Tisza disagreed, the decrease in velocity tends to confirm Tisza's prediction. The high Q of the resonating liquid column indicates a low transmission coefficient at the liquid surface, and the dissipation in the liquid appears to be small.

* Work done under Navy Contract N6ori-44.

W6. Pressure and Temperature Waves in Liquid Helium.* C. T. LANE, WILLIAM FAIRBANK, AND HENRY FAIRBANK, *Yale University.*—In connection with our second sound measurements in liquid helium II (see previous abstract) a number of subsidiary effects have been observed. In one experiment the resonant cavity was completely filled with liquid helium so that there was no observable vapor space between the microphone diaphragm and the liquid. The temperature was set at 1.75°K and allowed to rise slowly to the λ-point, the frequency of excitation remaining constant. A series of resonant peaks were observed, each peak corresponding to a temperature at which the second sound velocity was such as to render the fixed cavity resonant. These resonances were observed to disappear at the λ-point. A possible mechanism whereby temperature (second sound) waves are converted into pressure fluctuations capable of affecting the microphone diaphragm will be discussed. In addition it was found possible to excite normal sound vibrations in liquid hydrogen, liquid helium I, and possibly liquid helium II by using a fluctuating temperature source. In the case of hydrogen and helium I, this is caused by their comparatively large coefficient of expansion (thermophone effect). In helium II the effect is probably caused by normal sound in the vapor, produced by second sound in the liquid, in turn exciting normal sound in the liquid.

* Work done under Navy Contract N6ori-44.

W7. Ultrasonic Absorption and Velocity Measurements in Liquid Helium. J. R. PELLAM AND C. F. SQUIRE, *Massachusetts Institute of Technology.*—Electronic pulsed-circuit techniques have been applied to the measurement of absorption and velocity of ordinary sound waves in liquid He I and He II at 15 mc/sec. Short pulses (a few microseconds) are generated by a transducer, which also picks up the resultant echoes from a plane reflector. Velocity is determined from the increased time delay introduced in the echo by an increased sonic path length. Absorption is determined by keeping the ultrasonic attenuation within the liquid helium compensated electrically; i.e., the echo signal strength is held constant as the reflector is moved. Velocity measurements obtained agree with values reported[1] by investigators using continuous wave methods. Absorption coefficients measured above the λ-point (2.19°K) are in order-of-magnitude agreement with theoretically computed values based on viscous and thermal losses. A complete disappearance of the echo is observed in the immediate region of the λ-point. Absorption coefficients just below the λ-point have values comparable with those above the λ-point.

[1] J. C. Findlay, A. Pitt, H. Grayson Smith, and J. O. Wilhelm, Phys. Rev. **54**, 506 (1938); **56**, 122 (1939).

W8. On the Theory of "Second Sound" in Helium II. L. TISZA, *Massachusetts Institute of Technology.*—According to the theory based on Bose-Einstein condensation, He II is a mixture of a superfluid and a normal fluid with additive densities $\rho=\rho_s+\rho_n$. A gas type viscosity and an osmotic pressure P_n is associated with the normal fluid. In 1938, the author[1] concluded that inhomogeneities in the temperature will propagate in the form of waves (second sound) with the velocity

$$u_2=[dP_n/d\rho_n(\rho_s/\rho)]^{\frac{1}{2}}.$$

Subsequently Landau[2] advanced a theory based on quantum hydrodynamics leading to similar results and to the expression

$$u_2=[-d(1/s)/dT(\rho_n/\rho_s)]^{-\frac{1}{2}}$$

(s is the specific entropy). Recent measurements of Peshkov are in good agreement with the first expression, whereas Landau's formula shows considerable discrepancies. The author has rederived most of his earlier results from very general assumptions with a quasi-thermodynamic method. The two expressions for u_2 prove to be rigorously equiva-

lent provided that Landau's interpretation of the entropy is modified. With this proviso, the hydrodynamic model will conform to the requirements of the thermodynamic theory which thus admits two different molecular interpretations. A detailed paper is being completed.

[1] L. Tisza, Comptes rendus **207**, 1035 (1938), J. de Physique [8] 1, 164, 350 (1940).
[2] L. Landau, J. Phys. **5**, 71 (1941), E. Lifschitz, *ibid.* **8**, 110 (1944)

W9. The Quantum Corrections for the Second Virial Coefficient of Water. VERNON MYERS, *Yale University.*—The second virial coefficient for water has been calculated recently neglecting quantum effects.[1] The only quantum correction of any importance for moderate temperatures is that caused by the exchange of energy between the translational and rotational motions of the molecules caused by the angular dependence of the forces between the permanent electric moments borne by the water molecules. Using the method of Kirkwood,[2] this effect has been calculated in the 400°K–700°K temperature interval and is found to alter appreciably the previous results. The repulsive potential is assumed to be of the central field type in the present calculations. The discrepancy between the observed values of the second virial coefficient and the calculated values, including the quantum correction, is +6.7 percent for 400°K and −8.7 percent for 700°K. Better agreement with experiment could probably be obtained if an angularly dependent repulsive force were introduced in addition to the central force.

[1] H. Margenau and V. Myers, Phys. Rev. **66**, 307 (1944)
[2] J. G. Kirkwood, J. Chem. Phys. **1**, 597 (1933).

X1. The Distribution in Energy of Fission Fragments Near the Fast Fission Threshold.* DAVID H. FRISCH, *Los Alamos Laboratory, Los Alamos, New Mexico.*[1]—The distribution in kinetic energy of fission fragments from the compound nucleus $_{93}Np^{238}$ has been studied as a function of the energy of the neutrons causing fission. Mean neutron energies of 375, 475, 700, and 890 kev were used, covering a range of fission cross sections from approximately $.1\times10^{-24}$ to 1.2×10^{-24} cm², respectively 15 and $\frac{3}{4}$ of the high energy cross section. The energy distribution of uncollimated fragments from a thin foil was studied by differential recording of pulse heights in an electron-collecting ionization chamber. Only the high energy peak was recorded, and the resolution was limited by both the finite channel width of the discriminator and the spread in response of the ionization chamber. The latter was estimated by comparison of the observed minimum in the $_{92}U^{236}$ fragment distribution with that reported elsewhere.[2] Within the limits of resolution of the present experiment, there is no dependence of the distribution from $_{93}Np^{238}$ on neutron energy near the fission threshold. This work was carried out under contract between the University of California and the Manhattan District, Corps of Engineers, War Department.

* To be called for after paper X11 if time permits.
[1] Now at Massachusetts Institute of Technology.
[2] R. Sherr, Phys. Rev. **70**, 450 (1946), M. Deutsch, unpublished Los Alamos Report 510.

X2. Statistics of Single and Plural Scattering. S. A. GOUDSMIT AND H. S. SNYDER, *Northwestern University.*—It is generally assumed in scattering experiments that large deflections are caused by single scattering, small deflections to multiple, and the intermediate region to "plural" scattering. This implies that the statistical behavior of multiple scattering approaches the single scattering law for large deflections. A more precise analysis has shown that this is not necessarily so and that the scattering intensity for large deflections depends in a sensitive way upon the behavior of the single scattering law. Only if the second derivative of the logarithm of the single scattering law is positive, can the multiple scattering approach single scattering for large deflections. For example, if the single scattering law is Gaussian, this condition is not fulfilled. For this case large angle scattering is entirely caused by highly multiple small angle deflections. It is possible to write n-fold scattering as a series in which the successive terms represent contributions of single, double, triple, etc., scattering. For Rutherford scattering at large angles the multiple scattering approaches single scattering. The deviations from single scattering are caused by many small angle scatterings and not to double or triple scattering. It seems therefore impossible to define a region of "plural" scattering in this case.

X3. Theory of Multiple Scattering. H. S. SNYDER, *Northwestern University.*—A solution of the Fokker-Planck equation for the scattering of particles by a foil is found. If $W(\mathbf{v}, x)|v_x|d\mathbf{v}$ is the probable number of times a single incident particle will cross the plane $x=$constant having its velocity components lying in $d\mathbf{v}$, then $W(\mathbf{v}, x)$ can be written $W(\mathbf{v}, x)=W_0(\mathbf{v}, x)+W_1(\mathbf{v}, x)+\cdots$ in which $W_n(\mathbf{v}, x)$ determines the distribution for particles which have scattered n times. We find

$$W_n(\mathbf{v}, x)=\frac{1}{v_x}\int_0^x dx' \exp[-k(\mathbf{v})(x'-x)/v_x] \int d\mathbf{v}' f(\mathbf{v}, \mathbf{v}') W_{n-1}(\mathbf{v}', x')$$

for $v_x>0$, $0>x>a$. $f(\mathbf{v}, \mathbf{v}')d\mathbf{v}d\mathbf{v}'$ is rate of scattering from $d\mathbf{v}'$ to $d\mathbf{v}$, a is the thickness of the foil and $k(v)=\int f(\mathbf{v}', \mathbf{v})d\mathbf{v}'$. In an appropriate approximation this solution reduces to the one given by Goudsmit and Saunderson.[1] This solution should be particularly useful for determining the deviations from the single scattering law due to multiple scattering for neutrons scattered by any substance due to the fact that for neutrons the total scattering plus absorption cross-sections is sufficiently small so that for reasonable thickness of foil only the first few terms in the expansion of $W(\mathbf{v}, x)$ are important.

[1] Phys. Rev. **57**, 24 (1940); **58**, 36 (1940).

X4. Ionization Chamber Techniques in Measurement of C^{14}. W. P. JESSE, L. A. HANNUM, H. FORSTAT, AND A. L. HART, *Argonne National Laboratory.*—With the purpose of determining the reliability of the method and its limit of sensitivity, ionization chamber measurements have been carried out with the vibrating reed electrometer of Palevsky, Swank, and Grenchik and also a type of Lindemann electrometer as the measuring instrument. In each case, the rate of drift method was used. A few measurements on

thin solid samples showed self-consistent results. A greater number of measurements were carried out with gaseous CO_2 in a chamber of 150 cc volume at about one atmosphere pressure. An already dilute gas sample of approximate activity of 4×10^{-7} curie/g of carbon was successively diluted with inactive CO_2 by the use of calibrated volumes. For a further dilution of 420 times, the ionization current on vibrating reed agreed with the value calculated from the dilution to within 5 percent for runs of about an hour. At dilution of 5720 times an agreement within 20 percent was obtained. The arrangement with the Lindemann electrometer gives less accuracy but shows great promise as a very simple method for most measurements.

X5. Delays in Firing Time of Geiger-Müller Counters. CHALMERS W. SHERWIN, *University of Illinois.*—The average transit time of secondary electrons is measured by sending β-rays through a thin wall counter, through a slotted mask, and then into a mica window counter where their paths are parallel to the central wire, at known distances from the wire. The radial secondary electron velocity (cm/sec.) is represented empirically by $v=k(E/p)^{\frac{1}{2}}$, where E, the electric field, is in volts/cm; p, the pressure of the 92 percent argon, 8 percent amyl acetate mixture, is in millimeters of Hg; and k equals 4.5×10^{6}. The maximum transit time for a counter with 2.2 cm diameter cylinder and 0.012 cm diameter wire ($p=100$ mm) is 9.5×10^{-8} second. Furthermore, the average relative firing time of two counters is not zero even when the β-rays go near the wires of both counters so the secondary electron transit time is negligible. The average relative firing time varied in one case from one to 20×10^{-8} second as the over-voltage of one counter varied from 240 volts to zero volts. The counter fires sooner at high over-voltages.

X6. Spectroscopic Study of the Role of Hydrogen Peroxide in the Thermal Combination of Hydrogen and Oxygen. R. B. HOLT AND O. OLDENBERG, *Research Laboratory of Physics, Harvard University.*—The steady thermal combination of hydrogen and oxygen flowing through a hot vessel results in the presence of appreciable amounts of H_2O_2 in the exit gases.* It is questionable whether this is formed *in the reaction itself* since H_2O_2 should be too unstable at the high temperature. The alternative explanation assuming that it is formed *in the trap* from radicals swept out of the hot reaction vessel is hardly preferable since the most plausible radical, hydroxyl, does not build up a noticeable concentration in the reacting mixture. The question was decided by observing the absorption spectrum of the mixture itself during the progress of the reaction. This reveals the presence of H_2O_2 in fairly large concentration in the mixture in spite of the rapid decomposition it is sure to undergo under the conditions of the experiment. This result shows that H_2O_2 is the outstanding product of the chain reaction between hydrogen and oxygen. It is possible to follow the H_2O_2 concentration spectroscopically under varying conditions (temperature, ratio of reactants, etc.) and to correlate the observed concentrations with the amounts of H_2O_2 found by chemical analysis of the exit gases.

* R. N. Pease, J. Am. Chem. Soc. **52**, 5106 (1930).

X7. Absolute Intensities of Molecular Vibrational Absorption Bands. E. BRIGHT WILSON, JR. AND A. M. THORNDIKE.—The absolute intensities, $A=\int\alpha(\nu)d\nu$, of the infrared active fundamental vibrations of CH_4, C_2H_4, and N_2O have been measured using the method[1] of extrapolation to zero partial pressure of the absorbing gas in the presence of considerable inert gas pressure. (For N_2O and C_2H_4 one atmosphere of N_2; for CH_4 about five atmospheres of NH_3, which is several times as effective as non-polar gases.) The observed intensities are (all in cycles per cm-atmosphere): CH_4: 1304 cm^{-1} band—450×10^{10}, 3020 cm^{-1} band—900×10^{10}. C_2H_4: 950 and 995 cm^{-1} bands unresolved—1540×10^{10}, 1444 cm^{-1} band—210×10^{10}, 2990 and 3105 cm^{-1} bands unresolved—840×10^{10}. N_2O: 590 cm^{-1} band—120×10^{10}, 1285 cm^{-1} band—1150×10^{10}, 2224 cm^{-1} band—5600×10^{10}. The values for CH_4 agree within experimental error with 444×10^{10} and 967×10^{10} found by Rollefson and Havens[2] from measurements of infra-red dispersion. The values for C_2H_4 and N_2O are consistant with earlier results obtained by Wells.[3] These intensities correspond to "effective charges" on the vibrating atoms of from 0.05 to 2.0 times the charge on an electron.

[1] E. Bright Wilson, Jr. and A. J. Wells, J. Chem. Phys. **14**, 578 (1946)
[2] R. Rollefson and R. Havens, Phys. Rev. **57**, 710 (1940).
[3] A. J. Wells, Thesis, Harvard, 1941.

X8. Rotational Spectra of Some Linear Molecules Near 1 cm Wave-Length and Nuclear Quadrupole Moments of Br and Cl. C. H. TOWNES, A. N. HOLDEN, AND F. R. MERRITT, *Bell Telephone Laboratories, Murray Hill, New Jersey.*—Absorption lines due to the rotational transitions $J=1\rightarrow J=2$ for ClCN and $J=2\rightarrow J=3$ for the BrCN molecule have been observed at wave-lengths near 1.25 cm. A number of lines are found associated with each isotope of Cl and Br. Neither nuclear dipole moments nor molecular vibrational excitation appear responsible for the multiple lines. General features of these multiplets are explained by assuming the splitting is caused by electric quadrupole moments of the Cl and Br nuclei, and that the effect of any quadrupole moment of the N^{14} nucleus is small. On this basis, the two isotopes of Cl have nearly equal quadrupole moments, the moments for the two Br isotopes being also approximately equal but considerably larger than those for Cl. In addition the data allow a determination of moments of inertia for these molecules and internuclear distances. A comparison of the moments of inertia with electron diffraction data[1] shows that both molecules are cyanides rather than isocyanides. The distances are C—N=1.15A, Br—C=1.79A, Cl—C=1.64A, which are consistent with previous measurements.[1]

[1] J. Y. Beach and A. Turkevich, J. Am. Chem. Soc. **61**, 299 (1939).

X9. A Precision Ultrasonic Interferometer.* I. F. ZARTMAN, *Johns Hopkins University, and Muhlenberg College.*—A precision type ultrasonic interferometer has been developed. This interferometer is of the resonator type, the theory of which was developed by Hubbard.[1] This instrument incorporates high sensitivity, extreme stability, and is capable of yielding velocity, absorption, and reflection data of precision in gases and vapors from ordinary pressures to those less than one centimeter of mercury. The

temperature range of operation covers that from the lowest obtainable up to that permitted by the piezoelectric properties of the crystal plate. With the ability to use piezoelectric crystals of greatly differing frequencies measurements may be made over an extremely wide range of frequency to pressure ratios. Preliminary results using a 500-kilocycle quartz plate in CO_2 and H_2 at a temperature of 38°C yield data as a function of pressure to values less than one centimeter of mercury, i.e., f/p ratios of 30 megacycles per atmosphere. Evidence for molecular dispersion and absorption in these gases are presented.

* This work is supported by Contract NOrd 8036, U. S. Navy and a Research Corporation grant.

[1] J. C. Hubbard, Phys. Rev. **38**, 1011 (1931); Phys. Rev. **41**, 523 (1932).

X10. On the Existence of Single Magnetic Poles. ELLIOT T. BENEDIKT AND HERTA R. LENG, *Rensselaer Polytechnic Institute, Troy, New York.*—The present paper describes experiments devised to verify the existence of single magnetic poles as claimed by F. Ehrenhaft.[1] The method used was based on the observation of the motion of ferromagnetic particles under the action of a magnetic field generated by an electric current. If single magnetic poles were present, the magnetic field would cause motion in the direction of the closed lines of magnetic force. Observations were performed on a colloidal solution of Fe_3O_4[2] and with colloidal solutions of iron and nickel (approximate size of particles of order of 20 mμ). The solution was placed in an ebonite container in the center of which a straight conductor carrying a current of 3000 amperes was placed. The particles were illuminated by means of a carbon-arc lamp, and the scattered light was observed through a microscope. In the region of observation, the field was about 350 gauss. No motion such as would be expected from single magnetic poles was observed. Analysis of results shows no evidence of existence of single magnetic poles exceeding 1.5×10^{-12} e.m.u.

[1] F. Ehrenhaft, Phys. Rev. **60**, 169 (1941); **61**, 733 (1942); **63**, 216 and 461 (1943); **64**, 43 (1943).
[2] W. C. Elmore, Phys. Rev. **54**, 309 and 1092 (1938).

X11. The General Movement of Matter Possessing Six Degrees of Freedom in Fields is Helical. FELIX EHRENHAFT, *New York City.**—It has been experimentally proven and published in *ca.* 30 abstracts that single magnetic poles, north or south, do exist as predicted by Hertz (div $B\gtrless0$). This fact has been confirmed, no other explanation being valid.** The unipolar magnetic charge can in no way be explained away electrically, neither by Ampere's circuital currents nor by the spin of electrons, and thereby magnetic charges become equally important as electric charges. This broadened concept has to enter the whole of physics. Photomicrographs demonstrate that matter possessing six degrees of freedom moves in or against the direction of homogeneous constant magnetic and electric fields following helical paths with regularly spaced turns and reversing in direction with the reversal of the field. Movements of similar nature are observable in homogeneous constant beams of light (longitudinal and also transversal photophoresis). These facts have also been confirmed.*** In view of the similarity of helical paths in magnetic fields and light, it is clear that there must be a much closer connection between the two than heretofore believed. The author asserts that all these facts are irreconcilable with present theories.*** Some unpublished experimental details will appear in European scientific journals.

* The author can be reached during February and March 1947 c/o Professor John Plesch, 40 Hereford House, Park Lane, London W 1; beginning in April he will stay in Vienna.
** P. Tauzin; P. Tauzin, and L. Rault, Soc. Fran. de Physique, Nov. 16 (1945); May 17 (1946); Comptes rendus **222**, 1037 (1946).
*** F. Ehrenhaft, Comptes rendus **222**, 1100, 1345 (1946).

Y1. Fluctuations of Ionization Yield. U. FANO, *National Bureau of Standards.*—An ionizing radiation produces in a gas a number of ions closely proportional to the amount of energy absorbed, almost independent of the quality of the radiation, but subject to statistical fluctuations even when all pertinent factors are kept constant. The expected variance of the number of ionizations produced by a charged particle of energy E is FE/ϵ, where ϵ is the average energy absorbed per ionization and F is to be estimated. (If the number of ions were governed by a Poisson distribution, then $F=1$.) In general, $F=(\Sigma_p s_p(n_p-E_p/\epsilon)^2)/(\Sigma_p s_p n_p)$, where s_p is the cross section for an impact from which n_p ionizations arise and in which the energy E_p is spent. Following the method introduced in § 4 of a previous paper[1]

$$F=\Big(\sum_{E_j<I} s_j(E_j/\epsilon)^2+\sum_{I\le E_j<2I} s_j(1-E_j/\epsilon)^2+\sum_{E_j\ge 2I} s_j(1-I/\epsilon)^2\Big)/E_j\geq I\Sigma_j s_j,$$

where s_j is the cross section for an impact in which a molecule (together with all its electrons) absorbs the energy E_j, and I is the first ionization potential. F should be averaged over the energy of the impinging particle. Its order of magnitude is $\frac{1}{2}$ to $\frac{1}{3}$.

[1] U. Fano, Phys. Rev. **70**, 44 (1946).

Y2. Microwave Studies of Dielectric Properties of Arcs. DONALD E. KERR, SANBORN C. BROWN, WALTER P. KERN, *Massachusetts Institute of Technology.*—If the conductivity and dielectric constant of the center conductor of a coaxial transmission line are varied while the conductivity of the outer wall remains very high, the resulting transmission properties of the line vary widely. With high conductivity in the center conductor the line acts in the customary manner, transmitting all frequencies; but with zero conductivity the line becomes a circular wave guide with dielectric center rod, and has a cut-off frequency. If an arc is used as the center conductor, the current may be used to control the effective conductivity and dielectric constant, which may be determined through measurement of the propagation constant by standing wave techniques. These results may be used to study fundamental arc properties such as electron density and mean time between collisions. At a particular current density a rapid transition occurs between propagation of an exponentially attenuated wave and a guided transverse magnetic wave, the propagation constant of which is a continuous function of arc current. These properties suggest a means for obtaining a radio-frequency switch, a modulator, or an attenuator with variable slope.

Y3. High Frequency Probe Measurements of Electron Attachment and Ambipolar Diffusion. MANFRED A. BIONDI, SANBORN C. BROWN, *Massachusetts Institute of Technology*.—An electrodeless method of measuring electron attachment and diffusion in gases has been developed. An r-f field is used to break down a gas in a glass bottle inside a cavity resonant at 3000 Mc. This field is applied for 1000 microseconds, then turned off for 4000 microseconds. The electrons produced in the discharge then diffuse or attach depending on the gas used. If a small CW field is applied to the cavity, the free electrons will oscillate without having their energy distribution disturbed. The electron oscillation causes a shift of the resonant frequency of the cavity proportional to the number of free electrons. Thus the CW field may be used as a probe to detect the free electrons. The probe signal is set to a higher frequency than the resonance of the cavity in the absence of free electrons. The signal will undergo maximum transmission through the cavity when the effect of the free electrons plus the cavity constants give a resultant resonant frequency equal to that of the probe signal. By measuring the time at which maximum transmission occurs for various probe signal frequencies, the clean-up of electrons in the gas is determined. Data on the measured diffusion and attachment constants at thermal energies of various gases will be given.

Y4. Harmonic Components in s.c. Discharges.[1] LAWTON M. HARTMAN AND HENRY MARGENAU, *Yale University*.—In dealing with alternating current discharges in gases it is usually assumed that the electron distribution function consists of a time-constant part and a time-dependent part varying with the frequency of the impressed field. Actually, all frequencies should appear in the discharge, and the simple treatment is but an approximation. To determine its validity, the distribution function is here expanded as a Fourier series in the time and as a series of Legendre functions in the electron velocities. Differential equations relating all members of the expansion may be obtained with the use of the Boltzmann transfer equation, and approximate solutions for the second Fourier components, valid under different conditions of frequency, gas pressure and field strength, have been derived. These lead to a better appreciation of the limits of the "first-order treatment," which is on the whole correct. The results also show how for small frequencies of the external field, the distribution function alternates between the Maxwell form and the Druyvesteyn form, twice per cycle.

[1] Assisted by the Office of Naval Research under Contract N6ori-44.

Y5. Retrograde Motion of an Arc Cathode Spot in a Magnetic Field. C. J. GALLAGHER AND J. D. COBINE, *General Electric Company*.—A mercury arc cathode spot under the influence of a magnetic field perpendicular to the arc axis may be made to move contrary to the direction predicted by electromagnetic theory.[1] We have found this retrograde effect to exist not only in the mercury arc, but also in arcs between solid electrodes with different gases, including helium, argon, nitrogen, hydrogen, oxygen, and carbon dioxide. Electrode materials studied include carbon, tungsten, molybdenum, nickel, copper, aluminum, and cadmium. For retrograde motion, the arc column and anode spot tend to move in the conventional direction, but are "dragged" in the reverse direction by the cathode spot. Conditions for reversal for a particular gas-electrode combination are determined by pressure, magnetic field (B) and current. At constant current, the critical reversal pressure is proportional to B. Increasing current at constant B decreases the value of critical pressure. In general, gases with higher critical potentials have higher reversing pressures. Currents ranged from 2 to 10 amperes, magnetic fields from 10 to 450 gauss and reversal pressures from 60 to 0.8 cm Hg. In general, it was necessary to oxidize the electrodes to maintain a stable arc.

[1] C. G. Smith, Phys. Rev. 62, 48–54 (1942); 69, 96–100 (1946).

Y6. Gyroscopic Effects in a Vibratory System.* G. S. BENNETT, *Naval Ordnance Laboratory*.—An analytical investigation is made of the influence on a vibrating elastic system of a high speed rotating element. A fundamental condition for the presence of any gyroscopic effect is that the vibration be such as to produce a tilt of the spin vector of the rotor. Equations are derived showing (a) that if precession be prevented, no gyroscopic effects are present; and (b) that if precession be permitted, the gyroscopic action contributes a force opposed to the tilt, and proportional to the angle of tilt, in effect increasing the stiffness of the elastic system. Calculations based on an arbitrarily chosen rotor intended to approximate a typical small motor armature indicate that this additive spring force is small, and that the increase in natural frequency due to the added stiffness is exceedingly small—of the order of 0.1 percent—in the case where the precessional motion is not restrained.

* This work was done at Naval Research Laboratory, Washington, D. C.

Y7. An Experimental Investigation of Forced Vibrations in a Mechanical System Having a Non-Linear Restoring Force. CARL A. LUDEKE, *University of Cincinnati*.—This paper introduces a mechanical apparatus capable of generating and recording forced vibrations in a system having a non-linear restoring force. The experimental wave forms are then compared with the theoretical results given by three graphical methods. These are the methods of Martienssen, Hartog, and Rauscher. Provided a suitable first guess for the amplitude can be made, one application of Rauscher's method gives better results than the other methods. A graph is made of the experimental amplitude as a function of the disturbing frequency. These results are compared with the theoretical results of the above three methods. Again one application of Rauscher's method gives satisfactory results. In all experimental results it is noted that even though the restoring force is distinctly non-linear, the wave forms of the resulting motion are nearly sinusoidal as long as the frequency of the observed motion is the same as the frequency of the disturbing force. However, steady oscillations can be maintained for which the observed frequency is a sub-multiple of the disturbing frequency. Two such subharmonics were recorded and the experimental wave forms are shown.

Y8. A Linear Amplifier for General Laboratory Use. W. H. JORDAN AND P. R. BELL, *Clinton Laboratories.*—Twelve linear amplifiers have been built for general laboratory use. Feedback circuits have been used to stabilize the gain and improve the linearity. The high frequency cut-off of the amplifier can be varied by means of a three-position switch that changes the amount of capacitance and resistance in the feedback network. The low frequency cut-off is determined by a simple resistance-capacitance differentiator that is switched to match the high frequency response. The response of the amplifier to a voltage step applied to the input is a single pulse of fairly symmetric shape. The pulse rise time (10 percent to 90 percent) is 0.15 μsec. for the wide-band position, 0.7 μsec. for the medium-band position, and 4 μsec. in the narrow-band position. The amplifier will deliver pulses up to 100 volts for direct oscilloscope deflection, or 5 volts for driving a low impedance line. A pulse height selector is included on the amplifier chassis. It has been designed to measure accurately pulse heights up to 100 volts, independent of pulse duration or duty cycle. It delivers a pulse 3 volts high and 0.5 μsec. in length for scaler operation.

Y9. A Static Method of Simulating Accelerations Above One g. JOHN J. GILVARRY AND S. F. EYESTONE, *North American Aviation.*—In the developmental testing of accelerometers, accelerations above one g are usually simulated by a rotating table. A static method of simulating such accelerations is described. The accelerometer's moving element is assumed representable by an equivalent mass m such that accelerations are measured by determining the force on this mass. If a parameter i in the force-measuring unit is used as an acceleration index, a curve of i against acceleration can be constructed up to one g by tilting the accelerometer at various angles to the vertical. This curve is not necessarily linear but is assumed known. To simulate accelerations above one g, the accelerometer is turned so the earth's gravitation is not effective, and a force is applied to the moving member by a horizontal string passing over a pulley to a mass M_0. The mass M_0 is chosen so the corresponding parameter reading i_0 is in the range of the calibration curve below one g. If i_0 on this curve corresponds to g_0, the equivalent accelerometer mass is $m=M_0g/g_0$. If now the mass M_0 is replaced by an arbitrary mass M, the simulated acceleration is Mg_0/M_0. By suddenly cutting the thread, the step-function response can be obtained.

Y10. Fringing Flux Corrections for Magnetic Focusing Devices. NORMAN D. COGGESHALL, *Gulf Research & Development Company.*—In such an instrument as a sector type mass spectrometer the ions pass from a magnetic field free region into, through, and out of a region of uniform magnetic field. In calculating ion trajectories for such a system the physical boundaries of the magnet pole faces cannot be used for the boundaries of the uniform field region because of the fringing flux which is effective for some distance away from the pole faces. Therefore, the pole faces must be considered to have virtual boundaries which are displaced outwards from the actual boundaries. An analytical method of determining this displacement has been developed. The principal ray leaving the ion source travels on the median plane between the two pole faces. Since the fringing magnetic field on this plane may to a good approximation be represented as a function of one variable, the distance normal to the pole faces, the path of the principal ray may be calculated using the methods developed for ions moving in non-uniform magnetic fields.[1] The displacement d, of the virtual field boundary from the pole face boundary is found to be $d=r-\Delta$ where Δ satisfies the equation: $\int_{x_0}^{x} h(x)dx=r$, r is the radius of curvature of the ion paths in the uniform field region; the origin for the x coordinate is coincident with the edge of the pole faces; the unit length in the coordinate system is one gap width; x_0 is the value of the x coordinate at the ion source; and $h(x)$ is the function which expresses the magnetic field on the median plane in fractional value of the uniform field value. Using the Schwarz-Christoffel transformation to obtain $h(x)$ a number of specific cases have been evaluated and will be discussed.

[1] N. D. Coggeshall and M. Muskat, Phys. Rev. **66**, 187 (1944).

Y11. Alternating Current Probe for the Measurement of Magnetic Fields. E. C. GREGG, *Case School of Applied Science.*—A method of measuring magnetic field strengths is described which utilizes the change in alternating current permeability of a small Permalloy core transformer with superposed steady state magnetic fields.* One such transformer probe used for the measurement of the field of a scale model betatron consisted simply of a 150-turn primary and a 100-turn secondary wound on a 0.1 inch length of 0.01 inch diameter Permalloy wire. The completed probe had the dimensions of a cylinder 0.1 inch long and 0.08 inch in diameter. The primary winding was driven both with alternating and direct current while the secondary was connected to an amplifier and null indicator. The reference voltage for the null indicator was derived from the driving signal in order to minimize errors arising from drifts in this signal. The use of the null scheme and superposed primary direct current allowed the selection of any given magnetic field as a reference point and eliminated the necessity of calibrating the probe. The unknown magnetic field could then be determined in terms of the direct current through the probe required to return the probe to its initial condition. While the accuracy of this probe was about 0.2 percent, it is possible to improve this figure by increasing the gain and stability of the associated electronic equipment.

* G. W. Elmen, Bell Sys. Tech. J., January 1936.

Y12. Arterial Pulse Wave Velocities. ALLEN L. KING, *Dartmouth College, Hanover, New Hampshire.*—An expression for the instantaneous pulse pressure in terms of the radius of an elastomeric tube is inserted in the general differential equation for a pulse wave, and from the result a relation for pulse wave velocities is obtained. Numerical values of velocities for human aortas are computed by using data from an earlier paper* and the increase of velocity with mean blood pressure and age is shown. Results for other large arteries are given and a comparison of them

with directly measured values found in the literature is made. The Moens-Korteweg formula is shown to be inappropriate for tubes such as blood vessels.

* A. L. King, J. App. Phys. 17, 501 (1946).

Z1. A High Performance Photo-Galvanometer Feedback Amplifier. DEMETRIUS G. JELATIS, *Central Research Laboratories** and *Massachusetts Institute of Technology.*—The instrument described utilizes inverse feedback applied to a galvanometer to obtain a high current amplification combined with improved response and impedance characteristics. Using a commercial galvanometer (0.0005 microamperes per mm at 1 m) as the basic element, full scale output of 5 milliamperes is produced by 0.001 microampere input with thermal noise level less than one percent of full scale. Effective input resistance is reduced from 550 ohms to 0.1 ohm, and the critically damped response time from 6 seconds to under 0.1 second. Linearity is better than 0.1 percent over the entire range. The feedback current is derived from a d.c. amplifier actuated by a pair of balanced vacuum phototubes and normally contains two components: one proportional to the angular deflection, and the second to the angular velocity of the moving coil. Full output of 5 milliamperes is obtainable with a coil deflection of 0.1 microradian (0.0002 mm at 1 m). The shunt feedback circuit with the properties given above is useful in work with low level crystal rectifiers and boundary layer photocells where low input resistance is essential. For use with low impedance "voltage" sources, a series feedback arrangement can provide a full scale sensitivity of 0.1 microvolt with 0.1 megohm effective input resistance.

* Present location.

Z2. Wave Guides for Slow Waves. L. BRILLOUIN, *Harvard University.*—Many applications of T.M. waves in wave guides have been recently suggested for linear accelerators or decelerators of electrons. In order to obtain a good efficiency, it is necessary to match the wave velocity with electron velocity. Such a condition means that the phase velocity of the wave must be lower than c (light velocity) while ordinary wave guides yield a phase velocity larger than c. The present paper is devoted to a discussion of pipes fitted with equidistant diaphragms. These structures behave as band-pass filters and exhibit a very strong variation of the phase velocity with respect to frequency. Some special cases are completely discussed and serve as examples of a general method that can be applied to this class of problems.

Z3. Specular Reflection from Mercury Vapor. J. M. HANSEN AND H. W. WEBB, *Columbia University.*—The transition from diffuse scattering of the 2537A resonance line of mercury occurring at low vapor pressure to the specular reflection occurring at high pressure has been investigated by two methods: (1) Measurement upon a plane quartz—mercury vapor surface, using collimators to separate the specularly reflected from the diffusely scattered radiation, to determine their variation with pressure. (2) A study of the time elapsing between the incidence of the radiation on the vapor and its re-emission, using a modification of the method previously employed in this laboratory for measuring persistence of radiation.[1] These measurements show that diffuse scattering is inappreciable (less than 0.5 percent) at pressures above 247 mm (condensed mercury temperature 300°C), specular reflection is inappreciable below 0.27 mm (100°C), and both occur over the range 100°C–300°C. From the variation of the reflectivity with the angle of incidence, the optical constants of the vapor for the 2537A line were calculated. Persistence of radiation remains unchanged as diffuse scattering declines over the pressure range 0.066 mm to 2.8 mm (75°C to 150°C). Persistence of specular reflection is less than 1/40 of the lifetime of the excited state involved.

[1] H. W. Webb and H. A. Messenger, Phys. Rev. 66, 77 (1944).

Z4. The Decay Scheme of Cs^{134}. KAI SIEGBAHN AND MARTIN DEUTSCH, *Massachusetts Institute of Technology.*—The long-lived isomer of Cs^{134} has been studied by magnetic spectrometer and coincidence techniques, with a view to its use as a radioactive standard. The great majority of the disintegrations—about 95 percent—proceed by the emission of beta-particles of (0.645 ± 0.02) Mev maximum energy to an excited state of Ba^{134} with (1.36 ± 0.03) Mev excitation energy, followed by the successive emission of two gamma-rays of (0.584 ± 0.012) Mev and (0.776 ± 0.015) Mev, respectively. In a few percent of the disintegrations a gamma-ray of (1.35 ± 0.03) Mev is emitted. This is probably due to single-quantum de-excitation of the same excited state.

Z5. Pairs of Fission Fragments. PIERRE DEMERS,* *Chalk River Laboratory.*—Using new photographic emulsions[1] and a three-layer technique,[2] the tracks starting in a central U layer are recorded in two adjacent layers, with a short gap marking the origin. (1) The two tracks are most often (98 percent of cases) unequal. Mean values of the difference D between long (L) and short (S) tracks, of L, of S and of $T=L+S$, are as follows: D: 3.2 μ, 5.3 mm of air; L: 14.3 μ, 24.0 mm; S: 11.2 μ, 18.7 mm; T: 25.5 μ, 42.7 mm. Ionization along L near the origin is usually greater than along S. (2) A few long α tracks accompanying fission have been seen; spatial coincidence of the origin of the three tracks shows coincidence of emission in time within 2.10^{-14} second. (3) Three main kinds of recoils are recognized: Ag, Br; C, N, O; H. From rare H recoils a few μ long, a range velocity curve can be obtained for L and for S. Velocity can also be inferred as in Ref. 3 from the distribution of numerous very short protons (<0.5 μ, <75 kv) which are occasionally visible.

* Now at University of Montreal.
[1] Demers, Phys. Rev. 70, 86(L) (1946). Can. J. Research (to be published).
[2] Demers, Phys. Rev. 70, 974 (1946).
[3] Boggild, Brostrom, Lauritsen, D. K. Danske, V. S. Mfm. 18, 4 (1940).

Z6. Low Temperature Resistivity of Germanium Semi-Conductors. V. A. JOHNSON AND K. LARK-HOROVITZ, *Purdue University.*—Degeneracy criteria for the free electron gas in semi-conductors have been applied to various germanium samples, indicating that usually both at high and low temperatures the electron gas is not degenerate. In a

few cases, however, degeneracy occurs at about 150°K. Interpretation of resistance measurement at low temperatures[1] shows that a high purity germanium sample and an N-type sample (n electrons/cc at room temperature $\sim 4.\ 10^{17}$) behave as expected from the theory of semi-conductors; the resistance increases at low temperatures. However, the P-type sample ($n \sim 5.\ 10^{18}$) shows a behavior which cannot be accounted for by combining resistivities due to lattice scattering and impurity scattering. To account on this basis for the observed resistivity, one would have to assume Hall constant increasing with decreasing T, or if n remains constant throughout this range, a temperature independent resistance contribution similar to the so-called Mathiessen resistance in alloys seems to exist at these temperatures in semi-conductors. In the N-type sample, it is possible by extrapolating the Hall curve to low T to obtain a reproduction of the resistance curve, combining impurity and lattice scattering, using classical statistics. This is in agreement with the fact that this sample has a degeneracy temperature of about 10°K.

[1] See preceding abstract.

Z7. Resistivity of Germanium at Low Temperatures and the Effect of Additions. I. ESTERMANN, A. FONER, AND J. A. RANDALL, *Carnegie Institute of Technology.**—The resistivity ρ of several germanium samples** was measured between room temperature and 13°K. The purest sample shows a very steep increase of resistivity with cooling at temperatures below 30°K, giving a linear relation between

TABLE I.

Sample	Type	Resistivity in ohm-cm at 273°K	180°K	90°K	60°K	20°K	14°K	13°K
"pure"	—	17.5	19.2	11.2	9.2	73	1840	
P added	N	0.0242	0.0234	0.0301	0.0384	0.0551	0.0560	0.0560
0.006 at % Al	P	0.0324	—	—	0.0330	0.0641	0.0723	0.0712
0.04 at % Al (first run)	P	0.00510	0.00472	0.00520	0.00585	—	—	—
0.04 at % Al (fourth run)	P	0.00937	—	0.0086	0.0086	0.0088	0.0087	0.0087

$\log\rho$ and $1/T$. The samples with low impurity concentration (both N and P type), e.g., 0.006 atmos. percent Al, show a slight decrease in resistivity on cooling from room temperature to about 150°K, followed by an increase to about 2½ times the minimum value at 13°K. The sample with higher impurity concentration (0.04 atmos. percent Al) shows practically no change in resistivity over the whole temperature range. In this sample, however, the resistivity at all temperatures increased substantially after the first four cooling and warming up operations; the same effect, but to a much lesser degree, was observed in other samples. Typical results are given in Table I.

* This work has been carried out under Contract N6ori-47 with the Office of Naval Research.

** The samples were prepared at the Physics Department of Purdue University. Measurements of their properties at temperatures above 90°K were carried out at Purdue and are being correlated with our low temperature measurements.

Z8. Neutron Spectra of Li, Al, and Be Bombarded with 10-Mev Deuterons. J. S. LAUGHLIN AND P. G. KRUGER, *University of Illinois.*—A high pressure cloud chamber filled with methane gas has been used to detect neutrons above 2 Mev emitted from Li, Al, and Be thin targets bombarded with 10-Mev deuterons. In the first experimental arrangement the neutrons entered the cloud chamber after passing through a collimating hole in the water tanks. The lengths and scattering angles of the recoil protons were measured to obtain the neutron energies. In order to observe any influence of the collimator the beryllium spectrum measurement was repeated without collimation and with a minimum of scattering material near the target and chamber. 300 recoil protons were observed from Li, 400 from Al, and 1600 from Be. A single (d, n) reaction occurs with Be and Al targets and these neutron spectra have been used to plot the average level density *vs.* excitation energy for B^{10} and Si^{28}. The level densities increase in a regular manner with the excitation energy. The collimator appears to have no appreciable influence on the high energy neutron distribution. There is some evidence that a few low levels of B^{10} have been located. The number of neutrons detectable above 15 Mev from a lithium target is not greater than 2 percent of those below 7 Mev.

Z9. The Infra-Red Absorption Spectrum of H_2S. ROBERT H. NOBLE AND HARALD H. NIELSEN, *Ohio State University.*—The infra-red absorption bands of H_2S have been remeasured using an evacuated spectrometer with higher resolution than had been employed in previously published work. Data have been tabulated for the bands near 1290, 2440, 3790, and 5140 cm^{-1}. A careful survey of the included region resulted in the discovery of no bands or sub-bands not previously reported. Particular attention was paid to the region on the low frequency side of the band near 2694 cm^{-1}. King and Hainer[1] have suggested that this band should be interpreted as an "R" branch of a vibrational transition associated with a change in electric moment parallel to the axis of the least moment of inertia. Absorption of proper intensity for "Q" and "P" branches was not found. Tentative assignments of the measured bands have been made.

[1] G. W. King and R. M. Hainer, Abstract of paper given at the Chicago meeting of the American Chemical Society, September 1946.

SUPPLEMENTARY PROGRAMME

SP1. A Possible Effect of the Sun Upon Cosmic Radiation. W. F. G. SWANN, *Bartol Research Foundation.**—During the B-29 flights for the determination of latitude variation of the mesotron intensity reported in another paper, it was found that in one flight, made on June 18, the intensity continued to rise with increasing latitude beyond the knee of the curve as determined by other flights. Considerable sun-spot activity occurred during the period in question, culminating in other abnormal effects which have been cited by other observers. Our own apparatus gave considerable evidence of shower phenomena in the penetrating radiation. The paper comprises a discussion of these matters in relation to the sun as a possible origin (probably through betatron activity) of part, and possibly a considerable part, of the hard component of the cosmic radiation.

* To be given after paper A12 if time permits.

SP2. Piezoelectric Vibrations of Rochelle Salt Plates. N. CHAKO, *Kansas State College.**—The theory of vibration of Rochelle salt crystal plates is developed and the modes of vibration of square and rectangular plates with free edges are obtained. Since Rochelle salt has nine independent elastic constants and three priezolectric constants the natural modes of vibration of such a crystal are not of a simple harmonic type as one finds in the quartz crystal plates. However, for certain orientations of the plate (cut) the vibrations can be made simple harmonic. However, the frequencies in general are found to depend on four elastic constants c_{11}, c_{12}, c_{22}, and c_{66}, the last being the shearing constant along the x-y plane of the plate. The thickness vibrations were calculated and it was found that the Christoffel determinant was separable into a linear and one quadratic equation, thus giving rise to three independent frequencies. It was found that the lowest frequency for a plate of 1 cm thickness was approximately 93 kilo Hertz and that the highest frequency in the neighborhood of 102 kilo Hertz. Calculations have also been made for clamped edges and circular plates.

* To be given after paper L11 if time permits.

SP3. On the First Passage Time Problem for the Stationary Markoffian Random Function. A. J. F. SIEGERT, *Syracuse University.*[1]—A stationary Markoffian random function* $y(t)$ is completely defined by $P_2(y_0/y, t)dy$, the conditional probability, that $y<y(t)<y+dy$, provided that $y(0)=y_0$. The function $W(y_0/t, a)dt$ is defined as the conditional probability that $y(t)$ passes the value $a>y_0$ for the first time between $t>0$ and $t+dt$, provided that $y(0)=y_0$.

An adaptation of an argument of Schroedinger** yields the integral equation

$$\tfrac{1}{2}W(y_0/t, a)=U(y_0/t, a)-\int_0^t W(y_0/\vartheta a)U(a/t-\vartheta, a)d\vartheta$$

where $U(y_0/t, a)=-\dfrac{\partial}{\partial t}\int_{-\infty}^{a}P_2(y_0/y, t)dy$. Solving the integral equation by Laplace transformation, we obtain

$$\bar{W}(y_0/\lambda a)=\bar{U}(y_0/\lambda a)/[\tfrac{1}{2}+\bar{U}(a/\lambda a)],$$

where $\bar{W}(y_0/\lambda a)$ and $\bar{U}(y_0/\lambda a)$ are the Laplace transforms of $W(y_0/ta)$ and $U(y_0/ta)$, respectively.

[1] To be given after paper C12 if time permits.
* M. C. Wang and G. E. Uhlenbeck, Rev. Mod. Phys. 17, 323, 325 (1945).
** E. Schroedinger, Physik. Zeits. 16, 289 (1915). I am indebted to Prof. Uhlenbeck for calling my attention to this method.

PROGRAMME OF THE DIVISION OF HIGH-POLYMER PHYSICS

M1. Address of Retiring Chairman. H. A. ROBINSON, *Armstrong Cork Company* (45 min.).

M2. The Determination of Macromolecular Configurations in Dilute Solution by Light Scattering. P. M. DOTY,* W. A. AFFENS, AND B. H. ZIMM,** *Polytechnic Institute of Brooklyn* (30 min.).—The interference pattern produced by monochromatic light scattered from solutions of fractionated polystyrene has been studied. In particular, the dissymmetry coefficient of Debye, the fractional difference of the intensities of the light scattered at two different angles, has been investigated as a function of concentration, of solvent, and of molecular weight of the polymer. The variation with concentration is large and is characteristic of the particular solution, but it was found possible to extrapolate to infinite dilution to obtain a coefficient characteristic of the polymer alone. From this limiting or "intrinsic" coefficient the root-mean-square distance, R, between the ends of the chain molecule may be calculated by exact equations. It was found that R varied as the square root of the molecular weight, as predicted by the theories of chain statistics, but that it was only slightly dependent on the nature of the solvent. On the other hand, the intrinsic viscosity of the same materials was markedly dependent on the nature of the solvent. Some typical data are shown below:

Polystyrene molecular weight	Solvent	R	Mol. wt./R^3	Intrinsic viscosity
4,800,000	Toluene	2370A	—	7.6
4,800,000	Butanone	2100	1.10	2.3
11,800,000	Butanone	2770	1.53	4.10
2,100,00	Butanone	1230	1.38	1.45

* Present Address: Department of Colloid Science, Cambridge University, Cambridge, England.
** Present Address: Department of Chemistry, University of California, Berkeley 4 ,California.

M3. The Relation between Intrinsic Viscosity and Molecular Weight in Polymer Solutions. P. DEBYE, *Cornell University* (30 min.).—If a polymer molecule of the coiling type suspended in a liquid is exposed to forces caused by a flow pattern of the liquid as used in viscosity measurements, its center of gravity will move with the liquid and at the same time the molecule as a whole will rotate with an angular velocity determined by the velocity gradient. Notwithstanding this adaptation of the motion of the molecule to that of the liquid a relative flow of the liquid with respect to the molecule remains. With the assumption that the average density in space of the polymer molecule is so small that its disturbing effect on the motion of the liquid can be neglected, it can be shown that the intrinsic viscosity of a solution will be proportional to the average square of the distance of the average monomer group of the chain from the center of gravity of the whole molecule. This means that in this approximation Staudinger's rule should hold which makes the intrinsic viscosity proportional to the molecular weight. However, neglecting the disturbing effect of the molecule on the regular flow pattern of the liquid is too poor an approximation. A mathematical method has been developed which makes it possible to take care of this disturbance. The final conclusion is that the intrinsic viscosity depends on 2 fundamental constants, each of the dimension of a length, which characterize the molecule. The first of these constants is the familiar average distance D between the two ends of the chain or the corresponding spherical volume proportional to the third power of D, which can be taken to represent a measure for the average volume occupied by the polymer molecule in the solution. The second constant is a length L, determined by the average density with which the molecule fills its allotted space. It is a measure for the distance over which the outside velocity distribution makes itself felt into the interior of this space. The intrinsic viscosity is represented by a product of which the first factor is the specific volume of the molecule defined as the volume occupied divided by the mass of the polymer molecule. The second factor is a relatively simple function of the quotient D/L, a quantity which I would like to call the "shielding ratio." It turns out that for a linear polymer the intrinsic viscosity is proportional to the molecular weight (Staudinger's rule) for small values of the shielding ratio, whereas for large values of this ratio it becomes proportional to the square root of the molecular weight. In an intermediate case the curve can be approximated over a large range of molecular weights by the customary power-function. The exponent has some value intermediate between 1 and $\frac{1}{2}$ and is determined by the shielding ratio. Discussed in this way measurements on intrinsic viscosity give information about the actual size of the polymer molecule in solution and its changes with the solvent. As already indicated by measurements on the dissymmetry of light scattering it is found again that D is a good deal larger than would be expected from Eyring's theoretical formula (no interaction, free rotation). The way is also opened to the use of viscosity measurements in order to obtain information about branching, since branching will affect the space-density of the polymer molecule, which determines the shielding ratio.

M4. Time-Dependent Strain Birefringence in Viscoelastic Materials. TURNER ALFREY, JR., *Polytechnic Institute of Brooklyn* (30 min.).—The phenomenological theory of strain birefringence in viscoelastic materials is developed. The material is assumed to be homogeneous, amorphous, and (in the unstrained state) isotropic. The purely mechanical behavior is assumed to be representable in terms of a distribution of mechanical relaxation times—i.e., the material obeys the Boltzmann superposition principle. Each molecular mechanism of mechanical response to stress will have associated with it a certain strain-optical constant. This results in a definite pattern of (time-dependent) birefringence when stresses are applied. The theory has two possible applications: the use of photoelastic creep studies in the investigation of *molecular mechanisms* of viscoelastic behavior, and analysis of the optical creep effects which may occur when imperfectly elastic materials are used in photoelastic studies of stress distributions.

N1. Velocity and Attenuation of Sound in Rubber. W. B. THOMPSON, B. A. MROWCA, AND EUGENE GUTH, *University of Notre Dame* (30 min.).—Velocity and attenuation of sound in rubber strips were investigated by the standing wave method suggested by Bridgman and Trueblood, developed to measure the dynamic modulus by Silverman and Ballou, and extended by us and Nolle and Bolt (M.I.T.) to measure also attenuation. Amplitude of vibration in this method is below 0.001 percent. Velocity and attenuation of sound both decrease with temperature and with frequency in the range 500–6000 cycles per second for Hevea and synthetic gum stocks. From the velocity and attenuation of sound the dynamic modulus and internal friction constant were derived, assuming a proportionality of the viscous forces to the rate of deformation. Both the dynamic modulus and internal friction decrease with increasing temperature. The former fact is in contrast to the increase of the static and dynamic modulus at larger amplitudes predicted by the statistical theory of rubber elasticity and confirmed by experiment. Probably for such small amplitudes the intermolecular theories chiefly determine the temperature dependence of the dynamic modulus for rubber just as for all other materials. Although the measurements at Notre Dame were checked by those at M.I.T., both groups feel that more accurate data are needed before final conclusions can be reached, particularly about the temperature dependence of dynamic modulus. Financial support of ONR, Navy Department, is gratefully acknowledged.

N2. Elastic Losses of Natural and Synthetic Rubber as a Function of Frequency and Temperature.* H. S. SACK AND H. L. RAUB, *Cornell University* (30 min.).—The elastic losses of unloaded samples of natural rubber and synthetic rubber of the GRS types containing different amounts of styrene were measured. The sample, in the form of a reed, is acted upon by an alternating force of constant amplitude and adjustable frequency. The motion of the end of the reed is observed by means of an optical method. Signals proportional to and in phase with the force and the elonga-

tion, respectively, are obtained and applied to the two pairs of deflecting plates of an oscilloscope. Thus, a picture of the elastic hysteresis loop is obtained. The area of this loop is a measure for the elastic losses in the sample. Observations were made in a frequency range from 300 to 4000 c.p.s. and at temperatures from −60°C to +35°C. The results can be qualitatively interpreted by a relaxation theory, the relaxation time varying very strongly with temperature and with the styrene content. The crystallization of the samples is accompanied by a strong increase in the losses when the temperature decreases and then a decrease at still lower temperatures.

* This paper is partially based on work sponsored by the Office of Naval Research under Contract N6-ori-91.

N3. The Torsion of a Rubber Cylinder. R. S. RIVLIN,* *British Rubber Producers' Research Association* (30 min.).—In a series of papers pending publication[1] a mathematical formalism has been developed for the solution of problems concerning the deformation of highly elastic materials. The present paper is concerned with the experimental verification of the predictions of one paper of this series, in which the torsion of a rubber cylinder is discussed on the basis of this theory and it is found that, in order to produce pure torsion in a rubber cylinder, a compressive longitudinal thrust must be applied over the plane ends of the cylinder, in addition to the torsional couple. The distribution of this thrust over the ends of the cylinder and its dependence on torsion are investigated experimentally in the present paper and agreement with the theoretical conclusions is obtained.

* At present guest worker at the National Bureau of Standards.
[1] Rivlin, Phil. Trans. Roy. Soc. A.

N4. Heat Conductivity of Natural and Synthetic Rubbers under Stretch and at Low Temperatures. H. D. SMITH, T. MCC. DAUPHINEE, AND D. G. IVEY, *University of British Columbia, Canada* (*Introduced by Eugene Guth*) (30 min.).—Heat conductivity of natural and synthetic rubbers was studied in the range from +50° to −160°C. and from 0 to 100 percent stretch for two different cures and ages. The apparatus was a greatly modified version of one designed by Schallamach. Both for natural and synthetic rubbers, the value of the heat conductivity measured perpendicular to the direction of stretch was smaller and the rate of change of conductivity larger in the stretched than in the unstretched state. On lowering the temperature and raising it again natural rubber shows very complicated hysteresis phenomena due to progressing or regressing crystallization. Synthetic rubber shows a simpler behavior exhibiting a hysteresis loop caused by the transition of second-order from elastic to brittle, glassy material. The hysteresis phenomena for both types of rubber show great similarity (in particular in thermal conductivity near th brittle point) to the drop in specific heat observed by Bekkedahl and associates. The effect of cure and the effect of aging depends on the position of the temperature with regard to the transition temperature. Above and below the transition region, the heat conductivity decreases approximately linearly with temperature as one may expect from theory. Theoretical approaches to heat conductivity of polymers will be discussed briefly. Financial support by the National Research Council of Canada is gratefully acknowledged.

N5. Relaxation of Stress in Plastic Materials. M. MOCHULSKY, R. D. ANDREWS, AND A. V. TOBOLSKY, *Princeton University* (30 min.).—Studies of relaxation of stress at constant extension over a wide range of temperatures were extended from rubbery to plastic materials. These studies were interpreted in terms of such variables as molecular weight, cross linkage, chain stiffness, crystallinity, and interchain interaction. The effect of plasticizer was also investigated. Decay of stress due to chemical scission was observed in at least one linear thermoplastic.

P1. Six Rules for Analyzing Stress-Strain Curves. GEORGE HALSEY, *Textile Research Institute* (30 min.).—In the analysis of the stress-strain properties of a material there is a certain advantage to the making of haphazard stress-strain curves following no particular pattern. As more painstaking analyses are attempted and as the model is refined, this procedure becomes very wasteful. The writer has attempted to improve the situation by setting up a series of six rules for the analysis of the stress-strain curves. In the present paper the general distribution of non-Newtonian relaxation times is included in the scheme of analysis. Also, the existence of multiple equilibrium positions at the same value of the flow coordinate is discussed. The paper is organized into six rules of procedure, each containing a simplifying criterion. If all six criteria are obeyed, then the material under study is representable by a hyperbolic sine-law model. The six rules suggest an orderly mode of experiment.

P2. Studies of Cellulose Acetate with the Ultracentrifuge. S. SINGER AND H. MARK, *Polytechnic Institute of Brooklyn* (30 min.).—Measurements on a series of fractions of cellulose acetate in acetone have been performed with the velocity ultracentrifuge combined with free diffusion experiments. The molecular weights, M, of these fractions varied from 10,000 to 200,000, and in this range the sedimentation constant s varied considerably with M. In a system where s is independent of M, the particles may be considered "free-draining," that is, solvent freely penetrates the molecule. For particles that are impermeable to solvent and are randomly coiled, s is proportional to $M^{\frac{1}{2}}$. Our results indicate that the cellulose acetates are intermediate between these two cases. Moreover, on the assumption that the molecules may be satisfactorily represented by ellipsoids of revolution, axis ratios are calculated from sedimentation data and viscosity data independently, by Perrin's and Simha's equations respectively. The axis ratios so calculated differ by factors outside of experimental error, and indicate that the model is not a quantitative one for cellulose acetate in acetone.

P3. An Instrument for Measuring Particle Diameters and Constructing Histograms from Electron Micrographs. E. E. HANSON AND J. H. DANIEL, *Firestone Tire and Rubber Company* (30 min.).—An instrument for shortening

the time and labor required in constructing particle size histograms from electron micrographs is described. Representative histograms obtained with the instrument for GR-S latices are shown. Linear, surface, and volume-equivalent diameters of non-spherical particles are defined, and variations in the instrument for plotting such diameters are proposed.

P4. A Sound Velocity Method for Determination of Molecular Weight of Liquid Polymers. ALFRED WEISSLER, J. W. FITZGERALD, AND IRVING RESNICK, *Naval Research Laboratory.*—The molecular sound velocity $R=Mv^{\frac{1}{4}}/d$ (where M is molecular weight, d is density, and v is sound velocity in the liquid) has been shown by Rao to be (a) a temperature-independent constant for most pure liquids; (b) an additive property of the atoms in a molecule; and (c) therefore a linear function of molecular weight in each of several homologous series. Further, in each series, linear relationships were found by Lagemann and Dunbar to exist between any two of the following properties: molecular sound velocity, molecular refraction, parachor, molecular magnetic rotation, critical volume, Souders' molecular viscosity, and van der Waals b. Of these, the first two may be determined experimentally with relative ease and accuracy, by means of the acoustic interferometer using a frequency of one megacycle and the Abbe refractometer. These relations were utilized in the present work to give an expression for molecular weight:

$$M=\frac{Bd}{v^{\frac{1}{4}}-A\left(\frac{n^2-1}{n^2+2}\right)}.$$

This expression has yielded accurate results for the molecular weights of several pure members and commercial mixtures of the polyethylene glycol series. Comparisons are made between these results and the number average and weight average molecular weights. Excellent agreement was also observed for the calculated and experimental values of the slope A and for the calculated and observed values of the molecular sound velocities of these compounds.

P5. Diffraction of Visible Radiation by Cellulose Acetate Yarn. EMMETT MARTIN, *Tennessee Eastman Corporation.*—Filaments of cellulose acetate yarn have been found, under certain conditions at least, to have the property of diffracting visible radiation. The yarns in which this phenomenon has been observed were drafted at elevated temperatures to from 2 to 5 times their original length. When these yarns, either single or multiple filaments, are immersed in a colorless liquid having an index of refraction close to that of the yarn, and illuminated with approximately parallel white light incident on the fibers normal to their long axis, the fibers will appear to be colored when viewed at various angles from points in the plane containing both the fibers and the incident beam of light. The color at a particular angle is determined from the grating formula $\eta\lambda=d\sin\theta$, and does not depend upon the index of refraction of the immersion medium, except that the index of the medium should be near that of the fibers to reduce the white light scattering enough to make the colors visible. The distance apart of the diffracting centers, d, is directly proportional to draft factor, and varies from about 0.2 micron for undrafted fibers to approximately 1 micron for those drafted by a factor of 5.

Q1. Some Dielectric Properties of Butadiene-containing Polymers and Copolymers. R. F. BOYER, E. B. BAKER, AND P. C. WOODLAND, *Dow Chemical Company* (30 min.).—A study of the dielectric properties of mixtures of polystyrene and polybutadiene revealed a peak in the power factor-frequency curve at 100 megacycles. This peak was first ascribed to vinyl side groups, but it was then found that purified, natural rubber also showed a peak of about the same magnitude and at the same frequency. Consideration was next given to the idea that a long chain of conjugated double bonds is a perfect electrical conductor.[1] It was thought that a regular distribution of double bonds, as along a chain of polyisoprene, might cause dielectric dispersion when the transit time of electrons along the polymer chain was equal to the frequency of the applied field. Dispersions of carbon black in polyethylene were made to simulate roughly the proposed mechanism of dielectric loss. Such systems showed both a low frequency as well as a high frequency power factor peak. Both peaks depended in magnitude on the orientation of the carbon black particles with respect to the electric field being smaller when the long axis of the particle was perpendicular to the field.

[1] F. London, *Surface Chemistry* (American Assoc. for the Advancement of Science, Washington, D. C., 1943), p. 144.

Q2. Dielectric Properties of Rubber—Particularly of Loaded Stock. L. V. HOLROYD, B. A. MROWCA, AND EUGENE GUTH, *University of Notre Dame* (30 min.).—Dielectric constants and losses were measured in the range from 0–200 mc. In general, dielectric constants decrease with increasing frequency, with a drop corresponding to the peak in the loss-frequency curve. The peaks observed in the loss-frequency curve at low frequencies may be interpreted as caused by oxidation and to fillers, at high frequencies as caused by dipoles caused by the bonding of sulphur in vulcanization. Changes of dielectric constants and of losses, in particular shifts in peaks with temperature in the range from 0–70°C were also studied. Dielectric constants of rubber-carbon black mixtures from 0–25 percent volume concentration were observed and compared with theory of spherical particles indicated by Guth.[1] An extension of this theory to ellipsoids was also used in the interpretation of the data. Infinite conductivity of carbon black as compared to that of rubber was assumed. Results may be interpreted by assuming that carbon black particles preferentially form doublets. This result on doublets is also indicated in data kindly communicated to us by Dr. Breckenridge in von Hippel's laboratory (M.I.T.). Financial support by ONR, Navy Department, is gratefully acknowledged.

[1] J. App. Phys. (1944).

Q3. Frequency Response Characteristics of Dielectric Materials and Their Interpretation. A. VON HIPPEL, H. B. CALLEN AND W. B. WESTPHAL, *Massachusetts Institute of*

Technology (45 min.).—The paper presents dielectric constant and loss characteristics of gases, liquids, and solids measured over a broad frequency range and considers their interpretation in terms of molecular physics.

Q4. The Electrical Resistivity of Conducting Rubber. PAUL E. WACK, *University of Notre Dame* (30 min.).—The electrical resistivity of Gr-S loaded with Shawinigan and Continental R-40 carbon blacks was determined as a function of temperature, elongation, time, and percentage volume leading. The resistivity of Gr-S–Shawinigan mixes first increases with elongation, and then decreases, the peak occurring between 10 and 20 percent, but the resistivity of Gr-S–R-40 mixes increases for all elongations. The resistivity of all stretched samples decreased exponentially with time. The resistivity-temperature curves exhibited hysteresis loops for samples stretched to low elongations or for samples of low volume loadings, but did not show loops for samples stretched to high elongations or highly loaded. A plot of log-conductivity versus $1/T$ yielded straight lines. The temperature coefficient of resistivity for unstretched samples loaded with Shawinigan black is positive for all loadings investigated, and increases with loading. Both Shawinigan and R-40 blacks have a negative temperature coefficient of resistivity. Both positive and negative temperature coefficients were observed for unstretched samples loaded with R-40, the coefficient being negative for low loadings and positive for higher loadings. Log-resistivity versus carbon concentration yielded an exponentially decreasing curve and log-resistivity *vs.* log-concentration an approximately linear relationship. Interpretation of data will be discussed. Financial support of ONR, Navy Department, is gratefully acknowledged.

Q5. Measurements of the Refractive Index of Films. FRED W. BILLMEYER, JR., *E. I. duPont de Nemours and Company* (30 min.).—The refractive index of a film of transparent or translucent material may be determined by immersing the film in a suitable liquid mixture and observing the intensity of light reflected from the surface of the specimen. The composition of the immersion liquid is varied, and a record is made of its refractive index (measured on a refractometer) and of the reflected light intensity. The refractive index of the film is the same as that of the immersion liquid giving the lowest reflected intensity. This has been confirmed by experiments with a glass plate, whose refractive index was known. According to Fresnel's laws of reflection, the experimental data should fit a parabola with its minimum at the refractive index of the film. On fitting the data by the method of least squares, the minimum is obtained with a standard deviation of the order of 0.002 refractive index units. The method has been applied to several plastic materials.